Spatial genetic structure in the coral genus *Galaxea* (Euphyllidae) and their associated Symbiodiniaceae communities

アザミサンゴ属の種内と種間の空間的遺伝構造および共生する褐虫藻の群集構成

PhD Thesis

Patricia H. Wepfer

Submitted October 31st 2018

Okinawa Institute of Science and Technology Graduate University

I, Patricia Wepfer, declare that this thesis entitled "Spatial genetic structure in the coral genus *Galaxea* (Euphyllidae) and their associated Symbiodiniaceae communities" and the data presented in it are original and my own work.

I confirm that:

- No part of this work has previously been submitted for a degree at this or any other university.
- References to the work of others have been clearly acknowledged. Quotations from the work of others have been clearly indicated, and attributed to them.
- In cases where others have contributed to part of this work, such contribution has been clearly acknowledged and distinguished from my own work.
- None of this work has been previously published elsewhere

Signature:

Date: October 29th 2018

Abstract

The evolution and systematics of corals have been difficult to unravel despite being the fundament of one of the world's most charismatic ecosystems. Coral diversity and diversification processes are not well understood due to morphological plasticity, potential hybridization and generally high rates of dispersal. Both geographically and methodologically extensive studies are needed to improve our understanding of coral ecology and evolution, including spatial biodiversity processes involving hosts and their associated symbionts. This dissertation investigates coral evolution in three complementary studies using the genus *Galaxea* L. as a model. First, I ask whether endosymbiotic community composition differentiate among morphologically cryptic genetic lineages in *G. fascicularis*. The Symbiodiniaceae ITS2-sequence was metabarcoded using next generation sequencing (NGS) and community assembly was analyzed with joint distribution models. Symbiodiniaceae communities were found to cluster into three regular community types that cannot be explained by environment or host genotype, potentially indicating species interactions between Symbiodiniaceae types. Second, I assessed how spatial connectivity between geographic populations corresponds to neutral differentiation on the subspecies level using population genomic methods. Coral populations from the Ryukyu archipelago, the Daito Islands, and the Ogasawara Islands were characterized by restriction site-associated DNA sequencing (RAD) to investigate whether the Daito Islands could be a stepping stone between Ryukyu and Ogasawara. The Ogasawara population was found to be highly differentiated and to have diverged under little amounts of continuous gene flow since the early Pliocene. No stepping stone role of the Daito Islands was found and the Ogasawara population may receive most migrants from the Ryukyu Islands, which was consistent with the dispersal patterns predicted by a oceanographic dispersal model. Lastly, I investigated the evolutionary history in the genus *Galaxea* taking a phylogeographic approach. I asked whether the genetically well-differentiated and sympatric lineages within *G. fascicularis* in Okinawa maintain their separation over geographic space and to what extent their spatial distributions overlap in the genus distribution range. *Galaxea* field collections were gathered from across the Indo-Pacific, and complemented by museum specimens to increase geographical coverage. At the same time the relationship between genetic lineages and taxonomic species was evaluated based on five out of seven currently accepted species *(G. fascicularis, G. astreata, G. cryptoramosa, G. paucisepta, G. horrescens*). The genus *Galaxea* clustered into three highly divergent clades; one Indo-Pacific, one Pacific, and one basal small clade found in Chagos. All morphological species were part of the Pacific clade. Overall this study indicates spatial rather than ecological or symbiosis-related processes to drive diversification and that the current taxonomy does not reflect biological species in this genus.

Acknowledgements

I wish to thank Prof. Satoshi Mitarai and Prof. Evan Economo for their continuous support in planning, conducting, and completing this research. Prof. Satoshi Mitarai has taken me into his unit and has given me space, resources, administrative support for the numerous research collaborations with overseas institutions for sample acquisition, and has contributed the numerical dispersal model in chapter 2. Prof. Evan Economo has contributed largely to my intellectual growth through scientific discussions throughout my PhD, and has particularly supported me in the analysis and writing of chapter 1. I also thank Dr. Yuichi Nakajima for his groundbreaking guidance in finding this project. Without him, I would have never found my study taxon *Galaxea*, around which all questions of my PhD developed. For the very first and most important steps of my project, the specimen collections in the field, I wish to thank Dr. Shohei Suzuki, who accompanied me to almost all of my field trips. His large experience in scientific diving and his very careful and responsible planning of all fieldwork made him to the most competent dive buddy I could have wished for. I am very grateful to Sasha Mikheyev and Jo Tan for conducting the RAD-library preparations of my samples. An infinitely important role also played my international sample providers. Thanks to the kind support from Dr. Makamas Sutthacheep, Prof. Tamasak Yeemin, Dr. Veronica Radice, Prof. Put Ang, Prof. Allen Chen, Dr. Zoe Richards, Prof. Atsushi Fujimura, Dr. Mareike Sudek, Prof. James Reimer, and Tullia Terraneo *Galaxea* specimens from all over the Indo-Pacific could be gathered and enabled the phylogeographic study in my last chapter. Thanks to these people I was able to experience scientific exchange and networking with leading experts in the field, which was one of the most delightful sides of pursuing a PhD. Regarding sample collections, I am also very grateful to the OIST research support sections for helping me in passing numerous Joint Research Agreements and Material Transfer Agreements, and in obtaining CITES import permits for the samples from my collaborators. I am especially thankful to Dr. Makamas Sutthacheep, Prof. Tamasak Yeemin and their graduate students for hosting us several weeks for field collections in the Gulf of Thailand. Equally valuable, both regarding the science of my project as well as personal growth as a young researcher was my visit at the Hawai'i Institute of Marine Biology at the University of Hawai'i. I greatly appreciate the knowledgeable mentoring and discussions with all people of the ToBo Lab, and especially Prof. Rob Toonen for hosting me in his lab. I thank Dr. Bert Hoeksema from the Netherland Naturalis Biodiversitas for providing museum specimens and unpublished work regarding the taxonomy of *Galaxea.* I also wish to thank all members of the Marine Biophysics Unit and the Biodiversity and Biocomplexitiy Units for their kind support during all these years. In particular I would like to thank Kazumi Inoa, for teaching the basics of ROMS modeling, Nitish Narula for his help in phylogenomics, and Miguel Grau-Lopez for his general computational help. Thank you also to Kevin Reed for proof reading important sections of this thesis. I greatly appreciate the emotional support and discussions with other students, Maggi Mars Brisbin and Maki Thomas, for making everyday student life enjoyable throughout my PhD. I also would like to thank my family back in Switzerland for giving me strength and believing in me during all these years on the other side of the globe. Even though from so far, their support during these years were crucial for the completion of this work. Finally, I would like to thank OIST and JSPS (grant number 17J00366) for funding this research.

Index

List of Tables and Figures

Tables

Figures

Fig. S1.2. Parameter splines of Generalized Dissimilarity Model.

Fig. S1.3. Residual analysis of a pure latent variable model in Boral.

Fig. S1.4. Point estimates and 95% highest posterior density intervals for the OTU-specific regression coefficients fitted by Boral.

Figure S2.1. Principal component analysis for the separation of cryptic lineages 'L' 'L+' and 'S' based on 11'473 SNPs represented in at least 50% of all individuals.

Figure S2.2. Heatmaps of pairwise correlations for clone detection.

Figure S2.3. BayeScan output for the detection of sites under selection.

Figure S2.4. Admixture analysis based on SNPs present in > 70% of individuals.

Figure S2.5. Dadi site frequency spectra and residuals of 2D models.

Figure S2.6. Principle component analysis of immigration matrix according to inverse particle tracking per site to assess similarity in immigration patterns between collection sites.

Introduction

The concept of a species as a unit of evolutionary organization is fundamental to understanding biodiversity. However, corals (scleractinia) belong to one of the organismic groups for which delimitations and phylogenetic relationships of many species remain uncertain (Kitahara *et al.*, 2016). The scleractinia and Symbiodiniaceae together form the trophic and structural fundament of coral reef ecosystems and support thousands of species, including commercially important human foods. Due to local and global mass-bleaching events they have been in rapid decline (Hughes *et al.*, 2017), and the recognition of biologically meaningful species seems more important than ever for the effective implementation of conservation efforts (Beger *et al.*, 2014). Morphological plasticity, slow mutation rates of mitochondrial DNA (Shearer *et al.*, 2002), and frequent hybridization (Willis *et al.*, 1997; Willis *et al.*, 2006) have complicated the systematics in corals using classical phylogenetic and taxonomic approaches (Romano & Cairns, 2000; Fukami, 2008; Kitahara *et al.*, 2010) so that most of the conventional taxonomy to date may need critical revision with higher-resolution molecular methods. An additional logistical challenge is given by the easy dispersal of corals as pelagic larvae, which causes large and geographically widely spread populations. This leads to unrelated geographic and phylogenetic closeness (Jablonski, 1986), complicating a balanced sampling across even small evolutionary clades. Furthermore, corals live in tight symbiosis with the photosynthesizing dinoflagellate Symbiodiniaceae Freudenthal (1969), with which they share a co-evolutionary history (Thornhill *et al.*, 2014; LaJeunesse *et al.*, 2018). In order to better understand species and speciation in corals, the coral holobiont needs to be studied from multiple angles, applying a geographically and genetically intensive sampling. This thesis presents an integrative investigation of genetic differentiation within and among lineages of the coral genus *Galaxea* Oken (1815), in order to understand how ecological and evolutionary processes in a spatial context may relate to divergence and a potentially highly complex model of evolution in corals.

Symbiodiniaceae should be studied alongside with the coral host (Rosenberg *et al.*, 2007; Ainsworth *et al.*, 2010; Parkinson & Baums, 2014), since the holobiontic community as a whole responds to evolutionary forces such as natural selection and adaptation, and should thus be regarded as the unit of evolution (Rosenberg *et al.*, 2007). This is supported by host-symbiont specializations that have enabled co-adaptive radiations of the scleractinia with Symbiodiniaceae clade C in the Pacific (Thornhill *et al.*, 2014), and have facilitated the

adaptations of coral species to specific habitats (Stat *et al.*, 2006). The community structure of Symbiodiniaceae within a host is variable between species, and across time and space (Cunning & Baker, 2014) but a worldwide host-symbiont network analysis found an overall correlation between Symbiodiniaceae community and host community (Tonk *et al.*, 2013) and that even closely related species can differ in their Symbiodiniaceae composition (Pinzon & LaJeunesse, 2011; Warner *et al.*, 2015; Smith *et al.*, 2017). However, data on within species variation in Symbiodiniaceae community composition that also investigates the low abundance background types is still sparse. For understanding a potential influence of Symbiodiniaceae on coral differentiation, genetic variation within both the host and Symbiodiniaceae need to be investigated in detail while controlling for ecological and spatial factors. This was pursued with a metacommunity ecology approach using metabarcoding and joint species distribution modeling in *Galaxea fascicularis* from the Ryukyu and Daito Islands in Japan (Chapter 1).

Speciation in corals could be largely influenced by spatial processes, as is the case across the tree of life (Coyne & Orr, 2004). Populations that maintain limited genetic exchange with others due to spatial isolation will over long enough periods of time become genetically incompatible and speciate (Mayr, 1942; Mayr, 1963). This speciation process can be investigated at different stages. In order to understand the scales and mechanisms of ongoing spatially driven speciation, genetic and migratory relationships between populations may be studied in detail on ecological time scales using population genomic tools (Sousa & Hey, 2013). Understanding metapopulation structure and connectivity is also essential for preserving genetic diversity of local populations, which in turn relates to ecosystem resilience (Roberts, 1997; Sexton *et al.*, 2011; Manel & Holderegger, 2013). In corals, as in many other marine organisms, dispersal mostly occurs by passive transport in a pelagic larval stage. Gene flow between populations of pelagic dispersers may therefore be predicted by ocean current models (Roberts, 1997), and by combining population genetics with dispersal modeling approaches it is possible to gain a more comprehensive understanding for neutral divergence processes than with molecular methods alone. Lagrangian particle advection simulations with biological parameters of the dispersal propagules have been used to model larval dispersal across the globe (e.g. Cowen *et al.*, 2006; Paris *et al.*, 2007; Siegel *et al.*, 2008; Mitarai *et al.*, 2009; Kool *et al.*, 2011; Treml *et al.*, 2015) and an increasing number of studies have confirmed modeled dispersal to correspond to genetic differentiation (Selkoe *et al.*, 2010; White *et al.*, 2010; Crandall *et al.*, 2012; Crandall *et al.*, 2014; Raynal *et al.*, 2014), including

in corals (Foster *et al.*, 2012; Davies *et al.*, 2015). As the scales for spatial divergence could be very large in marine systems due to high dispersal capabilities (Palumbi, 1994), a geographically adequate, sufficiently wide sampling is needed in order to find the amounts of genetic differentiation necessary for incipient speciation. Spatially well-defined, isolated island systems are ideal to study spatial divergence, since dispersal is low between a limited number of potentially connected populations. Chapter 2 of this thesis presents a case study investigating potential incipient spatial speciation between populations of *Galaxea fascicularis* from the Ogasawara, the Daito, and the Ryukyu Islands, by analyzing divergence history and migratory relationships combining population genomic and dispersal modeling approaches.

In addition to population genetics, phylogenetic methods are able to reveal diversification processes on evolutionary time scales, i.e. identify the phylogenetic emergence of entities that have already developed reproductive barriers and have maintained genetic coherence through geologic times (species). For the correct estimation of species diversity and inference of their phylogenetic relationships, it is imperative to sample a clade as completely as possible (Zwickl & Hillis, 2002). Due to uncertain species delimitations in corals, the smallest level of likely monophyly may be the level of genus (Veron, 1995), which is why phylogenetic relationships in coral should be studied by including specimens from an entire genus comprehensively. A both taxonomically and geographically extensive sampling of a coral genus is logistically challenging but may be achieved in a small genus with only few extent taxonomic species. Toward this end I chose *Galaxea* (Euphyllidae), a genus with only ten extant morphospecies currently accepted in the World Register of Marine Species (WoRMS, 2015), to investigate species emergence histories in a spatial context, and to at the same time discuss the validity of the current taxonomy from a phylogenetic perspective. The genus is easily identifiable in the field and is common from the Res Sea to Micronesia. The most common species *G. fascicularis* L. 1767 is relatively well studied in Okinawa where anatomical (Hidaka, 1992), molecular (Watanabe *et al.*, 2005; Nakajima *et al.*, 2016), and reproductive studies (Abe *et al.*, 2008b) indicate the presence of three cryptic lineages referred to as 'L', 'S' and 'L+'. By investigating phylogenetic relationships and geographic distributions of these lineages in Chapter 3 I give a hypothetical explanation of a spatial speciation process between these lineages, and the evolutionary history of the genus *Galaxea.*

Specimen collection and DNA extraction

All specimens underlying the three chapters of this thesis were sampled and DNA extracted as described below, if not specified otherwise.

The collection of *Galaxea* specimens was approved by the prefectures of Okinawa (permit numbers 26–62, 27–64), Tokyo for the collections in Ogasawara (permit number 28–41), and Kagoshima for the collections in Tanega shima (no permit number assigned). Specimens were collected from various locations across Japan by SCUBA between 2014 and 2016. From the point of entry, a ca. 1 km^2 area was randomly searched for the target taxon, leaving at least 2 m distance between the selected colonies to minimize the chance of clonality. One or two typically sized polyps in the coral colony were taken per collection, from which one was used for molecular analysis and the second was kept as backup material and voucher specimen. The polyps were transferred on ice immediately after collection and into >99% EtOH within 3 hours. Sixty-seven colonies in total were selected for Symbiodiniaceae ITS2 metabarcoding. Each colony was photographed in the field with a color bar and scale and recorded in water depth using a dive computer. Remaining specimen materials were deposited in the Marine Biophysics Lab lead by Satoshi Mitarai at the Okinawa Institute of Science and Technology. Electronic specimen vouchers are available as field photographs upon request (patwepfer@gmail.com). A complete list of specimens collected for this thesis are listed in Appendix 3.

Polyps were grinded using mortar and pestle from which approximately 1 cm^3 of the material was used for DNA extraction. Holobiontic DNA was extracted using the Qiagen DNeasy Blood and Tissue Kit. The manufacturer's protocol was changed in the following steps: the initial incubation time for tissue lyses at 56ºC was extended to 4–10 h (step 1), 4ul of 100x RNAse A was applied after this first step. A 1.5–2 times larger volume of EtOH was applied for denaturation, in order to separate extensive amounts of mucus from the watery phase (step 3). DNA was eluted in several steps, using 200ul for a single elution or 40ul, 100ul, and 50ul for elution in three steps. Quantity and quality of genomic DNA were checked by Qubit and gel electrophoresis.

1. Chapter: Symbiodiniaceae metacommunity ecology in association with the coral *Galaxea fascicularis*

1.1. Introduction

Mutualisms between multicellular organisms and microbes form the basis of some of the most diverse ecosystems on the planet (Boucher *et al.*, 1982). In such systems, microbial symbionts form assemblages of potentially interacting individuals and species—ecological communities—within each host. The hosts often traverse space and environmental gradients, providing metacommunity structure to the local microbial assemblages (Leibold *et al.*, 2004). Thus, the application of questions, concepts, and methodologies from metacommunity ecology to the study of symbiont assemblages may help illuminate key aspects of their ecology, organization, and stability in the face of perturbation (Mihaljevic, 2012).

Perhaps the most fundamental question of community ecology is how individuals and species assemble into communities. In most terrestrial and marine systems, environmental gradients underlie variation in community composition to some degree, because climate strongly affects the physiology and fitness of most organisms (Simberloff & Dayan, 1991). However, positive and negative biotic interactions also influence community structure (Chesson, 2000). After accounting for the effects of the environment on individual species, there may be residual correlations between pairs of species that identify modules of interacting species—different communities or subcommunities that repeatedly assemble in space. Here, we analyze the metacommunity composition of Symbiodiniaceae in corals using metabarcoding and joint species distribution modeling approaches.

The Scleractinia-Symbiodiniaceae symbiosis may be viewed as the structural and trophic fundament of coral reef ecosystems that are renowned for their incredible diversity (Roberts *et al.*, 2002). Collapse of this symbiosis due to environmental stressors and diseases — coral bleaching — has repeatedly caused entire ecosystems to break down (Hughes *et al.*, 2017). The resistance of corals to bleaching is known to be affected by the composition of endosymbiotic Symbiodiniaceae communities (Sampayo *et al.*, 2008). We evaluated the extent to which composition and turnover of the Symbiodiniaceae community hosted in individual corals are driven by environmental and host factors, and after accounting for those, whether there are residual correlations indicating clusters of positively and negatively co-occurring variants. Such correlations could indicate that there are alternative stable symbiont

communities that can form within coral polyps that may respond differently to environmental stressors responsible for mutualism breakdown and coral bleaching.

Symbiodiniaceae are a family of dinoflagellates classified into nine ecologically distinct and phylogenetically highly divergent 'clades' denominated A-I, based upon the 18S rDNA region (Rowan & Powers, 1991; LaJeunesse, 2001; Pochon *et al.*, 2004; Pochon & Gates, 2010). This family was previously known as the genus *Symbiodinium* and has recently been lifted to family level (LaJeunesse *et al.*, 2018). Scleractinia most often host clades B, C, and D (Baker, 2003), with a predominance of clade C in the Indo-Pacific including Japan, to which they maintain intimate mutualistic relationships (Muscatine & Porter, 1977). The clades are further classified into hundreds of 'types' based on sequence variation of the ribosomal internally transcribed spacer 2 (ITS2). Because of host specializations and varying geographic and depth distributions, these types are considered to represent evolutionarily significant units that approximate species (e.g. LaJeunesse *et al.*, 2003; LaJeunesse, 2005) and formal species descriptions have been made based on ITS2 and the concordance with multiple other genetic markers (Lajeunesse *et al.*, 2012; LaJeunesse *et al.*, 2014; Parkinson & Coffroth, 2015). The community in a host individual usually consists of one dominant type and several minor background types (Mieog *et al.*, 2007). Background types may influence the recovery after a bleaching event (Berkelmans & van Oppen, 2006) and there is increasing evidence that they play a significant role for the stability of a regularly structured community (Boulotte *et al.*, 2016; but see Lee *et al.*, 2016; Ziegler *et al.*, 2018).

Generally, the physical environment is expected to have a strong influence on *in hospite* Symbiodiniaceae community assembly. For example, the dominant Symbiodiniaceae types within host species vary with latitude, seasons, and depths (reviewed in Baker, 2003). The host, as part of the endosymbiotic environment, may also have a significant influence on community composition. This is apparent from host-symbiont specifications, including between morphologically cryptic host lineages (Pinzon *et al.*, 2013; Warner *et al.*, 2015), as well as from the host health status or degree of bleaching, which directly mirrors the *in hospite* Symbiodiniaceae community (Rowan, 2004; Chen *et al.*, 2005). Coral skeletal morphology was also shown to affect the Symbiodiniaceae community since photosynthetic activity varies between Symbiodiniaceae clades and subclades and is linked to calcification and growth rate (Little *et al.*, 2004; Yost *et al.*, 2013; Diaz-Almeyda *et al.*, 2017). However, these observations have been made primarily on the dominant Symbiodiniaceae types in a community, and environmental variation or host impacts on the level of Symbiodiniaceae

ITS2 types are only beginning to emerge (Parkinson *et al.*, 2016; Diaz-Almeyda *et al.*, 2017). Community-level Symbiodiniaceae data have only recently become available at sufficient resolution, (e.g. Cunning *et al.*, 2015; Gorospe *et al.*, 2015; Boulotte *et al.*, 2016; Ziegler *et al.*, 2018) due to the decreasing cost of next-generation sequencing technology, and much remains unknown regarding their community assembly processes, such as the roles of environmental filtering versus biotic interactions.

While advances in next-generation sequencing have enabled characterizations of symbiont communities, new statistical methods facilitate both the evaluation of environmental effects on species distributions as well as residual correlations between species. In particular, joint species distribution modeling is an emerging paradigm that extends single species distribution models to include the potential biotic affects among species (Warton *et al.*, 2015). Unlike other common approaches for community analysis that are based on co-occurrence patterns alone, such as network analysis, joint species distribution models are able to correct for co-occurrences caused by similar environmental preferences. These "latent" correlations reflect blocks of species that do or do not tend to occur together, which can reflect positive and negative interactions among species (Kissling *et al.*, 2012). This approach of jointly modeling occurrence of multiple species complements other approaches that seek to explain community-level beta-diversity as a function of environmental or other factors, such as generalized dissimilarity modeling (GDM).

In this study, we used deep sequencing technology, joint distribution modeling (Warton *et al.*, 2015), and generalized dissimilarity modeling to analyze the metacommunity ecology of endosymbiotic Symbiodiniaceae on the example of the coral *Galaxea fascicularis* L. across the Nansei Islands in southwestern, Japan (Fig. 1.1). ITS2 was chosen as a genetic marker as it is the most commonly used describer of Symbiodiniaceae diversity. Despite the problems related to the multicopy nature (Arif *et al.*, 2014), it remains an essential marker to contextualize new studies with the large body of existing data (Cunning *et al.*, 2017). Moreover, in-depth variability of ITS2 on the level of endosymbiotic communities is still little explored. By finely resolving the ITS2 variation between and within individuals using deep-sequencing and Minimum Entropy Decomposition (Eren *et al.*, 2015) we also illuminate differentiation within what would cluster as a single ITS2 type using traditional OTU approaches.

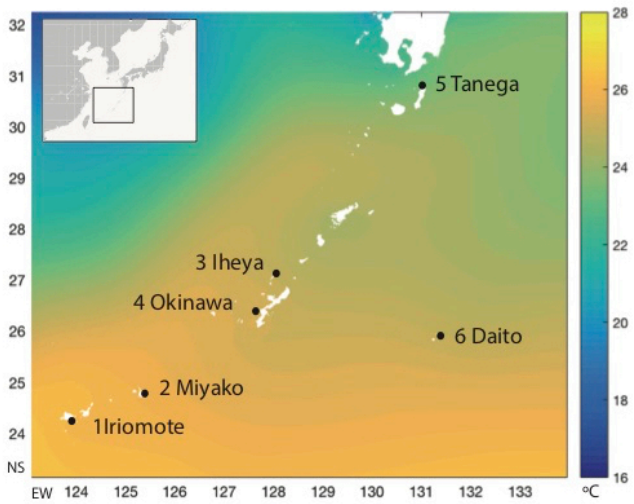

Figure 2.1. Mercator projected map of sampling sites along the Nansei Islands. Annual mean sea surface temperature is indicated as background color (data retrieved from WOA13). The numbers refer to the location IDs in Table 1.1.

Galaxea fascicularis is a suited model system to investigate the Symbiodiniaceae metacommunity ecology, since it is a widely distributed generalist species acquiring symbionts from the settlement location (Baird *et al.*, 2009) and occurs at all parts of the reef. There are several genetic lineages within this species with little morphological differentiation (Nakajima *et al.*, 2016). Associations with ITS2-types C1, C1b, C2r, C21, C21a, C27, C3, C3d, C3u, C40, C161, D1, D2, D17 have been reported (GeoSymbio: Franklin *et al.*, 2012; Zhou *et al.*, 2012; Tong *et al.*, 2017; Zhou *et al.*, 2017) indicating a rather flexible relationship potentially varying according to the environment and host characteristics. We specifically evaluated the extent to which geographic location, temperature, depth, host lineage, polyp size, and bleaching status, predict the distributions of Symbiodiniaceae types and communities between colonies of *Galaxea fascicularis*. After accounting for those factors, we further evaluated the extent to which residual modules of ITS2-types display non-random associations, a hallmark of discrete community assembly and a possible indication of communities structured by facilitating and competitive interactions.

1.2. Methods

1.2.1. Field sampling

Sixty-seven coral colonies of the taxon *Galaxea fascicularis* L. were collected from six locations along a latitudinal gradient in the Nansei Islands (Fig. 1.1, Table 1.1). They were collected by SCUBA from the fore reef, except for in Okinawa, where samples were picked

in the inner reef during walks at low tide. Collections since 2015 from the locations Miyako, Iheya, Tanega, and Daito include photo documentation, precise depth and *in situ* temperature recording and were used for the main analysis in this paper. Earlier collections from Iriomote and Okinawa have no associated metadata but were included to explore geographic variation for Symbiodiniaceae community composition. Sixty-seven colonies in total were selected for Symbiodiniaceae ITS2 metabarcoding.

Table 1.1. Sampling information and metadata. Specimens of the coral *Galaxea fascicularis* were collected from six different locations along the Nansei Islands, Japan. Locations marked with an asterisk were not used for joint distribution analysis due to missing host phenotype information.

ID	1	2	3	4	5*	6*
Location	Miyako, Yoshino	Iheya, northern tip	Tanega	Minami and Kita Daito	Okinawa, Zanpa	Iriomote, Haemida
Lat	24.74841	27.0927	30.82710	25.87795	26.43889	24.26833
Lon	125.44599	128.01216	131.03535	131.21427	127.71111	123.82972
Collection date	Jul. 20 2015	Jul. 29 2015	Sept. 14 2015	Nov. 11 2015	Nov. 16 2013	Aug. 24 2014
Depth [m]	6.7–19.8	9.3–12.6	6.7–11.4	14.8–23.9	~1 –2	~ 3 – 5
No. of samples	10	17	10	10	10	10
SST annual mean	25.9	24.6	22.9	25.6	25.6	26.1
SST mean col. month	29.4	27	28	25.9	26.3	28.4
in situ temp.	28	28	27	26	-	-
Host Genotype	L, S	L, S, L+	L, S	L, S	L, S	L, S
Colony photo	yes	yes	yes	yes	no	no

1.2.3. DNA sequencing and processing

Samples were deep-sequenced in the Symbiodiniaceae ITS2-region using the Illumina MiSeq platform. The primers IlluminaAmplicon-ITS-Dino-forward 5'-TCGTCGGCAGCG-TCAGATGTGTAT-AAGAGACAG-GTGAATTGCAGAACTCCGTG-3' and IlluminaAmplicon-its2rev2-reverse 5'-GTCTCGTGGGCT-CGGAGATGTGTA-TAAGAGACAG-CCTCCGCTTACT-TATATGCTT-3' (modified from Pochon *et al.* 2001) were used for amplification of the Symbiodiniaceae ITS2 region. 300x300 bp paired-end

sequencing was conducted by the Okinawa Institute of Science and Technology sequencing center on the Illumina MiSeq sequencing platform with v3 chemistry. The samples were sequenced in two sets, the first containing samples from Iriomote and Okinawa, and the second containing all other samples. The raw reads were quality filtered and trimmed with Trimmomatic software (Bolger et al. 2014) to have a minimal length of 80 bases, a minimal phred33 >15 over 4 subsequent bases and were then merged with their pairs using USEARCH (Edgar, 2013). A total of 10.9 M reads were gained, and after quality filtering and merging, 4.2 M sequences remained (average 56 k per sample). The samples from the first library were randomly subsampled to contain a comparable number of paired sequences as the samples from the second library (100 000 paired sequences per sample). Raw reads were submitted to the NCBI Sequence Read Archive (BioSample IDs SRR7528926 - 93).

1.2.4. Environment and host characteristics

Factors related to temperature and light intensity were chosen to characterize the environment, since these are well known to affect Symbiodiniaceae distribution (Baker, 2003). For each coral sample since 2015 (Table 1.1) precise water depth was recorded with a dive computer. Measured depths were corrected for tidal levels by subtracting the present tidal level from the dive computer reading. *In situ* temperature was measured and sea surface temperature (SST) was retrieved from the World Ocean Atlas 13 (Locarnini *et al.*, 2013) at the site-level. Annual mean SST was calculated from monthly values based upon the most recent available data (2005-2012, Fig. 1.1).

Genetic lineages of hosts were assessed based on mitochondrial data. There are at least three morphologically cryptic lineages ("L", "S", and "L+") within *Galaxea fascicularis* in the Nansei Islands, that differ in the length of a mitochondrial non-coding region (Watanabe *et al.*, 2005; Nakajima *et al.*, 2015; Nakajima *et al.*, 2016). Lineage identity was determined by fragment length analysis of this mitochondrial region following Nakajima *et al.* (2015). The host phenotype was characterized for samples with available photographs. Since the presence of Symbiodiniaceae reflects colony health, the degree of bleaching was recorded as 'healthy' if colonies showed no sign of bleaching, 'partially bleached' if individual polyps or colony margins were bleached, and 'bleached' if most of the colony was white, using a color card (Appendix 1: Fig. S1.1). Fluorescent green pigments produced by the host itself and the naturally lighter pigmentation in some colonies were disregarded in this assessment. To test a potential effect on skeleton growth, maximal polyp diameter was

measured for three to five centrally located polyps and averaged per colony using Fiji software (Schindelin *et al.*, 2012).

1.2.5. OTU delimitation and identification

A challenge for any microbial study is the delimitation of biologically meaningful operational taxonomic units (OTUs). Most commonly, sequences are grouped using heuristic clustering techniques according to predetermined percent identity radii; however, these clustering approaches are sometimes unable to detect low abundance diversity and the *a priori* setting of an identity radius can be arbitrary (Callahan *et al.*, 2017). For Symbiodiniaceae ITS2, a conservative identity threshold of 97% is often chosen so as to avoid splitting intragenomic variants (Arif *et al.*, 2014). Since this threshold may also lump ecologically distinct types (Sampayo *et al.*, 2007; LaJeunesse & Thornhill, 2011), higher percentage radii of 98–100% have also been applied (Kenkel & Bay, 2016; Smith *et al.*, 2017). We decided to use the Minimum Entropy Decomposition (MED) pipeline, as this approach requires no *a priori* similarity threshold and distinguishes OTUs based upon the highest resolution, applying the principle of entropy minimization (Eren *et al.*, 2015). This method is increasingly used in microbial studies, including those for Symbiodiniaceae (Smith *et al.*, 2017). We ran the MED pipeline with default parameters, setting the maximum number of informative positions for decomposing a node (OTU) to c=4, the threshold for defining zero entropy to m=0.0965 at any given nucleotide position, and the minimum substantive abundance of an OTU to M= N/10,000, N being the total number of reads. The pipeline removed 0.34 Million outlier sequences and determined that 99.11% (max. 3 nucleotide differences) was the optimal identity threshold to decompose the remaining N=3.86 Million sequences to OTUs constituting at least 843 sequences.

The resulting OTUs were checked for identity by searching the representative sequences against a Symbiodiniaceae ITS2-type database provided by Cunning *et al.* (2015) using nucleotide Blast. The same percentage sequence identity used for their delimitation by the MED was used (99.11%). One hundred eighty-two OTUs were mapped to a single best sequence in the database. Fourteen resulted in multiple best matches with equal e-values, for which the most abundant ITS2-type was assigned. The remaining 16 OTUs mapped to < 99.11% identity (96.2 – 98.9%, Table S1.1). All OTUs were referred to according the naming in (Cunning *et al.*, 2015) throughout the paper and respective accession numbers of the reference sequences are given in Table S1.1 of Appendix 1.

The taxonomic level of OTUs remains arbitrary and OTUs could be variants within the same genome, variants of the same species, or species with independent evolutionary histories. We decided to exploit the maximal resolution of our data using the MED pipeline and to interpret our results accordingly, but we also ran the analysis based on a heuristic clustering approach using a within-sample 97% clustering threshold, in order to evaluate our results. Filtered and merged ITS2-sequences were demultiplexed and cleaned for singletons and clustered with the USEARCH pipeline applying a 97% identity cut-off within each sample (Cunning *et al.*, 2017). OTUs were identified by blasting the representative sequence to the Symbiodiniaceae ITS2-database provided by Cunning *et al.* (2015). OTUs that were identified not to be Symbiodiniaceae or mapped to less than 97% identity to an existing reference sequence were removed. The OTU table was built by hand by listing the abundances of the same ITS2-type in columns for each sample in rows. The table was then filtered for outliers to contain only OTUs that were represented to a fraction of at least 0.001% of the total count over all samples.

1.2.6. Community analysis

The raw community matrix (OTUs × coral samples) was visualized as a heatmap using pheatmap package (Kolde, 2015) after standardization and log10-transforming non-zero counts of the matrix (Fig. 1.2). The matrix was then rarefied to represent relative abundances within samples. Two-dimensional non-metric multidimensional scaling was preformed based on Bray-Curtis community dissimilarities in the vegan package (Oksanen *et al.*, 2012) and boxplots were drawn to depict the most influential predictors (Fig. 1.3).

Overall community turnover was analyzed by fitting a generalized dissimilarity model (GDM) to Bray-Curtis community distances using the GDM package (Ferrier *et al.*, 2007). GDMs are extensions of regression based on distance matrices, but they allow for non-linear relationships between response and predictor variables (Ferrier *et al.*, 2007). Dissimilarity modeling was performed two times, once on the full sample set including the predictor variables mean SST, water depth, location, host lineage, and once on the subset of 47 samples that additionally included the predictors *in situ* temperature, host polyp size, and bleaching status. Sequencing depth (total count of raw fastq sequences per sample) was also included to control for a potential effect of sampling effort. The nominal factors 'host lineage' and 'location' were transformed to 0-1-coded Dummy variables. Significance and relative

importance of the variables were tested with 100 permutations (Table 1.2, Appendix 1: Fig. S1.2).

Distribution and co-occurrence patterns between individual Symbiodiniaceae OTUs were analyzed with a joint distribution model. Only the 47 samples having all metadata were used (Table 1.1) and OTUs that were not present in those were removed. A generalized linear latent variable model was applied to model residual variation not explained by the covariates and which may be interpreted as the influence of biotic interactions (Warton *et al.*, 2015). The latent variables are predictors introduced by the latent variable model based on correlations in abundance between taxa. Correlations in the latent variables imply shared character states of unmeasured predictors in the environment. As is common in ecological community data, the species abundances are not normally distributed but are over-dispersed with a high percentage of zero counts. In order to select the most appropriate modeling approach for the data, we first fitted two-dimensional, pure latent variable models assuming either a Poisson, a negative-binomial, or a zero-inflated Poisson distribution and compared their Akaike Information Criteria (AIC) following Niku *et al.* (2017). A negative binomial distribution resulted in the smallest AIC (75 713 vs. 1 476 784 for Poisson or 1 072 877 for zero-inflated Poisson) and was therefore chosen for subsequent analysis in the package 'Boral' (Hui, 2016). Boral fits models to distributions of individual OTUs using Bayesian Markov Chain Monte Carlo (MCMC) estimations. A pure latent variable model was first run again to verify the suitability of the chosen modeling approach by residual analysis (Fig. S1.3). Then the full model was run with the same covariates as for the GDM but replacing geographic distance with the PCA-transformed variable 'location' and adding two latent variables. Default priors for MCMC parameter estimations were used and parameter coefficients were visualized as trace plots (Fig. S1.4). Relative influence of covariates and latent variables were inferred by variation partitioning and illustrated using bar plots (Fig. 1.4a). Correlations between OTUs due to shared environmental responses and due to latent variables were inferred with a 95% probability cut-off (Figs. 1.4b, c). The same analysis was run for the community matrix resulting from OTUs delimited by 97% sequence identity (Fig. 1.5). All analyses were done in R version 3.4.0 (R Core Team, 2015).

1.3. Results

The MED pipeline distinguished 235 OTUs that mapped to 24 different Symbiodiniaceae ITS2-types (Fig. 1.2). The majority of OTUs (148) and 63% of all

sequences (total N=3.86 M) belonged either to C1, D1 or C21a (Fig. 1.2, Appendix 1: Table S1.1). The numerous C1-related types are mostly present at background levels and are a mix of well-known and rare types: C1b, C1c, C1h, and C1p have wide geographic distributions and are dominant in other coral taxa (Franklin *et al.*, 2012), while C1005, C1013, C1060, and C1085 have only been reported once in Japan (GenBank). Some types are both rare and previously unknown from Japan, such as C1148 from Western Australia, C1234 from the South China Sea, and C1002 from the Caribbean (Garren *et al.*, 2006), and some were found only as intragenomic variants of C1 (C1226, C1228, C1230) (Thornhill *et al.*, 2007).

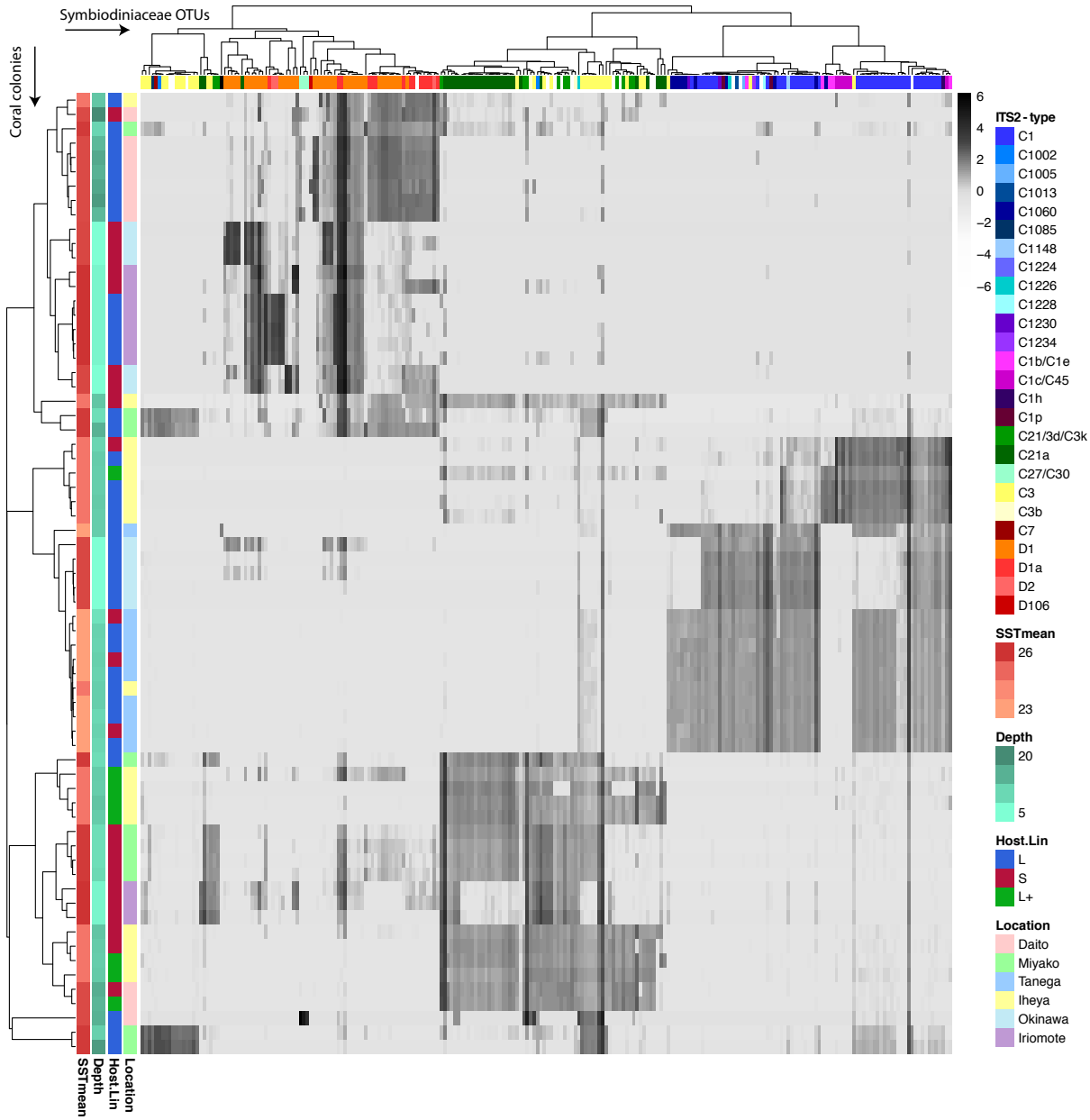

Figure 1.2. Heatmap illustrating abundances and co-occurrences of Symbiodiniaceae ITS2 types (columns) across *Galaxea fascicularis* colonies (rows). Symbiodiniaceae clustered into discrete communities that are characterized by the dominance of ITS2-types C1, D1, or C21a. Each community type associated with a different collection of background ITS2 types. 235 OTUs were defined by Minimum Entropy Decomposition across 67 coral samples. OTUs and communities were hierarchically clustered based on correlation and Bray-Curtis distance, respectively. OTU color indicates the closest matching ITS2-type (>99.11% ID, GenBank accession numbers in Appendix 1, Table S1.1, and communities are colored according to their source locations, annual mean SST, and depth. Uncolored OTUs represent previously unknown ITS2-types (Appendix 1: Table S1.1). Raw abundances were standardized across rows and log10-transformed for visualization of rare OTUs.

Symbiodiniaceae communities consistently clustered into three main community types, each characterized by the dominance of ITS2-types C1, C21a, or D1, except for three samples that were mostly inhabited by C3 or C27 (Figs. 1.2–3). The community types each associated with a different group of background ITS2-types and occurred at different frequencies among locations (Figs. 1.2–3). For example, C1-dominated communities were the most common community type in Tanega but were absent in Miyako, Iriomote and Daito, and D1-dominated communities were the most common in Daito and Iriomote, while being absent in Tanega. Within each community type there is some location-dependent variation, for example C1-OTUs varied between Iheya, Tanega, and Okinawa, and D1-OTUs varied between Daito, Iriomote, and Okinawa. D1-dominated communities were found both at the most shallow and deepest sampling sites (Fig. 1.3b). Host characteristics also co-varied with community type, in that larger polyps and less bleaching were associated with C1-dominated communities (Fig. 1.3a). Polyp diameters at least 2 mm larger on average were associated with C1-dominated communities (Fig. 1.3b).

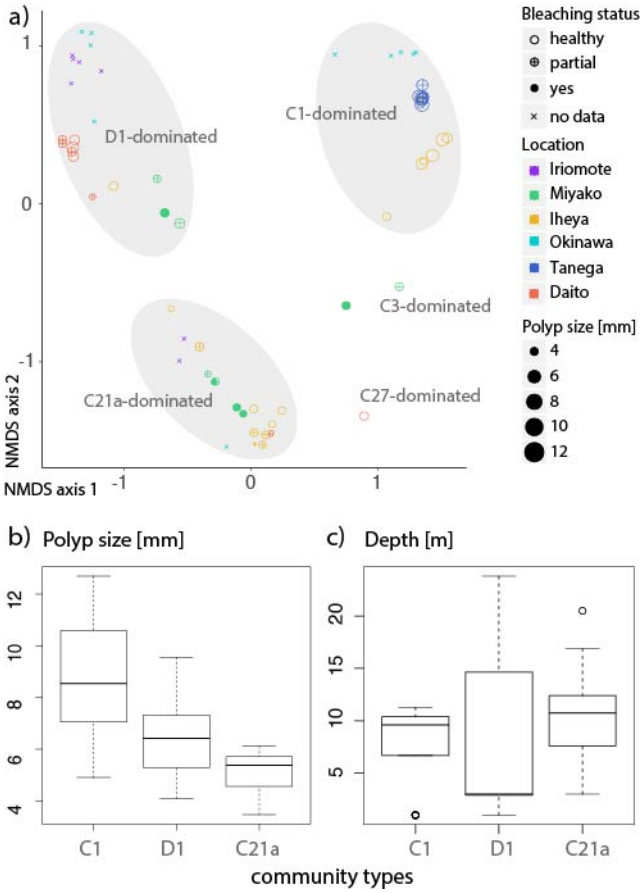

Figure 1.3. Variation between Symbiodiniaceae communities hosted by *G. fascicularis.* The NMDS (a, k=2, Stress1=0.087) is based on Bray-Curtis dissimilarity. The main community types vary across locations, in bleaching status and polyp size. C1-dominated communities are associated with the largest host polyps (b), and D1-dominated communities have the widest depth distribution (c). To depict polyp size (b), only 47 communities with available size information (Table 1.1) were used.

Accordingly, the generalized dissimilarity model over the first analysis identified polyp size as the most influential significant factor, followed by water depth, host lineage and sequencing depth, and further determined a minor effect of bleaching status on community turnover (Table 1.2, total explained deviance = 28.72%). The second analysis involving all specimens but only a part of the predictors identified host lineage as most important (total deviance explained = 11.61%). Temperature variables in both analyses were not significant and running the model with other SST parameters (annual minima, maxima, means of collection months, annual variation), did not change this result (results not shown).

Table 1.2. Relative importance and significance of environmental variables for Symbiodiniaceae community composition from generalized dissimilarity modeling. Once done for 47 samples with all metadata and once for all 67 samples with lacking host characteristics and *in situ* temperature.

Predictors	**47 samples** Relative importance	p	**67 samples** Relative importance	p
Bleaching status	0.89	0.00	NA	
Polyp size	12.2	0.00	NA	
Temp. in situ	1.69	0.30	NA	
SST mean	24.5	0.12	71.71	0.07
Depth	8.45	0.00	5.89	0.62
Sequ. depth	1.28	0.00	1.98	0.52
Host lineage (PC1+2)	6.76	0.00	18.59	0.00
Location (PC1 + PC2)	0.71	0.00	(dropped by GDM)	
Total deviance explained	28.72%		11.61%	
Model deviance	461.58	0.00	1172.65	0.03

The joint distribution model on MED-defined or 97% clustered OTUs revealed that the latent variables had a larger influence on the occurrence of an OTU (on average, 41% or 47%, respectively) than the predictors of the model (0%–14%,) (Fig. 1.4, 1.5; parameter coefficients in Fig. S1.4). The model predictors had similar influences on OTUs of the same ITS2-type, except for within types C3 and C21/3d/3k (Fig. 1.4a). The OTUs cluster into three arbitrary groups due to environmental and host similarity, one consisting of C3-strains, a second of C1-related types, and a third of C21-related types, C3 and clade D (Fig. 1.4b), but to three strongly correlated clusters due to residual variation characterized by types C1, C21a or D1 (Fig. 1.4c). The residual clusters show strong negative correlations with each other but less so between C21a and D1. The clusters aggregate similar genotypes, i.e. C1 with C1-related types, D1 with D1a and D2, and C21a with C21/3d/3k. The relative importance of the covariates and most of the co-occurrence patterns were largely consistent when using OTUs defined using a 97% identity cut-off (Fig. 1.5).

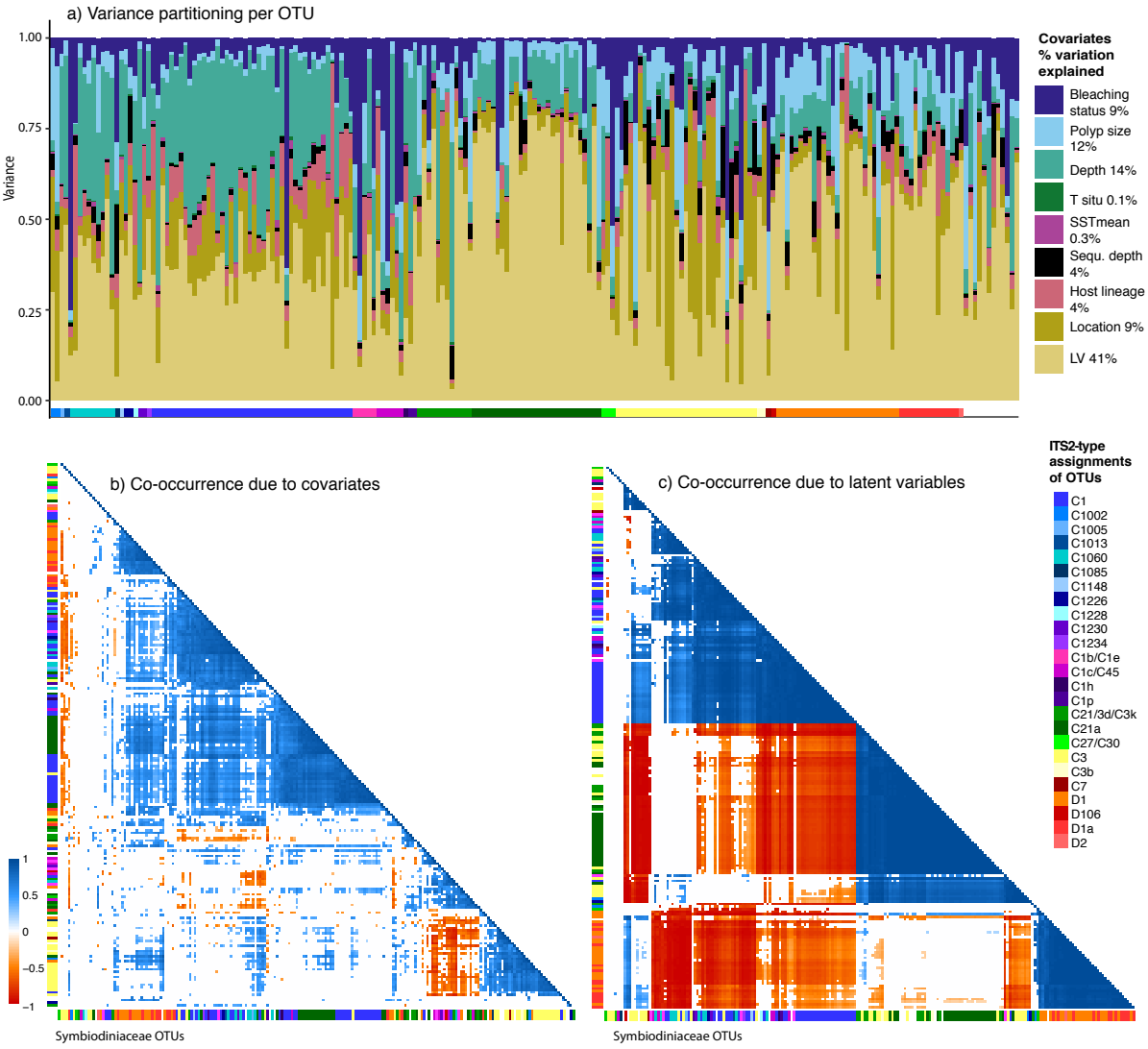

Figure 1.4. Joint distribution modeling of Symbiodiniaceae OTUs defined my Minimum Entropy Decomposition. The latent variables explain more of the OTUs occurrences in average than environmental and host covariates (a). While OTUs cluster arbitrarily due to the covariates of the model (b), three distinct clusters are formed due to the latent variables (c). OTUs are sorted by hierarchical clustering in the correlation matrices and are color-annotated by their ITS2-type assignments. Uncolored OTUs represent previously unknown ITS2-types (Appendix 1: Table S1.1).

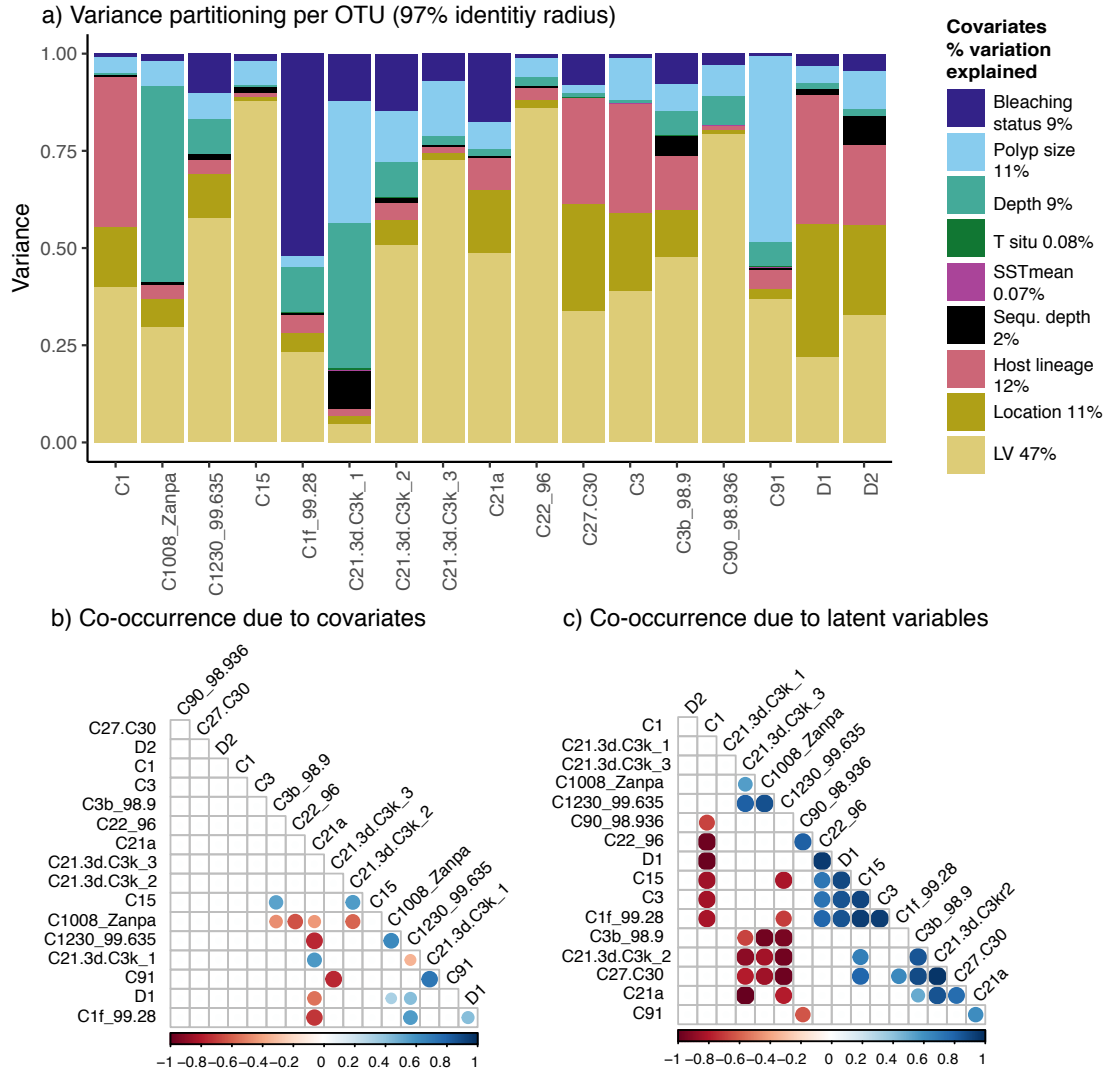

Figure 1.5. Joint distribution analysis of Symbiodiniaceae OTUs clustered to 97% identity using Boral. Variation partitioning (a) and co-occurrence patterns due to the predictors of the model (b) and due to latent variables (c). The clustering analysis resulted in 14 OTUs across all samples. The latent variables had the largest influence on the distribution of the OTUs, similar to in the main analysis, and co-occurrence between OTUs due to environmental and host factors was less pronounced than due to the latent variables (b, c). Strong negative interactions between C1 and D1 and C21a, and neutral relationships of C3 to almost all other types could be confirmed.

1.4. Discussion

Our results illuminate structure and assembly of endosymbiotic Symbiodiniaceae on the example of the coral *Galaxea fascicularis*. Most ITS2-types previously reported for *Galaxea* were confirmed, except for C3u from the Indian Ocean (Franklin *et al.*, 2012) and C2r, D17, and C161 from Hainan Island (Zhou *et al.*, 2017) (Fig. 1.1). We tested for the effects of environmental variation and host characteristics on community composition, using

generalized dissimilarity modeling to detect influences on community turnover. Further we used latent variable modeling to infer residual correlations among sets of OTUs (or variants), a possible signature of biotic interactions. Overall, we found detectable effects of the environment and host characteristics, but that these were rather modest compared to the latent variables (Fig. 1.4a, Fig. 1.5). This latent structure indicated three main community types hosted by the coral *Galaxea fascicularis*, characterized by the dominance of the ITS2-types C1, C21a, or D1, each of which was associated with a different group of background types that varied among locations (Fig. 1.2). We discuss each of these factors in turn.

1.4.1. Environmental influence

The most important environmental factor for both community turnover (Table 1.2) and distribution of individual OTUs (Fig. 1.4a) was water depth, known to cause zonation of Symbiodiniaceae types in many corals, particularly in broadcast spawning species (Bongaerts *et al.*, 2015). On the community level, we found D1-dominated communities to have the widest depth range, while C1- and C21a-dominated communities may be more common in intermediate to shallow depths (Fig. 3c). Accordingly, we find the occurrence of D1-OTUs to be less influenced by depth than the other ITS-types (Figs. 1.4a, Fig. 1.5). This was consistent with the previously described higher tolerance of clade D Symbiodiniaceae to deeper depths and to margins of the ideal coral habitat range in general (Toller *et al.*, 2001; Baker, 2003). There are several environmental factors that were not measured here but are correlated to water depth that may physiologically explain the found pattern in this study. Light levels, for example, decrease rapidly with depth and are known to relate to differential growth optima between Symbiodiniaceae types (Klueter *et al.*, 2017). Likewise, temperature and nutrient concentrations may also change with depth (Parsons *et al.*, 2013). Clade D is known to tolerate higher nutrient and temperature ranges than other clades (Cooper *et al.*, 2011), which could explain the higher abundance of type D at deeper, as well as shallower habitats of the reef (Baker, 2003). However, the found effect of depth could be influenced by the sampling design, as the sampling locations varied considerably in their depth ranges (Table 1.1). The coral reefs around the volcanic Daito Islands are generally deeper than in the other sites and may have influenced this result disproportionately in the generalized dissimilarity model (Table 1.2).

The main Symbiodiniaceae community types varied in frequency among locations and there was clear location-dependent variation within these main types that would not have been detected by a coarser OTU clustering approach, since locations sometimes differ in only

very similar OTUs of the same ITS2-type (Fig. 1.2). This indicates that Symbiodiniaceae may not vary according to locations on the scale of whole communities, and only on finer resolution may there be a spatially driven differentiation within ITS2-types, as for example in type C3, where some variants almost exclusively occurred in certain samples from Miyako, in which they were also dominant (Fig. 1.2). Accordingly, the factor location had a relatively constant influence on the occurrence of all OTUs (Fig. 1.4a) and had a minor influence on overall community turnover in the first GDM. Spatial differentiation in Symbiodiniaceae has been shown in population genetic investigations with microsatellite markers (Howells *et al.*, 2013; Baums *et al.*, 2014). The MED approach for decomposing ITS2-types could perhaps be used as an alternative to infer highly resolved differentiation patterns in Symbiodiniaceae. On a larger scale, however, it is evident that geographic location has an influence on *Galaxeas*'s Symbiodiniaceae composition, as entirely different ITS2-types (D17 and C2r) were found for example in Hainan (Zhou *et al.*, 2017).

The insignificance of temperature, both WOA-SST and *in situ* was unexpected, since temperature has long been established as one of the most influential factors for the distribution of Symbiodiniaceae taxa (Baker, 2003). This was found in numerous biogeographic field studies on the clade level regarding clade C versus clade D, as well as on the subclade level (Noda *et al.*, 2017) and in numerous laboratory experiments (Rowan, 2004; Sampayo *et al.*, 2008), and including in our study taxon (Chen *et al.*, 2005; Tong *et al.*, 2017; Zhou *et al.*, 2017). In contrast, we found clade D-dominated communities at almost every site, and therefore seemingly unlinked to mean temperatures of the sampling site. This indicates that fine-scale differences in heat distribution within the reef could be responsible for Symbiodiniaceae composition rather than latitudinal temperature gradients or average temperatures measured at a sampling site. Microhabitat differences related to temperature, water movement (Monismith, 2007), substrate (Cunning *et al.*, 2015) or syntopic fauna (Mihaljevic, 2012) influence the distribution of free-living Symbiodiniaceae and *in hospite* and should be monitored carefully in future studies. Another explanation may be that on-site temperature measurements at the time of collection are not representative for the temperature regimes that have caused the presented community patterns. *In-situ* temperature not only as a snapshot in time during collection but time histories may have revealed a better prediction for the distribution of Symbiodiniaceae types. Nevertheless, temperature may not be as influential for Symbiodiniaceae community composition in *Galaxea* as in other corals. *Galaxea* was shown to be relatively resistant to elevated temperatures (Marshall & Baird,

2000) and a recent study has found no seasonal variation in *Galaxea*-hosted Symbiodiniaceae communities in Hong Kong, where SST changes from 14ºC to 31ºC between winter and summer (Cai *et al.*, 2018). The relationship between temperature and Symbiodiniaceae composition may not be trivial in *Galaxea* and more detailed field measurements characterizing microhabitat variation are needed in order to understand this relationship under natural conditions.

1.4.2. Relation to host characteristics

Host characteristics had in average a larger influence on Symbiodiniaceae community turnover (Table 1.2) and the distributions of individual types (Fig. 1.4a, 1.5a) than the environment. C1-dominated communities were associated with the largest polyp sizes, healthiest colonies, and lineage 'L' of *Galaxea fascicularis*. C1 has been linked to faster skeletal growth (Jones & Berkelmans, 2010), higher efficiency in carbon (Little *et al.*, 2004) and nitrogen transfer rates to the host than clade D under normal temperature conditions (Baker *et al.*, 2013). In our study, these differences also existed within clades, i.e. between C1 and C21a. In return for less efficiency, C21a and D1 could have higher thermotolerance levels (Swain *et al.*, 2017) enabling them to associate with *Galaxea* colonies under higher bleaching levels (Fig. 1.2). Not much is known about how skeletal growth rate could affect polyp size in colonies directly, but an early study in *Acropora* branches identified by far the highest calcification rates in the terminal enlarged polyps of a branch (Goreau & Goreau, 1959). However, larger polyps correlated negatively with growth rate in the solitary coral *Balanophyllia* (Goffredo *et al.*, 2008). Computer tomographic analyses of the skeleton are needed to determine growth rate in *Galaxea fascicularis.*

Host lineage had a large influence on community turnover, particularly if not corrected for polyp size in the second analysis involving all specimens (Table 1.2), implying that generalist species may not be as 'general' in their symbiotic associations. Across our study sites, most C21a-dominated communities associated with lineages 'S' and 'L+', and C1 or D1-dominated communities were more associated with lineage 'L' (Fig. 1.3a). Differences in Symbiodiniaceae composition between cryptic species have been shown in other corals (Prada *et al.*, 2014; Warner *et al.*, 2015), emphasizing the importance of correct species delimitations in both symbiotic partners (Parkinson & Baums, 2014). Despite some indications for functional differentiation between the host lineages (Watanabe *et al.*, 2005), this matter is still unresolved and yet undetected variation in functional traits in the host may be related to differential symbiont or host selection. However, in this study we also observe

larger polyp sizes and healthier colonies to be associated with C1-dominated communities and correlating with host lineage 'L' (Fig. 1.3a). The causal relationships between host lineage, polyp size, colony health and Symbiodiniaceae composition remain to be resolved in future studies.

Our findings are based on the assumption that there is little variation in community composition within the host colony. Within colony-variation has been found in other coral species (van Oppen *et al.*, 2001b; Stat *et al.*, 2011) and could potentially confound our results regarding the role of explanatory predictors for Symbiodiniaceae community composition. However, although within colony-variation here was not tested in particular, there is evidence that the distribution of Symbiodiniaceae types in *Galaxea* could be rather uniform. The *Galaxea fascicularis* colonies sampled are usually planar with little chance for self-shading and therefore usually experience similar light levels across the colony. Further, two clonal colonies (PW112 and PW117) probably emerged by fragmentation (determined by RAD-seq), also hosted the same Symbiodiniaceae community, suggesting that once established, communities keep constant. The relatively high influence of total abundance on the distribution of OTUs indicate sensitivity to sequencing depth for the detection of rare OTUs. It was particularly important for some OTUs of C3 that occurred at background levels in strong correlation with C21a but also with C1 and C1060.

1.4.3. Co-occurrence between Symbiodiniaceae types

The communities studied assemble into three regular groups (Fig. 1.2), consistent with regularity of Symbiodiniaceae communities documented across a phylogenetically diverse set of coral hosts (Ziegler *et al.*, 2018). We find this to be true also on the colony-level within the same host species, and that this structure is only partly related to underlying variation in the environment or the host (Table 1.2, Figs. 1.4b, 1.5b). Instead, in both OTU clustering approaches community composition was most strongly determined by the latent variables (Figs. 1.4c, 1.5c), implying that other undetected predictors may be responsible for the co-occurrences of Symbiodiniaceae taxa. The undetected predictors could relate to microhabitat differences as mentioned above, other host characteristics such as differences in the life history, or possibly to metabolic or behavioral interactions between Symbiodiniaceae taxa them self, depending on the taxonomic level of the OTUs considered.

On the level of ITS2-types, which are traditionally regarded as species (LaJeunesse *et al.*, 2003; LaJeunesse, 2005; LaJeunesse *et al.*, 2014; Parkinson & Coffroth, 2015), co-

variation perhaps relates to synergistic or antagonistic species interactions. For example, the dominant ITS2-types C1, C21a and D1 tend to exclude each other in an endosymbiotic community even after controlling for environmental factors like temperature (Fig. 1.4c), that are known to influence the competitive success between for example C1 and D1 (Baker *et al.*, 2013). However, C21a may be less exclusive and co-exist with a more diverse set of ITS2-types, as indicated by the neutral correlations to clade D types and some of the C1-related types, and a positive correlation to C3 (Fig. 1.4c). Similarly, a recent study by Zhou *et al.* (2017) found C21a to occur with more different types to higher percentages than the other dominant lineages, suggesting that C21a may be generally more permissive for a more diverse community. The higher association of C21a-dominated communities with partially or fully bleached corals in this study (Fig. 1.3a) may further indicate that a more diverse community is able to accommodate stressful conditions better, as observed in other systems (Ives & Carpenter, 2007) and recently demonstrated numerically for Symbiodiniaceae (Ziegler *et al.*, 2018). A similar conclusion may be made for the two C3-dominated communities in our study (Fig. 1.2, 1.3a), however these were much less common and may therefore not represent a stable community state. To test a potentially higher tolerance of C21 and C3-dominated communities during stress, future research may conduct controlled bleaching experiments with *Galaxea* colonies hosting predominantly C21a vs. D1 or C1 or C3. Generally, more frequent co-occurrence was found between phylogenetically more similar ITS2-types, for example C21a with C21/3d/3k, D1 with D1a and D2, and C1 with other C1-related types, which may indicate a form of positive kin discrimination (Hamilton, 1964). Recognition of relatives is thought to be important in microbes, as many metabolic processes occur extracellularly and could benefit from co-occurrence of the same or similar species (Strassmann *et al.*, 2011). Little is known about co-occurrence patterns in Symbiodiniaceae to evaluate such a scenario and experimental manipulations of laboratory cultures are needed to advance this field. Statistical studies like the present could be improved by integrating functional species traits that interact with the physical environment evaluate the probable effects of such potential interactions more holistically (McGill *et al.*, 2006).

On the level of the numerous genetically very closely related OTUs the strong latent correlations may be the result of being intragenomic variants within the same genome. This could particularly be the case for OTUs of the same ITS2-type, as within C1, C21a, and D1. However, some OTUs of differing ITS2-types also correlate almost perfectly with one

another, for example C3 and C21a. C21 (and C21a) are derived states from the ancestral sequence C3 (Correa & Baker, 2009) and are known to occur in the same ribosomal repeat array (LaJeunesse *et al.*, 2004), which could explain the strong correlation between the two in our study. On the other hand, OTUs of the same ITS2 type have varying distributions across the communities, such as in C1 and C3 (Figs. 1.2, 1.4c). This and the finding that variants within certain ITS2-types vary in their ecological characterization underscores the challenges involved in using ITS2 as a descriptor of Symbiodiniaceae diversity, sometimes over-splitting intragenomic variants and sometimes over-aggregating ecologically distinct taxa (LaJeunesse & Thornhill, 2011; Reimer *et al.*, 2017). The necessity of an additional genetic marker such as the *psbA* region (as in LaJeunesse & Thornhill, 2011; Smith *et al.*, 2017) seems inevitable for clearly distinguishing intragenomic variation from actual species diversity.

Another approach to distinguish clusters of intragenomic variants from interspecific co-occurrences could be to use latent correlations such as inferred from joint species distribution models, similar to the metahaplotype approach presented by Smith (Smith *et al.*, 2017) who used clusters of co-associating ITS2 sequences to detect evolutionary significant units. Using the latent variables perfect correlation corrected for the environment (including host environment) could distinguish intragenomic variants from independent entities even between highly similar OTUs, as the obligatory co-existence in the same genome should result in perfect correlations, while weaker or inconsistent correlations between such clusters could indicate interspecific co-occurrence in a community. For example, there are two separate subclusters within the group of C1 and C1-related ITS2-types, one mainly consisting of C1, and another consisting of C1 and others like C1060 (Fig. 1.4c). These two subclusters may represent two distinct Symbiodiniaceae taxa that would have been classified as the same C1 type using a lower identity threshold. Several such differential correlation patterns between smaller latent clusters can be distinguished in this plot, which may each represent a different Symbiodiniaceae species. Correlational approaches, together with additional genetic markers, may be a promising strategy for understanding the nature of Symbiodiniaceae ITS2 diversity and for distinguishing biologically meaningful Symbiodiniaceae entities on lower taxonomic levels in the future.

Regardless of the difficulties for the correct delimitation of lower level taxa, we believe that co-occurrence patterns at least between ITS2-types that differ more than the maximally conservative 97% identity threshold (Arif *et al.*, 2014), and are consistent with our

analysis with OTUs clustered at this threshold (Fig. 1.5), could be the result of interspecific biotic interactions. This includes the co-occurrence patterns between C1, C21a, C3, and D1.

Chapter 2: Genetic divergence and connectivity patterns of a highly isolated coral population in the Ogasawara Islands

2.1. Introduction

Spatial barriers or isolation are thought to be the main cause of diversification and speciation in the evolutionary history on our planet (Coyne & Orr, 2004). Oceanic islands have markedly influenced our understanding of evolution (Darwin, 1859) as they represent naturally isolated systems to observe ongoing biodiversity processes related to geographic isolation (Kadmon & Pulliam, 1993). While the majority of island biogeography studies have focused on terrestrial systems, fewer studies exist for the marine world. Differentiation and speciation in the sea is generally known to be slower due to high dispersal capabilities in a pelagic larval stage, and effects of geographic isolation may be much less pronounced than on land (Palumbi, 1994). The oceanic Ogasawara Islands in southern Japan are an interesting example to study marine geographic divergence, as they are highly isolated and lack strong ocean currents that directly connect them to larger biomes in similar climates. Because of their high level of terrestrial endemism, they are referred to as the 'Galapagos of the Orient' and became a UNESCO World Heritage Site in 2011 (Kyodo, 2011). However, the marine diversity is relatively underexplored, and it is not clear if the marine ecosystems are as differentiated from surrounding regions. In this study, we analyzed genetic differentiation in a marine pelagic disperser on the Ogasawara Islands to surrounding potential source populations in Japan and the Mariana Islands using the coral species *Galaxea fascicularis* L.

The Ogasawara Islands, also known as the Bonin Islands, are an ancient volcanic island arch that first emerged approximately 40 Ma (Neall & Trewick, 2008). The sea surface temperatures and nutrient levels are equivalent to other subtropical regions, including the Ryukyu and the Daito islands, with sea surface temperatures (SST) ranging from 19 to 28 ºC (Inaba, 2004a). The oldest fossil coral atolls found on Ogasawara indicate that there has been marine life since 25 Ma (Yoshiwara, 1902). This distinguishes them from the much younger Daito and Ryukyu Islands in southwestern Japan, where the oldest fossils were dated to only 5 Ma and 3.5 Ma, respectively (PBDB, 2018). Due to their high isolation, fragmentation, and diverse habitat range, the Ogasawara Islands have facilitated adaptive radiations in many terrestrial organisms (Ito, 1998; Chiba, 1999). The terrestrial flora and fauna are suspected to largely originate from South East Asia, but Micronesian and Japanese mainland sources are also known (Ito, 1998). The marine fauna is relatively underrepresented in the literature and

primarily consists of taxonomic reports in fish, zoanthids, dinoflagellate algae, and gastropods (Shimada, 2002; Nakano *et al.*, 2008; Reimer *et al.*, 2010; Shih *et al.*, 2013; Reimer *et al.*, 2014). Coral communities are known to be less diverse and different than the climatically similar Ryukyu Islands located approximately 1200 km to the west (Inaba, 2004a). There are only 200 scleractinian species recorded in the whole Izu-Ogasawara archipelago as opposed to over 400 in the Ryukyu Islands (Veron, 1992; Inaba, 2004b), and unlike similar habitats in the Pacific there are only few occurrences of *Acropora* in Ogasawara (Inaba, 2004a). The Ogasawara Islands are therefore regarded to be their own ecoregion distinct from other Japanese regions as well as from the Mariana Islands (Veron *et al.*, 2015), indicating a high degree of isolation in corals despite their high dispersal capabilities. However, only little is known about the potential origins of the marine fauna in Ogasawara, and they have never been investigated for corals.

Several routes for the marine colonization of Ogasawara have been proposed similar to those for the terrestrial organisms. There are two main potential sources, the Izu Islands and the Mariana Islands, which lie north or south of the Ogasawara Islands, respectively. The route over the Izu Islands connects Ogasawara to the temperate Japanese main islands and subtropical Ryukyu Islands ('Izu route'), while the route over the Mariana Islands connects Ogasawara to tropical Guam and Micronesia ('Mariana route'). For fish, species composition seems to be more similar to the one in the Mariana Islands than in the Izu Islands (Senou, 2004) and a phylogeographic study in groupers revealed a distinct lineage from Ogasawara only rarely found in the rest of Japan (Kuriiwa *et al.*, 2014). Gastropod lineages in Ogasawara were also highly diverged from other Japanese regions, but both the Mariana and Izu routes of colonization were suggested (Yamazaki *et al.*, 2017). Both routes contain large gaps without suitable shallow water habitats. Along the Izu route the largest gap spans 330 km and mostly lies in temperate climates, making this path less likely for tropical species. However, the extensions of the Kuroshio current may enhance this connection in the eastward direction, as proposed for limpets (Nakano *et al.*, 2008) and zoanthids (Reimer *et al.*, 2011). The Kuroshio Current brings tropical waters from South East Asia along the Ryukyu Islands up to Shikoku and beyond, causing the occurrence of subtropical fauna at exceptionally high latitudes (Yamano *et al.*, 2001; Iwase, 2004; Nomura, 2004). Although these sites are sparsely distributed along the Japanese main islands, they could serve as stepping-stones for occasional dispersal from the Ryukyu to the Ogasawara Islands. The Mariana route lies in tropical waters but contains gaps of up to 500 km at present. These gaps

may have been even larger in the past since the Mariana Islands only began to emerge out of the ocean in the Pliocene (Tracey *et al.*, 1964; Kayanne *et al.*, 1993), or even as recent as in the Holocene in the case of the Northern Mariana Islands (Paulay, 2003). Both routes seem challenging even for species with high dispersal capabilities.

A third potential route has been suggested over the Daito islands ('Daito Route') based on studies in reef fish (Shimada, 2002; Senou *et al.*, 2003; Yoshigou, 2004; Matsuura & Senou, 2012), for example by using the Kuroshio Countercurrent for the occasional transportation from Ogasawara to the Ryukyu Islands (Kuriiwa *et al.*, 2014). Apart from the Daito Islands, there are only two other little islands located in between the Ogasawara and Ryukyu Islands, the Oki-Daito and Okinotori Islands (Fig. 2.1). Although distances between them are large and populations potentially small (island areas $< 7km^2$), these islands lie in subtropical latitudes and are surrounded by a well-developed coral reef (Kayanne *et al.*, 2012), making this path a valid alternative route of migration between the Ryukyu and Ogasawara Islands. However, previous observations have not been tested molecularly or did not include collections from the Daito Islands (Kuriiwa *et al.*, 2014). By sampling coral populations from all of the three island groups, we aimed at filling this gap and to resolve the potential role of the Daito Islands as a stepping-stone for a migratory connection between the Ogasawara and the Ryukyu Islands. We further compared the extent of this migration to the one between Ogasawara and Guam in order to evaluate the probability of the Ogasawaran marine colonization *via* the Mariana route.

Migration patterns and divergence histories may be analyzed from even a small number of samples if genetic data is abundant, such as those obtained from restriction site-associated DNA (RAD) sequencing (Davey & Blaxter, 2010). Demographic modeling approaches designed for large population genomic datasets are able to disentangle the effects of divergence time and migration rates for differentiation, and may therefore reveal a detailed and comprehensive picture of the shared divergence history between populations (Sousa & Hey, 2013). Moreover, they are potentially able to reveal processes further back in time than migration analysis focusing on recent levels of gene flow (Wilson & Rannala, 2003). Based on the joint allele frequency spectrum it is possible to test several alternative models of divergence, for example differing by presence or absence of migration, their directionality and temporal variability. In order to investigate the colonization history of Ogasawara, we therefore also analyzed the joint demographic histories between the populations in

Ogasawara, Daito, and Ryukyu, and between Ogasawara, Guam, and Ryukyu in addition to population summary statistics and migration analysis.

For marine pelagic dispersers, molecular dispersal assessments may be complemented with biophysical dispersal modeling. Contemporary migration pathways of marine organisms with a pelagic larval phase may be predicted based on ocean current models, since propagules disperse by passive drift on the water surface (Cowen *et al.*, 2006; Mitarai *et al.*, 2009; Kool *et al.*, 2011; Treml *et al.*, 2015). Using dispersal modeling, it is also possible to account for potential influences of genetically not-sampled locations in a dispersal network. Dispersal probabilities inferred by Lagrangian particle advection simulations were shown to correlate with genetic differentiation in many marine organisms (Selkoe *et al.*, 2010; White *et al.*, 2010; Crandall *et al.*, 2012; Raynal *et al.*, 2014), including corals (Foster *et al.*, 2012; Davies *et al.*, 2015; van der Ven *et al.*, 2015). Pelagic larvae potentially disperse 100s of km in only a few days, which generally results in well-connected populations with little genetic differentiation (Palumbi, 1994). The pelagic larvae reach competency for settlement after a few days but can last up to several months in the water column (Fadlallah, 1983; Babcock & Heyward, 1986). The majority of pelagic larvae settles within the same or neighboring habitat shortly after reaching competency (Cowen *et al.*, 2006), and it is the occasional long distance dispersal (LDD) of exceptionally long-living larvae that create smoothing effects between populations preventing divergence (Shanks, 2009). Using Regional Ocean Modeling System (ROMS; Shchepetkin & McWilliams, 2005) and Lagrangian particle advection simulations, we evaluated the probability of such LDD events over the three discussed routes of migration, including along the Izu Route, along the Mariana Route, and over the Daito Islands. We estimated dispersal for corals in general using a maximal PLD of 60 days (Markey *et al.*, 2016), and evaluated whether the hypothetical dispersal pathways as predicted by ocean currents match our genetic analysis.

In the this study, we RAD-sequenced 108 individuals of the coral *Galaxea fascicularis* type L (sensu Nakajima *et al.*, 2016) and used migration analysis and demographic modeling to answer whether the Daito islands could be a stepping stone between Ogasawara and Ryukyu, and whether the Ogasawara Islands are genetically more connected to Guam or the Ryukyu Islands. In addition, we implemented an oceanographic dispersal model to investigate patterns of contemporary dispersal. Based on genetic and oceanographic data, we discuss the potential of the alternative routes of colonization to the Ogasawara islands. We used *Galaxea fascicularis* as a model, since it is a typical broadcast

spawning species releasing gametes in large abundance, and is common throughout the Ryukyu Islands and one of the dominant species in the Ogasawara Islands (Inaba, 2004b). By the assessment of dispersal patterns between these island systems, we also shed light on the spatial limits of connectivity for a broadcast spawning coral, which may have implications for understanding spatiotemporal scales of peripatric divergence in the evolution of corals in general.

2.2. Materials and Methods

2.2.1. Sampling

Coral colonies from the taxon *Galaxea fascicularis* were sampled around five islands along a latitudinal gradient in the Ryukyu Islands, the Daito Islands, and two of the Ogasawara Islands (Fig. 2.1, Table 2.1). In addition, five individuals from Guam were included as outgroup specimens. In order to capture the genetic pool of an island and to reduce the chance of clonality, several sites per island were sampled and lumped for population statistics. Collections were done between 2014 and 2016 by intertidal walks in Zanpa or SCUBA (all other locations, Table 2.1; Appendix 3). The samples were first screened for their mitochondrial types "L", "S", or "L+" by fragment length analysis, as these fragment lengths correlate to lineage identity in this taxon (Nakajima *et al.*, 2016). 174 samples were finally selected for RAD sequencing.

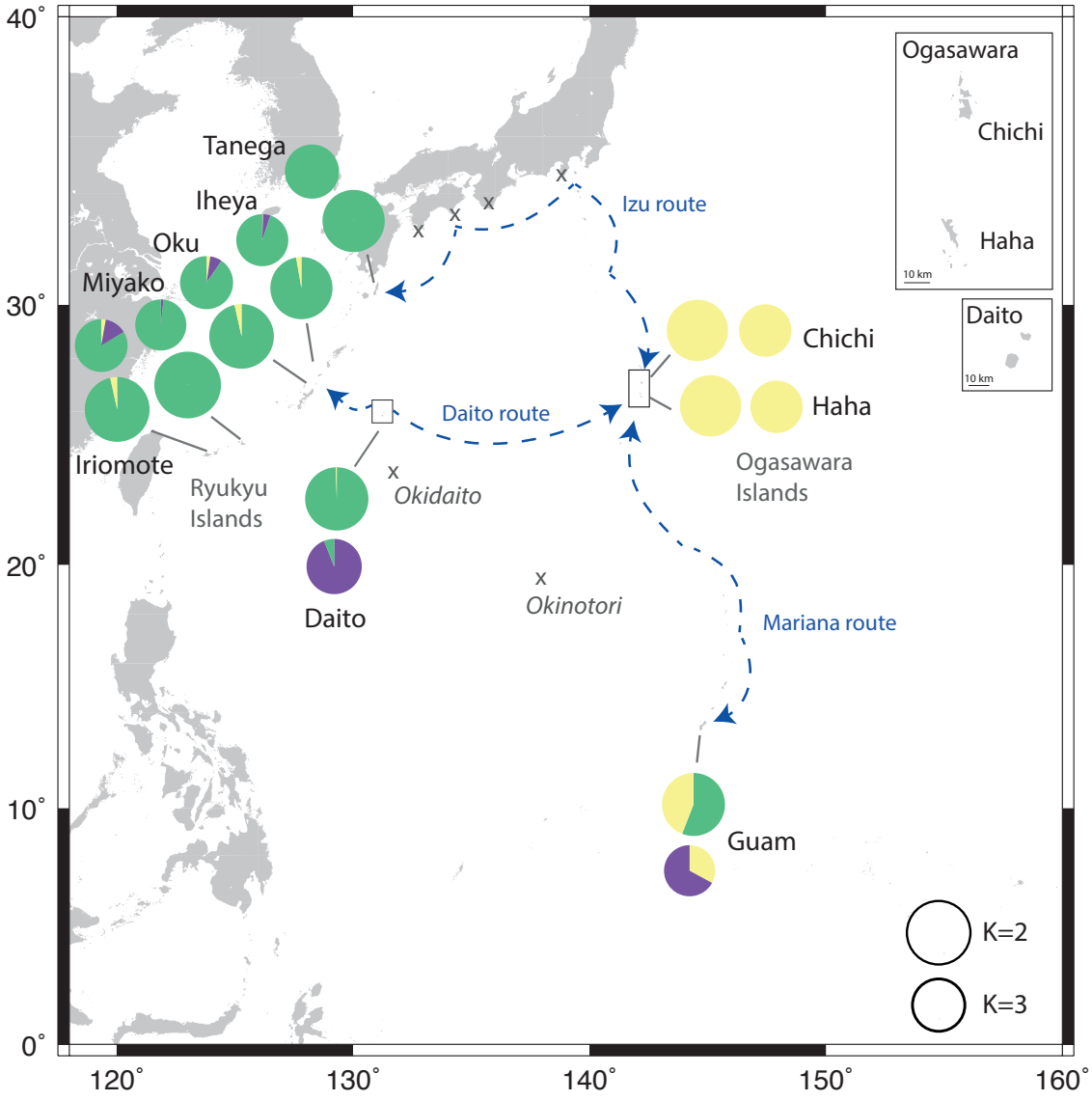

Figure 2.1. Geographic map showing sampling locations and potential migration routes to the Ogasawara Islands. Crosses (x) mark unsampled but potentially important stepping stone islands in the region. Admixture probabilities are summarized per island and are given for k=2 and k=3.

Table 2.1. Sampling sites per island, number of individuals and genetic lineage identity within *Galaxea fascicularis* "L", "S", "L+" *sensu* (Nakajima et al. 2016). The Total represents successfully sequenced individuals of lineage L per island that were used for population genetic analysis, after excluding clones and samples with ambiguous lineage identities.

Island	Site	NS	EW	Individuals sequenced	Total used for analysis
Iriomote	Haemida	24.268333	123.829722	9L 5S	4 L
Miyako	Ikema	24.93388	125.230555	10L 5S 1L+	18 L
	Yoshino	24.74841	125.44599	8L 5S	
Okinawa	Oku	26.84922	128.28717	7L 6S	7 L
Ihyea	North cape	27.0927	128.01216	12L 4S 8L+	7 L
Tanega	Tanega N	30.827102	131.03535	17L 12S	17 L
Daito	Kitadaito	25.95752	131.322	13L	21 L
	Minamidaito W	25.87795	131.21427	15L 1L+	
	Minamidaito S	25.81694	131.22034	1S	
Chichi	Chichi W	27.102365	142.21669	5L	15 L
	Anijima	27.111714	142.199749	4L	
	Nihoniwa	27.052554	142.171022	1L	
	Chichi SE	27.056147	142.228223	6L	
Haha	Haha N port	26.701905	142.140603	2L	13 L
	Haha E port	26.693478	142.151836	2L	
	Haha vlg. outer	26.635203	142.155223	5L	
	Haha vlg. beach	26.636437	142.157501	4L	
Guam	Agat Cementary	13.3900	144.6489	2L 1S	3 L
	Meriza Pier	13.2682	144.6639	1L 1S	

2.2.2. RAD sequencing and reference-based assembly

Quantity and extent of degradation of the genomic DNA was checked by Qubit and gel electrophoresis. Library preparation was done as described in (Tin *et al.*, 2014), involving a single digestion by the restriction enzyme EcoR1. This approach is designed for low quantities of degraded DNA and may be suited for marine invertebrate DNA, where DNA yield and quality are often low. This RAD protocol produces short fragments of 35-50 bp and uses as little as 20 ng of genomic DNA per sample as starting material. Sequencing was completed with Illumina HiSeq in three separate lanes containing each 90 samples. One of the lanes that included samples from Chichi, Haha, and some from Daito, were sequenced twice due to quality issues in the first run, which nevertheless resulted in more horizontal coverage in those samples than in the others.

Demultiplexed raw RAD reads were processed using dDocent software (Schmidt-Roach *et al.*, 2014), which combines quality filtering, mapping, and SNP calling in a single pipeline. Quality filtering is done with Trimmomatic (Bolger *et al.*, 2014), applying a quality score >20 to trim read ends and an average quality score >10 to remove bases in a sliding window of 5bp. Illumina adapters were removed at the same time. The cleaned reads were mapped against a *Galaxea* reference database with the MEM algorithm of the Burrows-Wheeler Aligner (Li & Durbin, 2009) and using dDocent default parameters (match value=1, mismatch value=3, gap open penalty =5). The *Galaxea* reference database included an unassembled *Galaxea fascicularis* genome provided by the Reef Future Genomics consortium (Voolstra *et al.*, 2015; Liew *et al.*, 2016), shotgun sequences previously produced for the development of microsatellite markers (Nakajima *et al.*, 2015), and a *Galaxea* mitochondrial genome (Niu *et al.*, 2016). Lastly, the pipeline used FreeBayes (Garrison & Marth, 2012) to call SNPs, giving an unfiltered VCF (variant calling format) file as output.

2.2.3. Individual and SNP filtering

The total SNP output file was filtered in multiple rounds. First, initial SNP quality filtering was conducted, so that average read depth was > 15 reads, quality score was >30, and minor allele count >3. After initial filtering, individuals with a high percentage of missing data (> 90% missing data) were removed (3 individuals). Second, SNPs were filtered to be present in at least 50% of all individuals to identify genetic lineages and clones (77'586 SNPs). Genetic lineages were identified by principal component analysis in R based on biallelic sites and separated by their factor loadings (Appendix 2: Fig. S2.1). Lineage L contained most individuals (123) from all locations (Table 2.1) and therefore was chosen for further analysis. Based on the same biallelic sites, potential clones were detected by pairwise correlations (13), where two individuals were deemed potential clones if their correlation coefficient was above a threshold of r >0.56 (Appendix 2: Fig. S2.2). This threshold was established based on previously known clone pairs from Iriomote within this data set.

Since we were interested in neutral differentiation, a further filtering step was conducted to identify F_{ST} -outlier sites that are under potential selection. We used BayeScan v.2.1 software (Foll & Gaggiotti, 2008), for which the input file was created using the make_bayescan_input.py script provided by De Wit *et al.* (2012). The analysis was run with samples divided into the populations Ogasawara, Daito, and Okinawa and using default parameters (1 chain, thinning interval = 100, 499801 iterations). Convergence of F_{ST} estimates was visualized with trace plots in R (Appendix 2: Fig. S2.3a). A false discovery

rate (q-value) of FDR=0.05 was applied to identify and remove nine outlier loci (Appendix 2: Fig. S2.3b). Further allele filtering steps were conducted following the dDocent_filter script distributed with the dDocent package. SNPs with read depth of > 55 reads within individuals, or SNPs with an allelic balance of AB < 0.2 and > 0.8 or >0.99 were discarded to avoid paralogy in a locus and to account for fixed alleles, respectively. As locus quality scores have shown to be inflated for high coverage loci, allele quality was then filtered respective to read depth (QUAL / DP >0.05). A further filter to ensure homology of the minor and reference allele was applied by filtering against mapping quality discrepancy between the reference and minor allele (MQM/MQMR >0.15 & MQM/MQMR < 1.85).

Two different thresholds for missing data across individuals were explored and used for subsequent analysis. For population summary statistics, which are known to be sensitive to missing data, a threshold of 70% presence across individuals was used. For all other analyses, a threshold of 50% was accepted. However, in order to evaluate the effect of missing data, the analyses (except for demographic modeling) was repeated for both threshold values and reported as supplementary information (Appendix 2: Tables S2.1, Fig. S2.4). The difference of genetic variation between the two thresholds was visualized by a principal component analysis (Fig. 2.2).

2.2.4. Population summary statistics and genetic structure

Genetic structure was analyzed by individual-based probabilistic ancestry analysis using Admixture software (Portik *et al.*, 2017). Admixture was run up to 8 replicate analyses to evaluate the potential presence of up to 8 distinct populations. The most likely number of ancestral populations (K) was chosen based on the smallest cross-validation error, which was determined to be K=2. However, since such population structuring approaches may often underestimate the number of populations in the data (Janes *et al.*, 2017), and in order to evaluate population substructure, we also showed results for the next most likely numbers of clusters K=3 and K=4. The results were illustrated with bar plots sorted by sampling site (Fig. 2.3) and pie charts per location (Fig. 2.1). Admixture analysis showed no indication for genetic structure among sampling sites within the islands of Haha, Chichi, and Miyako (Fig. 2.3c). Therefore, all sampling sites within an island were pooled to a single location for population summary statistics. The two Daito Islands (Kitadaito and Minamidaito, Table 2.1) showed signs for genetic differentiation in the Admixture analysis (Fig. 2.3), however, F_{ST} between the two was sites was very low (-0.002), which is why they were also pooled to a

single location 'Daito'. Classical population summary statistics between locations were inferred using vcftools (Danecek *et al.*, 2011). Inbreeding coefficient *(F)*, nucleotide diversity (*pi* = expected heterozygosity), and pairwise allele frequency variance (F_{ST}, weighted Weir and Cockerham) were calculated for each population (Table 2.2).

2.2.5. Migration analysis in BayesAss

Migration rates were investigated with a genetic assignment method implemented in BayesAss3-SNPs (Mussmann, 2017), a modified version of BayesAss v.3.0.4 (Wilson & Rannala, 2003). The input file was created from the BayeScan-filtered VCF file with PGDSpider v. 2.1.1.3 (Lischer & Excoffier, 2012), randomly selecting one SNP per locus. The PGDSpider output file was then corrected to discard loci not present in any of the samples. To diminish convergence problems (Meirmans, 2014), populations with less than 10 individuals were excluded (Oku, Iheya, Iriomote, Guam) and three separate runs were performed with different starting seeds (s=10, s=567, s=234). For all runs the same mixing parameters for m, a, and f were used, which were selected as suggested in the BayesAss manual to result in acceptance rates between 30 and 60%. Convergence of the parameter estimates was examined from the MCMC trace plots using Tracer v1.6.0 (Rambaut & Drummond, 2007). Additionally, the Bayesian deviance of each run was calculated using the R-script provided by Meirmans (2014). Results were taken from the run with the lowest deviance. All runs were performed with 10 M iterations, a sample interval of 1000 and a burn-in of 2 M iterations was discarded.

2.2.6. Analysis of joint demographic histories in dadi

The demographic histories, including patterns of gene flow, were investigated more in detail between island archipelagos using dadi (Gutenkunst *et al.*, 2009). Dadi uses a diffusion approximation method to find the most likely parameter values of a hypothetical demographic model, such as migration rates, population sizes, and divergence times (Gutenkunst *et al.*, 2009). Parameter values are found by maximizing similarity between the expected and the observed site frequency spectrum generated under a specific demographic scenario. The best fitting parameters are evaluated by computing a composite-likelihood and AIC. Dadi is able to account for missing data by 'projecting' actual sample sizes to a smaller size, which is why we used the more inclusive dataset of SNPs with up to 50% missing data. All islands in the Ryukyu archipelago with little genetic differentiation between each other (Iriomote, Miyako, Iheya, Oku, and Tanega) were combined to a single Ryukyu population

(56 individuals total), and Chichi and Haha Islands were combined to a single Ogasawara population (32 individuals total) for analyzing the divergence histories between the island groups.

Two three-dimensional (3D) models were tested. The first model was built in order to evaluate the potential role of Daito as a stepping-stone between Ryukyu and Ogasawara. We first tested the presence and symmetry of migration between each population pair, i.e. between Ogasawara and Ryukyu, between Ryukyu and Daito, and between Daito and Ogasawara. The fit of four different 2D models were compared, including a null model assuming no divergence between populations, and models implementing divergence with no migration, divergence under symmetric migration, and divergence under asymmetric migration (Appendix 2: Table S2.2, Fig. S2.5). Based on the migration patterns concluded from the pairwise analyses, a 3D model of all three populations was built. The model was built with two splits in time, the first splitting Ogasawara from the ancestral population of Okinawa and Daito, and the second splitting Ryukyu and Daito, according to what was known from the geologic histories of these three island systems (Yoshiwara, 1902; Ota & Omura, 1992) (Fig. 2.4). In addition, varying levels of gene flow in time were tested on the 2D level only. These additional models implemented either only ancient migration or migration only after secondary contact (Appendix 2: Table S2.2).

The second 3D model was built to compare migration rates between the Ogasawara islands and the southern Mariana Islands (Guam) to the migration between Ogasawara and western Japan (Ryukyu + Daito). Although the relatively small sample size in Guam may influence the detection of recent demographic events (due to the lack of rare alleles in small sample sizes), it should not affect the accuracy for distinguishing between relatively simple models based on common or fixed alleles. Similarly to above, pairwise 2D models were first tested between Guam and Ogasawara, and Guam and Ryukyu + Daito (Appendix 2: Table S2.2, Fig. S2.5). Based on the temporal order of emergence between the islands (Yoshiwara, 1902; Tracey *et al.*, 1964; Ota & Omura, 1992), the first split was implemented between Ogasawara and Guam + Ryukyu + Daito, and the second split between Guam and Ryukyu + Daito (Fig. 2.5).

Folded joint site frequency spectra for each analysis were computed using easySFS (Overcast, 2018). Only one biallelic site per locus was used. In order to account for missing data and to maximize the number of segregating sites, the populations Ogasawara, Daito,

Okinawa, and Guam were down-projected to 26, 16, 26, and 4 alleles, respectively. The parameter space of each tested model was searched in three optimization rounds following the workflow provided by (Portik *et al.*, 2017), where the most likely parameters (log Likelihood) from the previous round are given as start parameters in the subsequent round, starting with random parameters in the first round. The rounds differ by the level of parameter perturbation, the first round performing three-fold, the second round two-fold, and the third round a one-fold perturbation. The optimizations were run with 20 iterations in 30 repeats, with 30 iterations in 30 repeats, and 50 iterations in 50 repeats in the first, second and third rounds respectively. For the 3D models, the third optimization step was run in two subsequent rounds and with 100 maximal iterations. Final model fits were evaluated by Akaike Information Criterion (AIC) and by residual analysis between the observed and modeled joint frequency spectra (Fig. 2.4-5).

The modeled parameters in dadi are given in units of a reference population size N_{Ref}, which relates to theta θ by the equation $\theta = 4N_{Ref}\mu$. Migration rates are given in units of $M_{ij} = 2N_{Ref}*m_{ij}$ per generation and divergence times T are given in units of 2 N_{Ref} generations. μ is a product of the mutation rate and the total number of bp L from which SNPs were derived. L was estimated by multiplying the average read length of our RAD sequences (47.9 bp) by the number of loci that entered dadi analysis. The number of loci was estimated by dividing the total number of sites (8171) by the average number of sites found in a locus (2.2) and by multiplying this with the fraction, so which sites were present in the projected sample sizes relative to the total number of sites. This fraction was estimated to be 0.91 using vcftools, by subsequently excluding sites that were present in less than 13, 8, and 13 individuals in the populations Ogasawara, Daito, and Okinawa, resulting in a total L of 160826.56 bp. The precise mutation rate for our study taxon is not known, so we used a universal mutation rate of 2.5e-8 per generation suggested by the demographic program fastsimcoal (Excoffier & Foll, 2011). Based on these assumptions and approximations, migration rates were translated into number of migrated propagules per generation. Translating the number of generations into chronological times may be tricky, since corals have overlapping generations and the reproductive age of *G. fascicularis* is unknown. We assumed an average age of mothers of 35 years based on estimations in other coral species, including *Coleastrea aspera* (33 years), *Goniastrea favulus* (37 years), and *Platygyra sinensis* (35 years) (Madin *et al.*, 2016).

2.2.7. Biophysical dispersal model and isolation by distance analysis

In order to investigate dispersal patterns in a wider geographic context and to understand the influence of contemporary dispersal on genetic composition, a biophysical dispersal model was developed using the Regional Ocean Modeling System (ROMS; Shchepetkin & McWilliams, 2005) and life-history parameters of the larval stage. ROMS modeling was performed as described by Mitarai et *al.* (2009; 2016) and dispersal was assessed using an inverse particle tracking approach. One particle per day over the years of 2008-2017 were released from the grid mid points of reef sites. Particles were tracked back in time for 60 days every six hours. The tracking time of 60 days was chosen based on an overview given by Markey *et al.* (2016) showing that maximal longevity of coral larvae ranges between 23 and 244 days, and most being between 50 and 70 days. The distribution of coral reefs was inferred from the World Conservation Monitoring Center (UNEP-WCMC, 2010) and extended by the data provided by the Sangomap collaborative citizen science project (https://www.sangomap.jp/) and Kumagai *et al.* (2018). The potential amounts of immigrants from each source for a site were quantified for an advection time of 3–60 d (mimicking competency time windows of coral larvae) and assuming a larval mortality rate of 5% per day (Markey *et al.*, 2016). Expected connection times from a given source and destination site were calculated following the method of Mitarai *et al.* (2009).[1] Immigration probabilities were summarized in an immigration probability matrix listing collection sites as rows and possible source locations as columns, and standardized within rows by dividing by the sum (Appendix 2: Table S2.3).

The biophysical dispersal assessment was then compared to our genetic data. The immigration probability matrix was first transformed into eigenvalues by PCA to assess similarity in immigration patterns between collection sites (Appendix 2: Fig. S2.6). The collection sites were then averaged per island in order to obtain the same level of resolution as our genetic populations. Euclidean distances of Eigenvalue loadings were computed for immigration probabilities and compared to pairwise F_{ST} and geographic distance by Multiple Regression on Distance Matrices (MRM) using the ecodist package in R (Goslee & Urban, 2007) (Table 2.4). Results were illustrated by correlation plots (Fig. 2.7). The same analysis was also done using distances between the population centroids of the SNP-based PCA (Fig. 2.1) instead of F_{ST} (Appendix 2: Table S2.4). Lastly, we tested the relationship between

[1] ROMS modeling, particle tracking, and migration probabilities were performed by Satoshi Mitarai

nucleotide diversity *pi* and diversity of potential immigrants using community ecology metrics. The rational was that the immigration probabilities should predict the genetic composition of a population if it is constant in time, and that the more immigrants a population receives from different locations the higher genetic diversity should be at a site. Simpson alpha diversity per island was calculated based on the immigration probability matrix and regressed to genetic diversity *pi* per population in R (Fig. 2.8).

2.3. Results

Out of the 174 individuals sequenced, 39 were lineage S, 9 were lineage L+, one was ambiguous, and 126 were lineage L (Appendix 2: Fig. S2.1; Table 2.1). From lineage L, 108 remained after removing four individuals due to low coverage (Miyako_PW53, Daito_PW204, Daito_238, Chichi_PW507) and thirteen for being potential clones. All samples from the Ogasawara Islands and most from Daito (28 out of 31) were lineage L (Fig. S1). Each individual contained 1.78 M (sd=1.3 M) raw reads in average, from which 3% were filtered out due to poor base calling. In total, 785'312 unfiltered SNPs were called, and after full filtering and removing 9 sites under potential selection, 8171 SNPs were present in at least 50% of the individuals and 1756 SNPs were present in at least 70% of the individuals. We found that the lower filtering threshold regarding missing data among individuals (sites present in at least 50% *versus* 70% of individuals) did not increase noise but enhanced resolution (Fig. 2.2).

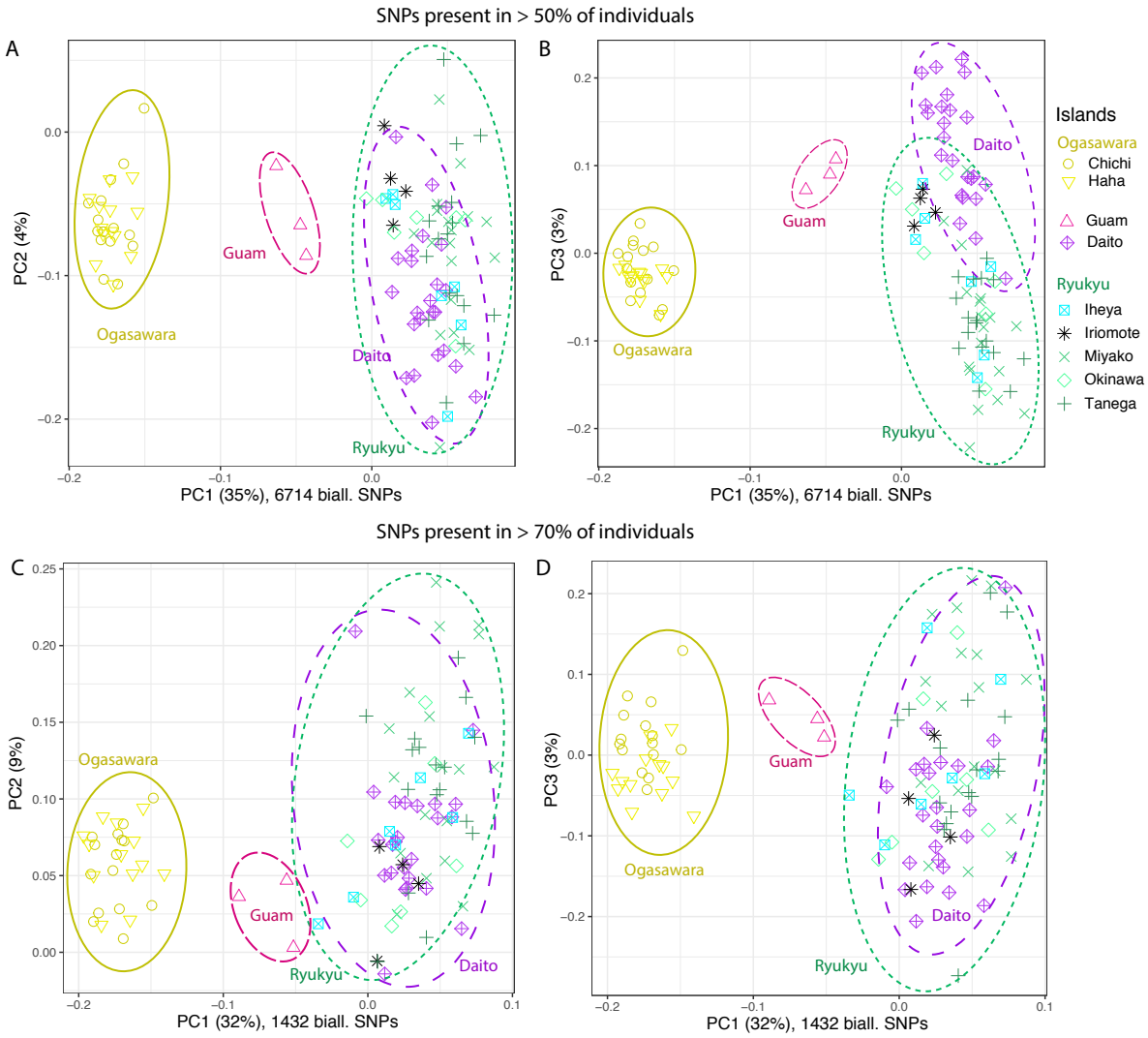

Figure 2.2. Principal component analysis based on biallelic sites (a, b) represented in at least 50% of all individuals and (c, d) represented in at least 70% of the individuals. The first and second principal components (a, b, and 3 c, d) explained similar proportions of the variations and are therefore both shown. A more inclusive dataset accepting more loci with higher percentage missing data (b, d) does not increase noise but enhances the resolution of population structure.

Population summary statistics confirm small F_{ST} values within island archipelagos (0.0 - 0.04) but higher among the island groups (0.03 - 0.19, Table 2.2). Inbreeding *F* was lowest in the Ogasawaran populations and highest in Miyako. In contrast, nucleotide diversity *Pi* was lowest in the Ogasawara populations (~ 0.2) and highest in the Ryukyu Islands (0.56 - 0.84). Both PCA and ancestry analysis find little spatial structuring within the Ryukyu archipelago and Daito islands but high differentiation to Ogasawara (Fig. 2.1-3). Ancestry analysis in Admixture determined two primary clusters, one from Ogasawara and

one from Ryukyu, with evidence for little mixing (Fig. 2.3). The third subcluster divided the Ryukyu cluster into a population predominant in Daito and Guam, and a fourth subcluster revealed further location-independent substructure within the Ryukyu Islands. The same analysis based on sites that are present in >70% of individuals were similar in K=2, but suggest more mixing in K=3 and K=4 (Appendix 2: Fig. S2.2), consistent to what would be expected from the PCA using this higher threshold (Fig. 2.2).

Table 2.2. Population summary statistics. Pairwise weighted Weir and Cockerham F_{ST}, inbreeding coefficient (*F*), and nucleotide diversity *Pi* (= nucleotide diversity) based on 1756 neutral SNPs present in >70% of individuals.

F_{ST}	*Ryukyu*						*Ogasawara*		
	Iriomote	Miyako	Oku	Iheya	Tanega	Daito	Haha	Chichi	Guam
Iriomote		0.023	-0.009	0.032	0.040	0.038	0.189	0.173	0.147
Miyako			0.014	0.019	0.011	0.039	0.197	0.189	0.144
Oku				0.005	0.039	0.042	0.174	0.165	0.111
Ihyea					0.026	0.032	0.175	0.169	0.164
Tanega						0.041	0.190	0.186	0.158
Daito							0.153	0.150	0.127
Haha								0.002	0.194
Chichi									0.168
F	0.563	0.839	0.761	0.580	0.710	0.422	0.201	0.272	0.560
Pi	0.442	0.317	0.417	0.346	0.284	0.240	0.288	0.281	0.520

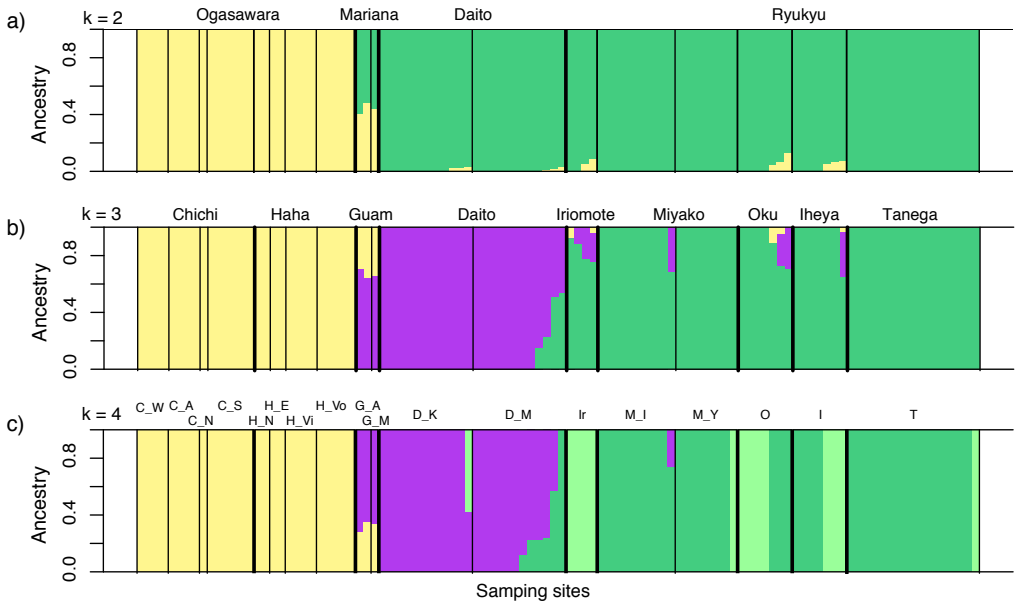

Figure 2.3. Individual population assignments for K=2 (CV error: 0.56), K=3 (CV error: 0.60) and K=4 (0.65) as inferred by Admixture analysis based on 8162 neutral sites present in >50% of individuals. Individuals are grouped by island archipelagos (a), islands (b), and sampling sites (c, Table 2.1).

BayesAss migration analysis (Table 2.3) had a Bayesian deviance of 135274.5 and found more dispersal in northward direction within the Ryukyu Islands, as evident from a higher proportion of migrants from Miyako in Tanega (0.0608) and Daito (0.0924) than the other way around (0.0112 and 0.0144). Migration between Ogasawara, Daito, and Ryukyu was estimated to be very small but slightly higher in eastward direction (0.0165 - 0.0187 *vs.* 0.0116 - 0.0154). According to this analysis, migration between Ogasawara and Daito was slightly lower than between Ogasawara and the Ryukyu Islands, inconsistent with what would be expected in a stepping-stone scenario over Daito. Reanalysis using the more filtered dataset (70% presence across individuals) revealed similar results, except for a ten times higher migration rate from Chichi to Haha (Appendix 2: Table S2.1). Migration rates may be hard to estimate between population pairs with very little genetic differentiation (Meirmans, 2014), which concerns the population pairs Chichi and Haha, and Miyako and Tanega here (Table 2.2). This should be kept in mind for the interpretation of our results.

Table 2.3. Migration rates estimated by BayesAss based on 6819 neutral, biallelic and unlinked SNPs present in at least 50% of all individuals. Rates represent the proportion of settlers in destination populations (rows) from source populations (columns) and their standard deviations between geographic populations. Only population with >10 individuals were included. Rates > 0.02 and < 0.8 are marked in bold.

Source >	*Ryukyu*		*Daito*	*Ogasawara*	
Dest. v	Miyako	Tanega		Chichi	Haha
Miyako	0.9276 (0.0280)	0.0144 (0.0137)	**0.0289 (0.0191)**	0.0147 (0.0140)	0.0143 (0.0138)
Tanega	**0.0608 (0.0267)**	0.8937 (0.0327)	0.0151 (0.0143)	0.0154 (0.0145)	0.0151 (0.0144)
Daito	**0.0924 (0.0269)**	0.0112 (0.0109)	0.8731 (0.0294)	0.0116 (0.0110)	0.0116 (0.0112)
Chichi	0.0168 (0.0159)	0.0165 (0.0157)	0.0168 (0.0162)	0.9169 (0.0319)	**0.0331 (0.0214)**
Haha	0.0182 (0.0171)	0.0187 (0.0177)	0.0186 (0.0177)	0.0184 (0.0173)	0.9260 (0.0322)

The 2D demographic modeling in dadi showed that divergence under asymmetric migration was the most likely scenario between Ogasawara and Ryukyu, Daito and Ogasawara, Guam and Ogasawara, and Guam and Ryukyu + Daito; and divergence under symmetric migration to be the most likely scenario between Ryukyu and Daito (Appendix 2: Table S2.2, Fig. S2.5). The final 3D model including Ogasawara, Daito, and Ryukyu estimated a higher migration rate eastward from Ryukyu to Ogasawara than the other way around, as well as from Daito to Ogasawara (Fig. 2.4). Migration from Daito to Ogasawara was slightly higher than from Ryukyu to Ogasawara, although the difference was small (10.9

vs. 9.61 / M migrants). Divergence times between Ogasawara and Ryukyu + Daito were estimated to 270,000 generations (T1 + T2), and between Ryukyu and Daito to 99,000 generations (T2), which translated to 9.45 and 3.46 M years, respectively (assuming an average generation time of 35 years). The second 3D demographic model between Guam, Ogasawara, and Ryukyu + Daito also generally estimated higher migration rates to than from Ogasawara estimated, and a higher rate from Guam than from Ryukyu + Daito to Ogasawara (27.2/M vs. 18.8/M, Fig. 2.5). Divergence times were estimated to be considerably shorter than by the first 3D model, estimating only 109,000 generations (T1 + T2) between Ogasawara and Ryukyu + Daito + Guam, corresponding to 3.8 M years. 55,900 generations were estimated to separate Guam from Ryukyu + Daito.

The additional more complex 2D models for Ryukyu and Daito estimated divergence at secondary contact with more migration from Ryukyu to Daito than the other way around to be the most likely scenario. Between Ryukyu and Ogasawara, Daito and Ogasawara, and Guam and Ogasawara divergence under ancestral asymmetric migration was slightly more likely than the simpler divergence models used to construct the 3D model (Appendix 2: Table S2.2).

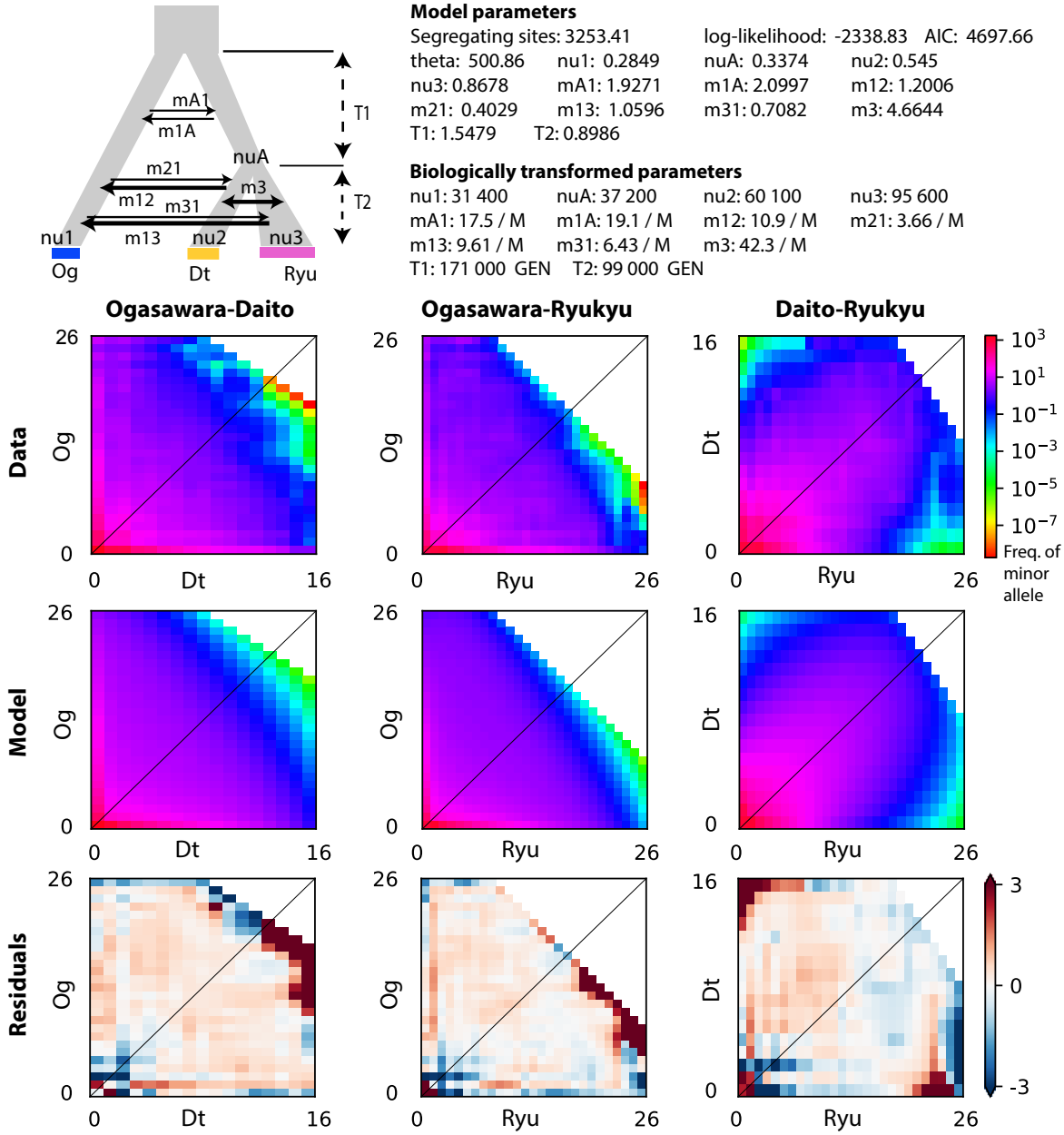

Figure 2.4. Joint demographic history between *Galaxea fascicularis* populations in Ogasawara (Og), Daito (Dt) and Ryukyu (Ryu) modeled by dadi. The demographic model was set to include continuous migration and each population to undergo an instantaneous size change. Site frequency spectra for observed and modeled alleles are given between each population pair. Residual plots illustrate mismatch between the model and data. Theta = the effective mutation rate of the ancestral population; nu1, nu2, nu3 = effective present population sizes relative to the ancestral population; nuA = relative effective size of ancestral population of Daito and Ryukyu before their separation; m12 = migration rate from Daito to Ogasawara, m21 = migration rate from Ogasawara to Daito (analogously for mA1, m1A, m13, m31), m3 = symmetric migration rate between Daito and Ryukyu; T1 = time between first and second population split, T2 = time since second population split.

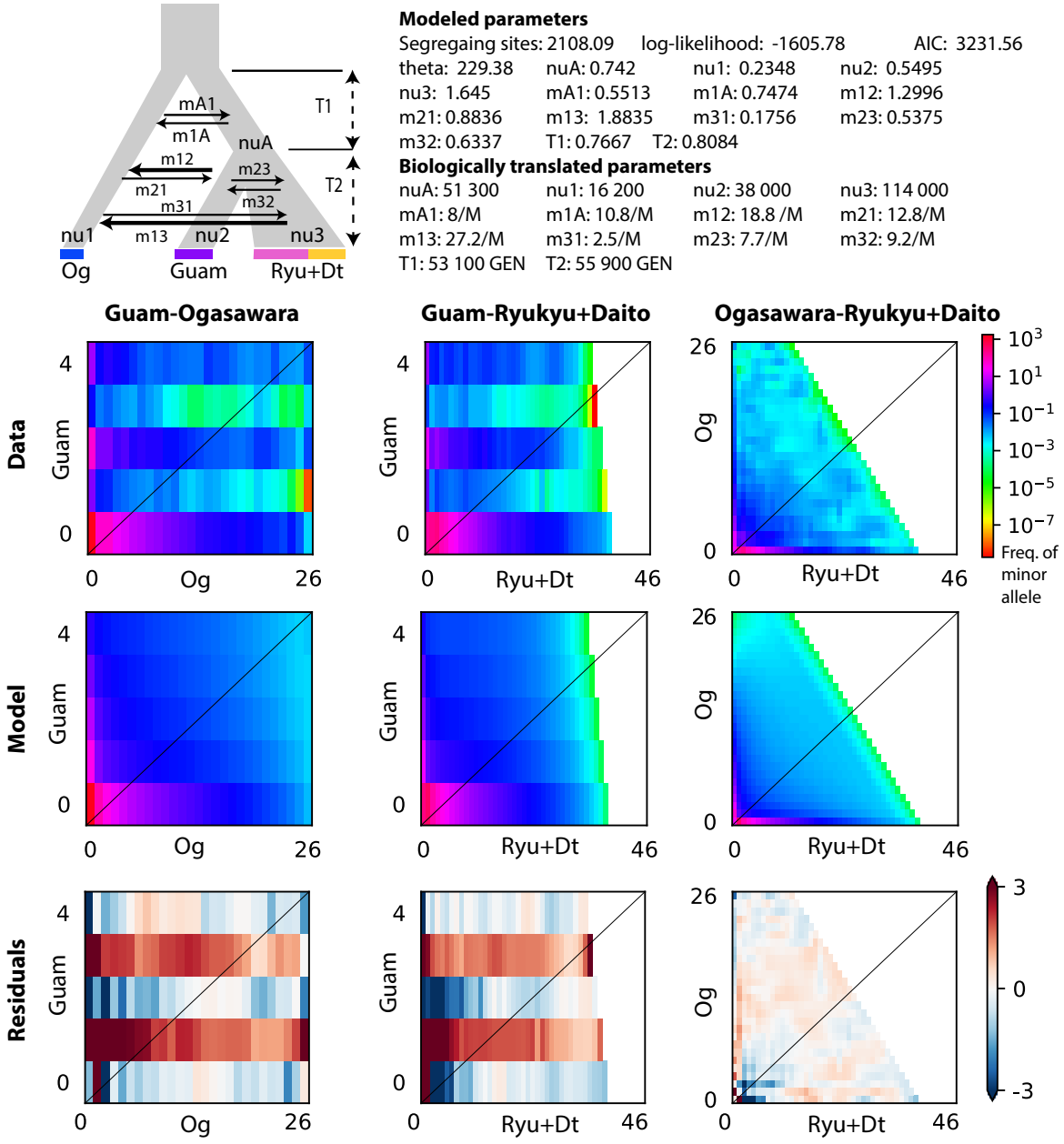

Figure 2.5. Joint demographic history between *Galaxea fascicularis* populations in Guam, Ogasawara (Og) and Ryukyu+Daito (Ryu+Dt) modeled by dadi. The demographic model was set to include continuous migration and each population to undergo an instantaneous size change. Site frequency spectra for observed and modeled alleles are given between each population pair. Residual plots illustrate mismatch between the model and data. Theta = the effective mutation rate of the ancestral population; nu1, nu2, nu3 = effective present population sizes relative to the ancestral population; nuA = relative effective size of ancestral population of Guam + Ryukyu + Daito before their separation; m1 = migration rate per generation between Ogasawara and Guam + Ryukyu + Daito, m23 = migration rate from Ryukyu + Daito to Ogasawara, m32 = migration rate from Ryukyu + Daito to Ogasawara

(analogously for mA1, m1A, m13, m31); T1 = time between first and second split, T2 = time since second population split.

Inverse particle tracking revealed that Ogasawara was a sink rather than source for surrounding populations and it received most immigrants from Tokara, Amami, and Luzon (Fig. 2.6; Appendix 2: Table S2.3). Only little dispersal was modeled to occur between Ogasawara along the Mariana Island chain. There was no direct dispersal between Daito and Ogasawara. The Ryukyu Islands received their immigrants from Philippines, Taiwan, and from other islands of the Ryukyu Archipelago (Fig. 2.6). The dissimilarity in immigration patterns did not relate to F_{ST} better than geographic distance alone (Fig. 2.7, Table 2.4), and trying the same analysis within the Ryukyu Islands only or replacing F_{ST} with population centroids of the SNP-based PCA was not significant (Appendix 2: Table S2.4). The genetic diversity *pi* had a negative relationship to diversity of immigration sources (adjusted R^2 = 0.025, p = 0.308; Fig. 2.8).

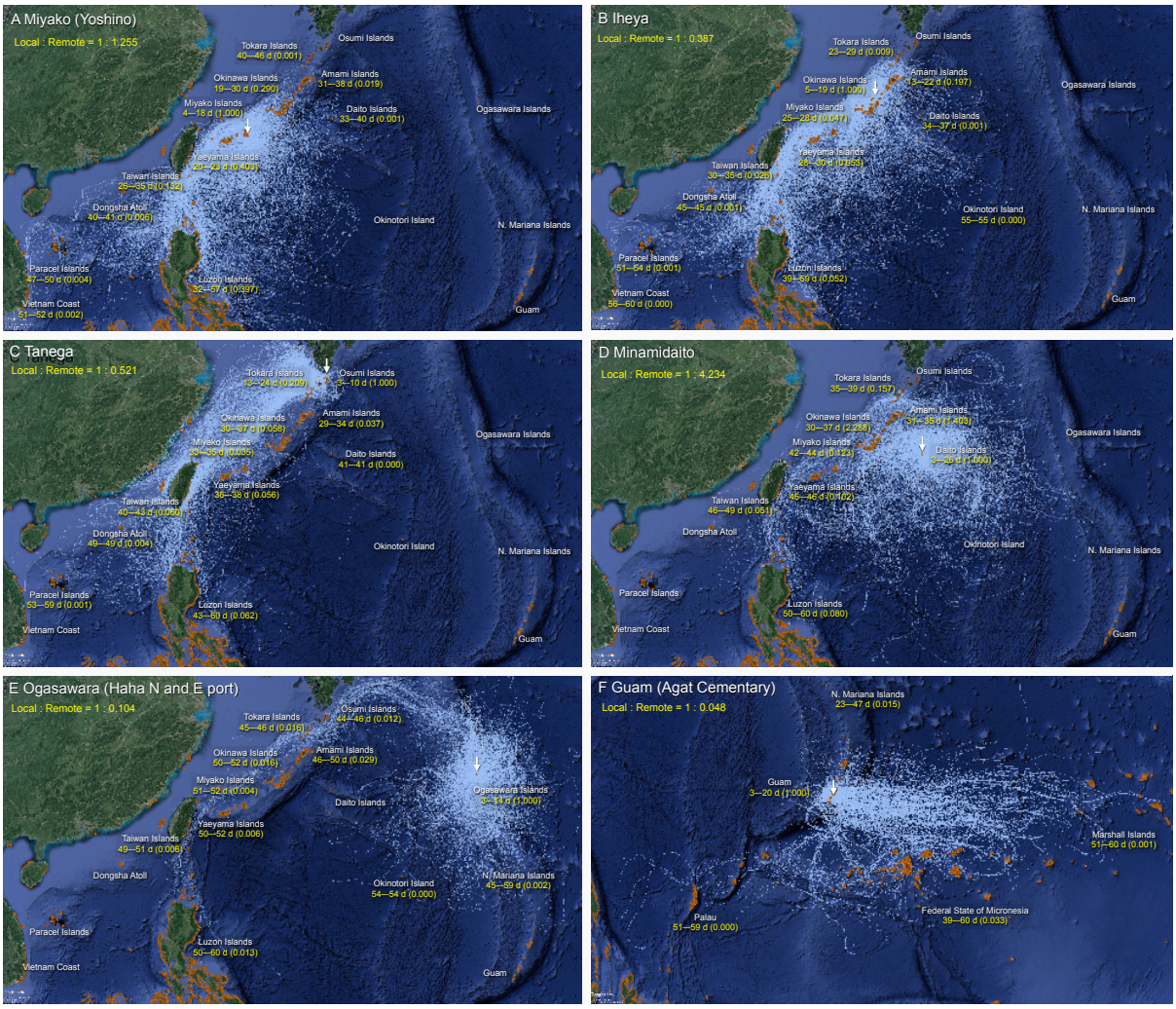

Figure 2.6. Examples of inverse particle tracking for 60 d. Immigration probabilities from different source regions (Taiwan Islands, Yaeyama Islands, Miyako Islands, Okinawa Islands, Amami Islands, Tokara Islands, Osumi Islands, Daito Islands, Ogasawara Islands, Okinotori Island, Northen Mariana Islands, and Guam) are shown for six example destinations (A–F). There is more northward dispersal in the Ryukyu Islands (A–C), but also southward (B). In the Daito Islands self-recruitment is small and settlers arrive mainly from the Ryukyu Islands. The Ogasawara Islands (E) theoretically receive more migrants from Luzon than from the Northern Mariana Islands, and Guam receives most settlers from Micronesia (F). Yellow numbers indicate expected connection times in days from a given source region. Numbers in the parentheses show transport probabilities from each source region normalized by the transport probabilities from its own region, while assuming 5% of daily larval mortality.[2]

[2] The figure components were made by Satoshi Mitarai.

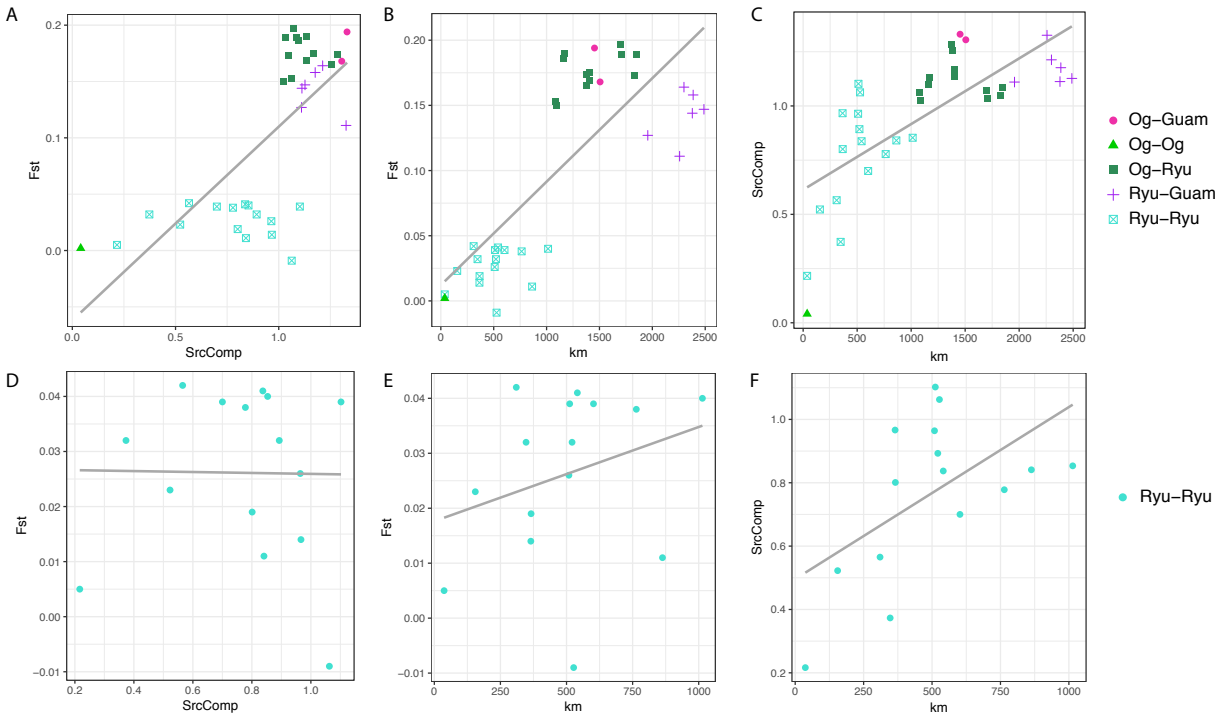

Figure 2.7. Correlations between pairwise geographic distance, F_{ST}, and dissimilarity in composition of migration sources according to inverse particle tracking. A-C: all islands, D-F: within Ryukyu and Daito Islands. Genetic differentiation correlates only weakly with dissimilarity in source composition across regions (A, C), but more to geographic distance alone (B, E), especially across regions (B). Genetic differentiation between Ryukyu islands and Guam are higher than between Ryukyu islands and Ogasawara islands, which are geographically closer to each other (B). Dissimilarity in source composition is related to geographic distance between sites (C, F), while this relationship is stronger within the Ryukyu Islands alone (F).

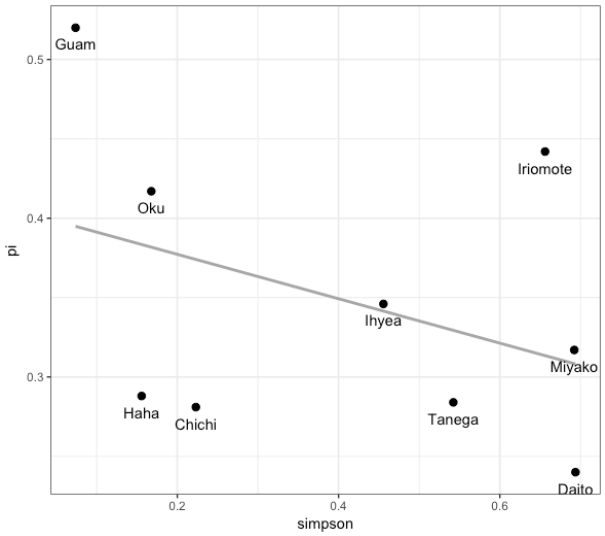

Figure 2.8. Correlation analysis between nucleotide diversity and Simpson index of alpha diversity based on potential source sites. The relationship is negative, contradicting to our expectations, indicating that other factors than connectivity to other populations is important for nucleotide diversity.

Table 2.4. Multiple regression of physical distance matrices (geographic distance and dissimilarity in potential source areas according to inverse particle tracking) to genetic differentiation F_{ST} and their percent variation explained. Over all populations, geographic distance explains genetic difference better than immigration dissimilarity (Dissim. source comp.). Within the Ryukyu Islands the regression was not significant.

Coefficients	All (*p*)	Ryukyu (*p*)
Geogr. Distance	$5.8\ 10^{-5}$ (0.010)	$2.5\ 10^{-5}$ (0.24)
Variation explained	15%	12%
Dissim. Source comp.	$7.1\ 10^{-2}$ (0.046)	$-1.5\ 10^{-2}$ (0.48)
Variation explained	4%	4%
total R^2	0.65	0.12
p	0.001	0.486

2.4. Discussion

Our study showed that the Ogasawaran *G. fascicularis* population is highly differentiated from populations in the Ryukyu Islands, Daito Islands, and Guam (Table 2.2, Figs. 2.1-3). The migration rates in the eastward direction from Ryukyu and Daito to Ogasawara were higher than the other way around (Fig. 2.4, Table 2.3), consistent with dispersal probabilities inferred from the biophysical dispersal model (Fig. 2.6, Appendix 2: Table S2.3). The role of Daito as a stepping-stone remains ambiguous from our genetic analysis (Table 2.3, Fig. 2.4), but is not supported by the oceanographic dispersal model (Figs. 2.6). Migration from Guam

to Ogasawara may be higher than from the Ryukyu and Daito Islands to Ogasawara (Fig. 2.5). As shown in previous studies (Nakajima *et al.*, 2010; Shinzato *et al.*, 2015; Nakajima *et al.*, 2016; Zayasu *et al.*, 2016), the Ryukyu Islands are a uniform population with little substructure (Table 2.2, Fig. 2.1-3), primarily receiving migrants from southern populations upstream the Kuroshio Current (Table 2.3, Fig. 2.6). At the Daito Islands, the amount of self-recruitment was relatively low, and most settlers came from the Ryukyu Islands (Fig. 2.6), which was supported by the model of divergence under secondary asymmetric migration between the two populations (Appendix 2: Table S2.2).

2.4.1. A small but healthy, isolated population in Ogasawara

The Ogasawara population had a smaller effective population size (Fig. 2.4) and despite having lower nucleotide diversity it showed less signs for inbreeding than the Ryukyu and Daito populations (Table 2.2). The small effective population size in Ogasawara is in line with what would be expected from its geographic isolation and small habitat area. The Ryukyu Islands in comparison are much larger and are closely connected to the diverse gene pool in the Coral Triangle (Roberts *et al.*, 2002) by the Kuroshio Current (Fig. 2.6), which could frequently provide the Ryukyu Islands with diverse larvae and explain the higher genetic diversity *pi* and population size there. Genetic diversity within the Ryukyu Islands generally decreased from South to North (Table 2.2), which is perhaps linked to the increasing distance to the Coral Triangle, similar to in Micronesia (Davies *et al.*, 2015). However, no such pattern had been found in *Acropora* from the same study area (Nakajima *et al.*, 2010).

The Ryukyu Islands may generally experience more frequent environmental disturbance than the Ogasawara Islands. Mass-bleaching events and typhoons (or the lack of typhoons causing overheating) in the Ryukyu Islands may have created several bottlenecks in the past, causing the high inbreeding coefficients observed here. For example, a severe mass-bleaching event in 1998 caused a massive depletion of coral populations throughout the Ryukyu Islands (Loya *et al.*, 2001; Hongo & Yamano, 2013). Although the coral coverage has recovered quite well in Okinawa (van Woesik *et al.*, 2011), the effects could still be present. Bleaching was observed on site during sampling in Miyako, which may, together with its relatively isolated position in the Ryukyu Islands, explain the particularly high inbreeding coefficient. Similarly in Guam, a significant decrease in coral coverage due to the Crown of Thorns starfish (*Acanthaster planci*) in 1969 (Colgan, 1987) could have caused a

bottleneck resulting in the high inbreeding coefficient (Table 2.2), however, population summary statistics for Guam should be interpreted with care due to the small sample size. In contrast, such extended coral dying has never been reported from Ogasawara (Inaba, 2004b).

The high genetic differentiation presently observed between Ogasawara and Ryukyu, Daito, and Guam seems to be the result of ancient divergence dated to the mid Miocene, with little amounts of migration ever since (Figs. 2.4 and 2.5, Table 2.3). This implies that LDD events along the Izu and the Daito route, as well as along the Mariana route have been too rare to cause smoothing effects between the *Galaxea* populations on Ogasawara and neighboring regions. Nevertheless, more gene flow was detected eastward from Ryukyu and Daito to Ogasawara than the other way around (Table 2.3, Fig. 2.4). This was consistent with our oceanographic dispersal model (Fig. 2.6) showing that at present Ogasawara seems to receive most direct migrants over the Izu route, confirming the extended influence of the Kuroshio Current hypothesized by previous studies (Nakano *et al.*, 2008; Reimer *et al.*, 2014). No *Galaxea* colonies have been reported from the southern coast of the Japanese main islands (Honshu and Shikoku), and a fossil occurrence of *Galaxea* in these areas is also unknown (PBDB, 2018), suggesting dispersal between the Ryukyu Islands and Ogasawara to entirely rely on rare direct dispersal events. At present, the Daito Islands do not seem to represent a direct stepping stone for migration between Ogasawara and Ryukyu in *Galaxea* from our contemporary oceanographic dispersal model (Fig. 2.6) and BayesAss analysis (Table 2.3). However, over an evolutionary time scale as addressed by our demographic model, migration from Daito to Ogasawara was estimated to be slightly higher than from the Ryukyu Islands (Fig. 2.4). This suggests that at least in the past, the Daito route has been travelled as much as the Izu route, consistent with expectations based on the fish species composition (Nonaka, 2004). As direct dispersal between Daito and Ogasawara seems not possible even at maximal pelagic larval duration of 60 d (Fig. 2.6), other potential stepping-stones like Okidaito and Okinotori (Fig. 2.1) may play an important role for this connection. Future connectivity assessments in this region should quantify stepping-stone probabilities of migration, which may reveal a better match between oceanographically and genetically inferred dispersal probabilities.

More migrants seem to reach Ogasawara from the Mariana Islands as from the Ryukyu and Daito Islands (Fig. 2.5). This disagreed with our biophysical dispersal model, according to which much fewer larvae should arrive from the Northern Mariana Island to Ogasawara than for example from the Philippines, however, it agreed with the higher

northward than southward migration estimated along the Mariana route (Fig. 2.6). In the case of *Galaxea,* the Mariana route of dispersal could be covered less than in other corals, as *Galaxea* was not reported from the northernmost Mariana Island Farallon de Pajaros (Brainard, 2012), extending the largest gap on this route to almost 600 km. In addition to large gaps, strong ocean currents may also present effective dispersal barriers in the sea, such as perhaps given by the Northequatorial Countercurrent flowing eastward. Major ocean currents were shown to prevent mixing within small distances, for example in damselfish by the Indonesian Throughflow (Raynal *et al.*, 2014), mantis shrimp by the Halmahera Eddy in (Barber *et al.*, 2006), or the bifurcation of the North Equatorial Current in boring clams (Ravago-Gotanco *et al.*, 2007). The absence of strong connectivity is also supported by a faunal break in *Galaxea* between Ogasawara and Mariana. *Galaxea* was never reported to be a dominant component of the coral community on any of the northern Mariana Islands (Brainard, 2012), while it is in Ogasawara (Inaba, 2004b). Moreover, only *G. fascicularis* lineage L was found in Ogasawara whereas both lineages L and S, as well as *G. horrescens* occur in Guam. This faunal break seems consistent with the presence of a strong dispersal barrier between the Mariana Islands and Ogasawara, agreeing more with our oceanographic dispersal model than with our demographic analysis. The genetic estimations of demographic parameters involving Guam may not be fully accurate given the small sample size available, and model fitting was generally challenging, as may be viewed from the error distribution (Fig. 2.6). This may also explain the difference in time estimations between the two 3D models. The small sample size from Guam clearly presents a limitation to our study and future work should include more specimens from the Mariana Islands to obtain more certain results. The oceanographic dispersal model could also be improved by including more islands along the Marina Islands and southern Ogasawara Islands (Io Islands) and by computing stepping stone dispersal between those. However, high genetic differentiation (Table 2.2) and the faunal break indicate that the Ogasawara coral fauna may be demographically isolated from the one in the Mariana Islands.

2.4.2. Connectivity between Guam and the Ryukyu and Daito Islands

In contrast, and despite further geographic distances and the lack of direct connectivity (Fig. 2.6), genetic differentiation between the Ryukyu populations and Guam was smaller than either of them to Ogasawara (Table 2.3, Fig. 2.7), indicating a potentially large effect of stepping-stones for migration between Ryukyu and Guam. Stepping-stone probabilities of dispersal were not quantified here, however, they may also be responsible for

the non-significant relationship between direct immigration probabilities and genetic differentiation, as well as the non-significant relationship between immigration probability and genetically derived parameters in our study (Tables 2.4, Figs. 2.7-8; Appendix 2: Table S2.4, Fig. S2.7). Low genetic differentiation among the Philippines, Guam, and Ryukyu has also been found in other organisms, for example in marine snails (Duda & Lessios, 2009), and crown of thorn starfish between the Philippines and Ryukyu (Yasuda *et al.*, 2009). This pattern may be caused by the homogenizing effect of a contiguous connection of habitats (Palumbi, 1994; Barber *et al.*, 2002) along the Philippine Islands. Guam could be connected to the eastern Coral Triangle by using Palau as a stepping stone, which is connected to the Kuroshio Current connecting the Philippines to the Ryukyu Islands. Even though there is high genetic diversity and differentiation in coral among the fragmented habitats in the Coral Triangle (Knittweis *et al.*, 2009), its eastern margin along the Philippines may be genetically relatively homogenous, consistent with modeled genetic diversity (Kool *et al.*, 2011) and the definition of ecoregions in this area (Spalding *et al.*, 2007; Veron *et al.*, 2015) (although genetic breaks within this ecoregion have also been shown (DeBoer *et al.*, 2014)).

The genetic similarity between Ryukyu and Guam may also be influenced by a direct migratory connection over the Daito Islands, since Daito and Guam were partially composed of the same subcluster on the K=3 level in the Admixture analysis (Figs. 2.1, 2.3). The Subtropical Countercurrent flowing from northern Japan roughly over the Daito Islands and the remote Okidaito and Okinotori Islands could connect the two regions over the Northern Mariana Islands. Occasional LDD was detected between the Daito and Okinotori, as well as between Okinotori and Northern Mariana. However, *Galaxea* has not been growing around Okinotori Island since at least the Holocene (Kayanne *et al.*, 2012) and the genetic similarity between Guam and Daito could also be due to historical reasons. The Daito Islands lie on the Philippine Sea plate and have drifted at least 220 km westward towards the Ryukyu trench subduction zone since emergence in the late Miocene (Ota & Omura, 1992), which could have facilitated more dispersal to the Mariana Islands in the past. Future studies may test demographic models, including ancestral gene flow based on more samples from Guam.

2.4.3. Potential incipient speciation in Ogasawara

The population of *G. fascicularis* in Ogasawara could be an incipient new species. It has been isolated from its three potential sister populations in Ryukyu, Daito, and Guam for at least 109,000 generations (Fig. 2.5), which corresponds to roughly 3.8 M years at a mean generation time of 35 years. There is a large margin of error in these estimations since exact

mutation rate and generation time for our taxon was not known. However, several million years of divergence probably separate the three populations from its common ancestor. This amount of time may be sufficient for incipient speciation, since time to speciation across various organisms are estimated to lie between 100,000s to millions of years (Coyne & Orr, 2004). Although this rate may be slower in marine species (Palumbi, 1992) the estimated speciation rate for scleractinia since the Pliocene is 1–4 /M years (Simpson *et al.*, 2011), which would cover the hypothesized time span of isolation of 3.8 M years in Ogasawara. Moreover, the time to speciation is thought to be generally shorter in allopatry or peripatry (Norris & Hull, 2012), such as appears to be the case in our study, since only little amount of gene-flow was detected in our demographic analysis. Spatially driven speciation in the sea has been regarded to be less common than on land due to fewer dispersal barriers, supported by the seemingly abrupt and geographically random appearance of new species in respect to their sisters in the fossil record (Jablonski, 1986). However, morphological variation does often not correspond to species-level genetic differentiation in corals, including in *Galaxea*. Although more micromorphological, ecological, and reproductive studies are needed to confirm speciation, the extent of genetic differentiation found here potentially indicate incipient speciation. According to theory, two spatially diverged lineages in the sea may develop prezygotic reproductive barriers (behavioral, recognition) after secondary contact, and develop further postzygotic barriers, such as hybrid inviability upon new increased geographic separation after many thousands of generations through environmentally variable geologic times (Norris & Hull, 2012). To further investigate a potential speciation event, future work may focus on the genetic composition of *Galaxea* in the Mariana Islands, since the two lineages may have mixed in Guam (Fig. 2.3).

Because of the long divergence time, it is difficult to determine whether the *Galaxea* population in Ogasawara has originally arrived *via* the Izu or the Mariana route from the present sample set. The colonization from Ryukyu would be supported by the contemporary dispersal probabilities according to ocean currents (Fig. 2.6). Even though the temperate northern habitats along the Izu route seem challenging to overcome at present, much warmer climates in the recent past (Hansen *et al.*, 2013; Snyder, 2016) could have facilitated dispersal along this route during most of their divergence time. However, at present the Ogasawara and Ryukyu do not share the same ancestral lineages; rather it is Guam that was mixed in its genetic composition with the lineage in Ogasawara (Admixture analysis Fig. 2.3).Colonization from the Mariana Islands was also supported by the migration rates

estimated by demographic modeling (Fig. 2.5). Colonization from the Mariana Islands would imply that the lineage found in Ogasawara originated perhaps in Guam, has colonized Ogasawara, and later became mixed in Guam with another lineage now dominant in the Ryukyu Islands. Contemporary dispersal seems to support this route of colonization, as northward but no southward migration was found along the Mariana chain (Fig. 2.6), although this finding should be verified after including a complete habitat map of this region in the dispersal model (northern Islands along the Izu-Bonin Arch). However, the mixed pattern could also be a result of secondary, southward migration of the Ogasawara population, perhaps since the relatively recent emergence of the Northern Mariana Islands, which would mean that the Ogasawaran lineage originated in Ogasawara.

The two possible explanations for the mixed genetic composition in Guam could be tested by sampling additional populations between Ogasawara and Guam, or by demographic modeling with more data from Guam. Colonization from the Mariana Islands would predict that the genetic composition on the younger islands between Ogasawara and Guam would have similar or smaller percentages of the Ogasawaran lineage than in Guam, and that ancestral migration northward to Ogasawara would be stronger than at present. On the other hand, secondary southward migration of the Ogasawara lineage would predict a gradual decrease of the Ogasawaran lineage from north to south and recent asymmetric migration from Ogasawara southward. We tested the likelihood of ancient gene-flow or secondary admixture in dadi, which revealed the best likelihood for strong ancient gene-flow from Ogasawara to Guam (Table S2), contradicting both of the above hypotheses. The small sample size in Guam was probably insufficient to detect recent levels of gene flow accurately. More sequencing to higher coverage, using more specimens and/or specimens from islands along the Northern Mariana Islands are needed to resolve the directionality of the relationship between Ogasawara and Guam, and to finally conclude whether the Ogasawaran lineage could have been colonized from Guam or the Ryukyu Islands.

Chapter 3: Phylogenetic and biogeographic evolution of *Galaxea*

3.1. Introduction

Our understanding of coral diversity and diversification processes is still underdeveloped despite their fundamental role in one of the world's most diverse ecosystems. Even on the family level the taxonomy and evolutionary history of the scleractinia are not fully resolved (Romano and Cairns 2000, Fukami 2008, Kitahara et al. 2010) and less than half of all scleractinian species have been analyzed phylogenetically (Huang & Roy, 2015; Kitahara *et al.*, 2016). Meaningful species delimitations are the basis for phylogenetic inference and are crucial for the implementation of accurate conservation measures. However, traditional species delimitations based on macromorphological characters such as attributes of the polyp skeleton or colony shape were shown to not agree with genetic differentiation, and many taxonomic species may not represent evolutionary coherent entities (Romano and Cairns 2000, Fukami 2008, Kitahara et al. 2010). Genetically very divergent but morphologically cryptic species are common in the scleractinia (e.g. Combosch *et al.* 2008; Flot *et al.*, 2011; Ladner & Palumbi, 2012) and may have led to an underestimation of diversity in many genera. Genetic and morphological delimitations may also be inconsistent when compared between geographic region. In order to understand coral diversity, it is therefore important to not *a-priori* link genetic to morphological variation, especially across geographically wide ranges (Veron 1995). Using a phylogeographic approach, we here attempt to holistically analyze the relationships between morphological, spatial, and genetic differentiation using the genus *Galaxea* Oken.

Galaxea may be one of the genera, for which taxonomic species may not reflect biological species. The small Indo-Pacific genus is the phylogenetic sister of *Simplastrea* Umbgrove and together they form the sister group to *Euphyllia* Dana (Huang, 2012) (although some uncertainties regarding the monophyly of *Galaxea* in respect to *Euphyllia* exist (Kitahara *et al.*, 2016)). The genus was recently reclassified from Oculinidae to Euphyllidae (WoRMS, 2015). There are ten extant taxonomic species accepted to date (WoRMS, 2015)(Table 3.1), which are differentiated by colony branching patterns, the number of septa cycles, and size (Veron and Stanfford-Smith, 2000). From the seven taxonomic species the most common is *G. fascicularis* L., distributed from the Red Sea to Micronesia, which is also the evolutionary oldest species with a fossil record dated to the

Oligocene (PBDB, 2018). It occurs in all parts of the reef and is thought to be one of the 'climate change winners' due to relatively high resistance to bleaching (Marshall and Baird 2000). The second most common taxon is *G. astreata* Lamarck, which geographically overlaps with *G. fascicularis*. The other eight species are much rarer and seem to be restricted to South East Asia (Table 3.1) (Veron and Stafford-Smith 2000). While the phylogenetic relationships between the taxonomic species are unknown, there are three genetically divergent lineages alone in the taxon *Galaxea fascicularis* (Watanabe *et al.* 2005; Nakajima *et al.* 2016), indicating that the current species concept in *Galaxea* may not be correct.

Two distinct 'types' of *G. fascicularis* had originally been found in the Ryukyu Islands, Japan, and distinguished based on variation in the nematocyst anatomy (Hidaka 1992). These types were later observed to differ in the length of a mitochondrial non-coding region between the genes *cytb* and *ND2* (Watanabe et al. 2005) and to somewhat vary in their coenosteum density (Wewengkang *et al.*, 2007). This mitochondrial region differs by almost 300 bp between the types (457 bp vs. 167 bp), which is why they have been referred to types 'S' for 'short' and 'L' for 'long' (Nakajima et al. 2015). The two types are also differentiated in their nuclear DNA as was revealed by microsatellite markers (Abe *et al.*, 2008a; Nakajima *et al.*, 2015). Reproductive studies indicate that they differ in spawning time (Heyward *et al.*, 1987; Yamazato, 1988) and mostly do not cross-fertilize under laboratory conditions (Abe et al. 2008a). A third lineage 'L+' has been found from Kume Island, which has a three base pairs longer mitochondrial control region than type L and is differentiated in the nuclear genome from both the L and S type (Nakajima et al. 2016). All lineages occur side by side on the reef in the Ryukyu Islands, however, their geographic distribution elsewhere that could shed light on their evolutionary origins are unknown.

Different neutral and selective processes could have caused the differentiation between the three cryptic lineages in *G. fascicularis*. For example, historical geographic isolation could have caused their divergence in the past, and the currently observed sympatry in the Ryukyu Islands may be the result of a more recent breakdown of a dispersal barrier. The divergence could also be caused ecologically, for example through water depth segregation, such as observed in other coral genera (Prada & Hellberg, 2013; Serrano *et al.*, 2014). In order to infer potential divergence mechanisms, it is therefore crucial to conduct a geographically comprehensive sampling. Furthermore, more distinct cryptic lineages may be found in *G. fascicularis* in other parts of the taxonomic distribution range. Cryptic species are very common in coral genera, as already shown in *Stylophora* (Flot *et al.*, 2011), *Acropora*

(Ladner & Palumbi, 2012), *Pocillopora* (Combosch *et al.*, 2008), *Heliopora* (Yasuda *et al.*, 2014; Yasuda *et al.*, 2015), and *Seriatopora* (Warner et al. 2015).

To this end, morphologically and taxonomically variable specimens in *Galaxea* from the entire Indo-Pacific distribution range were gathered for a comprehensive phylogenetic investigation. Field collections were complemented with museum specimens to increase geographical coverage. We used restriction site-associated DNA (RAD) sequencing to genomically characterize the specimens on a fine resolution. In addition, we analyzed the characteristic mitochondrial control region to relate our results to previous studies. By comparing genealogies between nuclear and mitochondrial regions, indications for hybridization may also be detected. Hybridization is known to occur frequently in corals (Veron 1995, Willis et al. 2006) and its potential influence on phylogenetic inference needs to be considered in any systematic study of corals. We further investigated the depth distribution and colony morphology between the cryptic lineages in *G. fascicularis* in order to shed light on potential environment-driven causes for their sympatric existence.

Table 3.1. Currently accepted species in *Galaxea* by the World Register of Marine Species. The age refers to the oldest fossil record listed the Paleo Biology Database (PBDB, 2018) where available. Abbreviations: na = not available, SE= South East

Species	First description	Distribution	Abundance	Age [Ma]
G. fascicularis	Linnaeus, 1767. Systema naturae sive regna tria naturae, secundum classes, ordines, genera, species, cum characteribus, differentiis, synonymis, locis. Laurentii Salvii, Holmiae. 12th ed. v. 1 (pt 2): 1278	Red Sea, Indo-Pacific	common	20.43
G. astreata	Lamarck, J.B.d.1816. Histoire naturelle des Animaux sans Vertèbres, présentant les caractères généraux et particuliers de ces animaux, leur distribution, leurs classes, leurs familles, leurs genres, et la citation des principales espèces qui s'y rapportent; précédée d'une Introduction offrant la Détermination des caractères essentiels de l'Animal, sa distinction du Végétal et des autres corps naturels, enfin, l'exposition des principes fondamentaux de la Zoologie: Paris, Déterville & Verdière. p. 227	Red Sea, Indo-Pacific	common	11.6
G. horrescens	Dana, J.D. 1846. United States Exploring Expedition during the years 1838-1842. Zoophytes 7: 1-740. Lea and Blanchard, Philadelphia.	Central Indo-Pacific	uncommon	2.5
G. paucisepta	Claereboudt, M. 1990. Galaxea paucisepta nom. nov. (for G. pauciradiata), rediscovery	SE Asia	rare	7.246

	and redescription of a poorly known scleractinian species (Oculinidae). Galaxea 9: 1-8.			
G. cryptoramosa	Veron, J.E.N. 2000. Corals of the World. Vol. 1–3. Australian Institute of Marine Science and CRR, Queensland, Australia.	SE Asia	uncommon	na
G. longisepta	Veron, J.E.N. 2000. Corals of the World. Vol. 1–3. Australian Institute of Marine Science and CRR, Queensland, Australia.	SE Asia	rare	na
G. pauciradiata *(synonym* G. astreata*)*	Blainville, H. M. de 1830. Zoophytes. In: Dictionnaire des sciences naturelles, dans lequel on traitre méthodiquement des differéns êtres de la nature, considérés soit en eux-mêmes, d'après l'état actuel de nos connaissances, soit relativement a l'utlité qu'en peuvent retirer la médicine, l'agriculture, le commerce et les arts. Edited by F. G. Levrault. Tome 60. Paris, Le Normat. Pp. 548, pls. 68.	Red Sea	uncommon	5.5
G. acrhelia *(synonym* G. cryptoramosa)	Veron, J.E.N. 2000. Corals of the World. Vol. 1–3. Australian Institute of Marine Science and CRR, Queensland, Australia.	SE Asia	uncommon	7.246
G. alta	Nemenzo, F., 1979. New species and new records of stony corals from west central Philippines. The Philippine Journal of Science 108: 1-25.	SE Asia	na	na
G. negrensis	Nemenzo 1979. Hoeksema, B.; Cairns, S. (2018). World List of Scleractinia. *Galaxea negrensis* Nemenzo, 1979.	SE Asia	na	na

3.2. Materials and Methods

3.2.1. Specimens

In order to evaluate species definitions, including the taxonomic (morphological) and genetically derived phylogenetic relationships, *Galaxea* specimens were collected from various places across the Indo-Pacific distribution range of the genus. Field collections were gathered from the Red Sea (15, KAUST), Maldives (10), Chagos (10), the Great Barrier Reef (5) (University of Queensland), Western Australia (12) (Curtin University), Thailand (6) (Ramkamhaeng University), Taiwan (6) and Dongsha (6) (Academia Sinica), Japan (~158), Hong Kong (13) (University of Hong Kong), Samoa (5) (National Marine Sanctuary American Samoa), and Guam (9) (University of Guam). DNA or specimens were exported with the CITES permit numbers PWS2016-AU-001320, PWS2016-AU-001565, AC.0510.2/18836), or processed in country of collection. To further increase geographic

coverage, field collections were complemented with museum specimens from the Smithsonian Institution (18), the Naturalis Biodiversity Center in Leiden (2), and the Museum of the University of the Ryukyus Fujukan (16). All specimens used, including their sampling location and available meta data are listed in Appendix 3, Tables S3.1 and S3.2.

Taxonomic species identities were assigned to specimens using field photographs (Fig. 3.1) and remaining collection material where available (Appendix 3, Table S3.1). Two sources were considered, the widely cited 'Corals of the World' (Veron and Stafford-Smith 2000) and an unpublished taxonomic treatment given by van der Veer (2007). In *G. fascicularis*, primary and secondary septa are similar or same in size so that the number of primary septa appears irregular or extended. This feature can be observed through the coral tissue, which is why this taxonomic species may be readily identified in the field or from field photographs, together with the feature of massive and unbranching colony morphology. Specimens, for which colony growth form was laminar and in which polyps had unequal septa cycles of six uniform septa each, and were > 3.5 mm in diameter were assigned to *G. astreata.* Specimens that were similar to *G. astreata* but had smaller polyps (< 3.5 mm) with strictly 2 septa cycles, out of which the second did often not reach the columnella, were assigned *G. paucisepta.* The identification of these two species required the examination of polyp skeleton material (Appendix 3, Table S3.1). Specimens that were thinly branched and had small polyps shorter than the width of the branch they were sitting on were assigned *G. horrescens.* Specimens that exhibited any form of cryptic branching pattern were assigned *G. cryptoramosa* following (van der Veer, 2007). For specimens from Dongsha, Taiwan, and most from Western Australia no photographs were available to verify the taxonomic labeling given by the sample providers. However, all sample providers (Put Ang, Allen Chen, Atsushi Fujimoto, Veronica Radice, Zoe Richards, Mareike Sudek, Tullia Terraneo) were experienced coral biologists so that the labeling may be trusted.

The distinction between *G. astreata* and *G. paucisepta* is ambiguous and disagrees between the two taxonomic sources considered. According to Veron and Stafford-Smith (2000) both taxa have 2 septa cycles and are only distinguished by polyp diameter (more or less than 3 mm) and the ability of *G. astreata* to extend the laminar growth form to columnar. In contrast, van der Veer (2007) distinguishes the two taxa by the number of septa cycles, *G. astreata* having 3 and *G. paucisepta* having only 2 complete cycles, and only *G. paucisepta* exhibiting laminar growth. According to van der Veer (2007), there is no *G. astreata* in Okinawa, as none of the colonies are columnar. In contrary, following Veron almost all of the

same specimens match the description of *G. astreata,* as most grow laminarly and have 2 septa cycles, except for a few specimens with smaller polyps (<3 mm) that would be assigned to *G. paucisepta.* Despite the ambiguous delimitation, there seems to be two separate forms in the field occurring side by side. I followed Veron's description but lifted the size threshold for separation from 3 to 3.5 mm polyp diameter, since polyp sizes of less than 3.5 mm were often linked to small and potentially juvenile colonies. Further, *G. cryptoramosa* found in Okinawa sometimes exhibited laminar growth forms in the same colony, complicating the distinction to *G. asterata.* In this study, all colonies that were branching in some part of the colony were assigned *G. cryptoramosa.*

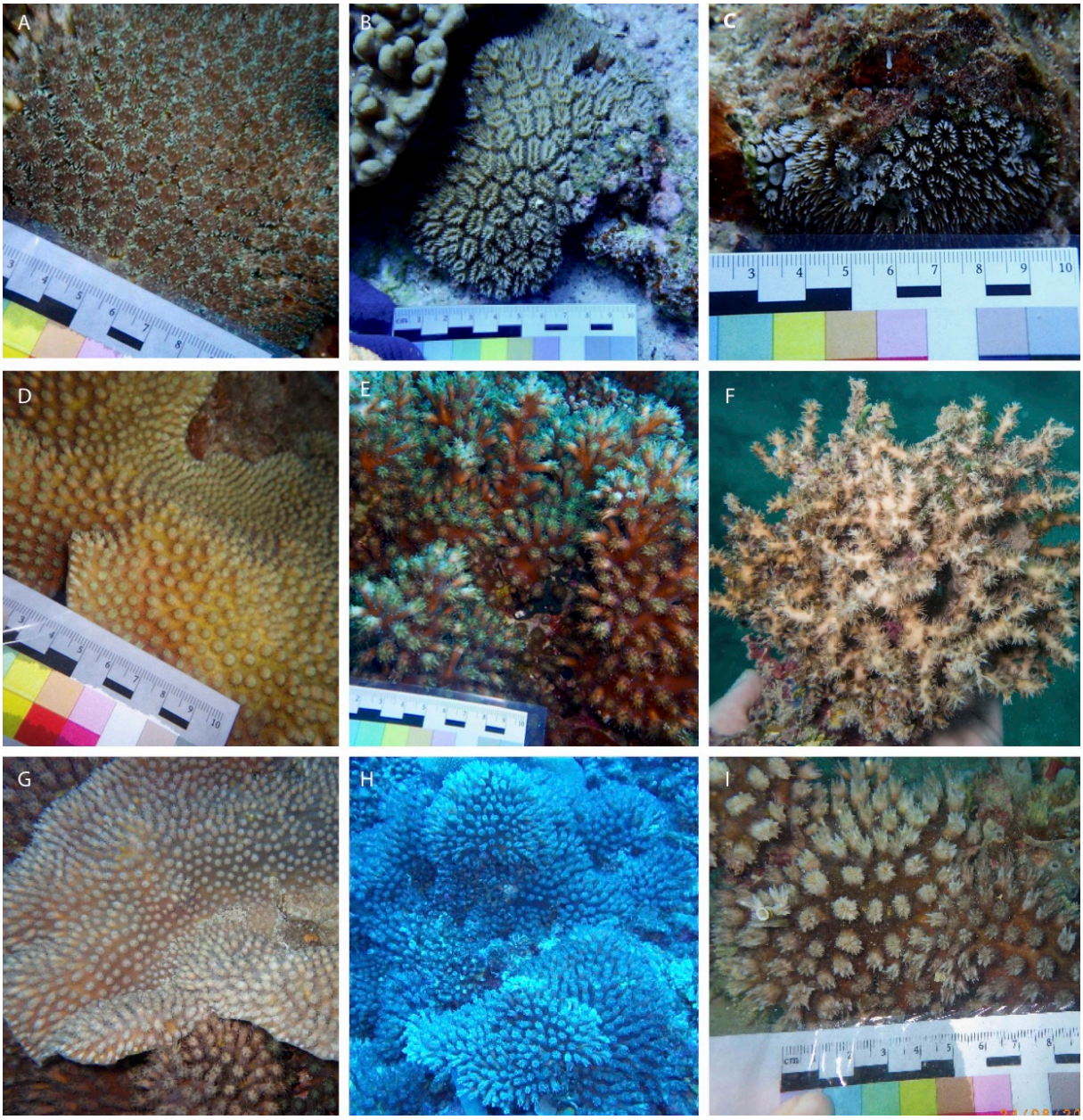

Figure 3.1. Example photographs of *Galaxea* specimens of different taxonomic species. A: *G. fascicularis,* lineage "S", PW575 from Seragaki; B: *G. fascicularis,* lineage "L", PW100 from Iheya, C: *G. fascicularis,* lineage "L+", PW42 from Miyako; D: *G. paucisepta,* PW571 from Seragaki; E: *G. cryptoramosa,* PW249 from Seragaki; F: *G. horrescens,* AF-3 from Guam; G: *G paucisepta* (overgrowing *G. astreata*), PW573 from Seragaki; H: *G. astreata,* PW572 from Seragaki; I: *G. astreata,* PW448 from Motobu.

Six outgroup specimens were added to the phylogenetic analysis for rooting purposes and to test for the monophyly of *Galaxea*. Three species within the "complex" clade of the scleractinia with two specimens each were chosen, including the closely related *Euphyllea* c.f. *ancora* and *Pachyseris* c.f. *speciosa* and two specimens of *Acropora digitifera* (Huang 2012).

3.2.2. DNA extraction

DNA from field collections were extracted as described in previously, however, for the extraction of ancient DNA from museum specimens, special precautions against contamination were necessary, as the yield is usually low and DNA is degraded. All tools were cleaned and sterilized with 10% bleach, 99% EtOH, and Bunsen burner in between processing of each specimen, and tubes and tips were autoclaved. To remove potential surface contamination from the dried specimens, skeleton pieces were soaked in 70% EtOH for 10 min to 1 h and air-dried. The QIAGEN DNeasy Blood and Tissue extraction protocol was adjusted to a larger quantity of extraction material of 0.2-1.3g per specimen and a longer denaturation incubation time of 18-22 h at 56 ºC with a larger amount of extraction buffer and protein kinase K (up to 10x more). After this step, the manufacturer's protocol was followed. Specimens from the Smithsonian Institution and the Naturalis Biodiversity Center Leiden were extracted and treated in collaboration with the ToBo laboratory at the Hawaii Institute of Marine Biology.

DNA was extracted from 40 museum samples that were satisfying the criteria of having sufficient material, being of acceptable quality (i.e. without visible mold or algal contamination), and not showing signs of chemical treatment for preservation purposes (i.e. smell of xylene). The extractions varied in yield and some of the samples showed signs of considerable DNA degradation (DNA fragments shorter than 500bp) when run on an Agarose gels. Based on DNA concentration and quality, 28 specimens were chosen for sequence analysis.

3.2.3. RAD-seq analysis

150 specimens were genotyped using RAD-tag sequencing. Libraries were prepared by the Ecological Genomics Pipeline (Economo & Mikheyev units). RAD-tag sequences are ideal not only for population genetics (Hohenlohe *et al.*, 2010) but also phylogenetic inference between recently diverged lineages (Emerson *et al.*, 2010). The protocol included single-digestion with the restriction enzyme EcoR1 and a size selection step (see (Tin *et al.* 2014) and previous chapter for more details). Libraries were single-end sequenced using the Illumina HiSeq platform. Raw reads were quality filtered and trimmed using Trimmomatic (Bolger *et al.* 2014). Loci were assembled in ipyrad software (Eaton 2015) based on partially assembled *Galaxea* reference sequences provided by the ReFuGe2020 consortium (Voolstra *et al.* 2015, Liew *et al.* 2016) and (Nakajima *et al.* 2015). Reads needed to be minimally 35 bp long to enter assembly analysis within ipyrad. A minimum depth of 6 and maximum depth

of 10,000 within samples were used for base calling. Only biallelic sites were considered. Maximally, four uncalled bases (Ns) and eight heterozygotes in consensus sequences were accepted. A locus needed to be represented in at least three samples and was allowed to have maximally 10 SNPs and 8 indels. Loci were trimmed at the 5' end by 5 bp because these contained too many and too inconsistently variable sites. From the mapping statistics, we then excluded individuals that had less than 1000 loci.

A phylogenetic tree was constructed from the SNP phylip output file with a maximum likelihood approach using ExaML v.3 (Kozlov *et al.*, 2015). Twenty random starting trees were generated using RAxML (Stamatakis, 2006) and given as input to ExaML. ExaML was run under the PSR model to find the most likely tree. Bootstrap analysis was performed with 100 iterations to estimate the likelihood of each node, creating bootstrapped alignments in RAxML and performing likelihood searches in ExML as described above. We used Booster (Lemoine *et al.*, 2018) to calculate branch supports. Booster implements a newly developed method of gradual distance measurements of branches between replicates and is thought to perform better for large datasets derived from next generation sequencing. The booster instability metric for each specimen is given in Appendix 3, Table S3.3.

3.2.4. Mitochondrial haplotype analysis

In addition, the *Galaxea* characteristic mitochondrial non-coding region between *cyt b* and *ND2* was analyzed by Sanger sequencing. Each polymerase chain reaction (PCR) contained 1ul of 8uM primers 188-1 3'-GAATAGGCTATACTAGCAGGTC-5' and 188-R3 3'-CATCATTATCCTCTTCAAGG-5', 2ul MilliQ water, 5ul AmpliTaq Gold Master Mix (Applied Biosystems, Thermo Fisher Scientific), and 1ul holobiontic DNA. The amplification protocol included an initial denaturation step of 95ºC for 9 minutes, 35 cycles of denaturation at the same temperature for 30 seconds, annealing at 54ºC for 30 seconds, an extension at 72ºC for 5 minutes, and a final extension at 72ºC for 5 minutes. Amplification success was evaluated in an agarose gel electrophoresis of similar size. PCR products of successfully amplified samples were cleaned with 1ul of 0.2x diluted Exo and 1ul of 0.2x diluted SAP per reaction, applying at 35ºC for 30 minutes followed by 80ºC for 15 minutes. Cleaned PCR products were sent for single-end sequencing to Macrogen Japan Corporation, except for 16 museum specimens from Fujukan, which were sequenced in-house. For these, 1ul of the cleaned PCR products were cycle-sequenced with 1ul 5x Sequencing Buffer, 1ul 3.2 pmol forward or reverse primers, 0.4 ul Big Dye and 6.6 ul MilliQ water, applying 96ºC for 1 min

for denaturation, 25 cycles of 10 seconds denaturation at the same temperature, 5 seconds for annealing at 50ºC and 4 minutes for extension at 60ºC. The cycle sequencing products were cleaned by ethanol precipitation and sequenced in an ABI sequencer. In total 135 specimens were sequenced.

DNA sequences were examined and processed using Geneious v. 9.1.2. Low quality base calls at the ends and primer sequences were removed. Some specimens, especially the museum specimens, showed signs for containing multiple haplotypes, i.e. both the longer L and shorter S sequences, resulting in double peaks in the DNA chromatograph. For these specimens (indicated in Appendix 3), only the dominant sequences were taken, if the peaks were an order of magnitude larger than those of the minor background sequence. Those samples were included in the analysis if one of the alternative sequences was identical to one of the other haplotypes and clearly more dominant than the others. Sequences of too low quality were removed entirely. The cleaned sequences were aligned to each other and previously published haplotype sequences by Watanabe *et al.* (2005), who has described five L-haplotypes LA-LE and three S-haplotypes SA-SC, and Nakajima *et al.* (2016), who published Watanabe *et al.*'s LA and SA sequences plus the sequences of two more L-haplotypes LF and L+ on Genbank (accession numbers LC155810 - 3). TCS haplotype networks were drawn using TCS v. 1.21(Clement *et al.*, 2002) and PopART (Bandelt *et al.*, 1999), and edited in Adobe Illustrator. A map showing the geographic distribution of the haplotypes was drawn using PopART software (Fig. 3.2).

3.2.5. Morphological and depth-differentiation between lineages of *G. fascicularis*

In order to infer any indications for potential ecological evolution between the three lineages L, S, L+ in *G. fascicularis*, we compared their depth distribution and morphology in some more detail. The lineages L and S were shown to differ in nematocyst morphology (Watanabe *et al.*; 2005), but not in tissue color (Wewengkang *et al.*, 2007), however, skeletal features have been examined less. To this end, we first identified the mitochondrial type of another 370 *Galaxea fascicularis* specimens collected from Japan and Thailand by fragment length analysis (Appendix 3, Table S3.1), following (Nakaema & Hidaka, 2015). Specimens were assigned type L if they had a fragment size of 457 bp, S if their fragment size was 167 bp, and L+ if their fragment size was 460 bp. Specimens with equally abundant multiple fragment sizes were excluded from the analysis. Specimens for which lineage identity was also identified with RAD data were marked as such (Fig. 3.3, 3.4).

We assessed depth distributions between the lineages based depth recordings of 176 specimens from Japan and 157 specimens from Thailand. Depth of occurrence was recorded for each specimen during field sampling using a dive computer (Scubapro Chromis). The reading was corrected for the tidal level of the sampling site at the time of collection to represent average depth. The distributions were visualized by boxplots for each sampling site and lineage separately (Fig. 3.3).

Colony morphology was quantified using 157 specimens from the Ryukyu, Daito and Ogasawara Islands using field photographs. Polyp maximal diameter, polyp minimal diameter, and distances between the polyps were measured using Fiji software (Schindelin et al. 2012). For each trait, 3–10 measurements were taken from fully-grown, typical polyps of the colony and averaged within a specimen. Fractions of minimal and maximal diameters were calculated and referred to as 'shape', and relative distances between polyps were calculated as fractions of measured distance to maximal diameter ('dist.rel'). A principal component analysis (PCA) was performed to depict morphological variation in two dimensions using the morph.pca function, and plotted with the ggbiplot function in R (Fig. 3.4). Variation in maximal polyp diameter between the lineages was additionally tested in a Kruskal-Wallis rank sum test, after confirming a non-normal distribution of this trait in a Shapiro-Wilk normality test. All analyses and plotting were done in R (R Development Core Team 2015) and edited in Adobe Illustrator.

Septa cycles were examined based on remaining collection material for 83 specimens with available material (Appendix 3, Table S3.1), including the number of septa cycles and their size proportions to each other. In addition, 8 specimens (Table 3.2) were chosen for micro-computer tomography (CT) in a ZEISS Xradia 5xx Versa to quantify the ratio of skeleton to open space in individual corallites. Individual polyps were bleached and dried prior to scanning. The 3D representation was reconstructed in Zeiss XM3DViewer and loaded into Amira v.6 software for virtual segmentation of skeleton and intra corallite air space. The volume ratio without air spaces to total volume including air spaces was taken as an indication for skeleton density and compared between the lineages L, S and L+.

3.3. Results

3.3.1. RAD-seq phylogeny and mitochondrial haplotype diversity

The RAD-seq analysis revealed 471 000 variable sites that were shared by more than 4 individuals. Unfortunately, most museum specimens (26), except for two from Tanzania and Indonesia, had to be discarded due to insufficient data (less than 1000 loci). Further five specimens from Miyako (1), Taiwan (2), Daito (1), and Chichi Island (1) also had to be discarded for the same reason. The phylogeny revealed that *Galaxea* is monophyletic in respect to the outgroup genera *Euphyllea, Pachyseris*, and *Acropora*, and clustered into three well-supported main clades (Fig. 3.2). The first clade was only found in Chagos and was basal to the other two clades. The second clade contained specimens from the Red Sea, the Indian Ocean, and the central Indo-Pacific (hereafter referred to as 'Indo-Pacific Clade'), and the third clade contained specimens from the central Indo-Pacific and all other parts of the Pacific (hereafter referred to as 'Pacific clade'). Within these main clades, specimens cluster according to geographical closeness. In the Indo-Pacific clade, individuals from the Red Sea are the phylogenetic sister to an Indian Ocean group and a clade containing samples from Asia and Australia. In the Pacific clade, the L+ - lineage formed a strongly supported clade basal to all other specimens, followed by the taxonomic species *G. horrescens.* The remaining specimens within this clade grouped to a south-eastern Pacific subclade, with specimens from Samoa and the Great Barrier Reef, and two subclades containing Western Australian and Asian specimens, respectively. An exception in the geographical structuring represented a specimen from Thailand PW297 in the Indo-Pacific clade, which was basal to all other individuals in this clade. The node support values were generally high for the deeper nodes (0.8-1) but nested, terminal clades within geographic locations had usually very low values (<0.7). Notably, all islands of the Ryukyu archipelago were mixed, and all sub clades had low supports, except for clusters of clones (for example Iheya_PW103, 100, 110, 112, 114, 117).

Taxonomically, the basal clade from Chagos and the Indo-Pacific clade consisted entirely of *G. fascicularis.* The Pacific clade contained *G. fascicularis* and all other taxonomic species included in this study, except for one specimen *G. astreata* with uncertain species identification from western Australia (no specimen photograph available). *Galaxea horrescens* was monophyletic, including specimens from Guam and Western Australia. *Galaxea paucisepta* and *G. cryptoramosa* clustered together and were distinct from other specimens from Okinawa. *Galaxea fascicularis* and *G. astreata* were polyphyletic.

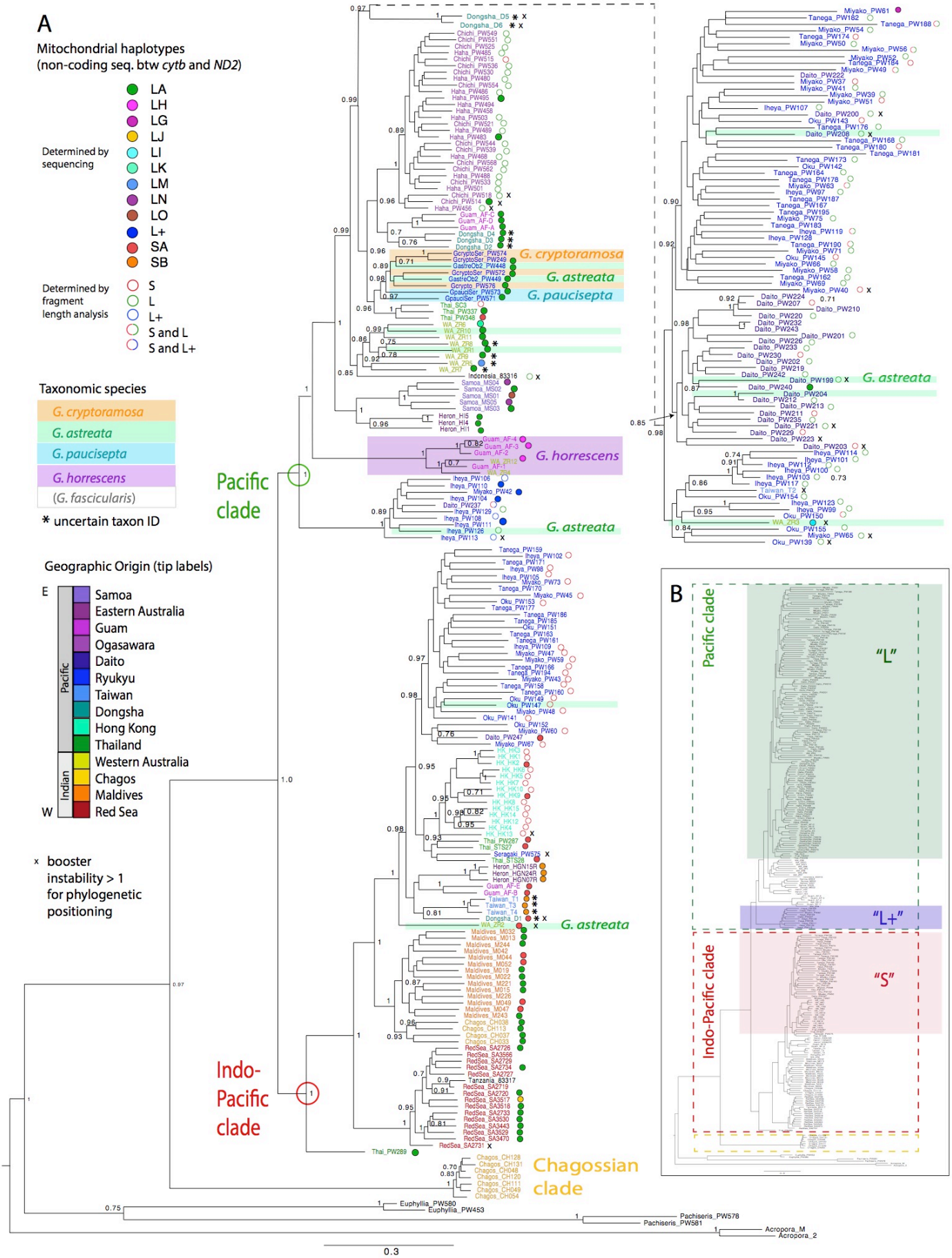
A
Mitochondrial haplotypes
(non-coding seq. btw cytb and ND2)
Determined by sequencing
LA
LH
LG
LJ
LI
LK
LM
LN
LO
L+
SA
SB
Determined by fragment length analysis
S
L
L+
S and L
S and L+
Taxonomic species
G. cryptoramosa
G. astreata
G. paucisepta
G. horrescens
(G. fascicularis)
* uncertain taxon ID
Geographic Origin (tip labels)
E
W
Pacific
Indian
Samoa
Eastern Australia
Guam
Ogasawara
Daito
Ryukyu
Taiwan
Dongsha
Hong Kong
Thailand
Western Australia
Chagos
Maldives
Red Sea
x booster instability > 1 for phylogenetic positioning
Pacific clade
Indo-Pacific clade
Chagossian clade
G. cryptoramosa
G. astreata
G. paucisepta
G. horrescens
G. astreata
G. astreata
B
Pacific clade
"L"
"L+"
Indo-Pacific clade
"S"
Euphyllia_PW580
Euphyllia_PW453
Pachiseris_PW578
Pachiseris_PW581
Acropora_M
Acropora_2
0.3

Figure 3.2. (previous page) RAD-seq phylogeny of *Galaxea.* Tip labels are colored according to geographic region and circles represent the mitochondrial haplotype retrieved by Sanger sequencing (filled circles) or fragment length analysis (empty circles, A). The insertion (B) shows the overview topology marking major clades and the cryptic lineages in *G. fascicularis.* All tips are *G. fascicularis,* except for the tips in colored background boxes in A, and asterisks (*) mark specimens with uncertain taxonomic species identification due to lacking sampling or specimen photographs. Node supports are given as Booster distances based on 100 bootstrap replicates, and crosses (x) mark specimens with booster instability >1 (Appendix 3: Table S3.3).

The cryptic lineages in *G. fascicularis* were split between the main clades; lineage S was contained in the Indo-Pacific clade, and lineages L and L+ were contained in the Pacific clade. However, the mitochondrial haplotypes mapped inconsistently to these clades. The Pacific clade consisted of type LA and most other subtypes of L, except for subtype LJ, which was found in the Red Sea. The Indo-Pacific clade contained both L and S haplotypes, with most Asian specimens containing haplotypes SA or SB, and the specimens from the Indian Ocean and the Red Sea containing mostly LA.

Across all locations and taxonomic species, 14 mitochondrial haplotypes were found, two haplotypes that were 135 bp short (S subtypes) and 12 haplotypes that had the longer 467 bp (L subtypes) or 470 bp (L+) sequences (Fig. 3.3). LA-LE, SA, and SB were previously reported by (Watanabe *et al.*, 2005), and the sequences LF, SA and L+ correspond to the sequences L2, S1, and L+ found by Nakajima *et al.* (2016). The other sequences have not been reported previously and were submitted to Genbank (accession numbers MK054259 - MK054269). LA and SA were the most widely distributed and most frequent types. The second SB subtype was common in Taiwan and in the Great Barrier Reef. Most L subtypes (LG-LP,) were rare and only found once from a single location, with the exceptions of LH which was common in *G. horrescens*. The specimens from Chagos in the basal RAD-seq clade could not be amplified in this marker (multiple bands of the PCR product in gel electrophoresis) and were not sequenced. This included the specimens CH048, CH049, CH054, CH111, CH120, CH128, and CH131.

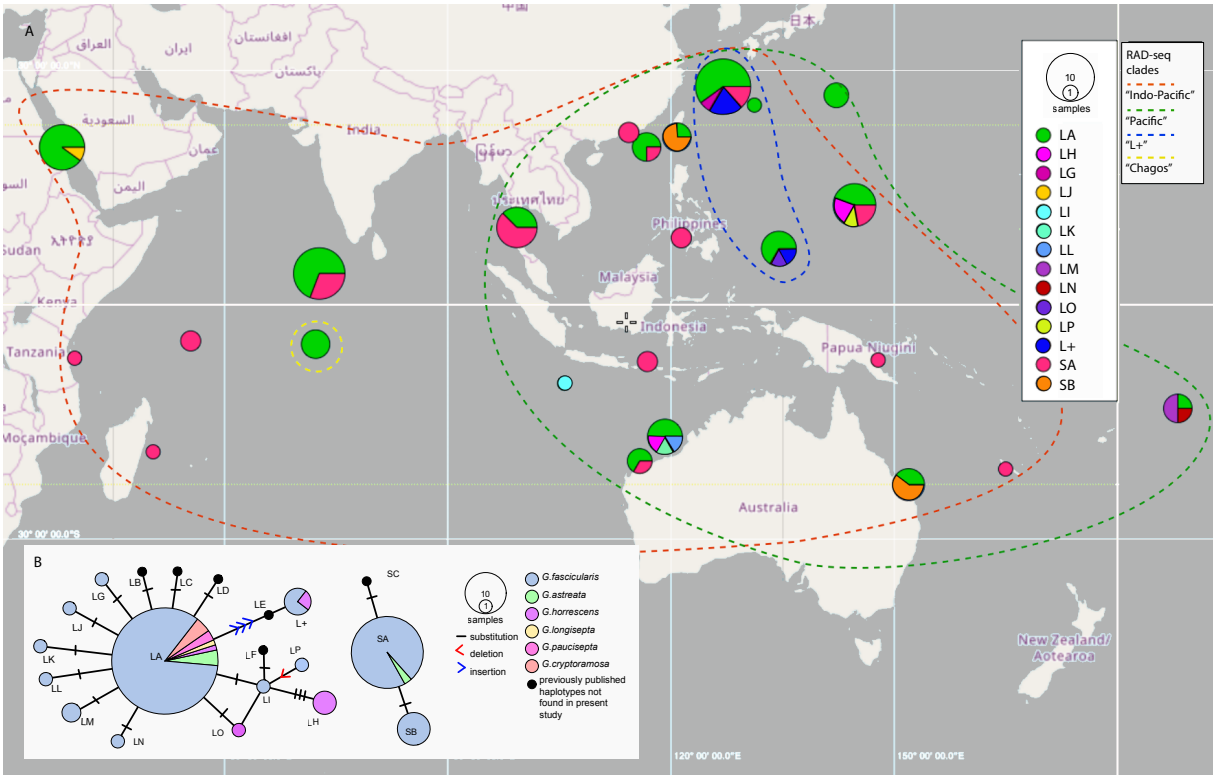

Figure 3.3. Geographic (A) and taxonomic (B) distribution of mitochondrial haplotypes in *Galaxea.* LA is the ancestral and most widely distributed haplotype. Most taxonomic species other than *G. fascicularis* contain haplotype LA, except for *G. horrescens,* which contained LH, and L+, and *G. astreata*, in which one specimen contained SA. The mitochondrial haplotype sequence consists of the non-coding region between *nt2* and *cytb.* The distribution of the major RAD-seq clades is shown by dotted lines.

3.3.2. Depth distribution and morphological variation between lineages in *G. fascicularis*

Within sampling sites, no obvious difference in depth distributions between the lineages S, L, and L+ were found (Fig. 3.4). However, in Thailand the sampling sites differed in the relative abundances of S and L. Sites in Trat were shallower and had more S than the L type, whereas sites in Chumphon were generally deeper and had more of the L type.

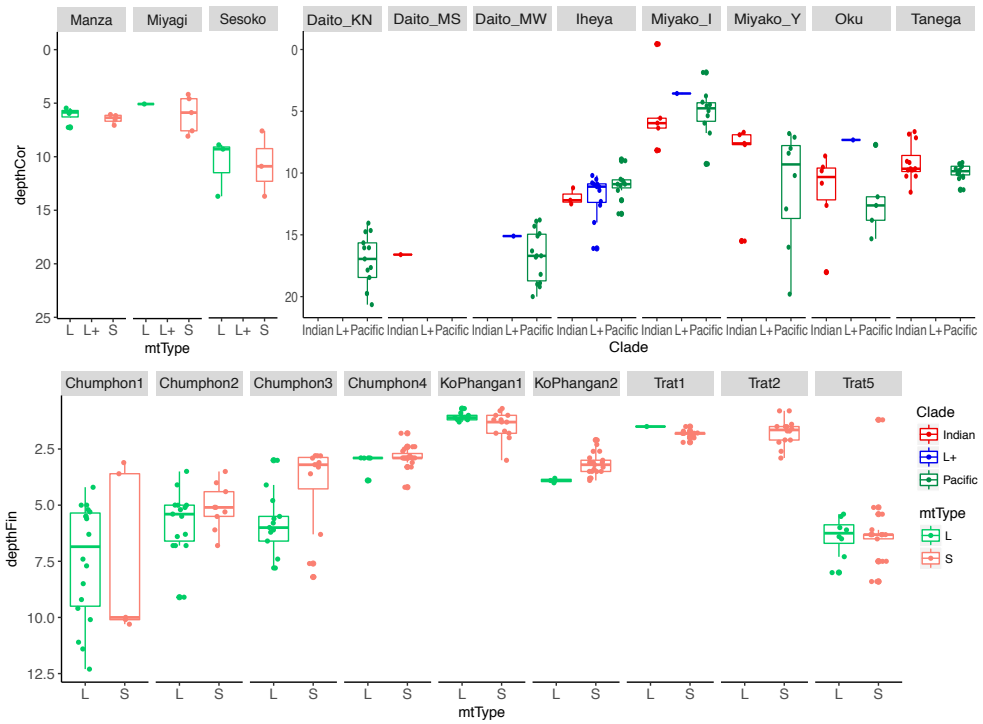

Figure 3.4. Depth distribution of cryptic lineages in *G. fascicularis* per sampling sites in Japan and Thailand. Lineages generally do not vary in their depth distributions. Specimens for which only mitochondrial data was available are colored in a lighter shade (mt-L, mt-S), specimens with RAD-seq information were colored in a darker shade (Indian = contained in the Indo-Pacific clade, Pacific = contained in the Pacific clade).

The three lineages L, L+, and S in *G. fascicularis* had overlapping variable spaces in the two-dimensional PCA, which explained 84% of the total variation (Fig. 3.5). However, lineage L may grow larger polyps, which tend to be slightly more asymmetric (more ellipsoid than circular) than the other lineages, as visible from its spread into positive direction along the first axis (PC1) corresponding to polyp size, and negative direction along the second axis corresponding to shape. The non-parametric Kruskal-Wallis test detected a significant difference in maximal polyp diameters between genetic lineages (chi-squared = 31.879, df = 2, p-value = <0.001), however, shape was not significant. The number of septa cycles or septa shapes were variable but did not differ between the three lineages. The CT scans resulted in a small difference of skeleton density between the lineages from the eight specimens measured, with lineage L, having larger air spaces or thinner walls in the corallite on average than lineages S and L+, resulting in smaller ratios of skeleton only and total corallite volume in the L type than in the other two types (Table 3.2).

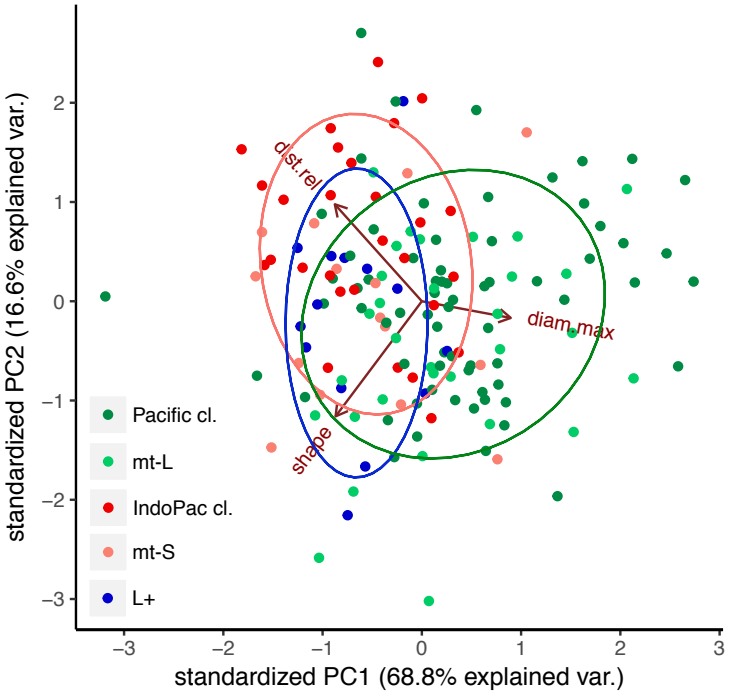

Figure 3.5. Morphology principal component analysis on lineages L (or 'Pacific clade;), S (or 'Indo-Pacific clade'), and L+ in *G. fascicularis* from the Ryukyu Islands. Mitochondrial type L grows somewhat larger polyps than the other lineages. Specimens for which only mitochondrial data was available are colored in a lighter shade (mt-L, mt-S). Abbreviations: diam.max = maximal polyp diameter, dist.rel = space between polyps, shape = ratio of shorter to longer polyp diameter.

Table 3.2. Skeleton density as measured by X-ray micro-computed tomography. The ration skeleton/total refers to the ratio between the volumes measured for the skeleton only without the air cavities and the total volume including air cavities. Specimens marked with an asterisk (*) represent clones.

Specimen	Source location	mtType	Skeleton/total	Example section
PW112*	Iheya	L	0.774	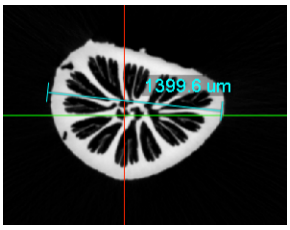
PW117*	Iheya	L	0.696	
PW107*	Iheya	L	0.677	
			mean: 0.716	
				PW112
PW116	Iheya	L+	0.935	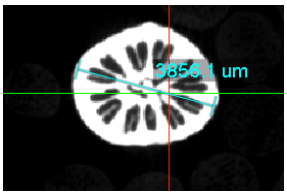
PW121	Oku	L+	0.807	
PW110	Iheya	L+	0.768	
			mean: 0.837	
				PW116
PW79	Miyako	S	0.830	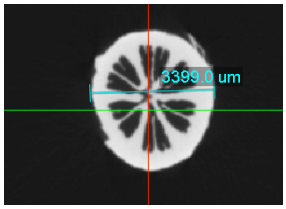
PW64	Miyako	S	0.730	
			mean: 0.780	
				PW64

3.4. Discussion

We investigated genetic differentiation in the genus *Galaxea* in the Indo-Pacific and assessed morphological variation and depth distribution between the cryptic lineages of *G. fascicularis.* We found that the genus is monophyletic and clustered into three distinct clades, an Indo-Pacific, a Pacific, and a basal clade represented in Chagos. The cryptic lineages in *G. fascicularis* were found to be highly divergent belonging to separate clades, the lineage S to the Indo-Pacific clade, and lineages L and L+ to the Pacific clade, respectively. No difference in depth distribution but some indications for morphological differentiation between the lineages exist in Okinawa. The taxonomic species and mitochondrial haplotypes only partially match the genomic divergence in the genus.

3.4.1. Origins and relationships between lineages L, S, L+ in *G. fascicularis*

The lineages L, S, L+ previously described from the Ryukyu Islands (Hidaka 1992, Watanabe et al. 2005) were genetically highly divergent and belonged to two different clades

in the genus phylogeny (Fig. 3.2). Lineages L and L+ were more closely related to each other than to lineage S and cluster exclusively with other Pacific specimens, indicating that these lineages have originated in the Pacific. Out of the two, lineage L+ was much rarer and could only be confirmed from the Ryukyu Islands and in one museum specimen of *G. horrescens* from Palau. Lineage S from the Ryukyu Islands, however, was more closely related to samples from the Red Sea and the Indian Ocean than to the other sympatric lineages, indicating that lineage S could have originated in the Indian Ocean and has only recently migrated into the Pacific. In the Pacific, lineage S was found in Thailand, Hong Kong, Dongsha, Taiwan, the Ryukyu Islands, and the Great Barrier Reef, but not in more disconnected and distant places like the Ogasawara Islands and Samoa. The Ogasawara Islands, for example, are disconnected from other Pacific islands (see previous chapter) and are known for their small coral species richness (Inaba 2004). Even in the Daito Islands, there was only one specimen out of more than thirty collected that belonged to lineage S. This suggests that lineage S could perhaps not have had enough time since its more recent immigration into the Pacific to disperse to these isolated places in detectable quantity, yet. Alternatively, both lineages could have inhabited the Pacific for similar times, but lineage L may have higher dispersal capabilities than lineage S. The often less dense coenosteum in lineage L (Hidaka 1992, Wewengkang et al. 2007) could result in more frequent fragmentation, which perhaps allows further dispersal by rafting than by larval dispersal alone (Thiel & Haye, 2006). However, the coenosteum density does not always predict the genetic lineage but could also be related to the environment (Wewengkang *et al.*, 2007), favoring the first of the two explanations.

The investigation of corallite characteristics in *Galaxea fascicularis* gave some indications for morphological differentiation between the lineages L, S, and L+ in the Ryukyu Islands. Lineages S and L+ seem to have smaller polyps and thicker corallite walls than lineage L, consistent with previous observations of softer and harder corallites in lineage L and S, respectively (Wewengkang et al. 2007). Unfortunately, genomic lineage information had not been available at the time of measurement and all specimens of the mitochondrial L type turned out to be clones. Further studies increasing the number of genomically identified specimens are needed to verify the observed trend in corallite wall thickness. The morphological differences are likely to be independent from depth of occurrence, because the lineages do not differ in their depth distribution (Fig. 3.4). Although in Thailand, a difference in depth distribution was found between the lineages, this was also correlated with sampling

site, indicating that other factors could be responsible for the found pattern. For example, the mass bleaching event in 1998 affected shallow regions within the Gulf of Thailand more than deeper regions (Yeemin *et al.*, 2009), which could have caused a selective dying of only one of the lineages. However, this is entirely speculative at this point and more investigations on differential environmental vulnerability between the lineages are needed to further develop this hypothesis. Whether there is an ecological differentiation between the two lineages in other microhabitat habitat characteristics than depth is not known so far, however, their phylogeographic distribution patterns and their similar morphology indicate that the two lineages have originated through long lasting ancient isolation instead of selective processes like habitat specializations. It was observed that the lineages have different spawning times in Okinawa (Heyward *et al.*, 1987; Yamazato, 1988), which could have prevented extended admixture since the breakdown of a historical dispersal isolation barrier, however indications for introgression exist from mismatches between the RAD (mostly nuclear) and mitochondrial data in some specimens (Fig. 3.2).

The mitochondrial haplotypes did not always correspond to the genomic differentiation between lineages L and S. About half of the specimens from Daito, a few from Miyako, and one from Ogasawara that genomically clearly belonged to lineage L contained the mitochondrial S haplotype (Fig. 3.2), suggesting introgressive gene flow (Moore, 1995; van Oppen *et al.*, 2001a). Fertilization success between the lineages has been tested in the laboratory by (Abe *et al.* 2008a), where the success between female lineage S (referred to as the hard type 'H') and male lineage L (referred to as the soft type - 'S') was significantly higher than the other way around. This is consistent with our observations particularly from Daito, where almost all specimens were genomically lineage L but many of them contained the mitochondrial haplotype S (Fig. 3.2). As mentioned above, the colonization of the isolated Daito islands by lineage S could be a recent phenomenon, and due to their isolation migratory connections to other islands in Okinawa are weaker. This may explain why the presence of lineage S is still primarily detected in the mitochondria of hybrid offspring in more isolated places like the Daito and Ogasawara Islands. Introgression between coral species is a common phenomenon and present in many groups, for example in *Acropora* (van Oppen *et al.*, 2001a; Ladner & Palumbi, 2012), fungiids (Gittenberger *et al.*, 2011), and *Pocillopora* (Combosch & Vollmer, 2015). Future research could test for genomic signs of hybridization between lineages L and S using for example *D*-statistics (Durand *et al.*, 2011).

Although apart from potential signs for introgression the genomic and mitochondrial data correlated relatively well in the Ryukyu Islands and other parts of Asia as expected from previous studies (Nakajima *et al.* 2015, Nakajima *et al*. 2016), this was not always true in the rest of the genus distribution range. In the Indian Ocean and the Red Sea specimens that were genomically closer to what was known as 'lineage S' usually also had haplotype L1. This indicates, that haplotype L1 could be the ancestral type of *Galaxea* and the characteristic deletion observed in the Pacific lineage S may have been coupled with its (recent) migration into the Pacific. Regardless of the point in time, the mitochondrial deletion in lineage S has probably happened only once shortly after immigration into the central Indo-Pacific, since there are no intermediate lengths and all specimens of lineage S in the Pacific contain this deletion. Most recently, lineage S could have begun to spread back into the central Indian Ocean, as indicated by a few Maldivian specimens containing the mitochondrial haplotype S1 (Figs. 3.2) and other individual museum specimen from the Indian Ocean (Fig. 3.3). In general, the investigated mitochondrial region was much more conserved compared to the rest of the genome and may not be sufficient to distinguish lineages or to represent diversity in this genus adequately. Evolutionary rates in mitochondria are known to be slow in corals (Shearer *et al*. 2002), and our results suggest that they could be inconsistent within the same genus, as mitochondrial diversity was higher in the Pacific clade than in the Indo-Pacific clade.

3.4.2. Biogeographic evolution of *Galaxea*

Explanations for the distribution and divergence histories of the major diversity patterns in scleractinia may be derived from the geologic history and well-preserved fossil record (Keith *et al.*, 2013). The fossil record indicates that *Galaxea* has originated in the Cenozoic, with the oldest occurrence dated to 33.9–28 Ma (stem group age) found in Jamaica, Iran, and Florida (PBDB 2018). Since the early Miocene 23–20 Ma and coinciding with the closing Tethys (Rögl, 1998), *Galaxea* has been extinct in the Atlantic and restricted to the Indo-Pacific. This is also from when the first records of the taxon *Galaxea fascicularis* were found in Indonesia, Fiji, Iran, and Australia. A record from Hawaii from the mid Miocene indicates that *Galaxea fascicularis* may have had its full (or bigger than) present range by 11 Ma (since it is not present in Hawaii to date). It is possible that the basal and rare clade found in Chagos is a relic from these early Miocene times, when the rotating African plate has caused considerable variation in marine dispersal barriers around the Middle Eastern and Mediterranean region (Rögl 1998). The existence of this basal clade indicates that the center of origin of *Galaxea*

may be located in the western Indian Ocean, similar to in *Stylophora* (Flot *et al*. 2011). It is curious that this clade was found only in Chagos. In *Stylophora* specimens from Chagos grouped with Madagassy and South-East African specimens, while specimens from the Red Sea grouped with Mid-Eastern African specimens (Keshavmurthy *et al.*, 2013). Consistent with the pattern, the museum specimen from Tanzania in this study clustered with specimens from the Red Sea (Fig. 3.2). Future research including more *Galaxea* specimens from the South-Eastern African coast and Madagascar may find more representatives of this basal clade from Chagos.

The divergence between the Indo-Pacific and Pacific clade may be a result of periods of restricted water flow between the Indian and Pacific Oceans during the late Miocene or Pliocene. The South-East Asian region has been tectonically dynamic throughout the Cenozoic era (Hall & Holloway, 1998), which is regarded to be an important driver of allopatric speciation in many marine organisms (Carpenter *et al.*, 2010). While the Australian plate was much further south during the late Oligocene (panmictic Tethys), it has moved up and has restricted marine dispersal towards the late Miocene, perhaps at times completely isolating the two basins in the Pliocene (Hall and Holloway 1998). The fossil record of other taxonomic species could also link to the divergence time between the two clades, as the morphological diversification in this genus seems to be a trait associated with the Pacific clade (Fig. 3.2). The oldest record of *Galaxea astreata* is from 11 Ma and was found in Fiji, *G. paucisepta* and *G. acrehelia* appeared at 7 Ma in Indonesia, and *'Acrhelia horrescens*' (synonym *G. horrescens*) was identified from 2.5 Ma in the Ryukyu Islands. Although the record of *G. astreata* should be treated with caution since the delimitation to *G. fascicularis* is not consistent, the record of *G. acrhelia* at 7 Ma suggests that the divergence between the Indo-Pacific and Pacific clade could be at least 7 M years old. The invasion of the Indo-Pacific clade by what we today see as lineage S into the Pacific could have been linked to the higher sea levels in the Pleistocene reconnecting the ocean basins again through the Indonesian flow through (Hoeksema, 2007). There were several climatic cycles since, and whether the invasion happened after the last glacial maximum (~ 15 000 a) or before cannot be inferred at this point and requires further analysis.

The morphological diversity in *Galaxea* is highest around the Coral Triangle, as it is in the majority of the Indo-Pacific coral genera (Veron & Stafford-Smith, 2000), and the highest morphological diversity was found in the Pacific clade. *Galaxea horrescens* out of the six taxa examined was the best-defined species, as specimens from multiple locations

formed a monophyletic clade based on the RAD data and were distinct also in their mitochondrial haplotype (mostly LH). Although the interpretation of branch lengths from this kind of data (SNPs) is tricky, the relatively long shared branch at their base indicates a long divergence time that started close to when the Indo-Pacific and Pacific clade started to diverge (Fig. 3.2). *Galaxea horrescens* has, in contrast to the other divergent lineages in this genus (linage L, S, L+, Chagossian), a fundamentally different ecological niche, given its branching growth form and brooding reproductive mode (Fadlallah, 1983). Its emergence could therefore be more related to ecological processes of speciation than neutral divergence. The other branching species *G. cryptoramosa* was only distantly related to *G. horrescens*, indicating that branching colony morphology has evolved multiple times in this genus. However, this hypothesis needs further investigation with more specimens of *G. cryptoramosa* from other locations, as well as the other branching species *G. acrhelia* (although van Veeren has synonymized this taxon with *G. cryptoramosa*). *Galaxea astreata, G. cryptoramosa,* and *G. paucisepta* in Okinawa were separate to *G. fascicularis* collected from the same island. These morphological species of *Galaxea* may be evolutionary relatively young, as they were molecularly undifferentiated in Okinawa. However, how these specimens relate to other conspecific individuals, for example from their respective type areas (all within Coral Triangle), remains to be analyzed in future studies.

3.4.3. Taxonomic implications and final remarks

The present study showed that *Galaxea fascicularis* is polyphyletic in respect to the other taxonomic species in *Galaxea.* The different lineages in this taxon tend to differ in polyp size and shape, but no other septa characteristics varied. Future studies may find more soft-tissue characteristics other than nematocyst length (Hidaka *et al.*, 1992) in order to eventually update the species description of the original *G. fascicularis* and to extend the genus by at least three more species (Chagos, L+, S, or L). *Galaxea horrescens* may be the only 'good' species recognized in this genus. For all other taxonomic species, more specimens needed to make taxonomic suggestions. Particularly problematic is *G. astreata,* for which the name is used inconsistently (Van der Veer, 2007; Veron & Stafford-Smith, 2000). Examination of type material is necessary to decide about the original morphological delimitation of this taxon.

A clear limitation to this study is the lack of any specimens from within the Coral Triangle, which is related to the challenging legal and administrative procedures to obtain

research permits in the involved countries. Policies that have originally been created to protect biodiversity are now increasingly causing limitations of basic biodiversity research (Prathapan *et al.*, 2018). What has already been shown for the Nagoya protocol also applies to the CITES (Convention on International Trade in Endangered Species of Wild Fauna and Flora) regulations. International and collaborative efforts to reveal true biodiversity patterns should be facilitated rather than hindered, in order to understand and address problems affecting biodiversity on a global level, such as global mass coral dying due to global climate change.

Conclusions

On the example of the genus *Galaxea,* this thesis investigated different aspects of coral diversity, which together may contribute to a better understanding of coral evolution in general. Based on a genus-wide sampling across the Indo-Pacific I showed that *Galaxea* is composed of three genetically highly divergent but morphologically little differentiated clades. These clades may have diverged during long times of allopatric isolation according to major changes in the seascape, such as the closure of the Tethys, the approximation of the Australian and Asian plate, and fluctuations in the flow-through between the Indian and Pacific Oceans. The morphological diversification, particularly in colony growth form, was associated with the Pacific clade and may have occurred relatively recently at the beginning the Pliocene (*G. horrescens*) or later (other taxa included here). This highlights the importance of a complete geographic sampling for detecting true diversity patterns in corals, and the necessity to investigate beyond the taxonomic species boundaries for revealing the evolutionary history of a genus (sampling focusing only on taxonomic completeness may not have detected the Indo-Pacific and Chagossian clades). The 'cryptic' lineages of *G. fascicularis* found in Okinawa (L, S, L+) were associated with different clades, and their sympatry in the central Indo-Pacific may be a recent phenomenon. Indications for introgression between the lineages clearly exist, suggesting that even after at least 7 M years of isolation, reproductive barriers are not completely formed between presumably neutrally diverging lineages. However, hybrids were relatively rare, suggesting that those could be selected against, perhaps currently reinforcing species boundaries between these lineages.

Neutral geographically driven differentiation was analyzed between populations from the Ogasawara, Daito and Ryukyu Islands within the Pacific clade of *G. fascicularis*. Our analysis showed that at migration rates of ~10 to 20 migrants per Million per generation the Ogasawara population has diverged over at least 109 000 generations from the populations in Ryukyu, Daito, and Guam. Regional oceanographic dispersal analysis indicated that Ogasawara is a sink population, receiving most migrants from the Ryukyu Archipelago, and that it was oceanographically isolated from a direct connection to the Daito Islands and the Mariana Islands. However, genetic estimations detected migration rates from the Daito Islands to be as high as from the Ryukyu Islands, and migration to exist in both directions between Guam and Ogasawara. This indicates the potential importance of indirect migration routes over non-sampled stepping stone populations, which may have a larger influence on

the genetic composition of a local population than rare cases of LDD at maximal larval competency periods. Overall, the Ogasawara *Galaxea* population was highly differentiated and may represent a case of incipient speciation that has happened over the course of several million years. However, it may have mixed with the other predominant lineage in Guam, indicating incomplete reproductive isolation.

The endosymbiotic composition of Symbiodiniaceae in *Galaxea* was investigated in detail across different locations, depth gradients, and host lineages. The communities structured into three main community types (C1, C21, or D1-dominated), which partially related to host attributes like polyp size, bleaching status, and location and depth, but not to host lineage. Thus, in the case of the broad-cast spawning generalist coral *Galaxea,* a co-evolutionary mode of diversification with Symbiodiniaceae seems unlikely, in contrast to what has been proposed on higher systematic levels (Thornhill *et al.*, 2014; LaJeunesse *et al.*, 2018). Depth segregation between lineages could also not be confirmed, suggesting a generally minor role of environmental or symbiotic factors for genetic differentiation. However, morphological differentiation sometimes related to genetic differentiation, hinting to the existence of also selective forces linked to functional diversification in this genus. Lineage L tended to have somewhat larger polyps than lineage S, and within the Pacific clade, morphology was indeed manifested in the genetic code and not due to phenotypic plasticity. More complete genomic data than was available here may also find genetic differentiation between the three, potentially quite young morphological species (*G. astreata, G. cryptoramosa, G. paucisepta*) in Okinawa.

In conclusion, this research confirmed the extremely slow emergence of reproductive barriers in corals under neutral processes such as geographic isolation, and a mismatch between morphological diversity and phylogenetic diversity, as well as between nuclear and mitochondrial markers (mitochondrial marker underestimating diversity). However, using high-resolution genomic DNA it was possible to infer a geographically well-resolved genus phylogeny and to provide an explanation for the co-occurrence patterns and emergence histories of morphologically and ecologically undifferentiated lineages. There is still much to learn about the speciation process in corals, but this research emphasizes the importance of genomic data and a geographically wide sampling for the correct inference of evolutionary histories.

References

Abe, M., Watanabe, T., Suzuki, Y. & Hidaka, M. (2008a) Genetic and morphological differentiation in the hermatypic coral *Galaxea fascicularis* in Okinawa, Japan. *Plankton Benthos Research*, **3**, 174-179.

Abe, M., Watanabe, T., Hayakawa, H. & Hidaka, M. (2008b) Breeding experiments of hermatypic coral *Galaxea fascicularis*: partial reproductive isolation between colonies of different nematocyst types and enhancement of fertilization success by presence of parental colonies. *Fisheries Science*, **74**, 1342-1344.

Ainsworth, T.D., Thurber, R.V. & Gates, R.D. (2010) The future of coral reefs: a microbial perspective. *Trends in Ecology & Evolution*, **25**, 233-240.

Arif, C., Daniels, C., Bayer, T., Banguera-Hinestroza, E., Barbrook, A., Howe, C.J., Lajeunesse, T.C. & Voolstra, C.R. (2014) Assessing *Symbiodinium* diversity in scleractinian corals via next-generation sequencing-based genotyping of the ITS2 rDNA region. *Molecular Ecology*, **23**, 4418-4433.

Babcock, R.C. & Heyward, A.J. (1986) Larval Development of Certain Gamete-Spawning Scleractinian Corals. *Coral Reefs*, **5**, 111-116.

Baird, A.H., Guest, J.R. & Willis, B.L. (2009) Systematic and Biogeographical Patterns in the Reproductive Biology of Scleractinian Corals. *Annual Review of Ecology Evolution and Systematics*, **40**, 551-571.

Baker, A.C. (2003) Flexibility and specificity in coral-algal symbiosis: Diversity, ecology, and biogeography of *Symbiodinium*. *Annual Review of Ecology Evolution and Systematics*, **34**, 661-689.

Baker, D.M., Andras, J.P., Jordan-Garza, A.G. & Fogel, M.L. (2013) Nitrate competition in a coral symbiosis varies with temperature among Symbiodinium clades. *Isme Journal*, **7**, 1248-1251.

Bandelt, H.-J., Forster, P. & Röhl, A. (1999) Median-joining networks for inferring intraspecific phylogenies. *Molecular biology and evolution*, **16**, 37-48.

Barber, P.H., Erdmann, M.V. & Palumbi, S.R. (2006) Comparative phylogeography of three codistributed stomatopods: Origins and timing of regional lineage diversification in the coral triangle. *Evolution*, **60**, 1825-1839.

Barber, P.H., Palumbi, S.R., Erdmann, M.V. & Moosa, M.K. (2002) Sharp genetic breaks among populations of *Haptosquilla pulchella* (Stomatopoda) indicate limits to larval transport: patterns, causes, and consequences. *Molecular Ecology*, **11**, 659-674.

Baums, I.B., Devlin-Durante, M.K. & Lajeunesse, T.C. (2014) New insights into the dynamics between reef corals and their associated dinoflagellate endosymbionts from population genetic studies. *Molecular Ecology*, **23**, 4203-4215.

Beger, M., Selkoe, K.A., Treml, E., Barber, P.H., von der Heyden, S., Crandall, E.D., Toonen, R.J. & Riginos, C. (2014) Evolving coral reef conservation with genetic information. *Bulletin of Marine Science*, **90**, 159-185.

Berkelmans, R. & van Oppen, M.J.H. (2006) The role of zooxanthellae in the thermal tolerance of corals: a 'nugget of hope' for coral reefs in an era of climate change. *Proceedings of the Royal Society B-Biological Sciences*, **273**, 2305-2312.

Bolger, A.M., Lohse, M. & Usadel, B. (2014) Trimmomatic: a flexible trimmer for Illumina sequence data. *Bioinformatics*, **30**, 2114-2120.

Bongaerts, P., Carmichael, M., Hay, K.B., Tonk, L., Frade, P.R. & Hoegh-Guldberg, O. (2015) Prevalent endosymbiont zonation shapes the depth distributions of scleractinian coral species. *Royal Society Open Science*, **2**, 140297.

Boucher, D.H., James, S. & Keeler, K.H. (1982) The Ecology of Mutualism. *Annual Review of Ecology and Systematics*, **13**, 315-347.

Boulotte, N.M., Dalton, S.J., Carroll, A.G., Harrison, P.L., Putnam, H.M., Peplow, L.M. & van Oppen, M.J.H. (2016) Exploring the *Symbiodinium* rare biosphere provides evidence for symbiont switching in reef-building corals. *Isme Journal*, **10**, 2693-2701.

Brainard, R. (2012) Coral reef ecosystem monitoring report of the Mariana archipelago, 2003-2007.

Cai, L., Zhou, G., Tong, H., Tian, R.-M., Zhang, W., Ding, W., Liu, S., Huang, H. & Qian, P.-Y. (2018) Season structures prokaryotic partners but not algal symbionts in subtropical hard corals. *Applied Microbiology and Biotechnology*, **102**, 4963–4973.

Callahan, B.J., McMurdie, P.J. & Holmes, S.P. (2017) Exact sequence variants should replace operational taxonomic units in marker gene data analysis. *The ISME Journal*, **11**, 2639-2643.

Carpenter, K.E., Barber, P.H., Crandall, E.D., Ablan-Lagman, M.C.A., Ambariyanto, Ngurah Mahardika, G., Manjaji-Matsumoto, B.M., Juinio-Meñez, M.-A., Santos, M.D., Starger, C.J. & Toha, A.H.A. (2010) Comparative phylogeography of the Coral Triangle and implications for marine management. *Journal of Marine Biology*, **2011**

Chen, C.A., Wang, A.T., Fang, L.S. & Yang, Y.W. (2005) Fluctuating algal symbiont communities in *Acropora palifera* (Scleractinia : Acroporidae) from Taiwan. *Marine Ecology Progress Series*, **295**, 113-121.

Chesson, P. (2000) Mechanisms of maintenance of species diversity. *Annual Review of Ecology and Systematics*, **31**, 343-366.

Chiba, S. (1999) Accelerated evolution of land snails Mandarina in the oceanic Bonin Islands: Evidence from mitochondrial DNA sequences. *Evolution*, **53**, 460-471.

Clement, M., Snell, Q., Walker, P., Posada, D. & Crandall, K. (2002) TCS: Estimating gene genealogies. *Parallel and Distributed Processing Symposium, International Proceedings*, **2**, 184.

Colgan, M.W. (1987) Coral-reef recovery on Guam (Micronesia) after catastrophic predation by *Acanthaster planci*. *Ecology*, **68**, 1592-1605.

Combosch, D.J. & Vollmer, S. (2015) Trans-Pacific RAD-Seq population genomics confirms introgressive hybridization in Eastern Pacific Pocillopora corals. *Molecular Phylogenetics and Evolution*, **in press**

Combosch, D.J., Guzman, H.M., Schuhmacher, H. & Vollmer, S.V. (2008) Interspecific hybridization and restricted trans-Pacific gene flow in the Tropical Eastern Pacific Pocillopora. *Molecular Ecology*, **17**, 1304-1312.

Cooper, T.F., Berkelmans, R., Ulstrup, K.E., Weeks, S., Radford, B., Jones, A.M., Doyle, J., Canto, M., O'Leary, R.A. & van Oppen, M.J.H. (2011) Environmental factors controlling the distribution of *Symbiodinium* harboured by the coral *Acropora millepora* on the Great Barrier Reef. *Plos One*, **6**, e25536.

Correa, A.M.S. & Baker, A.C. (2009) Understanding diversity in coral-algal symbiosis: a cluster-based approach to interpreting fine-scale genetic variation in the genus Symbiodinium. *Coral Reefs*, **28**, 81-93.

Cowen, R.K., Paris, C.B. & Srinivasan, A. (2006) Scaling of connectivity in marine populations. *Science*, **311**, 522-527.

Coyne, J.A. & Orr, H.A. (2004) *Speciation*. Sinauer Associates, Sunderland, Mass.

Crandall, E.D., Treml, E.A. & Barber, P.H. (2012) Coalescent and biophysical models of stepping-stone gene flow in neritid snails. *Molecular Ecology*, **21**, 5579-5598.

Crandall, E.D., Treml, E.A., Liggins, L., Gleeson, L., Yasuda, N., Barber, P.H., Worheide, G. & Riginos, C. (2014) Return of the ghosts of dispersal past: historical spread and contemporary gene flow in the blue sea star Linckia laevigata. *Bulletin of Marine Science*, **90**, 399-425.

Cunning, R. & Baker, A.C. (2014) Not just who, but how many: the importance of partner abundance in reef coral symbioses. *Frontiers in Microbiology*, **5**

Cunning, R., Gates, R.D. & Edmunds, P.J. (2017) Using high-throughput sequencing of ITS2 to describe *Symbiodinium* metacommunities in St. John, US Virgin Islands. *Peerj*, **5**, e3472.

Cunning, R., Yost, D.M., Guarinello, M.L., Putnam, H.M. & Gates, R.D. (2015) Variability of *Symbiodinium* communities in waters, sediments, and corals of thermally distinct reef pools in American Samoa. *Plos One*, **10**, e0145099.

Danecek, P., Auton, A., Abecasis, G., Albers, C.A., Banks, E., DePristo, M.A., Handsaker, R.E., Lunter, G., Marth, G.T. & Sherry, S.T. (2011) The variant call format and VCFtools. *Bioinformatics*, **27**, 2156-2158.

Darwin, C. (1859) *On the origin of species by means of natural selection*. J. Murray, London,.

Davey, J.L. & Blaxter, M.W. (2010) RADSeq: next-generation population genetics. *Briefings in Functional Genomics*, **9**, 416-423.

Davies, S.W., Treml, E.A., Kenkel, C.D. & Matz, M.V. (2015) Exploring the role of Micronesian islands in the maintenance of coral genetic diversity in the Pacific Ocean. *Molecular Ecology*, **24**, 70-82.

De Wit, P., Pespeni, M.H., Ladner, J.T., Barshis, D.J., Seneca, F., Jaris, H., Therkildsen, N.O., Morikawa, M. & Palumbi, S.R. (2012) The simple fool's guide to population genomics via RNA-Seq: an introduction to high-throughput sequencing data analysis. *Molecular Ecology Resources*, **12**, 1058-1067.

DeBoer, T.S., Naguit, M.R.A., Erdmann, M.V., Ablan-Lagman, M.C.A., Ambariyanto, Carpenter, K.E., Toha, A.H.A. & Barber, P.H. (2014) Concordance between phylogeographic and biogeographic boundaries in the Coral Triangle: conservation implications based on comparative analyses of multiple giant clam species. *Bulletin of Marine Science*, **90**, 277-300.

Diaz-Almeyda, E.M., Prada, C., Ohdera, A.H., Moran, H., Civitello, D.J., Iglesias-Prieto, R., Carlo, T.A., LaJeunesse, T.C. & Medina, M. (2017) Intraspecific and interspecific variation in thermotolerance and photoacclimation in *Symbiodinium* dinoflagellates. *Proceedings of the Royal Society B-Biological Sciences*, **284**, 20171767.

Duda, T.F. & Lessios, H.A. (2009) Connectivity of populations within and between major biogeographic regions of the tropical Pacific in *Conus ebraeus*, a widespread marine gastropod. *Coral Reefs*, **28**, 651-659.

Durand, E.Y., Patterson, D., Reich, D. & Slatkin, M. (2011) Testing for ancient admixture between closely related populations. *Molecular Biology and Evolution*, **28**, 2239–2252.

Edgar, R.C. (2013) UPARSE: highly accurate OTU sequences from microbial amplicon reads. *Nature Methods*, **10**, 996-998.

Emerson, K.J., Merz, C.R., Catchen, J.M., Hohenlohe, P.A., Cresko, W.A., Bradshaw, W.E. & Holzapfel, C.M. (2010) Resolving postglacial phylogeography using high-throughput sequencing. *Proceedings of the National Academy of Sciences of the United States of America*, **107**, 16196-16200.

Eren, A.M., Morrison, H.G., Lescault, P.J., Reveillaud, J., Vineis, J.H. & Sogin, M.L. (2015) Minimum entropy decomposition: Unsupervised oligotyping for sensitive partitioning of high-throughput marker gene sequences. *Isme Journal*, **9**, 968-979.

Excoffier, L. & Foll, M. (2011) fastsimcoal: a continuous-time coalescent simulator of genomic diversity under arbitrarily complex evolutionary scenarios. *Bioinformatics*, **27**, 1332-1334.

Fadlallah, Y.H. (1983) Sexual reproduciton, development and larval biology in Scleractinian Corals. *Coral Reefs*, **2**, 129-150.

Ferrier, S., Manion, G., Elith, J. & Richardson, K. (2007) Using generalized dissimilarity modelling to analyse and predict patterns of beta diversity in regional biodiversity assessment. *Diversity and Distributions*, **13**, 252-264.

Flot, J.-F., Blanchot, J., Charpy, L., Cruaud, C., Licuanan, W.Y., Nakano, Y., Payri, C. & Tillier, S. (2011) Incongruence between morphotypes and genetically delimited species in the coral genus *Stylophora*: phenotypic plasticity, morphological convergence, morphological stasis or interspecific hybridization? *BMC Ecology*, **11**, 22.

Foll, M. & Gaggiotti, O. (2008) A Genome-Scan Method to Identify Selected Loci Appropriate for Both Dominant and Codominant Markers: A Bayesian Perspective. *Genetics*, **180**, 977-993.

Foster, N.L., Paris, C.B., Kool, J.T., Baums, I.B., Stevens, J.R., Sanchez, J.A., Bastidas, C., Agudelo, C., Bush, P., Day, O., Ferrari, R., Gonzalez, P., Gore, S., Guppy, R., McCartney, M.A., McCoy, C., Mendes, J., Srinivasan, A., Steiner, S., Vermeij, M.J.A., Weil, E. & Mumby, P.J. (2012) Connectivity of Caribbean coral populations:

complementary insights from empirical and modelled gene flow. *Molecular Ecology*, **21**, 1143-1157.

Franklin, E.C., Stat, M., Pochon, X., Putnam, H.M. & Gates, R.D. (2012) GeoSymbio: a hybrid, cloud-based web application of global geospatial bioinformatics and ecoinformatics for *Symbiodinium*-host symbioses. *Molecular Ecology Resources*, **12**, 369-373.

Freudenthal, H. (1969) *Symbiodinium* gen. nov. and *Symbiodinium microadriaticum* Sp. nov., a zooxanthellae: taxonomy, life cycle and morphology. *The Journal of Protozoology*, **9**, 45-52.

Fukami, H. (2008) Short review: molecular phylogenetic analysis of reef corals. *Galaxea, Journal of Coral Reef Studies*, **10**, 47-55.

Garren, M., Walsh, S.M., Caccone, A. & Knowlton, N. (2006) Patterns of association between Symbiodinium and members of the Montastraea annularis species complex on spatial scales ranging from within colonies to between geographic regions. *Coral Reefs*, **25**, 503-512.

Garrison, E. & Marth, G. (2012) Haplotype-based variant detection from short-read sequencing. *arXiv preprint arXiv:1207.3907*,

Gittenberger, A., Reijnen, B.T. & Hoeksema, B.W. (2011) A molecularly based phylogeny reconstruction of mushroom corals (Scleractinia: Fungiidae) with taxonomic consequences and evolutionary implications for life history traits. *Contributions to Zoology*, **80**, 107-132.

Goffredo, S., Caroselli, E., Mattioli, G., Pignotti, E. & Zaccanti, F. (2008) Relationships between growth, population structure and sea surface temperature in the temperate solitary coral *Balanophyllia europaea* (Scleractinia, Dendrophylliidae). *Coral Reefs*, **27**, 623-632.

Goreau, T.F. & Goreau, N.I. (1959) The Physiology of Skeleton Formation in Corals .2. Calcium Deposition by Hermatypic Corals under Various Conditions in the Reef. *Biological Bulletin*, **117**, 239-250.

Gorospe, K.D., Donahue, M.J. & Karl, S.A. (2015) The importance of sampling design: spatial patterns and clonality in estimating the genetic diversity of coral reefs. *Marine Biology*, **162**, 917-928.

Goslee, S.C. & Urban, D.L. (2007) The ecodist package for dissimilarity-based analysis of ecological data. *Journal of Statistical Software*, **22**, 1-19.

Gutenkunst, R.N., Hernandez, R.D., Williamson, S.H. & Bustamante, C.D. (2009) Inferring the joint demographic history of multiple populations from multidimensional SNP frequency data. *PLoS Genet*, **5**, e1000695.

Hall, R. & Holloway, J.D. (1998) *Biogeography and geological evolution of SE Asia*. Backhuys.

Hamilton, W.D. (1964) The genetical evolution of social behaviour. II. *Journal of theoretical biology*, **7**, 17-52.

Hansen, J., Sato, M., Russell, G. & Kharecha, P. (2013) Climate sensitivity, sea level and atmospheric carbon dioxide. *Philosophical Transactions of the Royal Society A: Mathematical, Physical and Engineering Sciences*, **371**, 20120294.

Heyward, A., Yamazato, K., Yeemin, T. & Minei, M. (1987) Sexual reproduction of corals in Okinawa. *Galaxea*, **6**, 331-343.

Hidaka, M. (1992) Use of nematocyst morphology for taxonomy of some related species of scleractinian corals. *Galaxea*, **11**, 21-28.

Hoeksema, B.W. (2007) Delineation of the Indo-Malayan centre of maximum marine biodiversity: the Coral Triangle. *Biogoegraphy, time, and place: distributions, barriers, and islands* (ed. by W. Renema), pp. 117-178. Springer, Dordrecht, The Netherlands.

Hohenlohe, P.A., Bassham, S., Etter, P.D., Stiffler, N., Johnson, E.A. & Cresko, W.A. (2010) Population Genomics of Parallel Adaptation in Threespine Stickleback using Sequenced RAD Tags. *Plos Genetics*, **6**

Hongo, C. & Yamano, H. (2013) Species-specific responses of corals to bleaching events on anthropogenically turbid reefs on Okinawa Island, Japan, over a 15-year period (1995–2009). *PLoS One*, **8**, e60952.

Howells, E.J., Willis, B.L., Bay, L.K. & van Oppen, M.J.H. (2013) Spatial and temporal genetic structure of *Symbiodinium* populations within a common reef-building coral on the Great Barrier Reef. *Molecular Ecology*, **22**, 3693-3708.

Huang, D.W. (2012) Threatened Reef Corals of the World. *Plos One*, **7**, e34459.

Huang, D.W. & Roy, K. (2015) The future of evolutionary diversity in reef corals. *Philosophical Transactions of the Royal Society B-Biological Sciences*, **370**, 20140010.

Hughes, T.P., Kerry, J.T., Alvarez-Noriega, M., Alvarez-Romero, J.G., Anderson, K.D., Baird, A.H., Babcock, R.C., Beger, M., Bellwood, D.R., Berkelmans, R., Bridge,

T.C., Butler, I.R., Byrne, M., Cantin, N.E., Comeau, S., Connolly, S.R., Cumming, G.S., Dalton, S.J., Diaz-Pulido, G., Eakin, C.M., Figueira, W.F., Gilmour, J.P., Harrison, H.B., Heron, S.F., Hoey, A.S., Hobbs, J.P.A., Hoogenboom, M.O., Kennedy, E.V., Kuo, C.Y., Lough, J.M., Lowe, R.J., Liu, G., Culloch, M.T.M., Malcolm, H.A., Mcwilliam, M.J., Pandolfi, J.M., Pears, R.J., Pratchett, M.S., Schoepf, V., Simpson, T., Skirving, W.J., Sommer, B., Torda, G., Wachenfeld, D.R., Willis, B.L. & Wilson, S.K. (2017) Global warming and recurrent mass bleaching of corals. *Nature*, **543**, 373-377.

Hui, F.K.C. (2016) Boral - Bayesian Ordination and Regression Analysis of Multivariate Abundance Data in r. *Methods in Ecology and Evolution*, **7**, 744-750.

Inaba (2004a) Ogasawara Islands. Status of coral reefs around the country. *Coral Reefs of Japan*, pp. 160-163. The Japanese Coral Reef Society and MOE.

Inaba, M. (2004b) Ecological feature and status of hermatypic corals in the Ogasawara Islands. *Midoriishi*, **14**, 20-23.

Ito, M. (1998) Origin and evolution of endemic plants of the Bonin (Ogasawara) Islands. *Researches on Population Ecology*, **40**, 205-212.

Ives, A.R. & Carpenter, S.R. (2007) Stability and diversity of ecosystems. *Science*, **317**, 58-62.

Iwase, F. (2004) East of Muroto. *Coral Reefs of Japan* (ed. by J.C.R. Society). Ministry of Environment Japan.

Jablonski, D. (1986) Larval ecology and macroevolution in marine invertebrates. *Bulletin of Marine Science*, **39**, 565-587.

Janes, J.K., Miller, J.M., Dupuis, J.R., Malenfant, R.M., Gorrell, J.C., Cullingham, C.I. & Andrew, R.L. (2017) The K=2 conundrum. *Molecular Ecology*, **26**, 3594-3602.

Jones, A. & Berkelmans, R. (2010) Potential costs of acclimatization to a warmer climate: Growth of a reef coral with heat tolerant vs. sensitive symbiont types. *Plos One*, **5**, e10437.

Kadmon, R. & Pulliam, H.R. (1993) Island Biogeography - Effect of Geographical Isolation on Species Composition. *Ecology*, **74**, 977-981.

Kayanne, H., Ishii, T., Matsumoto, E. & Yonekura, N. (1993) Late Holocene sea-level change on Rota and Guam, Mariana Islands, and its constraint on geophysical predictions. *Quaternary research* **40**, 189-189.

Kayanne, H., Hongo, C., Okaji, K., Ide, Y., Hayashibara, T., Yamamoto, H., Mikami, N., Onodera, K., Ootsubo, T. & Takano, H. (2012) Low species diversity of hermatypic

corals on an isolated reef, Okinotorishima, in the northwestern Pacific. *Galaxea, Journal of Coral Reef Studies*, **14**, 73-95.

Keith, S.A., Baird, A.H., Hughes, T.P., Madin, J.S. & Connolly, S.R. (2013) Faunal breaks and species composition of Indo-Pacific corals: the role of plate tectonics, environment and habitat distribution. *Proceedings of the Royal Society B-Biological Sciences*, **280**, 20130818.

Kenkel, C.D. & Bay, L.K. (2016) The role of vertical symbiont transmission in altering cooperation and fitness of coral-*Symbiodinium* symbioses. *bioRxiv*, doi: https://doi.org/10.1101/067322.

Keshavmurthy, S., Yang, S.Y., Alamaru, A., Chuang, Y.Y., Pichon, M., Obura, D., Fontana, S., De Palmas, S., Stefani, F., Benzoni, F., MacDonald, A., Noreen, A.M.E., Chen, C.S., Wallace, C.C., Pillay, R.M., Denis, V., Amri, A.Y., Reimer, J.D., Mezaki, T., Sheppard, C., Loya, Y., Abelson, A., Mohammed, M.S., Baker, A.C., Mostafavi, P.G., Suharsono, B.A. & Chen, C.A. (2013) DNA barcoding reveals the coral "laboratory-rat", *Stylophora pistillata* encompasses multiple identities. *Scientific Reports*, **3**, 1520.

Kissling, W.D., Dormann, C.F., Groeneveld, J., Hickler, T., Kuhn, I., McInerny, G.J., Montoya, J.M., Romermann, C., Schiffers, K., Schurr, F.M., Singer, A., Svenning, J.C., Zimmermann, N.E. & O'Hara, R.B. (2012) Towards novel approaches to modelling biotic interactions in multispecies assemblages at large spatial extents. *Journal of Biogeography*, **39**, 2163-2178.

Kitahara, M.V., Fukami, H., Benzoni, F. & Huang, D. (2016) The New Systematics of Scleractinia: Integrating Molecular and Morphological Evidence. *The Cnidaria, Past, Present and Future: The world of Medusa and her sisters* (ed. by S. Goffredo and Z. Dubinsky), pp. 41-59. Springer International Publishing, Cham.

Kitahara, M.V., Cairns, S.D., Stolarski, J., Blair, D. & Miller, D.J. (2010) A Comprehensive Phylogenetic Analysis of the Scleractinia (Cnidaria, Anthozoa) Based on Mitochondrial CO1 Sequence Data. *Plos One*, **5**

Klueter, A., Trapani, J., Archer, F.I., McIlroy, S.E. & Coffroth, M.A. (2017) Comparative growth rates of cultured marine dinoflagellates in the genus *Symbiodinium* and the effects of temperature and light. *Plos One*, **12**, e0187707.

Knittweis, L., Kraemer, W.E., Timm, J. & Kochzius, M. (2009) Genetic structure of *Heliofungia actiniformis* (Scleractinia: Fungiidae) populations in the Indo-Malay

Archipelago: implications for live coral trade management efforts. *Conservation Genetics*, **10**, 241-249.

Kolde, R. (2015) *pheatmap: Pretty heatmaps. R package version 1.0. 8*.

Kool, J.T., Paris, C.B., Barber, P.H. & Cowen, R.K. (2011) Connectivity and the development of population genetic structure in Indo-West Pacific coral reef communities. *Global Ecology and Biogeography*, **20**, 695-706.

Kozlov, A.M., Aberer, A.J. & Stamatakis, A. (2015) ExaML version 3: a tool for phylogenomic analyses on supercomputers. *Bioinformatics*, **31**, 2577-2579.

Kumagai, N.H., Yamano, H. & Sango-Map-Project, C. (2018) High-resolution modeling of thermal thresholds and environmental influences on coral bleaching for local and regional reef management. *Peerj*, **6**, e4382.

Kuriiwa, K., Chiba, S.N., Motomura, H. & Matsuura, K. (2014) Phylogeography of Blacktip Grouper, *Epinephelus fasciatus* (Perciformes: Serranidae), and influence of the Kuroshio Current on cryptic lineages and genetic population structure. *Ichthyological Research*, **61**, 361-374.

Kyodo (2011) Ogasawara Islands join World Heritage family. In: *Japan Times*

Ladner, J.T. & Palumbi, S.R. (2012) Extensive sympatry, cryptic diversity and introgression throughout the geographic distribution of two coral species complexes. *Molecular Ecology*, **21**, 2224-2238.

LaJeunesse, T.C. (2001) Investigating the biodiversity, ecology, and phylogeny of endosymbiotic dinoflagellates in the genus *Symbiodinium* using the ITS region: In search of a "species" level marker. *Journal of Phycology*, **37**, 866-880.

LaJeunesse, T.C. (2005) "Species" radiations of symbiotic Dinoflagellates in the Atlantic and Indo-Pacific since the Miocene-Pliocene transition *Molecular Biology and Evolution*, **22**, 1158-1158.

LaJeunesse, T.C. & Thornhill, D.J. (2011) Improved resolution of reef-coral endosymbiont (*Symbiodinium*) species diversity, ecology, and evolution through *psbA* non-coding region genotyping. *Plos One*, **6**, e29013.

Lajeunesse, T.C., Parkinson, J.E. & Reimer, J.D. (2012) A genetics-based description of *Symbiodinium minutum* sp. nov. and *S. psygmophilum* sp. nov. (dinophyceae), two dinoflagellates symbiotic with cnidaria. *Journal of Phycology*, **48**, 1380-1391.

LaJeunesse, T.C., Loh, W.K.W., van Woesik, R., Hoegh-Guldberg, O., Schmidt, G.W. & Fitt, W.K. (2003) Low symbiont diversity in southern Great Barrier Reef corals, relative to those of the Caribbean. *Limnology and Oceanography*, **48**, 2046-2054.

LaJeunesse, T.C., Wham, D.C., Pettay, D.T., Parkinson, J.E., Keshavmurthy, S. & Chen, C.A. (2014) Ecologically differentiated stress-tolerant endosymbionts in the dinoflagellate genus *Symbiodinium* (Dinophyceae) Clade D are different species. *Phycologia*, **53**, 305-319.

LaJeunesse, T.C., Parkinson, J.E., Gabrielson, P.W., Jeong, H.J., Reimer, J.D., Voolstra, C.R. & Santos, S.R. (2018) Systematic revision of Symbiodiniaceae highlights the antiquity and diversity of coral endosymbionts. *Current Biology*, **28**, 1-11.

LaJeunesse, T.C., Bhagooli, R., Hidaka, M., DeVantier, L., Done, T., Schmidt, G.W., Fitt, W.K. & Hoegh-Guldberg, O. (2004) Closely related Symbiodinium spp. differ in relative dominance in coral reef host communities across environmental, latitudinal and biogeographic gradients. *Marine Ecology Progress Series*, **284**, 147-161.

Lee, M.J., Jeong, H.J., Jang, S.H., Lee, S.Y., Kang, N.S., Lee, K.H., Kim, H.S., Wham, D.C. & LaJeunesse, T.C. (2016) Most low-abundance "background" *Symbiodinium* spp. are transitory and have minimal functional significance for symbiotic corals. *Microbial Ecology*, **71**, 771-783.

Leibold, M.A., Holyoak, M., Mouquet, N., Amarasekare, P., Chase, J.M., Hoopes, M.F., Holt, R.D., Shurin, J.B., Law, R., Tilman, D., Loreau, M. & Gonzalez, A. (2004) The metacommunity concept: a framework for multi-scale community ecology. *Ecology Letters*, **7**, 601-613.

Lemoine, F., Domelevo Entfellner, J.B., Wilkinson, E., Correia, D., Dávila Felipe, M., De Oliveira, T. & Gascuel, O. (2018) Renewing Felsenstein's phylogenetic bootstrap in the era of big data. *Nature*, **556**, 452-456.

Li, H. & Durbin, R. (2009) Fast and accurate short read alignment with Burrows-Wheeler transform. *Bioinformatics*, **25**, 1754-1760.

Liew, Y.J., Aranda, M. & Voolstra, C.R. (2016) Reefgenomics.Org - a repository for marine genomics data. *Database*, **2016**, baw152.

Lischer, H.E.L. & Excoffier, L. (2012) PGDSpider: an automated data conversion tool for connecting population genetics and genomics programs. *Bioinformatics*, **28**, 298-299.

Little, A.F., van Oppen, M.J.H. & Willis, B.L. (2004) Flexibility in algal endosymbioses shapes growth in reef corals. *Science*, **304**, 1492-1494.

Locarnini, R., Mishonov, A., Antonov, J., Boyer, T., Garcia, H., Baranova, O., Zweng, M., Paver, C., Reagan, J. & Johnson, D. (2013) World Ocean Atlas 2013, NOAA Atlas NESDIS 73 Vol. 1: Temperature. In:

Loya, Y., Sakai, K., Yamazato, K., Nakano, Y., Sambali, H. & van Woesik, R. (2001) Coral bleaching: the winners and the losers. *Ecology Letters*, **4**, 122-131.

Madin, J.S., Anderson, K.D., Andreasen, M.H., Bridge, T.C., Cairns, S.D., Connolly, S.R., Darling, E.S., Diaz, M., Falster, D.S. & Franklin, E.C. (2016) The Coral Trait Database, a curated database of trait information for coral species from the global oceans. *Scientific Data*, **3**, 160017.

Manel, S. & Holderegger, R. (2013) Ten years of landscape genetics. *Trends in Ecology & Evolution*, **28**, 614-621.

Markey, K.L., Abdo, D.A., Evans, S.N. & Bosserelle, C. (2016) Keeping It Local: Dispersal Limitations of Coral Larvae to the High Latitude Coral Reefs of the Houtman Abrolhos Islands. *Plos One*, **11**, e0147628.

Marshall, P.A. & Baird, A.H. (2000) Bleaching of corals on the Great Barrier Reef: differential susceptibilities among taxa. *Coral Reefs*, **19**, 155-163.

Matsuura, K. & Senou, H. (2012) Introduction of Fishes in the Kuroshio Current. *Fishes in the Kuroshio Current* (ed. by K. Matsuura). Tokai University Press, Kanagawa.

Mayr, A. (1963) *Animal species and evolution*. Harvard University Press/Belknap Press, Cambridge, MA.

Mayr, E. (1942) *Systematics and the origin of species from the viewpoint of a zoologist*. Columbia University Press, New York.

McGill, B.J., Enquist, B.J., Weiher, E. & Westoby, M. (2006) Rebuilding community ecology from functional traits. *Trends in Ecology & Evolution*, **21**, 178-185.

Meirmans, P.G. (2014) Nonconvergence in Bayesian estimation of migration rates. *Molecular Ecology Resources*, **14**, 726-733.

Mieog, J.C., van Oppen, M.J.H., Cantin, N.E., Stam, W.T. & Olsen, J.L. (2007) Real-time PCR reveals a high incidence of *Symbiodinium* clade D at low levels in four scleractinian corals across the Great Barrier Reef: implications for symbiont shuffling. *Coral Reefs*, **26**, 449-457.

Mihaljevic, J.R. (2012) Linking metacommunity theory and symbiont evolutionary ecology. *Trends in Ecology & Evolution*, **27**, 323-329.

Mitarai, S., Siegel, D.A., Watson, J.R., Dong, C. & McWilliams, J.C. (2009) Quantifying connectivity in the coastal ocean with application to the Southern California Bight. *Journal of Geophysical Research-Oceans*, **114**

Mitarai, S., Watanabe, H., Nakajima, Y., Shchepetkin, A.F. & McWilliams, J.C. (2016) Quantifying dispersal from hydrothermal vent fields in the western Pacific Ocean.

Proceedings of the National Academy of Sciences of the United States of America, **113**, 2976-2981.

Monismith, S.G. (2007) Hydrodynamics of coral reefs. *Annual Review of Fluid Mechanics*, **39**, 37-55.

Moore, W.S. (1995) Inferring Phylogenies from Mtdna Variation - Mitochondrial-Gene Trees Versus Nuclear-Gene Trees. *Evolution*, **49**, 718-726.

Muscatine, L. & Porter, J.W. (1977) Reef corals - mutualistic symbioses adapted to nutrient-poor environments. *Bioscience*, **27**, 454-460.

Mussmann, S. (2017) BayesAss3-SNPs. available at: https://github.com/smussmann82/BayesAss3-SNPs.

Nakaema, S. & Hidaka, M. (2015) GFP distribution and fluorescence intensity in *Galaxea fascicularis*: developmental changes and maternal effects *Platax*, **12**, 1-9.

Nakajima, Y., Nishikawa, A., Iguchi, A. & Sakai, K. (2010) Gene Flow and Genetic Diversity of a Broadcast-Spawning Coral in Northern Peripheral Populations. *Plos One*, **5**, e11149.

Nakajima, Y., Shinzato, C., Satoh, N. & Mitarai, S. (2015) Novel polymorphic microsatellite markers reveal genetic differentiation between two sympatric types of *Galaxea fascicularis*. *Plos One*, **10**, e0130176.

Nakajima, Y., Zayasu, Y., Shinzato, C., Satoh, N. & Mitarai, S. (2016) Genetic differentiation and connectivity of morphological types of the broadcast-spawning coral *Galaxea fascicularis* in the Nansei Islands, Japan. *Ecology and Evolution*, **6**, 1457-1469.

Nakano, T., Yazaki, I., Kurokawa, M., Yamaguchi, K. & Kuwasawa, K. (2008) The origin of the endemic patellogastropod limpets of the Ogasawara Islands in the northwestern Pacific. *Journal of Molluscan Studies*, **75**, 87-90.

Neall, V.E. & Trewick, S.A. (2008) The age and origin of the Pacific islands: a geological overview. *Philosophical Transactions of the Royal Society B-Biological Sciences*, **363**, 3293-3308.

Niku, J., Warton, D.I., Hui, F.K. & Taskinen, S. (2017) Generalized Linear Latent Variable Models for Multivariate Count and Biomass Data in Ecology. *Journal of Agricultural, Biological and Environmental Statistics*, 1-25.

Niu, W., Huang, H., Lin, R., Chen, C.-H., Shen, K.-N. & Hsiao, C.-D. (2016) The complete mitogenome of the Galaxy Coral, *Galaxea fascicularis* (Cnidaria: Oculinidae). *Mitochondrial DNA Part B*, **1**, 10-11.

Noda, H., Parkinson, J.E., Yang, S.Y. & Reimer, J.D. (2017) A preliminary survey of zoantharian endosymbionts shows high genetic variation over small geographic scales on Okinawa-jima Island, Japan. *Peerj*, **5**, e3740.

Nomura, K. (2004) Kii Peninsula. *Coral Reefs of Japan* (ed. by J.C.R. Society). Ministry of Environment Japan.

Nonaka, M. (2004) Daito Islands. *Coral reefs of Japan. Tokyo: Ministry of the Environment*, 199-201.

Norris, R.D. & Hull, P.M. (2012) The temporal dimension of marine speciation. *Evolutionary Ecology*, **26**, 393-415.

Oksanen, J., Blanchet, F.G., Kindt, R., Legendre, P., Minchin, P.R., O'Hara, R.B., Simpson, G.L., Solymos, P., Stevens, M.H.H. & Wagner, H. (2012) *vegan: Community Ecology Package. R package version 2.0-5*.

Ota, Y. & Omura, A. (1992) Contrasting styles and rates of tectonic uplift of coral reef terraces in the Ryukyu and Daito Islands, southwestern Japan. *Quaternary International*, **15**, 17-29.

Overcast, I. (2018) *easy SFS. Available from: https://github.com/isaacovercast/easySFS. Accessed 2018 February 6th.*

Palumbi, S.R. (1992) Marine Speciation on a Small Planet. *Trends in Ecology & Evolution*, **7**, 114-118.

Palumbi, S.R. (1994) Genetic-Divergence, Reproductive Isolation, and Marine Speciation. *Annual Review of Ecology and Systematics*, **25**, 547-572.

Paris, C.B., Cherubin, L.M. & Cowen, R.K. (2007) Surfing, spinning, or diving from reef to reef: effects on population connectivity. *Marine Ecology Progress Series*, **347**, 285-300.

Parkinson, J.E. & Baums, I.B. (2014) The extended phenotypes of marine symbioses: ecological and evolutionary consequences of intraspecific genetic diversity in coral-algal associations. *Frontiers in Microbiology*, **5**

Parkinson, J.E. & Coffroth, M.A. (2015) New Species of Clade B *Symbiodinium* (Dinophyceae) from the Greater Caribbean belong to different functional guilds: *S. aenigmaticum* Sp Nov., *S. antillogorgium* Sp Nov., *S. endomadracis* Sp Nov., and *S. pseudominutum* Sp Nov. *Journal of Phycology*, **51**, 850-858.

Parkinson, J.E., Baumgarten, S., Michell, C.T., Baums, I.B., LaJeunesse, T.C. & Voolstra, C.R. (2016) Gene expression variation resolves species and Individual strains among coral-associated dinoflagellates within the genus *Symbiodinium*. *Genome Biology and Evolution*, **8**, 665-680.

Parsons, T.R., Takahashi, M. & Hargrave, B. (2013) *Biological oceanographic processes*. Elsevier.

Paulay, G. (2003) Marine biodiversity of Guam and the Marianas: overview. *Micronesica*, **35**, 3-25.

PBDB (2018) *The data were downloaded from the Paleobiology Database, using the taxon name 'Galaxea'.* . Available at: https://paleobiodb.org/#/ (accessed 15 July, 2018

Pinzon, J.H. & LaJeunesse, T.C. (2011) Species delimitation of common reef corals in the genus *Pocillopora* using nucleotide sequence phylogenies, population genetics and symbiosis ecology. *Molecular Ecology*, **20**, 311-325.

Pinzon, J.H., Sampayo, E., Cox, E., Chauka, L.J., Chen, C.A., Voolstra, C.R. & LaJeunesse, T.C. (2013) Blind to morphology: genetics identifies several widespread ecologically common species and few endemics among Indo-Pacific cauliflower corals (*Pocillopora*, Scleractinia). *Journal of Biogeography*, **40**, 1595-1608.

Pochon, X. & Gates, R.D. (2010) A new *Symbiodinium* clade (Dinophyceae) from soritid foraminifera in Hawai'i. *Molecular Phylogenetics and Evolution*, **56**, 492-497.

Pochon, X., LaJeunesse, T.C. & Pawlowski, J. (2004) Biogeographic partitioning and host specialization among foraminiferan dinoflagellate symbionts (*Symbiodinium*; Dinophyta). *Marine Biology*, **146**, 17-27.

Portik, D.M., Leache, A.D., Rivera, D., Barej, M.F., Burger, M., Hirschfeld, M., Rodel, M.O., Blackburn, D.C. & Fujita, M.K. (2017) Evaluating mechanisms of diversification in a Guineo-Congolian tropical forest frog using demographic model selection. *Molecular Ecology*, **26**, 5245-5263.

Prada, C. & Hellberg, M.E. (2013) Long prereproductive selection and divergence by depth in a Caribbean candelabrum coral. *Proceedings of the National Academy of Sciences of the United States of America*, **110**, 3961-3966.

Prada, C., Mcilroy, S.E., Beltran, D.M., Valint, D.J., Ford, S.A., Hellberg, M.E. & Coffroth, M.A. (2014) Cryptic diversity hides host and habitat specialization in a gorgonian-algal symbiosis. *Molecular Ecology*, **23**, 3330-3340.

Prathapan, K.D., Pethiyagoda, R., Bawa, K.S., Raven, P.H., Rajan, P.D. & Countries, C.-S. (2018) When the cure kills-CBD limits biodiversity research National laws fearing biopiracy squelch taxonomy studies. *Science*, **360**, 1405-1406.

R Core Team (2015) *R: A language and environment for statistical computing*. R Foundation for Statistical Computing.

Rambaut, A. & Drummond, A.J. (2007) *Tracer v1.6. Available from* http://beast.bio.ed.ac.uk/Tracer. *Accessed 2018 April 6.*

Ravago-Gotanco, R.G., Magsino, R.M. & Juinio-Menez, M.A. (2007) Influence of the North Equatorial Current on the population genetic structure of *Tridacna crocea* (Mollusca : Tridacnidae) along the eastern Philippine seaboard. *Marine Ecology Progress Series*, **336**, 161-168.

Raynal, J.M., Crandall, E.D., Barber, P.H., Mahardika, G.N., Lagman, M.C. & Carpenter, K.E. (2014) Basin isolation and oceanographic features influencing lineage divergence in the humbug damselfish (*Dascyllus aruanus*) in the Coral Triangle. *Bulletin of Marine Science*, **90**, 513-532.

Reimer, J.D., Hirose, M., Yanagi, K. & Sinniger, F. (2011) Marine invertebrate diversity in the oceanic Ogasawara Islands: a molecular examination of zoanthids (Anthozoa: Hexacorallia) and their *Symbiodinium* (Dinophyceae). *Systematics and Biodiversity*, **9**, 133-143.

Reimer, J.D., Albinsky, D., Yang, S.Y. & Lorion, J. (2014) Zoanthid (Cnidaria: Anthozoa: Hexacorallia: Zoantharia) species of coral reefs in Palau. *Marine Biodiversity*, **44**, 37-44.

Reimer, J.D., Shah, M.M.R., Sinniger, F., Yanagi, K. & Suda, S. (2010) Preliminary analyses of cultured *Symbiodinium* isolated from sand in the oceanic Ogasawara Islands, Japan. *Marine Biodiversity*, **40**, 237-247.

Reimer, J.D., Herrera, M., Gatins, R., Roberts, M.B., Parkinson, J.E. & Berumen, M.L. (2017) Latitudinal variation in the symbiotic dinoflagellate *Symbiodinium* of the common reef zoantharian *Palythoa tuberculosa* on the Saudi Arabian coast of the Red Sea. *Journal of Biogeography*, **44**, 661-673.

Roberts, C.M. (1997) Connectivity and management of Caribbean coral reefs. *Science*, **278**, 1454-1457.

Roberts, C.M., McClean, C.J., Veron, J.E.N., Hawkins, J.P., Allen, G.R., McAllister, D.E., Mittermeier, C.G., Schueler, F.W., Spalding, M., Wells, F., Vynne, C. & Werner,

T.B. (2002) Marine biodiversity hotspots and conservation priorities for tropical reefs. *Science*, **295**, 1280-1284.

Rögl, F. (1998) Palaeogeographic Considerations for Mediterranean and Paratethys Seaways (Oligocene to Miocene). *Annalen des Naturhistorischen Museums in Wien. Serie A für Mineralogie und Petrographie, Geologie und Palāontologie, Anthropologie und Prāhistorie*, **99**, 279-310.

Romano, S.L. & Cairns, S.D. (2000) Molecular phylogenetic hypotheses for the evolution of scleractinian corals. *Bulletin of Marine Science*, **67**, 1043-1068.

Rosenberg, E., Koren, O., Reshef, L., Efrony, R. & Zilber-Rosenberg, I. (2007) The role of microorganisms in coral health, disease and evolution. *Nature Reviews Microbiology*, **5**, 355-362.

Rowan, R. (2004) Coral bleaching - Thermal adaptation in reef coral symbionts. *Nature*, **430**, 742-742.

Rowan, R. & Powers, D.A. (1991) Molecular Genetic Identification of Symbiotic Dinoflagellates (Zooxanthellae). *Marine Ecology Progress Series*, **71**, 65-73.

Sampayo, E., Ridgway, T., Bongaerts, P. & Hoegh-Guldberg, O. (2008) Bleaching susceptibility and mortality of corals are determined by fine-scale differences in symbiont type. *Proceedings of the National Academy of Sciences*, **105**, 10444-10449.

Sampayo, E.M., Franceschinis, L., Hoegh-Guldberg, O. & Dove, S. (2007) Niche partitioning of closely related symbiotic dinoflagellates. *Molecular Ecology*, **16**, 3721-3733.

Schindelin, J., Arganda-Carreras, I., Frise, E., Kaynig, V., Longair, M., Pietzsch, T., Preibisch, S., Rueden, C., Saalfeld, S., Schmid, B., Tinevez, J.Y., White, D.J., Hartenstein, V., Eliceiri, K., Tomancak, P. & Cardona, A. (2012) Fiji: an open-source platform for biological-image analysis. *Nature Methods*, **9**, 676-682.

Schmidt-Roach, S., Miller, K.J., Lundgren, P. & Andreakis, N. (2014) With eyes wide open: a revision of species within and closely related to the *Pocillopora damicornis* species complex (Scleractinia; Pocilloporidae) using morphology and genetics. *Zoological Journal of the Linnean Society*, **170**, 1-33.

Selkoe, K.A., Watson, J.R., White, C., Ben Horin, T., Iacchei, M., Mitarai, S., Siegel, D.A., Gaines, S.D. & Toonen, R.J. (2010) Taking the chaos out of genetic patchiness: seascape genetics reveals ecological and oceanographic drivers of genetic patterns in three temperate reef species. *Molecular Ecology*, **19**, 3708-3726.

Senou, H. (2004) The fish of Ogasawara. *Ogasawara, the Galapagos of the East: The appeal of endemic organisms and the crisis they face* (ed. by H. Karube and M. Takakuwa), pp. 55-62. Kanagawa Prefectural Museum of Natural History, Odawara.

Senou, H., Morita, Y. & Morishita, O. (2003) Notes on the distribution of a surgeonfish *Ctenochaetus hawaiiensis* (Perciformes: Acanthuridae) *I.O.P Diving News*, **14**, 2-4 (in Japanese).

Serrano, X., Baums, I.B., O'Reilly, K., Smith, T.B., Jones, R.J., Shearer, T.L., Nunes, F.L.D. & Baker, A.C. (2014) Geographic differences in vertical connectivity in the Caribbean coral *Montastraea cavernosa* despite high levels of horizontal connectivity at shallow depths. *Molecular Ecology*, **23**, 4226-4240.

Sexton, J.P., Strauss, S.Y. & Rice, K.J. (2011) Gene flow increases fitness at the warm edge of a species' range. *Proceedings of the National Academy of Sciences of the United States of America*, **108**, 11704-11709.

Shanks, A.L. (2009) Pelagic larval duration and dispersal distance revisited. *The biological bulletin*, **216**, 373-385.

Shchepetkin, A.F. & McWilliams, J.C. (2005) The regional oceanic modeling system (ROMS): a split-explicit, free-surface, topography-following-coordinate oceanic model. *Ocean modelling*, **9**, 347-404.

Shearer, T.L., Van Oppen, M.J.H., Romano, S.L. & Worheide, G. (2002) Slow mitochondrial DNA sequence evolution in the Anthozoa (Cnidaria). *Molecular Ecology*, **11**, 2475-2487.

Shih, H.T., Komai, T. & Liu, M.Y. (2013) A new species of fiddler crab from the Ogasawara (Bonin) Islands, Japan, separated from the widely-distributed sister species *Uca* (*Paraleptuca*) *crassipes* (White, 1847) (Crustacea: Decapoda: Brachyura: Ocypodidae). *Zootaxa*, **3746**, 175-193.

Shimada, K. (2002) Family Chaetodontidae. *Fishes of Japan with pictorial keys to the species, English edition* (ed. by T. Nakabo), pp. 884-897. Toaki University Press, Tokyo.

Shinzato, C., Mungpakdee, S., Arakaki, N. & Satoh, N. (2015) Genome-wide SNP analysis explains coral diversity and recovery in the Ryukyu Archipelago. *Scientific Reports*, **5**, 18211.

Siegel, D.A., Mitarai, S., Costello, C.J., Gaines, S.D., Kendall, B.E., Warner, R.R. & Winters, K.B. (2008) The stochastic nature of larval connectivity among nearshore

marine populations. *Proceedings of the National Academy of Sciences of the United States of America*, **105**, 8974-8979.

Simberloff, D. & Dayan, T. (1991) The Guild Concept and the Structure of Ecological Communities. *Annual Review of Ecology and Systematics*, **22**, 115-143.

Simpson, C., Kiessling, W., Mewis, H., Baron-Szabo, R.C. & Muller, J. (2011) Evolutionary Diversification of Reef Corals: A Comparison of the Molecular and Fossil Records. *Evolution*, **65**, 3274-3284.

Smith, E.G., Ketchum, R.N. & Burt, J.A. (2017) Host specificity of *Symbiodinium* variants revealed by an ITS2 metahaplotype approach. *Isme Journal*, **11**, 1500-1503.

Snyder, C.W. (2016) Evolution of global temperature over the past two million years. *Nature*, **538**, 226.

Sousa, V. & Hey, J. (2013) Understanding the origin of species with genome-scale data: modelling gene flow. *Nature Reviews Genetics*, **14**, 404-414.

Spalding, M.D., Fox, H.E., Halpern, B.S., McManus, M.A., Molnar, J., Allen, G.R., Davidson, N., Jorge, Z.A., Lombana, A.L., Lourie, S.A., Martin, K.D., McManus, E., Molnar, J., Recchia, C.A. & Robertson, J. (2007) Marine ecoregions of the world: A bioregionalization of coastal and shelf areas. *Bioscience*, **57**, 573-583.

Stamatakis, A. (2006) RAxML-VI-HPC: Maximum Likelihood-based Phylogenetic Analyses with Thousands of Taxa and Mixed Models. *Bioinformatics*, **22**, 2688-2690.

Stat, M., Carter, D. & Hoegh-Guldberg, O. (2006) The evolutionary history of *Symbiodinium* and scleractinian hosts - Symbiosis, diversity, and the effect of climate change. *Perspectives in Plant Ecology Evolution and Systematics*, **8**, 23-43.

Stat, M., Bird, C.E., Pochon, X., Chasqui, L., Chauka, L.J., Concepcion, G.T., Logan, D., Takabayashi, M., Toonen, R.J. & Gates, R.D. (2011) Variation in *Symbiodinium* ITS2 sequence assemblages among coral colonies. *Plos One*, **6**, e15854.

Stemann, T.A. (2003) Reef corals of the White Limestone Group of Jamaica. *Cainozoic Research* **3**, 83-107.

Strassmann, J.E., Gilbert, O.M. & Queller, D.C. (2011) Kin Discrimination and Cooperation in Microbes. *Annual Review of Microbiology, Vol 65*, **65**, 349-367.

Swain, T.D., Chandler, J., Backman, V. & Marcelino, L. (2017) Consensus thermotolerance ranking for 110 *Symbiodinium* phylotypes: an exemplar utilization of a novel iterative partial-rank aggregation tool with broad application potential. *Functional Ecology*, **31**, 172-183.

Thiel, M. & Haye, P.A. (2006) The ecology of rafting in the marine environment. III. Biogeographical and evolutionary consequences. *Oceanography and Marine Biology - an Annual Review, Vol 44*, **44**, 323-429.

Thornhill, D.J., Lajeunesse, T.C. & Santos, S.R. (2007) Measuring rDNA diversity in eukaryotic microbial systems: how intragenomic variation, pseudogenes, and PCR artifacts confound biodiversity estimates. *Molecular Ecology*, **16**, 5326-5340.

Thornhill, D.J., Lewis, A.M., Wham, D.C. & LaJeunesse, T.C. (2014) Host-specialist lineages dominate the adaptive radiation of reef coral endosymbionts. *Evolution*, **68**, 352-367.

Tin, M.M.Y., Economo, E.P. & Mikheyev, A.S. (2014) Sequencing degraded DNA from non-destructively sampled museum specimens for RAD-tagging and low-coverage shotgun phylogenetics. *Plos One*, **9**, e96793.

Toller, W.W., Rowan, R. & Knowlton, N. (2001) Zooxanthellae of the *Montastraea annularis* species complex: Patterns of distribution of four taxa of *Symbiodinium* on different reefs and across depths. *Biological Bulletin*, **201**, 348-359.

Tong, H.Y., Cai, L., Zhou, G.W., Yuan, T., Zhang, W.P., Tian, R.M., Huang, H. & Qian, P.Y. (2017) Temperature shapes coral-algal symbiosis in the South China Sea. *Scientific Reports*, **7**, 40118.

Tonk, L., Sampayo, E.M., Weeks, S., Magno-Canto, M. & Hoegh-Guldberg, O. (2013) Host-Specific Interactions with Environmental Factors Shape the Distribution of Symbiodinium across the Great Barrier Reef. *Plos One*, **8**, e68533.

Tracey, J.I., Schlanger, S.O., Stark, J.T., Doan, D.B. & May, H.G. (1964) *General geology of Guam*. U.S. Government Printing Office.

Treml, E.A., Roberts, J., Halpin, P.N., Possingham, H.P. & Riginos, C. (2015) The emergent geography of biophysical dispersal barriers across the Indo-West Pacific. *Diversity and Distributions*, **21**, 465-476.

UNEP-WCMC, W.C., WRI, TNC (2010) Global distribution of warm-water coral reefs, compiled from multiple sources including the Millennium Coral Reef Mapping Project. Version 3.0. Includes contributions from IMaRS-USF and IRD (2005), IMaRS-USF (2005) and Spalding et al. (2001). In, Cambridge (UK): UN Environment World Conservation Monitoring Centre. URL: http://data.unep-wcmc.org/datasets/1.

van der Veer, E. (2007) *Towards a revision of the coral genus Galaxea (Scleractinia: Oculinidae)*. University of Leiden, Leiden.

van der Ven, R.M., Triest, L., De Ryck, D.J.R., Mwaura, J.M., Mohammed, M.S. & Kochzius, M. (2015) Population genetic structure of the stony coral *Acropora tenuis* shows high but variable connectivity in East Africa. *Journal of Biogeography*,

van Oppen, M.J.H., McDonald, B.J., Willis, B. & Miller, D.J. (2001a) The evolutionary history of the coral genus *Acropora* (Scleractinia, Cnidaria) based on a mitochondrial and a nuclear marker: Reticulation, incomplete lineage sorting, or morphological convergence? *Molecular Biology and Evolution*, **18**, 1315-1329.

van Oppen, M.J.H., Palstra, F.P., Piquet, A.M.T. & Miller, D.J. (2001b) Patterns of coral-dinoflagellate associations in *Acropora*: significance of local availability and physiology of *Symbiodinium* strains and host-symbiont selectivity. *Proceedings of the Royal Society B-Biological Sciences*, **268**, 1759-1767.

van Woesik, R., Sakai, K., Ganase, A. & Loya, Y. (2011) Revisiting the winners and the losers a decade after coral bleaching. *Marine Ecology Progress Series*, **434**, 67-76.

Veron, J.E.N. (1992) Conservation of Biodiversity - a Critical Time for the Hermatypic Corals of Japan. *Coral Reefs*, **11**, 13-21.

Veron, J.E.N. (1995) *Corals in space and time : the biogeography and evolution of the Scleractinia*. Comstock/Cornell, Ithaca.

Veron, J.E.N. & Stafford-Smith, M. (2000) *Corals of the orld*. Australian Institute of Marine Science, Townsville, Australia.

Veron, J.E.N., Stafford-Smith, M., DeVantier, L. & Turak, E. (2015) Overview of distribution patterns of zooxanthellate Scleractinia. *Frontiers in Marince Science*, **1**, Article 81.

Voolstra, C., Miller, D., Ragan, M., Hoffmann, A., Hoegh-Guldberg, O., Bourne, D., Ball, E., Ying, H., Foret, S., Takahashi, S., Weynberg, K., van Oppen, M., Morrow, K., Chan, C.X., Rosic, N., Leggat, W., Sprungala, S., Imelfort, M., Tyson, G., Kassahn, K., Lundgren, P., Beeden, R., Ravasi, T., Berumen, M., Abel, E. & Fyffe, T. (2015) The ReFuGe 2020 Consortium—using “omics” approaches to explore the adaptability and resilience of coral holobionts to environmental change. *Frontiers in Marine Science*, **2**, 68.

Warner, P.A., van Oppen, M.J.H. & Willis, B.L. (2015) Unexpected cryptic species diversity in the widespread coral *Seriatoporahystrix* masks spatial-genetic patterns of connectivity. *Molecular Ecology*, **24**, 2993-3008.

Warton, D.I., Blanchet, F.G., O'Hara, R.B., Ovaskainen, O., Taskinen, S., Walker, S.C. & Hui, F.K.C. (2015) So Many Variables: Joint Modeling in Community Ecology. *Trends in Ecology & Evolution*, **30**, 766-779.

Watanabe, T., Nishida, M., Watanabe, K., Wewengkang, D.S. & Hidaka, M. (2005) Polymorphism in nucleotide sequence of mitochondrial intergenic region in scleractinian coral (*Galaxea fascicularis*). *Marine Biotechnology*, **7**, 33-39.

Wewengkang, D.S., Watanabe, T. & Hidaka, M. (2007) Studies on morphotypes of the coral *Galaxea fascicularis* from Okinawa: polyp color, nematocyst shape, and coenosteum density. *Journal of the Japanese Coral Reef Society*, **9**, 49-59.

White, C., Selkoe, K.A., Watson, J., Siegel, D.A., Zacherl, D.C. & Toonen, R.J. (2010) Ocean currents help explain population genetic structure. *Proceedings of the Royal Society B-Biological Sciences*, **277**, 1685-1694.

Willis, B., Babcock, R., Harrison, P. & Wallace, C. (1997) Experimental hybridization and breeding incompatibilities within the mating systems of mass spawning reef corals. *Coral Reefs*, **16**, 53-65.

Willis, B.L., van Oppen, M.J.H., Miller, D.J., Vollmer, S.V. & Ayre, D.J. (2006) The role of hybridization in the evolution of reef corals. *Annual Review of Ecology Evolution and Systematics*, **37**, 489-517.

Wilson, G.A. & Rannala, B. (2003) Bayesian inference of recent migration rates using multilocus genotypes. *Genetics*, **163**, 1177-1191.

WoRMS, E.B. (2015) *World Register of Marine Species*. Available at: http://www.marinespecies.org at VLIZ (accessed 2015-03-04

Yamano, H., Hori, K., Yamauchi, M., Yamagawa, O. & Ohmura, A. (2001) Highest-latitude coral reef at Iki Island, Japan. *Coral Reefs*, **20**, 9-12.

Yamazaki, D., Miura, O., Ikeda, M., Kijima, A., Tu, D.V., Sasaki, T. & Chiba, S. (2017) Genetic diversification of intertidal gastropoda in an archipelago: the effects of islands, oceanic currents, and ecology. *Marine Biology*, **164**, 184.

Yamazato, K. (1988) Reproductive mechanism of *Galaxea fascicularis*. *Report for Grant-in-Aid on "Early phase of reproduction of marine resource organisms" from the Ministry of Education, Science and Culture, Japan*, 148-155.

Yasuda, N., Nagai, S., Hamaguchi, M., Okaji, K., Gerard, K. & Nadaoka, K. (2009) Gene flow of *Acanthaster planci* (L.) in relation to ocean currents revealed by microsatellite analysis. *Molecular Ecology*, **18**, 1574-1590.

Yasuda, N., Taquet, C., Nagai, S., Fortes, M., Fan, T.-Y., Phongsuwan, N. & Nadaoka, K. (2014) Genetic structure and cryptic speciation in the threatened reef-building coral *Heliopora coerulea* along Kuroshio Current. *Bulletin of Marine Science*, **90**, 233-255.

Yasuda, N., Taquet, C., Nagai, S., Fortes, M., Fan, T.-Y., Harii, S., Yoshida, T., Sito, Y. & Nadaoka, K. (2015) Genetic diversity, paraphyly and incomplete lineage sorting of mtDNA, ITS2 and microsatellite flanking region in closely related *Heliopora species* (Octocorallia). *Molecular Phylogenetics and Evolution*, **93**, 161-171.

Yeemin, T., Saenghaisuk, C., Sutthacheep, M., Pengsakun, S., Klinthong, W. & Saengmanee, K. (2009) Conditions of coral communities in the Gulf of Thailand: a decade after the 1998 severe bleaching event. *Galaxea, Journal of Coral Reef Studies*, **11**, 207-217.

Yoshigou, H. (2004) The fishes fround from tide-pools and surge sublittral zone in the Minami-daito (South-Borodino) Island, Japan. *Misc Rep Hiwa Mus Natl Hist Hiroshima*, **43**, 1-51.

Yoshiwara, S. (1902) III.—Geological Age of the Ogasawara Group (Bonin Islands) as indicated by the occurrence of Nummulites. *Geological Magazine*, **9**, 296-303.

Yost, D.M., Wang, L.H., Fan, T.Y., Chen, C.S., Lee, R.W., Sogin, E. & Gates, R.D. (2013) Diversity in skeletal architecture influences biological heterogeneity and *Symbiodinium* habitat in corals. *Zoology*, **116**, 262-269.

Zayasu, Y., Nakajima, Y., Sakai, K., Suzuki, G., Satoh, N. & Shinzato, C. (2016) Unexpectedly complex gradation of coral population structure in the Nansei Islands, Japan. *Ecology and Evolution*, **6**, 5491-5505.

Zhou, G., Huang, H., Lian, J., Zhang, C. & Li, X. (2012) Habitat correlation of *Symbiodinium* diversity in two reef-building coral species in an upwelling region, eastern Hainan Island, China. *Journal of the Marine Biological Association of the United Kingdom*, **92**, 1309-1316.

Zhou, G.W., Cai, L., Li, Y.C., Tong, H.Y., Jiang, L., Zhang, Y.Y., Lei, X.M., Guo, M.L., Liu, S., Qian, P.Y. & Huang, H. (2017) Temperature-driven local acclimatization of *Symbiodnium* hosted by the Coral *Galaxea fascicularis* at Hainan Island, China. *Frontiers in Microbiology*, **8**, 2487.

Ziegler, M., Eguíluz, V.M., Duarte, C.M. & Voolstra, C.R. (2018) Rare symbionts may contribute to the resilience of coral–algal assemblages. *The ISME Journal*, **12**, 161-172.

Zwickl, D.J. & Hillis, D.M. (2002) Increased taxon sampling greatly reduces phylogenetic error. *Systematic Biology*, **51**, 588-598.

Appendices

Appendix 1

Table S1.1. Symbiodiniaceae ITS2-types found in 67 *Galaxea fascicularis* colonies across the Nansei Islands. OTUs with <99.11% identity to an existing reference were submitted as new ITS2-types to GenBank. GenBank accession numbers, number of OTUs and the total abundance as a fraction of the total (N= 3.86 M) are given per ITS2 type.

ITS2 reference type	GenBank Accession Number	# OTUs	Abundance
dominant			
C1	JN558041	45	0.23 N
D1	AF334660	40	0.23 N
C21a	AY589744	31	0.16 N
common			
D1a	JN558078	14	0.085 N
C3	AB778606	32	0.072 N
C21/3d/C3k	AY239372	12	0.050 N
C1060	DQ480600	10	0.035 N
C1b/C1e	AY239363	5	0.033 N
C1c/C45	AY239364	6	0.027 N
C27/C3	AY239379	3	0.013 N
rare			
C1h	AY258473	1	0.008 N
C1p	GU907652	1	0.007 N
C1230	EU074889	2	0.007 N
D2	AY686649	3	0.007 N
C1228	EU074883	1	0.006 N
C1002	DQ838544	1	0.004 N
C1226	EU074881	2	0.002 N
C3b	AF499791	2	0.002 N
C7	AF499797	1	0.0017 N
C1148	EU040178	1	0.001 N
C1005	DQ480633	1	0.0007 N
C1013	DQ480642	1	0.0007 N
C1234	EU118165	1	0.0007 N
C1085	AY624605	1	0.0004 N
D106	AF174559	1	0.0003 N
other ITS2-types			
OTU7 (98.9% C21/3d/3k)		1	0.0006 N
OTU 14 (98.6% C21/3d/3k)		1	0.0016 N
OTU25 (98.57% C3)		1	0.0008 N
OTU40 (98.9% C21/3d/3k)		1	0.0012 N
OTU297 (98.5% C21a)		1	0.0005 N
OTU350 (98.9% D111)		1	0.0006 N
OTU1387 (98.9% C3b)		1	0.0022 N

OTU1503 (98.9% C21/3d/3k)	1	0.0005 N
OTU1507 (98.9 % C21/3d/3k)	1	0.0005 N
OTU1675 (98.9% C3)	1	0.0004 N
OTU2094 (98.9% C21/3d/3k)	1	0.0004 N
OTU35 (97.5% C18)	1	0.00223 N
OTU45 (98.2% C3.1)	1	0.0004 N
OTU43 (96.8% C22)	1	0.0018 N
OTU52 (96.2% C1008)	1	0.0010 N
OTU18 (96.8% C1)	1	0.0009 N

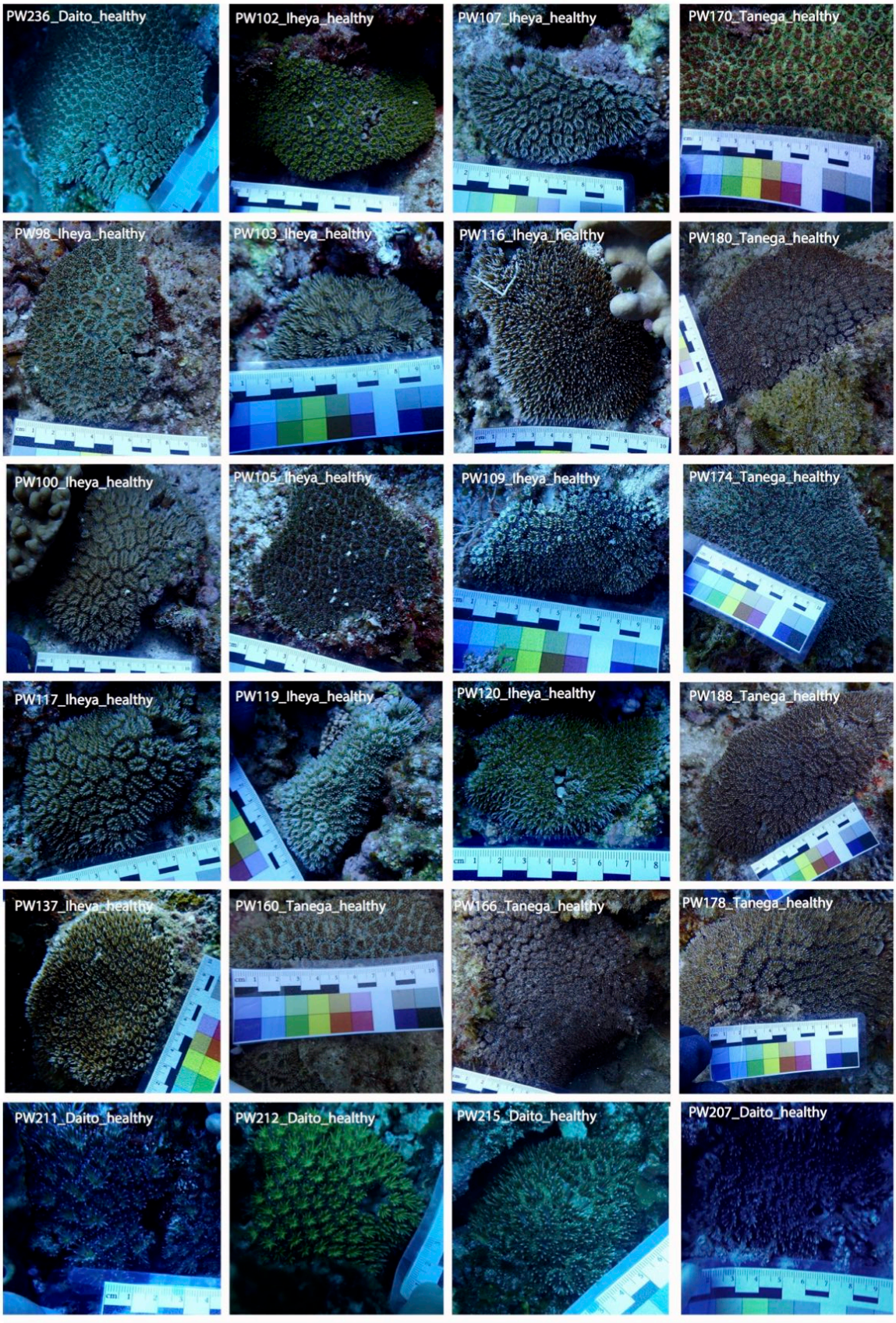

Figure S1.1. Sampling photographs of 47 *Galaxea fascicularis* specimens from four locations.

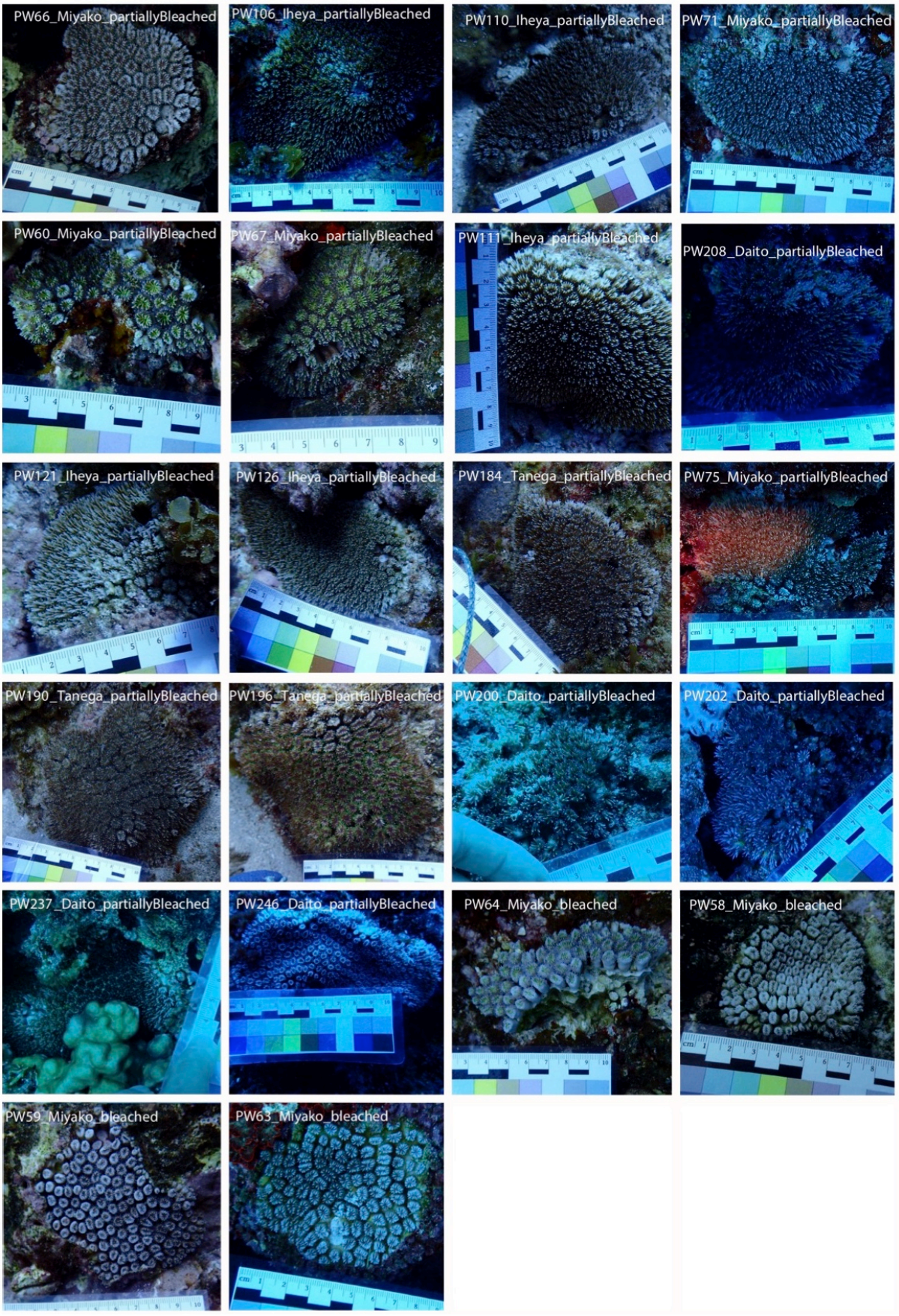

Figure S1.1. Sampling photographs of 47 *Galaxea fascicularis* specimens from four locations (continued)

A

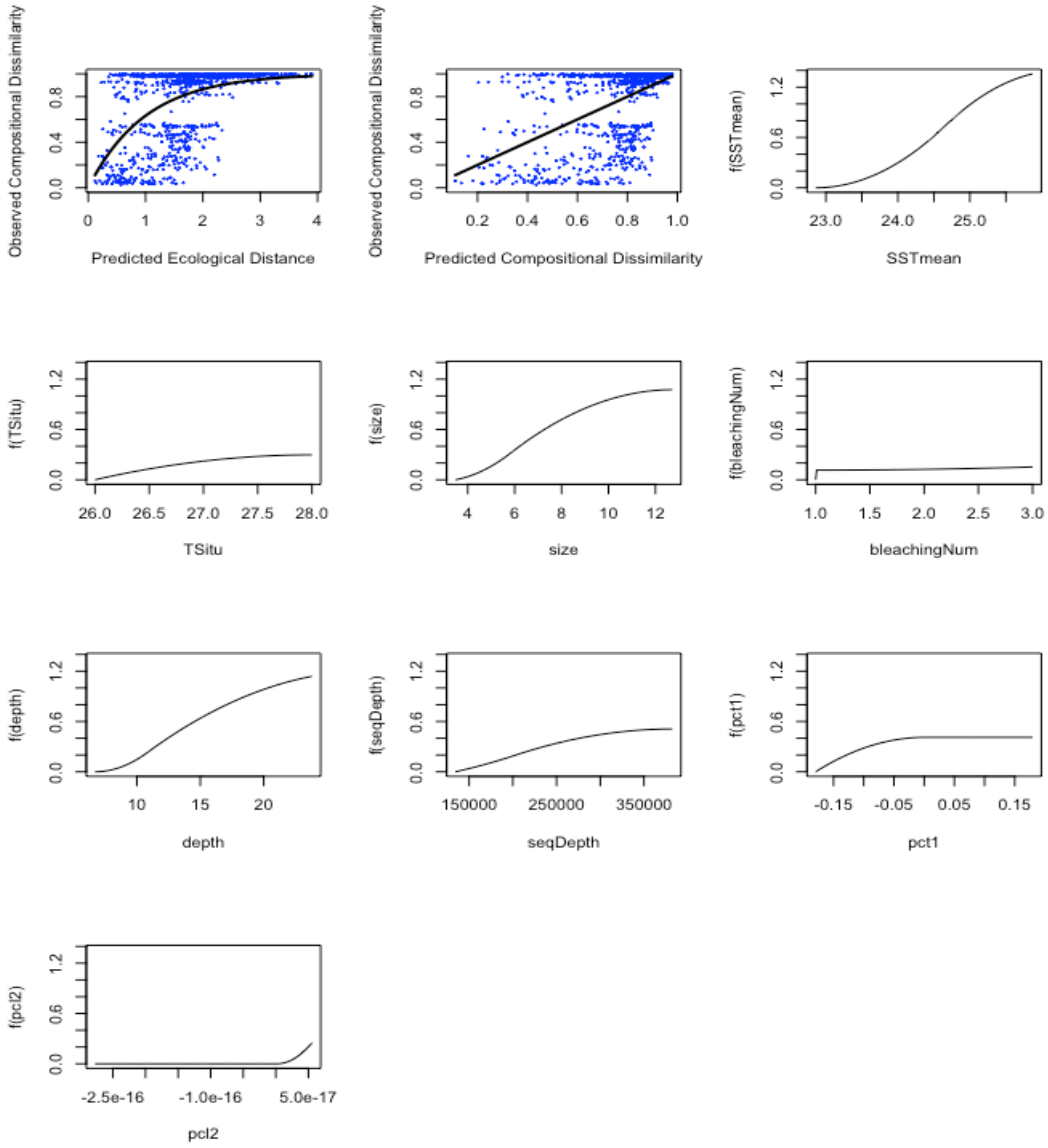
Observed Compositional Dissimilarity
Predicted Ecological Distance
Predicted Compositional Dissimilarity
f(SSTmean)
SSTmean
f(TSitu)
TSitu
f(size)
size
f(bleachingNum)
bleachingNum
f(depth)
depth
f(seqDepth)
seqDepth
f(pct1)
pct1
f(pcl2)
pcl2

B

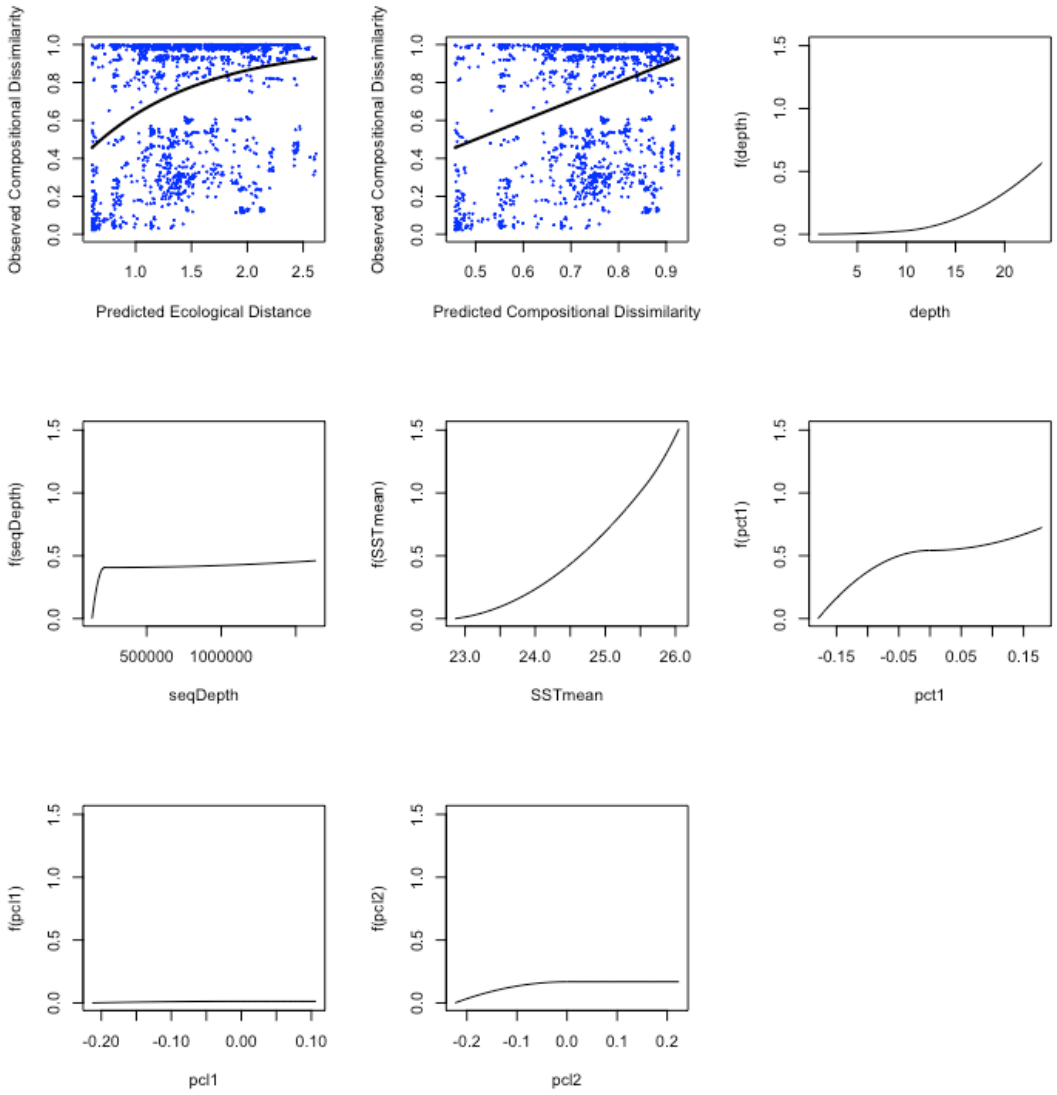

Fig. S1.2. Parameter splines of Generalized Dissimilarity Model on 47 samples with all metadata (A), and on 67 samples with reduced metadata (no T *in situ*, bleaching status, polyp size).

A

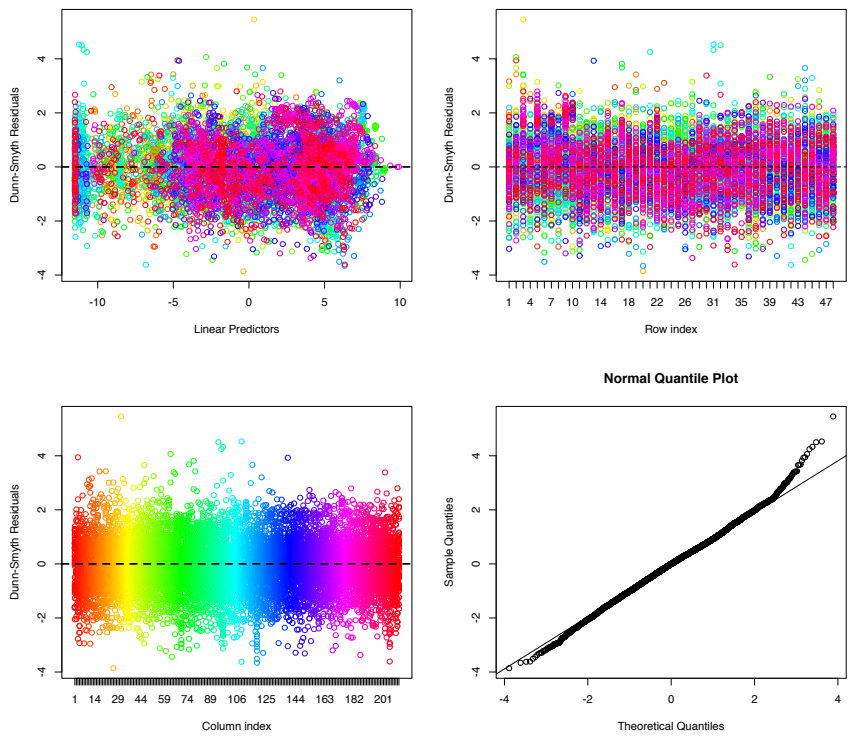
Dunn-Smyth Residuals
Linear Predictors
Row index
Normal Quantile Plot
Column index
Sample Quantiles
Theoretical Quantiles

B

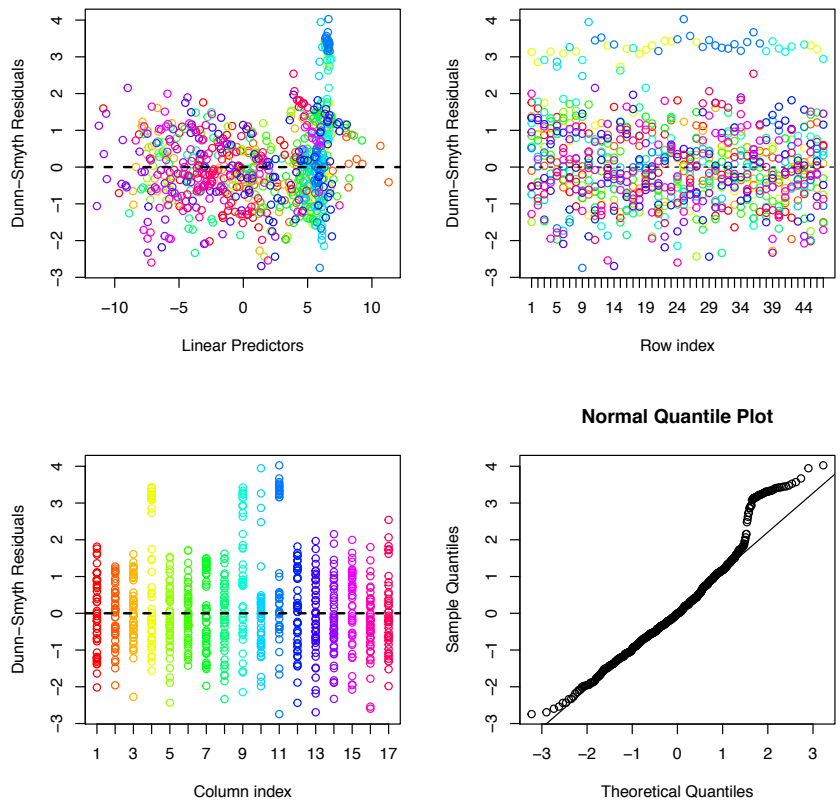
Dunn–Smyth Residuals
Linear Predictors
Row index
Normal Quantile Plot
Column index
Sample Quantiles
Theoretical Quantiles

Fig. S1.3. Residual analysis of a pure latent variable model in Boral verifies the suitability of a modelling approach assuming a negative-binomial distribution of the data. Top left: Dunn– Smyth residuals vs. linear predictors. Top right: Dunn–Smyth residuals vs. row index; Bottom left: Dunn–Smyth residuals vs. column index; Bottom right: normal quantile plot of Dunn–Smyth residuals. A: Analysis based on OTUs defined by minimum entropy decomposition. B: Analysis based on OTUs defined by 97% identity radius.

A

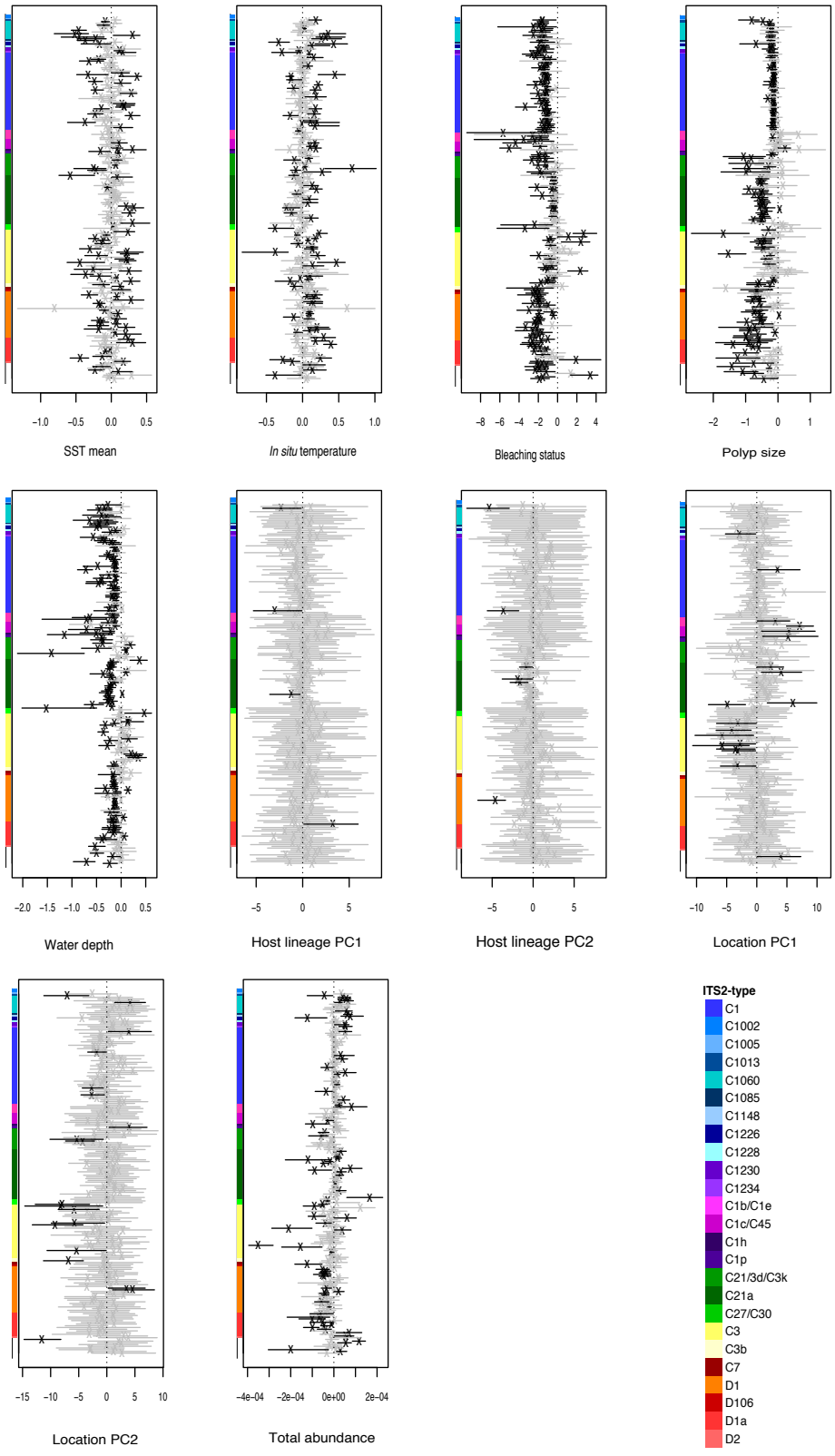
SST mean
In situ temperature
Bleaching status
Polyp size
Water depth
Host lineage PC1
Host lineage PC2
Location PC1
Location PC2
Total abundance
ITS2-type
C1
C1002
C1005
C1013
C1060
C1085
C1148
C1226
C1228
C1230
C1234
C1b/C1e
C1c/C45
C1h
C1p
C21/3d/C3k
C21a
C27/C30
C3
C3b
C7
D1
D106
D1a
D2

B

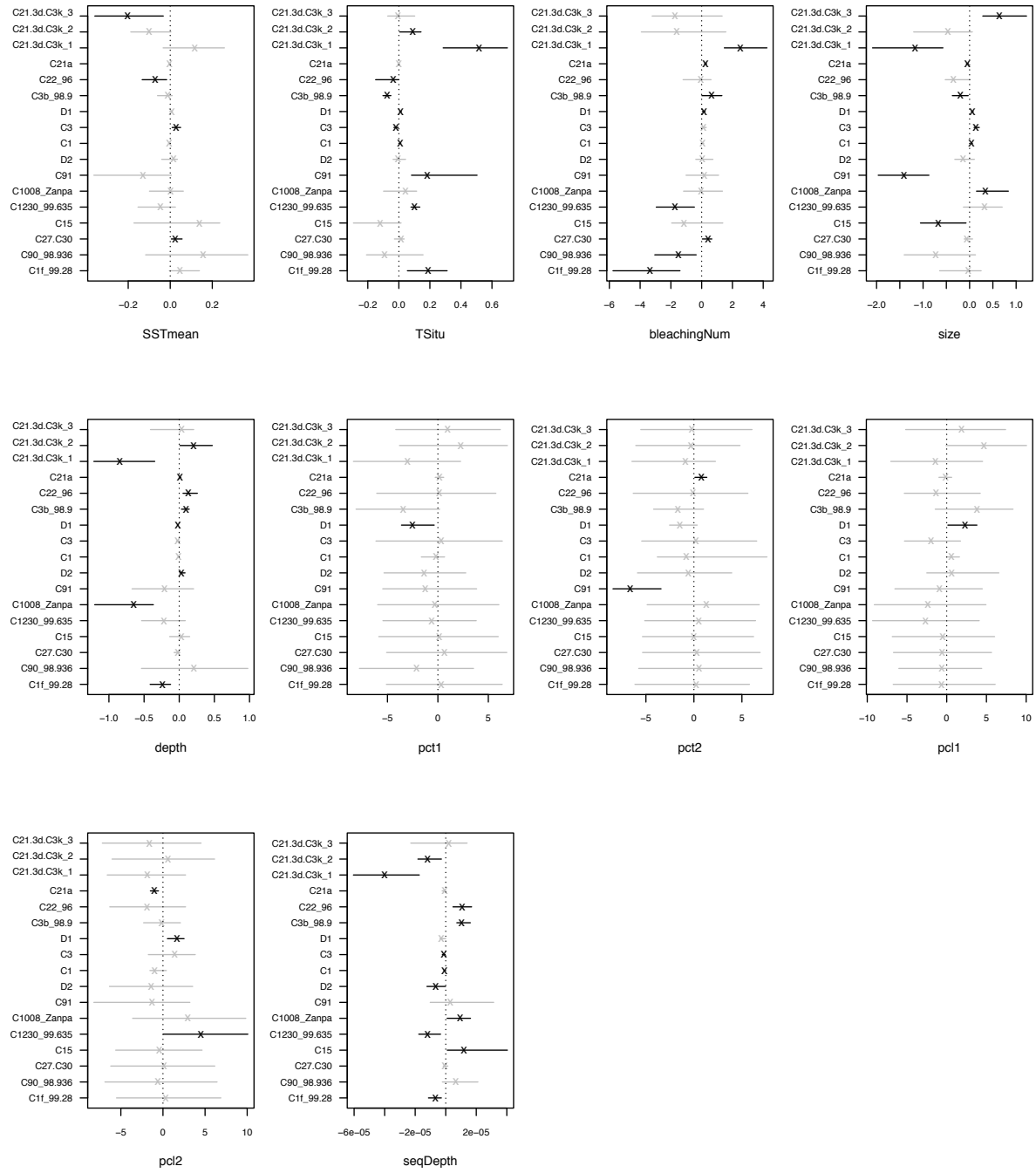

Fig. S1.4. Point estimates and 95% highest posterior density intervals for the OTU-specific regression coefficients corresponding to a covariate fitted in the Boral model. Density intervals that include zero are colored gray. A: Analysis based on OTUs defined by minimum entropy decomposition. B: Analysis based on OTUs defined by 97% identity radius.

Appendix 2

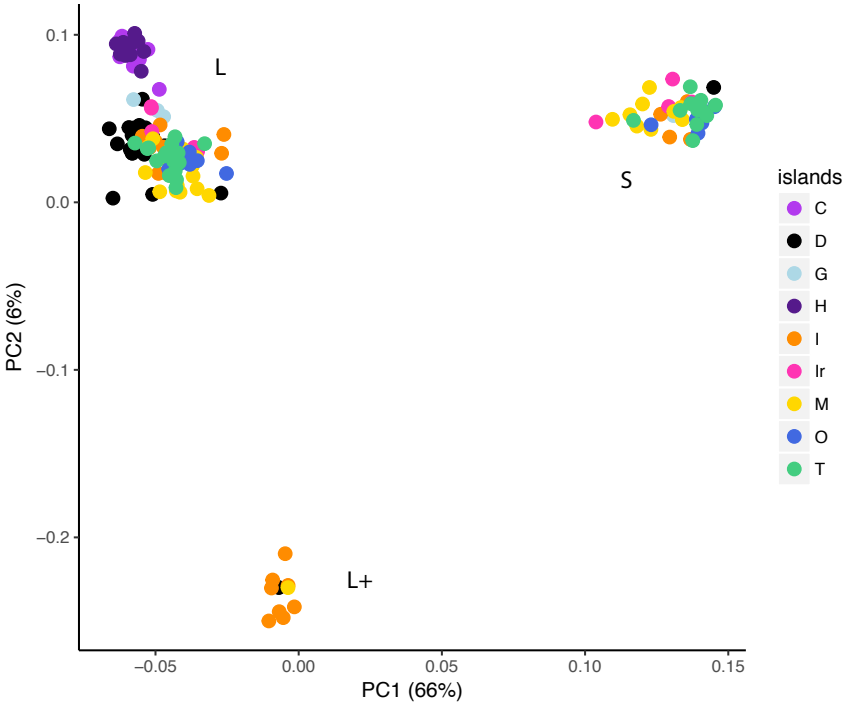

Figure S2.1. Principal component analysis for the separation of cryptic lineages 'L' 'L+' and 'S' based on 11'473 SNPs represented in at least 50% of all individuals.

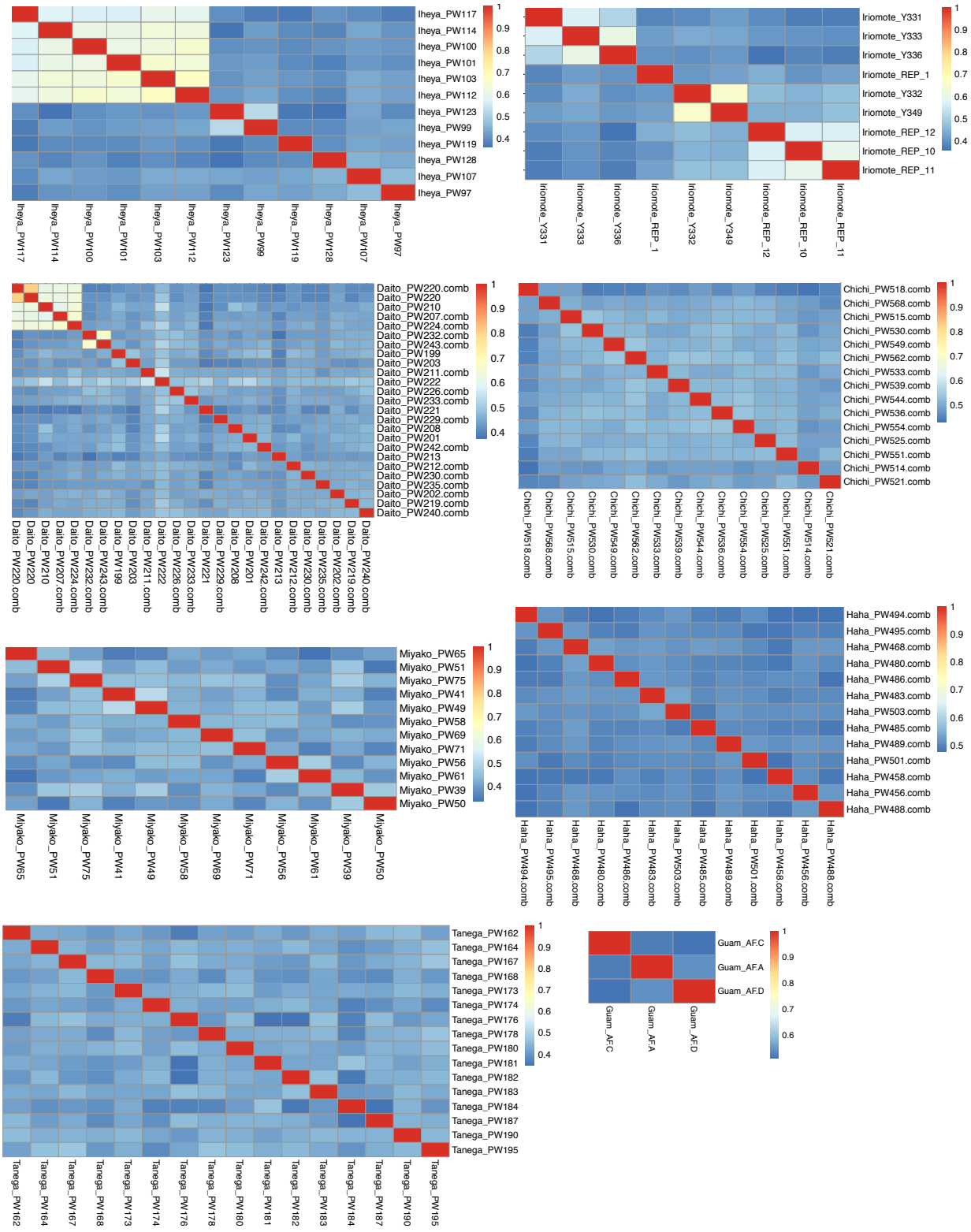

Figure S2.2. Heatmaps of pairwise correlations for clone detection. Correlation coefficients for each sampling location are given. Clone pairs were identified based on a correlation coefficient >0.56, as this is the correlation between known clone pairs from Iriomote.

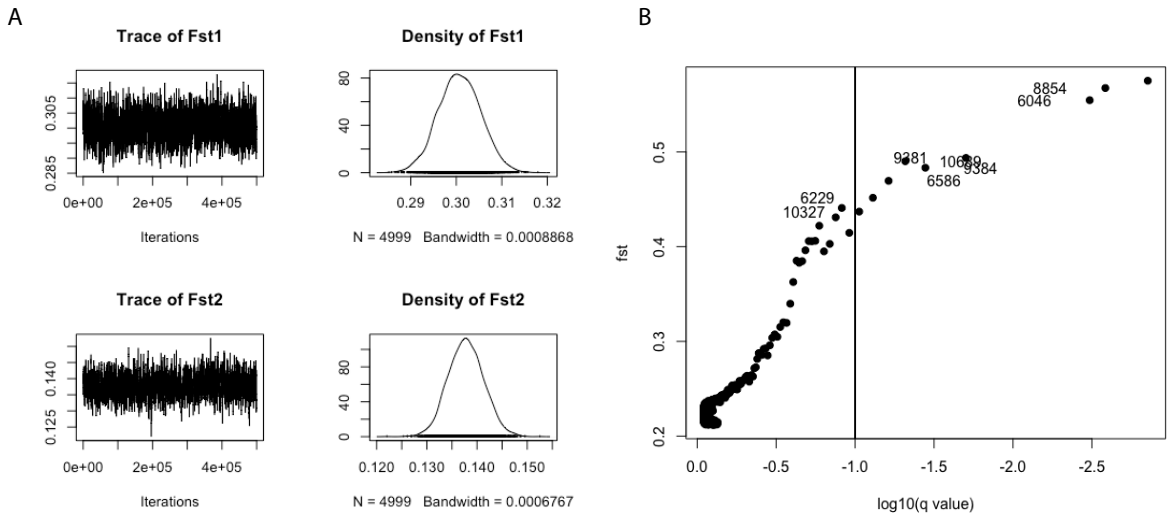

Figure S2.3. BayeScan output for the detection of sites under selection. A: Trace plots based on two main populations Ogasawara and Ryukyu + Daito. B: Nine loci under potential selection were identified based on the recommended False Discovery Rate of FRD=0.1 (q-value cut-off). The outlier loci have Fst > 0.437.

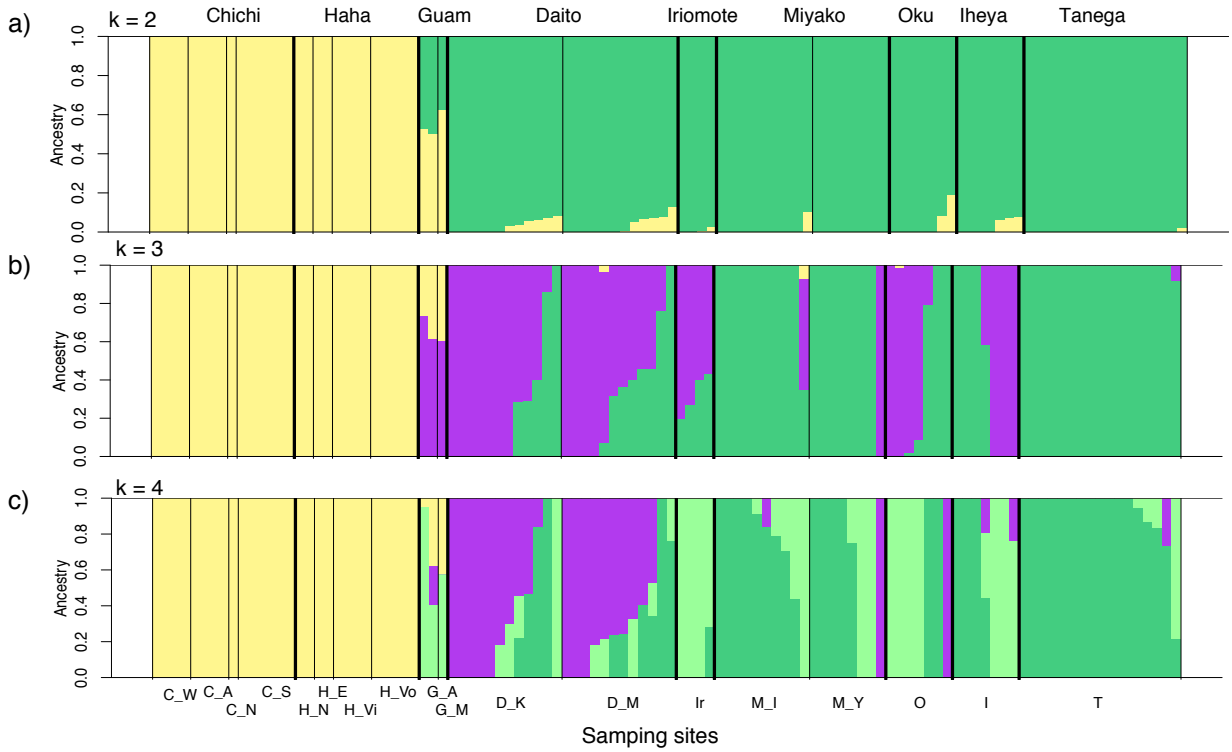

Figure S2.4. Admixture analysis based on SNPs present in > 70% of individuals. Individual population assignments for K=2 (CV error: 0.483), K=3 (CV error: 0.511), and K=4 (0.545) as inferred by Admixture based on 1756 neutral sites present in >70% of the individuals. Individuals are grouped by sampling site.

Table S2.1. Migration rates estimated by BayesAss based on 1979 neutral and biallelic SNPs present in at least 70% of individuals. Rates represent the proportion of settlers in destination populations (rows) from source populations (columns) and their standard deviations between geographic populations. Only population with >10 individuals were included. Rates > 0.02 and < 0.8 are marked in bold.

	Source				
Dest.	Chichi	Haha	Daito	Miyako	Tanega
Chichi	0.9329 (0.0295)	0.0170 (0.0163)	0.0169 (0.0161)	0.0167 (0.0157)	0.0165 (0.0156)
Haha	**0.2589** (0.0319)	0.6854 (0.0173)	0.0188 (0.0179)	0.0184 (0.0176)	0.0185 (0.0174)
Daito	0.0114 (0.0111)	0.0114 (0.0110)	0.8855 (0.0292)	**0.0801** (0.0261)	0.0115 (0.0113)
Miyako	0.0146 (0.0138)	0.0146 (0.0139)	**0.0288** (0.0193)	0.9274 (0.0283)	0.0146 (0.0139)
Tanega	0.0152 (0.0146)	0.0152 (0.0143)	0.0151 (0.0145)	**0.0609** (0.0273)	0.8936 (0.0325)

Table S2.2. 2D demographic models tested in *dadi* to infer symmetry of pairwise migratory relationships. Projections, number of segregating sites, and final parameter values after three rounds of optimization are given. Models used for the 3D model is printed in bold and refers to the site frequency spectra in Figure S5. The most likely 2D model is printed in italic.

Populations	Model	log-lik	theta	AIC	nu1	nu2	m12 (m)	m21	T1	T2
Og-Dt	no div	-5156.81	594.89	10319.62						
S: 2544	no mig	-606.82	613.5	1219.64	0.3154	0.6706	0.1273			
proj: 26, 16	sym mig	-534.01	223.55	1076.02	1.0467	2.12	0.4155	3.2804		
	asym mig	**-530.51**	**99.25**	**1071.02**	**2.1044**	**5.1664**	**0.2422**	**0.1362**	**8.6079**	
	anc sym mig	*-529.54*	*145.9*	*1069.08*	*1.6254*	*3.2109*	*0.2978*	*5.7315*	*0.0388*	
	anc asym mig	-554.31	1256.44	1120.62	0.1841	0.2954	2.2857	4.4724	5.5964	0.0082
	sec cont sym mig	-534.37	319.76	1078.74	0.7324	1.4749	0.5873	0.0039	1.8593	
	sec cont asym	-530.73	191.31	1073.46	1.0665	2.7211	0.4865	0.2487	0.0047	3.8745
Og-Ryu	no div	-6830.57	667.59	13667.14						
S: 2998.212	no mig	-847.93	710.84	1701.86	0.1769	0.6951	0.0743			
proj: 26, 26	sym mig	-752.23	189.34	1512.46	1.0039	3.1471	0.4291	5.2475		
	asym mig	**-742.49**	**277.31**	**1494.98**	**0.5387**	**2.4165**	**0.9897**	**0.4081**	**2.6545**	
	anc sym mig	-749.75	283.72	1509.5	0.6769	2.0899	0.6897	3.0695	0.0125	
	anc asym mig	*-739.91*	*444.76*	*1491.82*	*0.3302*	*1.4787*	*1.8095*	*0.6265*	*1.1196*	*0.0068*
	sec cont sym mig	-752.29	266.57	1514.58	0.7117	2.2432	0.6063	0.0999	3.211	
	sec cont asym	-742.18	186.73	1496.36	0.7892	3.5428	0.6766	0.2789	0.7577	3.9584
Dt-Ryu	no div	-1398.79	692.84	2803.58						
S: 2963.46	no mig	-552.04	737.02	1110.08	0.1324	0.339	0.0146			
proj: 16, 26	**sym mig**	**-549.68**	**225.67**	**1107.36**	**1.2523**	**2.3462**	**1.7908**	**4.2156**		
	asym mig	-549.81	322.45	1109.62	0.7878	1.7177	3.1138	2.2851	2.4041	
	anc sym mig	-534.79	504.95	1079.58	0.564	1.0031	19.9212	4.387	0.0406	
	anc asym mig	-540.1	103.13	1092.2	2.0333	5.9508	3.1874	1.0778	9.4945	0.1184
	sec cont sym mig	-549.63	132.43	1109.26	2.1472	3.998	1.0484	0.2614	7.7444	
	sec cont asym	*-526.02*	*249.71*	*1064.04*	*0.2848*	*1.8384*	*13.1354*	*0.6378*	*9.996*	*0.3724*
G-Ryu+Dt	no div	-1568.8	437.3	3143.6						
S: 1955.085	no mig	-518.26	433.39	1042.52	0.0956	0.9093	0.0838			
proj: 4, 46	sym mig	-518.33	433.04	1044.66	0.0968	0.9111	0.0114	0.0848		
	asym mig	**-503.56**	**112.73**	**1017.12**	**0.3004**	**4.3402**	**1.1996**	**0.0595**	**4.5957**	
G-Og	no div	-1437.89	279.07	2881.78						
S: 1099	no mig	-336.79	320.14	679.58	0.1935	0.4607	0.1509			
proj: 4, 26	sym mig	-348.07	285.2	704.14	0.3541	0.5967	0.5914	0.3858		
	asym mig	**-334.63**	**303.1**	**679.26**	**0.2711**	**0.5369**	**0.0399**	**0.2894**	**0.2302**	
	anc_sym_mig	-340.71	80.95	691.42	1.2099	2.1523	0.3384	8.1019	0.2779	
	anc_asym_mig	*-331.34*	*176.3*	*674.68*	*0.3769*	*1.0823*	*1.4361*	*0.3116*	*8.4823*	*0.0858*
	sec cont sym	-336.09	320.24	682.18	0.2054	0.4621	0.2488	0.1281	0.0391	
	sec cont asym	-341.54	96.19	695.08	0.5827	2.0692	0.6914	0.1037	3.8337	2.0034

Abbreviations: Og = Ogasawara, Ryu = Ryukyu, Dt = Daito, proj. = projection, S = average number of segregating sites per individual, theta = the effective mutation rate of the ancestral population, nu1(2) = effective population sizes relative to ancestral population, m = symmetric migration rate, m12 = migration rate from population two to population 1, m21 = migration rate from population one to population two, T = time between population split and the present. Models: no div = no divergence, no mig = divergence without migration, (a)sym mig = divergence under (a)symmetric migration, anc (a)sym mig = divergence under ancestral (a)symmetric migration until T1 and no migration since T2, sec cont (a)sym mig = divergence under no migration until T1, then (a)symmetric migration.

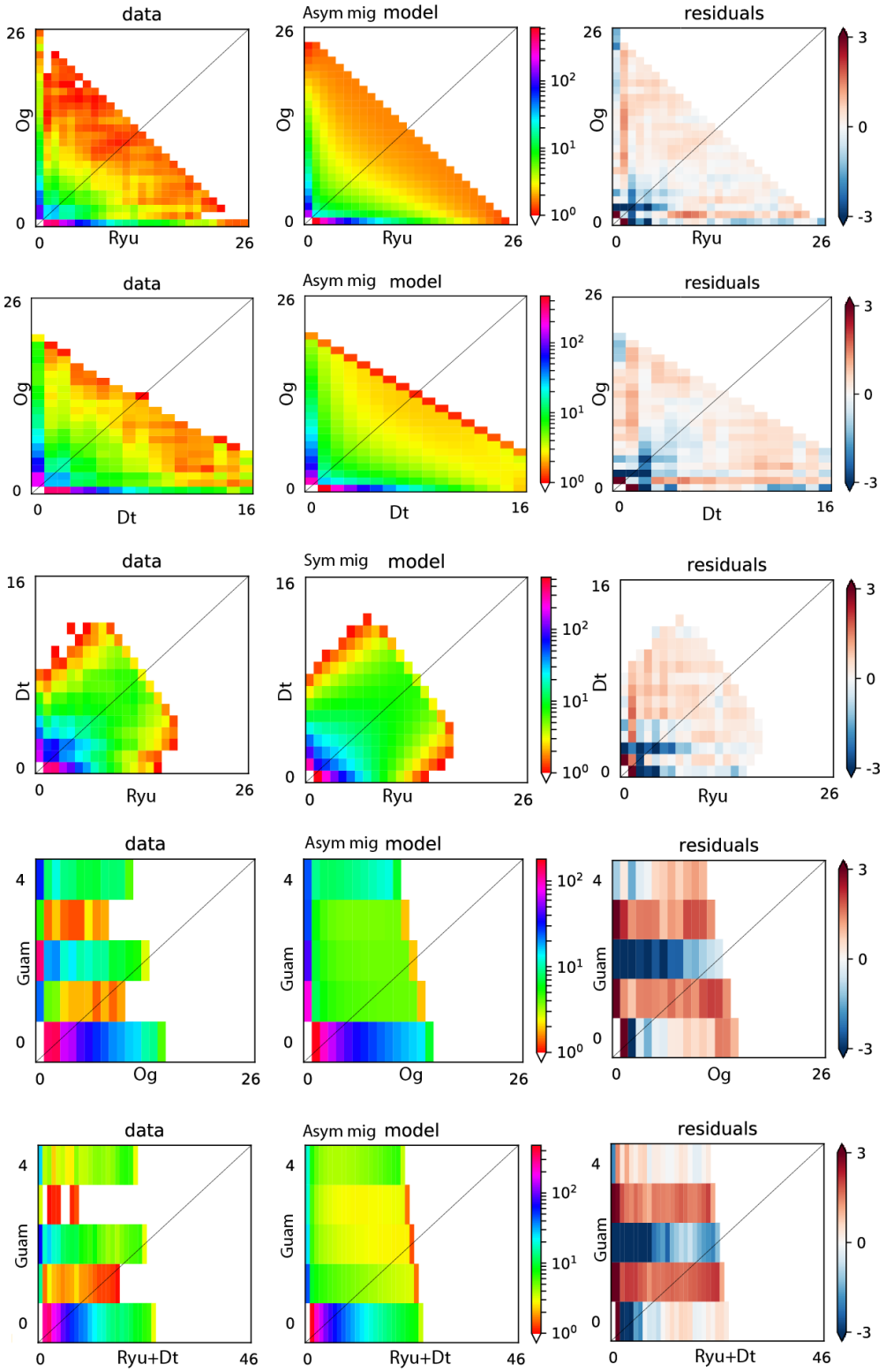

Figure S2.5. Dadi site frequency spectra and residuals of 2D models. Models of divergence used for the 3D models are given. Parameter values are given in Table S2 (bold). Abbreviations: Og = Ogasawara, Dt = Daito, Ryu = Ryukyu, Asym mig = Divergence under asymmetric migration, Sym mig = Divergence under symmetric migration.

Table S2.3. Immigration probability matrix according to inverse particle tracking. Propagules are modeled to settle between 3 and 60 d with an average mortality rate of 5% per day.

Source > Destination v	Palau	Nmariana	Micronesia	Marshall	Vietnam	Paracel	Dongsha	Luzon	Taiwan	Amami	Tokara	Iriomote	Miyako	Oku	Tanega	Daito	Ogasawara	Guam	Okinotori
Iriomote	0.000	0.000	0.000	0.000	0.002	0.003	0.003	0.300	0.087	0.001	0.001	0.485	0.102	0.015	0.000	0.000	0.000	0.000	0.000
Miyako Y	0.000	0.000	0.000	0.000	0.001	0.002	0.003	0.144	0.050	0.005	0.000	0.178	0.535	0.081	0.000	0.001	0.000	0.000	0.000
Miyako I	0.000	0.000	0.000	0.000	0.001	0.002	0.003	0.176	0.059	0.008	0.000	0.179	0.443	0.129	0.000	0.000	0.000	0.000	0.000
Oku	0.000	0.000	0.000	0.000	0.000	0.000	0.000	0.011	0.005	0.049	0.003	0.011	0.010	0.911	0.000	0.000	0.000	0.000	0.000
Ihyea	0.000	0.000	0.000	0.000	0.000	0.001	0.001	0.037	0.019	0.142	0.006	0.038	0.034	0.721	0.000	0.001	0.000	0.000	0.000
Tanega	0.000	0.000	0.000	0.000	0.000	0.001	0.003	0.041	0.039	0.024	0.137	0.037	0.023	0.038	0.657	0.000	0.000	0.000	0.000
MinamiDaito	0.000	0.000	0.000	0.000	0.000	0.000	0.000	0.015	0.010	0.269	0.030	0.020	0.024	0.440	0.000	0.192	0.000	0.000	0.000
KitaDaito	0.000	0.000	0.000	0.000	0.000	0.000	0.000	0.011	0.008	0.306	0.034	0.017	0.018	0.427	0.005	0.175	0.000	0.000	0.000
Haha3-4	0.000	0.000	0.000	0.000	0.000	0.000	0.000	0.011	0.006	0.015	0.011	0.006	0.004	0.009	0.009	0.000	0.929	0.000	0.000
Haha1-2	0.000	0.000	0.000	0.000	0.000	0.000	0.000	0.012	0.005	0.026	0.015	0.005	0.004	0.015	0.011	0.000	0.907	0.000	0.000
Chichi	0.000	0.000	0.000	0.000	0.000	0.000	0.000	0.019	0.010	0.026	0.018	0.010	0.005	0.018	0.014	0.000	0.880	0.000	0.000
Guam A	0.000	0.014	0.031	0.001	0.000	0.000	0.000	0.000	0.000	0.000	0.000	0.000	0.000	0.000	0.000	0.000	0.000	0.953	0.000
Guam M	0.000	0.011	0.018	0.000	0.000	0.000	0.000	0.000	0.000	0.000	0.000	0.000	0.000	0.000	0.000	0.000	0.000	0.971	0.000

Table S2.4. Multiple regression of physical distance matrices (geographic distance and dissimilarity in potential source areas according to inverse particle tracking) on distances between PCA centroids of populations and their percent variation explained. Over all populations, geographic distance explains genetic difference better than the dissimilarity in potential sources (Dissim. source comp.). Within the Ryukyu Islands the regression was not significant but dissimilarity in source composition could be more important.

Coefficients	All (*p*)	Ryukyu (*p*)
Geogr. Distance	$2.07\ 10^{-5}$ (0.45)	$-6.99\ 10^{-5}$ (0.96)
Dissim. Source comp.	$-8.08\ 10^{-2}$ (0.19)	$-4.62\ 10^{-2}$ (0.44)
total R2	0.076	0.075
p	0.44	0.59

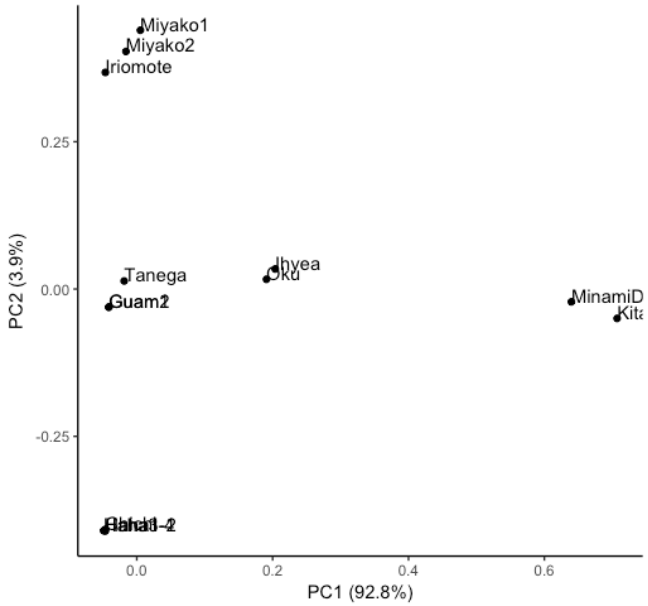

Figure S2.6. Principle component analysis of immigration matrix according to inverse particle tracking per site to assess similarity in immigration patterns between collection sites.

Appendix 3: Table S3.1 - List of specimens

specID	locality	Date	collector	taxon	mt type FA	mt type seq	RAD lineage	meta bar	RAD-plateNo	skeleton examined	polypDia Max [mm]	polypDia Min [mm]	polyp Dist	depth Situ	depth Tide Correct	notes
PW1	Sesoko	14.06.2015	P. Wepfer	G.fascicularis							6.48	4.01	2.05	6.6	7.46	
PW2	Sesoko	14.06.2015	P. Wepfer	G.fascicularis							4.85	3.38	1.83	6.3	7.16	
PW3	Sesoko	14.06.2015	P. Wepfer	G.fascicularis	S						5	3.56	2.31	6.8	7.66	
PW4	Sesoko	14.06.2015	P. Wepfer	G.fascicularis							5.87	4.34	3.08	6.9	7.76	
PW5	Sesoko	14.06.2015	P. Wepfer	G.fascicularis							7.91	4.84	2.34	7.8	8.66	
PW6	Sesoko	14.06.2015	P. Wepfer	G.fascicularis	L						5.95	3.57	1.86	8.1	8.96	
PW7	Sesoko	14.06.2015	P. Wepfer	G.fascicularis							5.78	4.17	2.23	8	8.86	
PW8	Sesoko	14.06.2015	P. Wepfer	G.fascicularis							5.19	3.9	2.41	8.2	9.06	
PW9	Sesoko	14.06.2015	P. Wepfer	G.fascicularis	L						4.74	3.7	1.76	8.5	9.36	
PW10	Sesoko	14.06.2015	P. Wepfer	G.fascicularis							5.65	4.15	2	10.2	11.06	
PW11	Sesoko	14.06.2015	P. Wepfer	G.fascicularis							4.22	3.29	1.86	10.8	11.66	
PW12	Sesoko	14.06.2015	P. Wepfer	G.fascicularis	L						5.48	3.7	2.1	12.9	13.76	
PW13	Sesoko	14.06.2015	P. Wepfer	G.fascicularis							4.91	3.28	1.79	11.8	12.66	
PW14	Sesoko	14.06.2015	P. Wepfer	G.fascicularis	S						4.47	3.93	1.86	12.9	13.76	
PW15	Sesoko	14.06.2015	P. Wepfer	G.fascicularis							6.77	4.29	2.11	11.5	12.36	
PW16	Sesoko	14.06.2015	P. Wepfer	G.fascicularis	S/L						9.08	6.32	2.9	12.2	13.06	
PW17	Sesoko	14.06.2015	P. Wepfer	G.fascicularis	S						5.66	4.26	2.77	10.1	10.96	
PW18	Sesoko	14.06.2015	P. Wepfer	G.fascicularis							6.79	3.92	1.48	6.6	7.46	
PW19	Manza	21.06.2015	P. Wepfer	G.fascicularis	S						5.13	4.25	2.67	7.5	7.06	
PW20	Manza	21.06.2015	P. Wepfer	G.fascicularis							4.61	3.49	1.52	7.1	6.66	
PW21	Manza	21.06.2015	P. Wepfer	G.fascicularis							6.67	4.23	2.19	6.8	6.36	
PW22	Manza	21.06.2015	P. Wepfer	G.fascicularis							7.73	4.33	1.93	6	5.56	
PW23	Manza	21.06.2015	P. Wepfer	G.fascicularis	L						6.23	4.55	2.47	5.9	5.46	
PW24	Manza	21.06.2015	P. Wepfer	G.fascicularis	S						3.85	3.09	1.56	6.6	6.16	
PW25	Manza	21.06.2015	P. Wepfer	G.fascicularis	L						6.75	4.72	2.02	7.7	7.26	
PW26	Manza	21.06.2015	P. Wepfer	G.fascicularis							4.19	2.72	1.38	6.8	6.36	
PW27	Manza	21.06.2015	P. Wepfer	G.fascicularis							7	3.77	1.91	6.8	6.36	
PW28	Manza	21.06.2015	P. Wepfer	G.fascicularis	S						4.56	3.34	1.91	7	6.56	
PW29	Manza	21.06.2015	P. Wepfer	G.fascicularis							6.37	3.59	1.96	7	6.56	
PW30	Manza	21.06.2015	P. Wepfer	G.fascicularis	L						na	na	na	6.4	5.96	
PW31	Manza	21.06.2015	P. Wepfer	G.fascicularis							5.5	4.33	1.85	7.2	6.76	
PW32	Manza	21.06.2015	P. Wepfer	G.fascicularis							5.41	3.18	1.91	7	6.56	
PW33	Manza	21.06.2015	P. Wepfer	G.fascicularis	S						6.91	4.52	3.01	6.5	6.06	
PW34	Manza	21.06.2015	P. Wepfer	G.fascicularis	L						4.45	2.81	1.49	6.2	5.76	
PW35	Manza	21.06.2015	P. Wepfer	G.fascicularis							5.32	3.62	1.97	6.7	6.26	
PW36	Manza	21.06.2015	P. Wepfer	G.fascicularis							3.59	2.62	1.17	8	7.56	
PW37	Ikema	18.07.2015	P. Wepfer	G.fascicularis	S		L		EGP0129	na	8.79	5.1	2.22	2.3	1.86	
PW38	Ikema	18.07.2015	P. Wepfer	G.fascicularis	L						8.71	4.53	2.55	2.5	2.06	
PW39	Ikema	18.07.2015	P. Wepfer	G.fascicularis	L		L		EGP0129	yes	7.47	4.97	1.94	4.9	4.46	
PW40	Ikema	18.07.2015	P. Wepfer	G.fascicularis	S		L		EGP0129	na	na	na	na	4.2	3.76	
PW41	Ikema	18.07.2015	P. Wepfer	G.fascicularis	L		L		EGP0129	yes	5.78	3.9	1.8	4.7	4.26	
PW42	Ikema	18.07.2015	P. Wepfer	G.fascicularis	L+	L+	L+		EGP0129	na	5.97	4	2.2	4	3.56	
PW43	Ikema	18.07.2015	P. Wepfer	G.fascicularis	S		S		EGP0129	na	6.5	4.03	2.35	6.8	6.36	
PW44	Ikema	18.07.2015	P. Wepfer	G.fascicularis	L						na	na	na	5.6	5.16	
PW45	Ikema	18.07.2015	P. Wepfer	G.fascicularis	S		S		EGP0129	na	[2.9]	?	?		-0.44	
PW46	Ikema	18.07.2015	P. Wepfer	G.fascicularis	L						na	na	na	7.1	6.66	
PW47	Ikema	18.07.2015	P. Wepfer	G.fascicularis	S		S		EGP0129	yes	2.61	1.89	1.2	6.4	5.96	
PW48	Ikema	18.07.2015	P. Wepfer	G.fascicularis	S		S		EGP0129	na	[3.64]	3.11]		6	5.56	
PW49	Ikema	18.07.2015	P. Wepfer	G.fascicularis	S/L		L		EGP0129	yes	5.83	3.84	1.51	5.4	4.96	
PW50	Ikema	18.07.2015	P. Wepfer	G.fascicularis	L		L		EGP0129	yes	3.81	3.09	1.46	5	4.56	
PW51	Ikema	18.07.2015	P. Wepfer	G.fascicularis	S		L		EGP0129	na	na	na	na	5.8	5.36	
PW52	Ikema	18.07.2015	P. Wepfer	G.fascicularis	L		L		EGP0129	na	7.72	5.17	1.93	7.2	6.76	
PW53	Ikema	18.07.2015	P. Wepfer	G.fascicularis	S		na		EGP0129	yes	5.88	3.94	1.92	8.6	8.16	
PW54	Ikema	18.07.2015	P. Wepfer	G.fascicularis	L		na		EGP0129		6.46	4.79	2.06	6.4	5.96	
PW55	Ikema	18.07.2015	P. Wepfer	G.fascicularis	S						4.17	3.18	1.28	7.3	6.86	
PW56	Ikema	18.07.2015	P. Wepfer	G.fascicularis	S/L		L		EGP0129	yes	5.91	3.99	1.69	9.7	9.26	
PW57	Yoshino	19.07.2015	P. Wepfer	G.fascicularis							4.13	2.91	2.12	4.7	4	
PW58	Yoshino	19.07.2015	P. Wepfer	G.fascicularis	L		L	2: C21	EGP0129	yes	5.2	3	1.05	7.8	7.1	
PW59	Yoshino	19.07.2015	P. Wepfer	G.fascicularis	S		S	2	EGP0129	yes	4.32	3.38	1.65	8.3	7.6	
PW60	Yoshino	19.07.2015	P. Wepfer	G.fascicularis	S		S	2: C21	EGP0129	na	5.4	3.93	1.78	7.6	6.9	CT-scan
PW61	Yoshino	19.07.2015	P. Wepfer	G.fascicularis	S	LG	L	2: D1	EGP0129	yes	6.63	4.12	1.96	9.1	8.4	CT-scan
PW62	Yoshino	19.07.2015	P. Wepfer	G.fascicularis							5.57	4.28	2.98	11.4	10.7	
PW63	Yoshino	19.07.2015	P. Wepfer	G.fascicularis	S/L		L	2	EGP0129	na	6.12	3.71	1.71	10.9	10.2	
PW64	Yoshino	19.07.2015	P. Wepfer	G.fascicularis	S		S		EGP0129	yes	5.63	3.8	2.1	7.4	6.7	CT-scan
PW65	Yoshino	19.07.2015	P. Wepfer	G.fascicularis	L		L		EGP0129	yes	5.81	2.84	1.42	8.7	8	
PW66	Yoshino	19.07.2015	P. Wepfer	G.fascicularis	L		L	2	EGP0129	na	7.58	5.15	1.81	7.5	6.8	
PW67	Yoshino	19.07.2015	P. Wepfer	G.fascicularis	S		S	2	EGP0129	yes	4.39	2.69	1.23	8.4	7.7	
PW68	Yoshino	19.07.2015	P. Wepfer	G.fascicularis							5.29	3.28	1.63	7.9	7.2	
PW69	Yoshino	19.07.2015	P. Wepfer	G.fascicularis	L		L	(cancel	EGP0129	yes	7.57	5.17	2.65	13.6	12.9	
PW70	Yoshino	19.07.2015	P. Wepfer	G.fascicularis							5.9	4.5	1.77	15.9	15.2	
PW71	Yoshino	19.07.2015	P. Wepfer	G.fascicularis	L		L	2	EGP0129	yes	5.27	3.78	1.69	16.7	16	
PW72	Yoshino	19.07.2015	P. Wepfer	G.fascicularis							5.24	4.22	1.79	14.7	14	
PW73	Yoshino	19.07.2015	P. Wepfer	G.fascicularis	S		S	(cancel	EGP0129	na	6.2	4.52	1.8	16.2	15.5	
PW74	Yoshino	19.07.2015	P. Wepfer	G.fascicularis	L			(cancelled)			7.54	5.05	2.28	17	16.3	
PW75	Yoshino	19.07.2015	P. Wepfer	G.fascicularis	L		L	2	EGP0129	na	5.8	3.94	1.9	20.5	19.8	
PW76	Yoshino	19.07.2015	P. Wepfer	G.fascicularis							5.81	3.85	1.82	18.3	17.6	
PW77	Miyagi	22.07.2015	P. Wepfer	G.fascicularis							5.93	3.84	1.85	4.3	4.18	
PW78	Miyagi	22.07.2015	P. Wepfer	G.fascicularis	S						6.31	4.77	2.1	6	5.88	
PW79	Miyagi	22.07.2015	P. Wepfer	G.fascicularis	S/L+						4	3.25	1.43	7.9	7.78	
PW80	Miyagi	22.07.2015	P. Wepfer	G.fascicularis							4.27	3.2	1.29	7	6.88	
PW81	Miyagi	22.07.2015	P. Wepfer	G.fascicularis	S						5.64	4.04	2.23	4.7	4.58	
PW82	Miyagi	22.07.2015	P. Wepfer	G.fascicularis							5.27	3.54	1.68	8.1	7.98	
PW83	Miyagi	22.07.2015	P. Wepfer	G.fascicularis	S/L						5.88	3.57	1.72	8.1	7.98	
PW84	Miyagi	22.07.2015	P. Wepfer	G.fascicularis							5.67	3.89	1.6	8.6	8.48	
PW85	Miyagi	22.07.2015	P. Wepfer	G.fascicularis	S/L						7.04	4.08	2.47	7.5	7.38	
PW86	Miyagi	22.07.2015	P. Wepfer	G.fascicularis	S/L+						3.51	2.61	1.4	9.3	9.18	
PW87	Miyagi	22.07.2015	P. Wepfer	G.fascicularis							5.23	3.64	1.74	8.5	8.38	
PW88	Miyagi	22.07.2015	P. Wepfer	G.fascicularis							5.01	2.8	1.77	8.4	8.28	
PW89	Miyagi	22.07.2015	P. Wepfer	G.fascicularis	L						7.08	4.22	1.98	5.2	5.08	
PW90	Miyagi	22.07.2015	P. Wepfer	G.fascicularis							4.14	2.81	1.93	4.2	4.08	
PW91	Miyagi	22.07.2015	P. Wepfer	G.fascicularis	S						5.12	3.68	1.86	4.3	4.18	
PW92	Miyagi	22.07.2015	P. Wepfer	G.fascicularis							5.49	3.57	1.94	8.8	8.68	
PW93	Miyagi	22.07.2015	P. Wepfer	G.fascicularis	S						6.31	4.14	1.64	8.2	8.08	
PW94	Miyagi	22.07.2015	P. Wepfer	G.fascicularis							4.04	2.46	1.74	8	7.88	
PW95	Miyagi	22.07.2015	P. Wepfer	G.fascicularis	S						7.89	4.17	2.7	7.7	7.58	
PW96	Miyagi	22.07.2015	P. Wepfer	G.fascicularis							5.84	4.15	2.08	8.4	8.28	
PW97	Iheya	28.07.2015	P. Wepfer	G.fascicularis	L		L		EGP0124	yes	5	42	22	8.9	9	

specID	locality	Date	collector	taxon	mt type FA	mt type seq	RAD lineage	meta bar	RAD-plateNo	skeleton examined	polypDia Max [mm]	polypDia Min [mm]	polyp Dist	depth Situ	depth Tide Correct	notes
PW98	Iheya	28.07.2015	P. Wepfer	G.fasciularis	S		S	2: C1	EGP0124	yes	5.6	4.44	3.36	9.2	9.3	
PW99	Iheya	28.07.2015	P. Wepfer	G.fasciularis	L		L		EGP0124	yes	5.7	3.5	2.56	8.8	8.9	
PW100	Iheya	28.07.2015	P. Wepfer	G.fasciularis	L		L	2: C1	EGP0124	yes	11.2	5.52	2.41	10.4	10.5	CT-scan
PW101	Iheya	28.07.2015	P. Wepfer	G.fasciularis	L		L		EGP0124	na	4.01	2.85	1.5	10.8	10.9	
PW102	Iheya	28.07.2015	P. Wepfer	G.fasciularis	S		S	2: C21	EGP0124	na	4.73	3.21	2.23	11.1	11.2	
PW103	Iheya	28.07.2015	P. Wepfer	G.fasciularis	L		L	2: C1	EGP0124	yes	10.61	5.55	2.69	11.3	11.4	
PW104	Iheya	28.07.2015	P. Wepfer	G.fasciularis	S	L+	L+		EGP0124	na	4.44	3.38	2.08	11.4	11.5	
PW105	Iheya	28.07.2015	P. Wepfer	G.fasciularis	S		S	2: D/C2	EGP0124	na	4.1	3.27	2.01	12.1	12.2	
PW106	Iheya	28.07.2015	P. Wepfer	G.fasciularis	L+		L+	2: C21	EGP0124	na	5.81	4.19	2.41	12.5	12.6	
PW107	Iheya	28.07.2015	P. Wepfer	G.fasciularis	L		L	2: D1	EGP0124	yes	6.36	3.47	2.36	12.1	12.2	
PW108	Iheya	28.07.2015	P. Wepfer	G.fasciularis	L+		L+		EGP0124	yes	6.15	5.28	2.11	12.2	12.3	
PW109	Iheya	28.07.2015	P. Wepfer	G.fasciularis	S		S	2	EGP0124	na	5.5	3.71	2.35	12.4	12.5	
PW110	Iheya	28.07.2015	P. Wepfer	G.fasciularis	L+	L+	L+	2	EGP0124	na	6.02	3.68	2.7	11	11.1	
PW111	Iheya	28.07.2015	P. Wepfer	G.fasciularis	S	L+	L+	2: C21	EGP0124	na	5.61	4	2.61	10.8	10.9	CT-scan
PW112	Iheya	28.07.2015	P. Wepfer	G.fasciularis	L		L	2: C1	EGP0124	na	7.87	4.7	2.82	10.5	10.6	CT-scan
PW113	Iheya	28.07.2015	P. Wepfer	G.fasciularis	L+		L+	(cancel	EGP0124	na	5.19	4.11	1.97	10.1	10.2	
PW114	Iheya	28.07.2015	P. Wepfer	G.fasciularis	L		L	(cancel	EGP0129	yes	11.17	5.63	3.19	9.8	9.9	
PW115	Iheya	28.07.2015	P. Wepfer	G.fasciularis	L						9.15	5.54	3.11	9.9	10	
PW116	Iheya	28.07.2015	P. Wepfer	G.fasciularis	L+			2: C1			5.44	3.99	2.37	10.4	10.5	CT-scan
PW117	Iheya	28.07.2015	P. Wepfer	G.fasciularis	L		L	2: C1	EGP0129	yes	8.94	4.48	2.62	10.8	10.9	CT-scan
PW118	Iheya	28.07.2015	P. Wepfer	G.fasciularis	L						8.48	4.76	2.15	11.4	11.5	
PW119	Iheya	28.07.2015	P. Wepfer	G.fasciularis	S/L		L	2: C1	EGP0129	yes	7.06	4.64	2.68	10.9	11	
PW120	Iheya	28.07.2015	P. Wepfer	G.fasciularis	L+			2			5.38	3.6	1.51	11.3	11.4	
PW121	Iheya	28.07.2015	P. Wepfer	G.fasciularis	L+			2: C21			4.97	3.5	1.38	10.7	10.8	CT-scan
PW122	Iheya	28.07.2015	P. Wepfer	G.fasciularis	L						5.27	3.49	2.29	10.6	10.7	
PW123	Iheya	28.07.2015	P. Wepfer	G.fasciularis	L		L		EGP0129	na	3.43	?	1.64	10.6	10.7	
PW124	Iheya	28.07.2015	P. Wepfer	G.fasciularis	L		L				6.36	4.25	2.51	10.8	10.9	
PW125	Iheya	28.07.2015	P. Wepfer	G.fasciularis	L+						5.73	4.65	1.91	11	11.1	
PW126	Iheya	28.07.2015	P. Wepfer	G.fasciularis	L		L+	2	EGP0129	yes	3.47	2.7	1.42	10.8	10.9	
PW127	Iheya	28.07.2015	P. Wepfer	G.fasciularis	L		L				5.34	3.49	1.71	11.1	11.2	
PW128	Iheya	28.07.2015	P. Wepfer	G.fasciularis	-		-		EGP0129	na	4.86	2.94	2.41	13.2	13.3	
PW129	Iheya	28.07.2015	P. Wepfer	G.fasciularis	L		L+		EGP0129	na	5.26	3.63	1.89	16	16.1	
PW130	Iheya	28.07.2015	P. Wepfer	G.fasciularis	L+						4.1	3.12	1.7	13.9	14	
PW131	Iheya	28.07.2015	P. Wepfer	G.fasciularis							4.46	2.9	1.77	13.4	13.5	
PW132	Iheya	28.07.2015	P. Wepfer	G.fasciularis							4.77	3.27	1.58		0.1	
PW133	Iheya	28.07.2015	P. Wepfer	G.fasciularis							5.21	3.72	2	12.8	12.9	
PW134	Iheya	28.07.2015	P. Wepfer	G.fasciularis							5.49	4.03	1.7	12.6	12.7	
PW135	Iheya	28.07.2015	P. Wepfer	G.fasciularis							4.43	3.43	1.64	13.3	13.4	
PW136	Iheya	28.07.2015	P. Wepfer	G.fasciularis							4.66	3.66	2.19	14.4	14.5	
PW137	Oku	29.07.2015	P. Wepfer	G.fasciularis	L+		L+	2			4.76	3.5	2.07	6.5	7.32	
PW138	Oku	29.07.2015	P. Wepfer	G.fasciularis							6.94	4.79	2.77	6.1	6.92	
PW139	Oku	29.07.2015	P. Wepfer	G.fasciularis	L		L		EGP0129	yes	5.35	3.88	2.29	6.9	7.72	
PW140	Oku	29.07.2015	P. Wepfer	G.fasciularis							7.53	4.95	2.24	8.2	9.02	
PW141	Oku	29.07.2015	P. Wepfer	G.fasciularis	S		S		EGP0129		4.56	3.3	1.78	9	9.82	
PW142	Oku	29.07.2015	P. Wepfer	G.fasciularis			L		EGP0129	na	7.03	4.84	2.79	11.8	12.62	
PW143	Oku	29.07.2015	P. Wepfer	G.fasciularis	S		L		EGP0129	yes	8.39	4.98	2.36	13	13.82	
PW144	Oku	29.07.2015	P. Wepfer	G.fasciularis							4.91	3.68	2.4	14.5	15.32	
PW145	Oku	29.07.2015	P. Wepfer	G.fasciularis	S		L		EGP0129	yes	6.92	4.6	2.3	14.5	15.32	
PW146	Oku	29.07.2015	P. Wepfer	G.fasciularis							5.37	4.07	2.19	16.5	17.32	
PW147	Oku	29.07.2015	P. Wepfer	G.fasciularis	S		S		EGP0129	yes	4.86	2.92	2.26	17.2	18.02	
PW148	Oku	29.07.2015	P. Wepfer	G.fasciularis							5.73	3.69	2.14	14	14.82	
PW149	Oku	29.07.2015	P. Wepfer	G.fasciularis	S		S		EGP0129	yes	6.8	4.63	2.05	11.8	12.62	
PW150	Oku	29.07.2015	P. Wepfer	G.fasciularis	S/L		L		EGP0129	yes	8.49	5.66	2.71	11.1	11.92	
PW151	Oku	29.07.2015	P. Wepfer	G.fasciularis			S		EGP0129	yes	5.88	4.06	2.81	10	10.82	
PW152	Oku	29.07.2015	P. Wepfer	G.fasciularis			S		EGP0129	yes	5.16	3.88	2.26	8.7	9.52	
PW153	Oku	29.07.2015	P. Wepfer	G.fasciularis	S		S		EGP0129	yes	5.88	4.47	2.57	7.8	8.62	
PW154	Oku	29.07.2015	P. Wepfer	G.fasciularis	L		L		EGP0129	yes	7.57	5.71	3.13	7.3	8.12	
PW155	Oku	29.07.2015	P. Wepfer	G.fasciularis	L		L		EGP0129	na	4.84	3.05	1.49	7.9	8.72	
PW156	Oku	29.07.2015	P. Wepfer	G.fasciularis							3.96	3.07	1.77	6	6.82	
PW157	Oku	29.07.2015	P. Wepfer	G.fasciularis	S						3.79	3.01	1.39	4.2	5.02	
PW158	Tanega	13.09.2015	Y. Nakajima	G.fasciularis	S		S		EGP0129	na	6.9	4.45	3.25	7.2	7.15	
PW159	Tanega	13.09.2015	Y. Nakajima	G.fasciularis			S		EGP0129	na	6.21	4.34	2.6	6.9	6.85	
PW160	Tanega	13.09.2015	Y. Nakajima	G.fasciularis	S		S	2	EGP0129	na	7.19	4.8	2.93	6.7	6.65	
PW161	Tanega	13.09.2015	Y. Nakajima	G.fasciularis			S		EGP0129	na	6.33	3.77	2.76	9.2	9.15	
PW162	Tanega	13.09.2015	Y. Nakajima	G.fasciularis	L		L		EGP0129	na	8.29	5.79	2.44	9.3	9.25	
PW163	Tanega	13.09.2015	Y. Nakajima	G.fasciularis			S		EGP0129	na	5.24	4.1	2.9	9.7	9.65	
PW164	Tanega	13.09.2015	Y. Nakajima	G.fasciularis	L		L		EGP0129	na	11.74	5.8	3.59	9.9	9.85	
PW165	Tanega	13.09.2015	Y. Nakajima	G.fasciularis										9.9	9.85	
PW166	Tanega	13.09.2015	Y. Nakajima	G.fasciularis	S		S	2	EGP0129	na	5.08	3.47	2.52	9.7	9.65	
PW167	Tanega	13.09.2015	Y. Nakajima	G.fasciularis			L		EGP0129	na	9.34	6.69	2.93	9.8	9.75	
PW168	Tanega	13.09.2015	Y. Nakajima	G.fasciularis	L		L		EGP0129	na	5.7	4.37	1.86	10.5	10.45	
PW169	Tanega	13.09.2015	Y. Nakajima	G.fasciularis										10.4	10.35	
PW170	Tanega	13.09.2015	Y. Nakajima	G.fasciularis	S		S	2	EGP0129	na	4.91	3.49	2.28	10.3	10.25	
PW171	Tanega	13.09.2015	Y. Nakajima	G.fasciularis			S		EGP0129	yes				10.3	10.25	
PW172	Tanega	13.09.2015	Y. Nakajima	G.fasciularis	L									9.7	9.65	
PW173	Tanega	13.09.2015	Y. Nakajima	G.fasciularis			L		EGP0129	yes	9.9	6.89	3.25	10.1	10.05	
PW174	Tanega	13.09.2015	Y. Nakajima	G.fasciularis	S		L	2	EGP0129	na	10.36	5.81	2.89	10.4	10.35	
PW175	Tanega	13.09.2015	Y. Nakajima	G.fasciularis										7.1	7.05	
PW176	Tanega	13.09.2015	Y. Nakajima	G.fasciularis	L		L		EGP0129	na				8.6	9.15	
PW177	Tanega	13.09.2015	Y. Nakajima	G.fasciularis			S		EGP0129	na	6.01	4.75	2.96	9.2	9.75	
PW178	Tanega	13.09.2015	Y. Nakajima	G.fasciularis	L		L	2	EGP0129	na	11.25	6.07	2.7	8.9	9.45	
PW179	Tanega	13.09.2015	Y. Nakajima	G.fasciularis										9.2	9.75	
PW180	Tanega	13.09.2015	Y. Nakajima	G.fasciularis	S		L	2	EGP0129	na	12.06	5.48	2.96	9.5	10.05	
PW181	Tanega	13.09.2015	Y. Nakajima	G.fasciularis			L		EGP0129	na				9.3	9.85	
PW182	Tanega	13.09.2015	Y. Nakajima	G.fasciularis	L		L		EGP0129	na				9.1	9.65	
PW183	Tanega	13.09.2015	Y. Nakajima	G.fasciularis			L		EGP0129	na	6.81	4.81	2.16	8.9	9.45	
PW184	Tanega	13.09.2015	Y. Nakajima	G.fasciularis	S		L	2	EGP0129	na	8.55	4.38	2.26	8.7	9.25	
PW185	Tanega	13.09.2015	Y. Nakajima	G.fasciularis			S		EGP0129	na	6.86	5.08	2.36	9.2	9.75	
PW186	Tanega	13.09.2015	Y. Nakajima	G.fasciularis	S		S		EGP0129	na				8.5	9.05	
PW187	Tanega	13.09.2015	Y. Nakajima	G.fasciularis			L		EGP0129	na	8.98	4.83	2.28	7.5	8.05	
PW188	Tanega	13.09.2015	Y. Nakajima	G.fasciularis	S/L		L	2	EGP0129	na	12.72	6.39	2.67	9.7	10.25	
PW189	Tanega	13.09.2015	Y. Nakajima	G.fasciularis										9.8	10.35	
PW190	Tanega	13.09.2015	Y. Nakajima	G.fasciularis	S/L		L	2	EGP0129	na	9.11	4.69	2.28	10.8	11.35	
PW191	Tanega	13.09.2015	Y. Nakajima	G.fasciularis										9.2	9.75	
PW192	Tanega	13.09.2015	Y. Nakajima	G.fasciularis	L									10.6	11.15	
PW193	Tanega	13.09.2015	Y. Nakajima	G.fasciularis										10.8	11.35	
PW194	Tanega	13.09.2015	Y. Nakajima	G.fasciularis	S		S		EGP0129	na	5.84	4.77	3.08	11	11.55	

speID	locality	Date	collector	taxon	mt type FA	mt type seq	RAD lineage	meta bar	RAD-plateNo	skeleton examined	polypDia Max [mm]	polypDia Min [mm]	polyp Dist	depth Situ	depth Tide Correct	notes
PW195	Tanega	13.09.2015	Y. Nakajima	G.fascicularis			L		EGP0129	na	10.36	6.14	3.22	9.2	9.75	
PW196	Tanega	13.09.2015	Y. Nakajima	G.fascicularis	S/L			2			8.11	5.32	2.24	9.4	9.95	
PW197	Tanega	13.09.2015	Y. Nakajima	G.fascicularis										9	9.55	
M1	Guam		na	G.fascicularis	S	SA			EGP0124	yes						74-G-18
M2	Guam		na	G.fascicularis	S	LA			EGP0124	yes						74-G-21
M3	Guam		na	G.horrescens	S	LP			EGP0124	na						74-G-8
M4	Palau		na	G.horrescens	NA	LA			EGP0124	na						74-P-26
M5	Palau		na	G. paucisepta	S				EGP0124	yes						74-P-45
M6	Palau		na	G.horrescens	S	L+			EGP0124	na						74-P-46
M7	Palau		na	G.horrescens	NA				EGP0124							74-P-60
M8	Palau		na	G.horrescens	S	LO			EGP0124	yes						74-P-77
M9	Palau		na	G.horrescens	S	SA				yes						P76-153B
M10	Palau		na	G. astreata	S	LA			EGP0124							P76-332
M11	Palau		na	G.longisepta	S	LA			EGP0124	yes						P76-609
M12	Palau		na	G.longisepta	S					yes						P76-609(b)
M13	Palau		na	G.fascicularis	S	SA			EGP0124	yes						P76-659
M14	Palau		na	G. paucisepta	S				EGP0124	yes						P76-698
M15	Palau		na	G.horrescens	S	SA			EGP0124							P76-728
M16	Palau		na	G.horrescens	S					yes						P76-728(B)
M17	Palau		na	G.horrescens					EGP0124							P76-728(c)
M18	Palau		na	G.fascicularis					EGP0124							P76-833
M19	Palau		na	G.fascicularis												P76-918
M20	Ryukyu		Kawaguchi	G. astreata												RUMF-ZG-02971
PW198	KitadaitoNorth	02.11.2015	P. Wepfer	G.fascicularis	S/L						7.98	4.52	2.77	18.3	18.45	
PW199	KitadaitoNorth	02.11.2015	P. Wepfer	G.fascicularis	L		L		EGP0129	yes	na	na	na	19.6	19.75	
PW200	KitadaitoNorth	02.11.2015	P. Wepfer	G.fascicularis	L		L	2	EGP0129	yes	5.32	3.72	1.85	20.5	20.65	
PW201	KitadaitoNorth	02.11.2015	P. Wepfer	G.fascicularis	L		L		EGP0129	yes	na	na	na	19.6	19.75	
PW202	KitadaitoNorth	02.11.2015	P. Wepfer	G.fascicularis	L		L	2	EGP0130	yes	6.51	4.69	2.01	18.3	18.45	
PW203	KitadaitoNorth	02.11.2015	P. Wepfer	G.fascicularis	S		L		EGP0129	yes	11.32	8.12	2.72	16.8	16.95	
PW204	KitadaitoNorth	02.11.2015	P. Wepfer	G.fascicularis			L		EGP0129	yes				17.5	17.65	
PW205	KitadaitoNorth	02.11.2015	P. Wepfer	G.fascicularis	L						5.46	3.95	2.27	NA		
PW206	KitadaitoNorth	02.11.2015	P. Wepfer	G.fascicularis										17.5	17.65	
PW207	KitadaitoNorth	02.11.2015	P. Wepfer	G.fascicularis	S		L	2	EGP0130	na	7.44	5.33	2.24	17.7	17.85	CT-scan
PW208	KitadaitoNorth	02.11.2015	P. Wepfer	G.fascicularis	L		L	2	EGP0129	yes	5.72	3.71	1.85	15.9	16.05	
PW209	KitadaitoNorth	02.11.2015	P. Wepfer	G.fascicularis	L						6.99	4.74	2.56	15.9	16.05	
PW210	KitadaitoNorth	02.11.2015	P. Wepfer	G.fascicularis			L		EGP0129	yes				15.5	15.65	
PW211	KitadaitoNorth	02.11.2015	P. Wepfer	G.fascicularis	S		L	2	EGP0130	yes	7.24	4.84	2.56	14.6	14.75	
PW212	KitadaitoNorth	02.11.2015	P. Wepfer	G.fascicularis	L		L	2	EGP0130	yes	5.92	4.62	1.83	15.9	16.05	
PW213	KitadaitoNorth	02.11.2015	P. Wepfer	G.fascicularis	L		L		EGP0129	na	7.21	4.94	2.11	14.5	14.65	
PW214	KitadaitoNorth	02.11.2015	P. Wepfer	G.fascicularis	L						8.24	4.81	2.6	14.4	14.55	
PW215	KitadaitoNorth	02.11.2015	P. Wepfer	G.fascicularis	S/L			2			9.57	5.27	3.98	14.5	14.65	CT-scan
PW216	KitadaitoNorth	02.11.2015	P. Wepfer	G.fascicularis	L						10.41	5.5	2.02	14.4	14.55	
PW217	KitadaitoNorth	02.11.2015	P. Wepfer	G.fascicularis	L			(cancelled)			12.41	6.71	3.29	13.8	13.95	
PW218	KitadaitoNorth	02.11.2015	P. Wepfer	G.fascicularis	L						na	na	na	14.9	15.05	
PW219	KitadaitoNorth	02.11.2015	P. Wepfer	G.fascicularis	?		L		EGP0130	na				13.9	14.05	
PW220	MinamidaitoWes	03.11.2015	P. Wepfer	G.fascicularis	L		S		EGP0130	na				14.4	14.3	
PW221	MinamidaitoWes	03.11.2015	P. Wepfer	G.fascicularis	L		L		EGP0129	yes				NA		
PW222	MinamidaitoWes	03.11.2015	P. Wepfer	G.fascicularis			L		EGP0129	yes				13.9	13.8	
PW223	MinamidaitoWes	03.11.2015	P. Wepfer	G.fascicularis			L		EGP0129	na				14	13.9	
PW224	MinamidaitoWes	03.11.2015	P. Wepfer	G.fascicularis			L		EGP0130	na				15	14.9	
PW225	MinamidaitoWes	03.11.2015	P. Wepfer	G.fascicularis	L									15.8	15.7	
PW226	MinamidaitoWes	03.11.2015	P. Wepfer	G.fascicularis	L		L		EGP0130	na				18.3	18.2	
PW227	MinamidaitoWes	03.11.2015	P. Wepfer	G.fascicularis										19	18.9	
PW228	MinamidaitoWes	03.11.2015	P. Wepfer	G.fascicularis										20.4	20.3	
PW229	MinamidaitoWes	03.11.2015	P. Wepfer	G.fascicularis	S		L		EGP0130	na				20.1	20	
PW230	MinamidaitoWes	03.11.2015	P. Wepfer	G.fascicularis	S		L		EGP0130	na				19.3	19.2	
PW231	MinamidaitoWes	03.11.2015	P. Wepfer	G.fascicularis	L									19.4	19.3	
PW232	MinamidaitoWes	03.11.2015	P. Wepfer	G.fascicularis			L		EGP0130	na				19	18.9	
PW233	MinamidaitoWes	03.11.2015	P. Wepfer	G.fascicularis	L		L		EGP0130		4.47	3.32	1.39	19.1	19	
PW234	MinamidaitoWes	03.11.2015	P. Wepfer	G.fascicularis	L									17.5	17.4	
PW235	MinamidaitoWes	03.11.2015	P. Wepfer	G.fascicularis			L		EGP0130	na	6.72	4.51	1.94	16.8	16.7	
PW236	MinamidaitoWes	03.11.2015	P. Wepfer	G.fascicularis	S			2			3.77	2.94	1.88	16.9	16.8	
PW237	MinamidaitoWes	03.11.2015	P. Wepfer	G.fascicularis	S/L+		L+	2	EGP0130	na	3.68	2.89	1.47	15.2	15.1	
PW238	MinamidaitoWes	03.11.2015	P. Wepfer	G.fascicularis	S		?		EGP0130	na				15.2	15.1	
PW239	MinamidaitoWes	03.11.2015	P. Wepfer	G.fascicularis	L									15.5	15.4	
PW240	MinamidaitoWes	03.11.2015	P. Wepfer	G.fascicularis	L		L		EGP0130	na	4.57	4.03	1.46	15.2	15.1	
PW241	MinamidaitoWes	03.11.2015	P. Wepfer	G.fascicularis	L									16.3	16.2	
PW242	MinamidaitoWes	03.11.2015	P. Wepfer	G.fascicularis	L		L		EGP0130	na	9.08	6.52	2.65	16.8	16.7	
PW243	MinamidaitoWes	03.11.2015	P. Wepfer	G.fascicularis			L		EGP0130	na				16.4	16.3	
PW244	MinamidaitoWes	03.11.2015	P. Wepfer	G.fascicularis	L									17.1	17	
PW245	MinamidaitoWes	03.11.2015	P. Wepfer	G.fascicularis	L									15.3	15.2	
PW246	MinamidaitoSou	03.11.2015	P. Wepfer	G.fascicularis	S			2			4.24	3.06	2.16	23.8	23.9	
PW247	MinamidaitoSou	03.11.2015	P. Wepfer	G.fascicularis	S	SA	S		EGP0130	yes	7.88	5.57	1.89	16.5	16.6	
PW248	SeragakiRyugu	04.06.2016	P. Wepfer	G. astreata	L						7.3	5.79	5.41	23	23.81	
PW249	SeragakiRyugu	04.06.2016	P. Wepfer	G. cryptoramosa	S	LA	L		EGP0135		5.64	4.81	4.95	23	23.81	
PW250	SeragakiRyugu	04.06.2016	P. Wepfer	G. paucisepta	L						3.17	2.73	2.59	26	26.81	
PW251	SeragakiRyugu	04.06.2016	P. Wepfer	G. paucisepta	L						2.73	2.16	2.12	26	26.81	
PW252	SeragakiRyugu	04.06.2016	P. Wepfer	G. pauciradiata/	L					yes	3.17	3	2.34	23	23.81	
PW253	Trat1	10.07.2016	P. Wepfer	G.fascicularis	L	L, S					4.92	3.93	1.89	1.5		
PW254	Trat1	10.07.2016	P. Wepfer	G.fascicularis	S	S					9.97	6.72	3.03	1.5		
PW255	Trat1	10.07.2016	P. Wepfer	G.fascicularis	S						5.18	3.94	2.18	1.7		
PW256	Trat1	10.07.2016	P. Wepfer	G.fascicularis	S									1.8		
PW257	Trat1	10.07.2016	P. Wepfer	G.fascicularis	S									2		
PW258	Trat1	10.07.2016	P. Wepfer	G.fascicularis	S									2.2		
PW259	Trat1	10.07.2016	P. Wepfer	G.fascicularis	S						6.67	4.81	2.59	1.95		mean site depth
PW260	Trat1	10.07.2016	P. Wepfer	G.fascicularis	S									1.8		
PW261	Trat1	10.07.2016	P. Wepfer	G.fascicularis	S									1.8		
PW262	Trat1	10.07.2016	P. Wepfer	G.fascicularis	S									1.7875		mean site depth
PW263	Trat1	10.07.2016	P. Wepfer	G.fascicularis	S									1.7875		mean site depth
PW264	Trat1	10.07.2016	P. Wepfer	G.fascicularis	S									1.7875		mean site depth
PW265	Trat1	10.07.2016	P. Wepfer	G.fascicularis	S									1.7875		mean site depth
YN531	Trat1	10.07.2016	Y. Nakajima	G.fascicularis										1.7875		mean site depth
YN532	Trat1	10.07.2016	Y. Nakajima	G.fascicularis										1.7875		mean site depth
PW266	Trat2	11.07.2016	P. Wepfer	G.fascicularis										2.1		
PW267	Trat2	11.07.2016	P. Wepfer	G.fascicularis	S									1.4		
PW268	Trat2	11.07.2016	P. Wepfer	G.fascicularis	S									0.8		
PW269	Trat2	11.07.2016	P. Wepfer	G.fascicularis	S	S								0.8		

Appendix 3: Table S3.1 - List of specimens

specID	locality	Date	collector	taxon	mt type FA	mt type seq	RAD lineage	meta bar	RAD-plateNo	skeleton examined	polypDia Max [mm]	polypDia Min [mm]	polyp Dist	depth Situ	depth Tide Correct	notes
PW270	Trat2	11.07.2016	P. Wepfer	G.fascicularis	S	S								1.6		
PW271	Trat2	11.07.2016	P. Wepfer	G.fascicularis	S	S								na		
PW272	Trat2	11.07.2016	P. Wepfer	G.fascicularis										2.2		
PW273	Trat2	11.07.2016	P. Wepfer	G.fascicularis										2.4		
PW274	Trat2	11.07.2016	P. Wepfer	G.fascicularis	S									na		
PW275	Trat2	11.07.2016	P. Wepfer	G.fascicularis	S									2.1		
PW276	Trat2	11.07.2016	P. Wepfer	G.fascicularis	S									2.9		
PW277	Trat2	11.07.2016	P. Wepfer	G.fascicularis	S									1.7		
PW278	Trat2	11.07.2016	P. Wepfer	G.fascicularis	S									na		
PW279	Trat2	11.07.2016	P. Wepfer	G.fascicularis	S									2.6		
PW280	Trat2	11.07.2016	P. Wepfer	G.fascicularis	S									1.5		
PW281	Trat2	11.07.2016	P. Wepfer	G.fascicularis	S									2.2		
PW282	Trat2	11.07.2016	P. Wepfer	G.fascicularis	S									1.7		
PW283	Trat2	11.07.2016	P. Wepfer	G.fascicularis	S									1.5		
PW284	Trat2	11.07.2016	P. Wepfer	G.fascicularis	S									1.5		
PW285	Trat2	11.07.2016	P. Wepfer	G.fascicularis	S									2.1		
PW286	Trat2	11.07.2016	P. Wepfer	G.fascicularis	S									na		
PW287	Trat3	11.07.2016	P. Wepfer	G.fascicularis	S	SA	S		EGP0130					2.9		
PW288	Trat3	11.07.2016	P. Wepfer	G.fascicularis	S									2.9		mean site depth
PW289	Trat3	11.07.2016	P. Wepfer	G.fascicularis	L	LA	L		EGP0130		5.79	4.45	2.85	2.9		mean site depth
PW290	Trat3	11.07.2016	P. Wepfer	G.fascicularis	S									2.7		
PW291	Trat3	11.07.2016	P. Wepfer	G.fascicularis	S									na		
PW292	Trat4	11.07.2016	P. Wepfer	G.fascicularis	S									2.9		mean site depth
PW293	Trat4	11.07.2016	P. Wepfer	G.fascicularis	S									2.9		mean site depth
PW294	Trat4	11.07.2016	P. Wepfer	G.fascicularis	S									2.9		mean site depth
PW295	Trat4	11.07.2016	P. Wepfer	G.fascicularis	S									2.9		mean site depth
PW296	Trat4	11.07.2016	P. Wepfer	G.fascicularis	S									2.9		mean site depth
PW297	Trat4	11.07.2016	P. Wepfer	G.fascicularis	L									2.9		mean site depth
PW298	Trat4	11.07.2016	P. Wepfer	G.fascicularis										2.9		mean site depth
PW299	Trat4	11.07.2016	P. Wepfer	G.fascicularis	S									2.9		mean site depth
PW300	Trat4	11.07.2016	P. Wepfer	G.fascicularis										2.9		mean site depth
PW301	Trat4	11.07.2016	P. Wepfer	G.fascicularis	S									2.9		mean site depth
PW302	Trat4	11.07.2016	P. Wepfer	G.fascicularis	S									2.9		mean site depth
PW303	Trat4	11.07.2016	P. Wepfer	G.fascicularis	S									2.9		mean site depth
PW304	Trat4	11.07.2016	P. Wepfer	G.fascicularis	S									2.9		mean site depth
PW305	Trat4	11.07.2016	P. Wepfer	G.fascicularis	S									2.9		mean site depth
PW306	Trat4	11.07.2016	P. Wepfer	G.fascicularis										2.9		mean site depth
PW307	Trat4	11.07.2016	P. Wepfer	G.fascicularis	S									2.9		mean site depth
PW308	Trat4	11.07.2016	P. Wepfer	G.fascicularis	S									2.9		mean site depth
PW309	Trat4	11.07.2016	P. Wepfer	G.fascicularis	S									2.9		mean site depth
PW310	Trat4	11.07.2016	P. Wepfer	G.fascicularis	S									2.9		mean site depth
Poan1	Trat4	11.07.2016	Sitterporn	G.fascicularis	S									na		
Poan2	Trat4	11.07.2016	Sitterporn	G.fascicularis										na		
Poan3	Trat4	11.07.2016	Sitterporn	G.fascicularis										na		
Poan4	Trat4	11.07.2016	Sitterporn	G.fascicularis										na		
Poan5	Trat4	11.07.2016	Sitterporn	G.fascicularis										na		
PW310	Trat5	12.07.2016	P. Wepfer	G.fascicularis	S									1.2		
PW311	Trat5	12.07.2016	P. Wepfer	G.fascicularis	S									6.31176		mean site depth
PW312	Trat5	12.07.2016	P. Wepfer	G.fascicularis	S									6.31176		mean site depth
PW313	Trat5	12.07.2016	P. Wepfer	G.fascicularis	S									6.31176		mean site depth
PW314	Trat5	12.07.2016	P. Wepfer	G.fascicularis	S									6.31176		mean site depth
PW315	Trat5	12.07.2016	P. Wepfer	G.fascicularis	S									6.31176		mean site depth
PW316	Trat5	12.07.2016	P. Wepfer	G.fascicularis	S									6.31176		mean site depth
PW317	Trat5	12.07.2016	P. Wepfer	G.fascicularis	S									6.31176		mean site depth
PW318	Trat5	12.07.2016	P. Wepfer	G.fascicularis	S									5.1		
PW319	Trat5	12.07.2016	P. Wepfer	G.fascicularis	L									6.1		
PW320	Trat5	12.07.2016	P. Wepfer	G.fascicularis	L									5.5		
PW321	Trat5	12.07.2016	P. Wepfer	G.fascicularis	S									6.1		
PW322	Trat5	12.07.2016	P. Wepfer	G.fascicularis	L									6.4		
PW323	Trat5	12.07.2016	P. Wepfer	G.fascicularis	L									6		
PW324	Trat5	12.07.2016	P. Wepfer	G.fascicularis	L									5.4		
PW325	Trat5	12.07.2016	P. Wepfer	G.fascicularis	S									6.31176		mean site depth
PW326	Trat5	12.07.2016	P. Wepfer	G.fascicularis	S									6.5		
PW327	Trat5	12.07.2016	P. Wepfer	G.fascicularis	L									6.5		
PW328	Trat5	12.07.2016	P. Wepfer	G.fascicularis	L									7.3		
PW329	Trat5	12.07.2016	P. Wepfer	G.fascicularis	L									8		
PW330	Trat5	12.07.2016	P. Wepfer	G.fascicularis	S									8.4		
PW331	Trat5	12.07.2016	P. Wepfer	G.fascicularis	S									8.4		
PW332	Trat5	12.07.2016	P. Wepfer	G.fascicularis	S									7.5		
PW333	Trat5	12.07.2016	P. Wepfer	G.fascicularis	S									7.5		
PW334	Trat5	12.07.2016	P. Wepfer	G.fascicularis	S									5.4		
Poan6	Trat5	12.07.2016	Sitterporn	G.fascicularis										6.31176		mean site depth
Poan7	Trat5	12.07.2016	Sitterporn	G.fascicularis										6.31176		mean site depth
PW335	Chumphon1	15.07.2016	P. Wepfer	G.fascicularis	L									5.2		
PW336	Chumphon1	15.07.2016	P. Wepfer	G.fascicularis	L									5		
PW337	Chumphon1	15.07.2016	P. Wepfer	G.fascicularis	L	LA	L		EGP0130					5		
PW338	Chumphon1	15.07.2016	P. Wepfer	G.fascicularis	S									3.6		
PW339	Chumphon1	15.07.2016	P. Wepfer	G.fascicularis	S									3.1		
PW340	Chumphon1	15.07.2016	P. Wepfer	G.fascicularis	L									4.2		
PW341	Chumphon1	15.07.2016	P. Wepfer	G.fascicularis	L									5.6		
PW342	Chumphon1	15.07.2016	P. Wepfer	G.fascicularis	L									5.5		
PW343	Chumphon1	15.07.2016	P. Wepfer	G.fascicularis	L									5.3		
PW344	Chumphon1	15.07.2016	P. Wepfer	G.fascicularis	L									5.5		
PW345	Chumphon1	15.07.2016	P. Wepfer	G.fascicularis	L									6.3		
PW346	Chumphon1	15.07.2016	P. Wepfer	G.fascicularis	L									8.5		
PW347	Chumphon1	15.07.2016	P. Wepfer	G.fascicularis	L									9.6		
PW348	Chumphon1	15.07.2016	P. Wepfer	G.fascicularis	S	SA	L		EGP0130					10		
PW349	Chumphon1	15.07.2016	P. Wepfer	G.fascicularis	L									10.1		
PW350	Chumphon1	15.07.2016	P. Wepfer	G.fascicularis	L									11.4		
PW351	Chumphon1	15.07.2016	P. Wepfer	G.fascicularis	L									12.3		
PW352	Chumphon1	15.07.2016	P. Wepfer	G.fascicularis	S									10.3		
PW353	Chumphon1	15.07.2016	P. Wepfer	G.fascicularis	L									11.1		
PW354	Chumphon1	15.07.2016	P. Wepfer	G.fascicularis	L									na		
PW355	Chumphon1	15.07.2016	P. Wepfer	G.fascicularis	L									10.1		
PW356	Chumphon1	15.07.2016	P. Wepfer	G.fascicularis	L									9.2		
PW357	Chumphon1	15.07.2016	P. Wepfer	G.fascicularis	L									7.7		
PW358	Chumphon1	15.07.2016	P. Wepfer	G.fascicularis	L									7.4		

specID	locality	Date	collector	taxon	mt type FA	mt type seq	RAD lineage	meta bar	RAD-plateNo	skeleton examined	polypDia Max [mm]	polypDia Min [mm]	polyp Dist	depth Situ	depth Tide Correct	notes
PW359	Chumphon1	15.07.2016	P. Wepfer	G.fascicularis	?									6.1		
PW360	Chumphon2	15.07.2016	P. Wepfer	G.fascicularis	L									9.1		
PW361	Chumphon2	15.07.2016	P. Wepfer	G.fascicularis	L									6.8		
PW362	Chumphon2	15.07.2016	P. Wepfer	G.fascicularis	L									6.8		
PW363	Chumphon2	15.07.2016	P. Wepfer	G.fascicularis	L									5.2		
PW364	Chumphon2	15.07.2016	P. Wepfer	G.fascicularis	S									5.3		
PW365	Chumphon2	15.07.2016	P. Wepfer	G.fascicularis	L									5.5		
PW366	Chumphon2	15.07.2016	P. Wepfer	G.fascicularis	L									4.1		
PW367	Chumphon2	15.07.2016	P. Wepfer	G.fascicularis	L									6.3		
PW368	Chumphon2	15.07.2016	P. Wepfer	G.fascicularis	L									6.8		
PW369	Chumphon2	15.07.2016	P. Wepfer	G.fascicularis	L									5.4		
PW370	Chumphon2	15.07.2016	P. Wepfer	G.fascicularis	L									6.4		
PW371	Chumphon2	15.07.2016	P. Wepfer	G.fascicularis	S									6.1		
PW372	Chumphon2	15.07.2016	P. Wepfer	G.fascicularis	S									6.8		
PW373	Chumphon2	15.07.2016	P. Wepfer	G.fascicularis	L									na		
PW374	Chumphon2	15.07.2016	P. Wepfer	G.fascicularis	S									5.1		
PW375	Chumphon2	15.07.2016	P. Wepfer	G.fascicularis	S									5.1		
PW376	Chumphon2	15.07.2016	P. Wepfer	G.fascicularis	S									5.5		
PW377	Chumphon2	15.07.2016	P. Wepfer	G.fascicularis	L									5		
PW378	Chumphon2	15.07.2016	P. Wepfer	G.fascicularis	L									5		
PW379	Chumphon2	15.07.2016	P. Wepfer	G.fascicularis	L									5.1		
PW380	Chumphon2	15.07.2016	P. Wepfer	G.fascicularis	S									4.4		
PW381	Chumphon2	15.07.2016	P. Wepfer	G.fascicularis	L									5		
PW382	Chumphon2	15.07.2016	P. Wepfer	G.fascicularis	S									4		
PW383	Chumphon2	15.07.2016	P. Wepfer	G.fascicularis	S									na		
PW384	Chumphon2	15.07.2016	P. Wepfer	G.fascicularis	S									3.5		
PW385	Chumphon2	15.07.2016	P. Wepfer	G.fascicularis	L									3.5		
PW386	Chumphon3	16.07.2017	P. Wepfer	G.fascicularis	L									4.1		
PW387	Chumphon3	16.07.2017	P. Wepfer	G.fascicularis	L									3		
PW388	Chumphon3	16.07.2017	P. Wepfer	G.fascicularis	S									2.8		
PW389	Chumphon3	16.07.2017	P. Wepfer	G.fascicularis	S									2.8		
PW390	Chumphon3	16.07.2017	P. Wepfer	G.fascicularis	S									3.3		
PW391	Chumphon3	16.07.2017	P. Wepfer	G.fascicularis	L									5.8		
PW392	Chumphon3	16.07.2017	P. Wepfer	G.fascicularis	L									6		
PW393	Chumphon3	16.07.2017	P. Wepfer	G.fascicularis	L									6.1		
PW394	Chumphon3	16.07.2017	P. Wepfer	G.fascicularis	L									6.2		
PW395	Chumphon3	16.07.2017	P. Wepfer	G.fascicularis	L									5.5		
PW396	Chumphon3	16.07.2017	P. Wepfer	G.fascicularis	S									6.3		
PW397	Chumphon3	16.07.2017	P. Wepfer	G.fascicularis	L/S									8		
PW398	Chumphon3	16.07.2017	P. Wepfer	G.fascicularis	L									7.8		
PW399	Chumphon3	16.07.2017	P. Wepfer	G.fascicularis	S									7.6		
PW400	Chumphon3	16.07.2017	P. Wepfer	G.fascicularis	S									8.2		
PW401	Chumphon3	16.07.2017	P. Wepfer	G.fascicularis	L									6.6		
PW402	Chumphon3	16.07.2017	P. Wepfer	G.fascicularis	L									7.8		
PW403	Chumphon3	16.07.2017	P. Wepfer	G.fascicularis	L									7.4		
PW404	Chumphon3	16.07.2017	P. Wepfer	G.fascicularis	L									5.6		
PW405	Chumphon3	16.07.2017	P. Wepfer	G.fascicularis	S									3.1		
PW406	Chumphon3	16.07.2017	P. Wepfer	G.fascicularis	L									4.8		
PW407	Chumphon3	16.07.2017	P. Wepfer	G.fascicularis	S									3.6		
PW408	Chumphon3	16.07.2017	P. Wepfer	G.fascicularis	S									3.2		
PW409	Chumphon3	16.07.2017	P. Wepfer	G.fascicularis	S									2.8		
PW410	Chumphon3	16.07.2017	P. Wepfer	G.fascicularis	S									2.9		
PW411	Chumphon3	16.07.2017	P. Wepfer	G.fascicularis	S									3.2		
PW412	Chumphon4	16.07.2017	P. Wepfer	G.fascicularis	S									3.3		
PW413	Chumphon4	16.07.2017	P. Wepfer	G.fascicularis	S									2.4		
PW414	Chumphon4	16.07.2017	P. Wepfer	G.fascicularis	S									3.1		
PW415	Chumphon4	16.07.2017	P. Wepfer	G.fascicularis	S									4.2		
PW416	Chumphon4	16.07.2017	P. Wepfer	G.fascicularis	L									3.9		
PW417	Chumphon4	16.07.2017	P. Wepfer	G.fascicularis	S									2.8		
PW418	Chumphon4	16.07.2017	P. Wepfer	G.fascicularis	S									2.6		
PW419	Chumphon4	16.07.2017	P. Wepfer	G.fascicularis	S									2.4		
PW420	Chumphon4	16.07.2017	P. Wepfer	G.fascicularis	S									2.5		
PW421	Chumphon4	16.07.2017	P. Wepfer	G.fascicularis	S									1.8		
PW422	Chumphon4	16.07.2017	P. Wepfer	G.fascicularis	L									2.9		mean site depth
PW423	Chumphon4	16.07.2017	P. Wepfer	G.fascicularis	S									2.9		mean site depth
PW424	Chumphon4	16.07.2017	P. Wepfer	G.fascicularis	L									2.9		mean site depth
PW425	Chumphon4	16.07.2017	P. Wepfer	G.fascicularis	L									2.9		mean site depth
PW426	Chumphon4	16.07.2017	P. Wepfer	G.fascicularis	S									2.9		mean site depth
PW427	Chumphon4	16.07.2017	P. Wepfer	G.fascicularis	S									2.9		mean site depth
PW428	Chumphon4	16.07.2017	P. Wepfer	G.fascicularis	S									2.9		mean site depth
PW429	Chumphon4	16.07.2017	P. Wepfer	G.fascicularis	S									2.9		mean site depth
PW430	Chumphon4	16.07.2017	P. Wepfer	G.fascicularis	S									2.9		mean site depth
PW431	Chumphon4	16.07.2017	P. Wepfer	G.fascicularis	S									2.9		mean site depth
PW432	Chumphon4	16.07.2017	P. Wepfer	G.fascicularis	L									2.9		mean site depth
PW433	Chumphon4	16.07.2017	P. Wepfer	G.fascicularis	S									2.9		mean site depth
PW434	Chumphon4	16.07.2017	P. Wepfer	G.fascicularis	S									2.9		mean site depth
PW435	Chumphon4	16.07.2017	P. Wepfer	G.fascicularis	S									2.9		mean site depth
PW436	Maeda	04.06.2016	P. Wepfer	Porites										na		
PW437	Maeda	04.06.2016	P. Wepfer	Porites										na		
PW438	Maeda	04.06.2016	P. Wepfer	Porites										na		
PW439	Maeda	04.06.2016	P. Wepfer	Porites										na		
PW440	SeragakiRyugu	21.08.2016	P. Wepfer	G. astreata/ pa	L	LA				yes	3.42	3.41	2.82	14.5	15.51	
PW441	SeragakiRyugu	21.08.2016	P. Wepfer	Euphyllidae	S									na		
PW442	SeragakiRyugu	21.08.2016	P. Wepfer	Porites										na		
PW443	SeragakiRyugu	21.08.2016	P. Wepfer	Porites										na		
PW444	SeragakiRyugu	21.08.2016	P. Wepfer	Porites										na		
PW445	Observatory2	24.08.2016	P. Wepfer	Porites												
PW446	Observatory2	24.08.2016	P. Wepfer	Porites												
PW447	Observatory2	24.08.2016	P. Wepfer	Porites												
PW448	Observatory2	24.08.2016	P. Wepfer	G. astreata / (cr	L	LA	L				6.66	5.04	3.39	17.3	17.16	
PW449	Observatory2	24.08.2016	P. Wepfer	G. astreata / (cr	L	LA	L				3.63	3	2.35	na		
PW450	Observatory1	24.08.2016	P. Wepfer	G.fascicularis	L									17.6	17.46	
PW451	Observatory1	24.08.2016	P. Wepfer	G.fascicularis	L									17.5	17.36	
PW452	Observatory1	24.08.2016	P. Wepfer	G.fascicularis	S									17.5	17.36	
STG01	KoPhangan1	Oct. 2016	Sitterporn	G.fascicularis	S									3		
STG02	KoPhangan1	Oct. 2016	Sitterporn	G.fascicularis	S									1.8		
STG03	KoPhangan1	Oct. 2016	Sitterporn	G.fascicularis	S									1.3		

specID	locality	Date	collector	taxon	mt type FA	mt type seq	RAD lineage	meta bar	RAD-plateNo	skeleton examined	polypDia Max [mm]	polypDia Min [mm]	polyp Dist	depth Situ	depth Tide Correct	notes
STG04	KoPhangan1	Oct. 2016	Sitterporn	G.fasciularis	L									1.3		
STG05	KoPhangan1	Oct. 2016	Sitterporn	G.fasciularis	S									0.8		
STG06	KoPhangan1	Oct. 2016	Sitterporn	G.fasciularis	S									1.8		
STG07	KoPhangan1	Oct. 2016	Sitterporn	G.fasciularis	L									1		
STG08	KoPhangan1	Oct. 2016	Sitterporn	G.fasciularis										1		
STG09	KoPhangan1	Oct. 2016	Sitterporn	G.fasciularis	L									0.7		
STG10	KoPhangan1	Oct. 2016	Sitterporn	G.fasciularis	S									1.2		
STG11	KoPhangan1	Oct. 2016	Sitterporn	G.fasciularis	S									1		
STG12	KoPhangan1	Oct. 2016	Sitterporn	G.fasciularis	S									2		
STG13	KoPhangan1	Oct. 2016	Sitterporn	G.fasciularis	L									1.2		
STG14	KoPhangan1	Oct. 2016	Sitterporn	G.fasciularis	L									1.2		
STG15	KoPhangan1	Oct. 2016	Sitterporn	G.fasciularis	S									1.3		
STG16	KoPhangan1	Oct. 2016	Sitterporn	G.fasciularis	L									1.1		
STG17	KoPhangan1	Oct. 2016	Sitterporn	G.fasciularis	S									1		
STG18	KoPhangan1	Oct. 2016	Sitterporn	G.fasciularis	L									1.1		
STG19	KoPhangan1	Oct. 2016	Sitterporn	G.fasciularis	L									0.9		
STG20	KoPhangan1	Oct. 2016	Sitterporn	G.fasciularis	S									1.2		
STG21	KoPhangan1	Oct. 2016	Sitterporn	G.fasciularis	L									1.1		
STG22	KoPhangan1	Oct. 2016	Sitterporn	G.fasciularis	S									0.7		
STG23	KoPhangan1	Oct. 2016	Sitterporn	G.fasciularis	S									1.7		
STS26	KoPhangan2	Oct. 2016	Sitterporn	G.fasciularis	S									2.1		
STS27	KoPhangan2	Oct. 2016	Sitterporn	G.fasciularis	S	SA	S		EGP0130					2.6		
STS28	KoPhangan2	Oct. 2016	Sitterporn	G.fasciularis	L	SA	L		EGP0130	yes				nophoto		
STS29	KoPhangan2	Oct. 2016	Sitterporn	G.fasciularis	L									3.9		
STS30	KoPhangan2	Oct. 2016	Sitterporn	G.fasciularis	S									3.5		
STS31	KoPhangan2	Oct. 2016	Sitterporn	G.fasciularis	S									3.5		
STS32	KoPhangan2	Oct. 2016	Sitterporn	G.fasciularis	S									3.1		
STS33	KoPhangan2	Oct. 2016	Sitterporn	G.fasciularis	S									3.1		
STS34	KoPhangan2	Oct. 2016	Sitterporn	G.fasciularis	S									3.1		
STS35	KoPhangan2	Oct. 2016	Sitterporn	G.fasciularis	S									3.8		
STS36	KoPhangan2	Oct. 2016	Sitterporn	G.fasciularis	L									3.8		
STS37	KoPhangan2	Oct. 2016	Sitterporn	G.fasciularis	S									3.4		
STS38	KoPhangan2	Oct. 2016	Sitterporn	G.fasciularis	L									4		
STS39	KoPhangan2	Oct. 2016	Sitterporn	G.fasciularis	S									3.8		
STS40	KoPhangan2	Oct. 2016	Sitterporn	G.fasciularis	S									3.2		
STS41	KoPhangan2	Oct. 2016	Sitterporn	G.fasciularis	S									3.5		
STS42	KoPhangan2	Oct. 2016	Sitterporn	G.fasciularis	S									3.8		
STS43	KoPhangan2	Oct. 2016	Sitterporn	G.fasciularis	S									3.9		
STS44	KoPhangan2	Oct. 2016	Sitterporn	G.fasciularis	S									3.5		
STS45	KoPhangan2	Oct. 2016	Sitterporn	G.fasciularis	S									3.1		
STS46	KoPhangan2	Oct. 2016	Sitterporn	G.fasciularis	S									2.6		
STS47	KoPhangan2	Oct. 2016	Sitterporn	G.fasciularis	S									2.3		
STS48	KoPhangan2	Oct. 2016	Sitterporn	G.fasciularis	S									2.9		
STS49	KoPhangan2	Oct. 2016	Sitterporn	G.fasciularis	S									3.3		
STS50	KoPhangan2	Oct. 2016	Sitterporn	G.fasciularis	S									3		
PW453	AnaHotelBeach	8.10.16	P. Wepfer	Euphyllia ancora										na		
PW454	AnaHotelBeach	8.10.16	P. Wepfer	Euphyllia ancora										na		
D1	Dongsha	2016	Allen Chen	G.fasciularis	L	SA	S		EGP0130							
D2	Dongsha	2016	Allen Chen	G.fasciularis		LA	L		EGP0130							
D3	Dongsha	2016	Allen Chen	G.fasciularis		LA	L		EGP0130							
D4	Dongsha	2016	Allen Chen	G.fasciularis		LA	L		EGP0130							
D5	Dongsha	2016	Allen Chen	G.fasciularis			L		EGP0130							
D6	Dongsha	2016	Allen Chen	G.fasciularis			L		EGP0130							
T1	Taiwan	2016	Allen Chen	G.fasciularis	S		S		EGP0130							
T2	Taiwan	2016	Allen Chen	G.fasciularis			na		EGP0130							
T3	Taiwan	2016	Allen Chen	G.fasciularis	S		S		EGP0130							
T4	Taiwan	2016	Allen Chen	G.fasciularis	S		S		EGP0130							
T5	Taiwan	2016	Allen Chen	G.fasciularis			na		EGP0130							
T6	Taiwan	2016	Allen Chen	G.fasciularis	S		S		EGP0130							
PW455	HahaNorthPort	27.10.2016	P. Wepfer	G.fasciularis										3		mean site depth
PW456	HahaNorthPort	27.10.2016	P. Wepfer	G.fasciularis	L	LA	L		EGP0130					3		mean site depth
PW457	HahaNorthPort	27.10.2016	P. Wepfer	G.fasciularis										3		mean site depth
PW458	HahaNorthPort	27.10.2016	P. Wepfer	G.fasciularis			L		EGP0130					3		mean site depth
PW459	HahaNorthPort	27.10.2016	P. Wepfer	G.fasciularis	L									3		mean site depth
PW460	HahaNorthPort	27.10.2016	P. Wepfer	G.fasciularis	L									3		mean site depth
PW461	HahaNorthPort	27.10.2016	P. Wepfer	G.fasciularis	L									3		mean site depth
PW462	HahaNorthPort	27.10.2016	P. Wepfer	G.fasciularis										3		mean site depth
PW463	HahaNorthPort	27.10.2016	P. Wepfer	G.fasciularis	L									3		mean site depth
PW464	HahaNorthPort	27.10.2016	P. Wepfer	G.fasciularis										3		mean site depth
PW465	HahaNorthPort	27.10.2016	P. Wepfer	G.fasciularis										3		mean site depth
PW466	HahaNorthPort	27.10.2016	P. Wepfer	G.fasciularis	L									3		mean site depth
PW467	HahaEastPort	27.10.2016	P. Wepfer	G.fasciularis	L						?	?	?	3		mean site depth
PW468	HahaEastPort	27.10.2016	P. Wepfer	G.fasciularis	L		L		EGP0130		5.28	3.78	2.09	3		mean site depth
PW469	HahaEastPort	27.10.2016	P. Wepfer	G.fasciularis	L						5.8	4.85	1.96	3		mean site depth
PW470	HahaEastPort	27.10.2016	P. Wepfer	G.fasciularis							4.9	3.46	1.58	3		mean site depth
PW471	HahaEastPort	27.10.2016	P. Wepfer	G.fasciularis	L						7.53	5.55	3.29	3		mean site depth
PW472	HahaEastPort	27.10.2016	P. Wepfer	G.fasciularis	L						9.58	7.29	3.77	3		mean site depth
PW473	HahaEastPort	27.10.2016	P. Wepfer	G.fasciularis	L						11.43	7.2	3.36	3		mean site depth
PW474	HahaEastPort	27.10.2016	P. Wepfer	G.fasciularis						yes				3		mean site depth
PW475	HahaEastPort	27.10.2016	P. Wepfer	G.fasciularis										3		mean site depth
PW476	HahaEastPort	27.10.2016	P. Wepfer	G.fasciularis	L									3		mean site depth
PW477	HahaEastPort	27.10.2016	P. Wepfer	G.fasciularis										3		mean site depth
PW478	HahaEastPort	27.10.2016	P. Wepfer	G.fasciularis										3		mean site depth
PW479	HahaEastPort	27.10.2016	P. Wepfer	G.fasciularis	L									3		mean site depth
PW480	HahaEastPort	27.10.2016	P. Wepfer	G.fasciularis	L		L		EGP0130	yes				3		mean site depth
PW481	HahaEastPort	27.10.2016	P. Wepfer	G.fasciularis	L									3		mean site depth
PW482	HahaVillageOute	28.10.2016	P. Wepfer	G.fasciularis							5.89	3.47	1.58	7		mean site depth
PW483	HahaVillageOute	28.10.2016	P. Wepfer	G.fasciularis	S	LA	L		EGP0130	yes	7.32	5.63	3.23	7		mean site depth
PW484	HahaVillageOute	28.10.2016	P. Wepfer	G.fasciularis							5.73	3.87	2.09	7		mean site depth
PW485	HahaVillageOute	28.10.2016	P. Wepfer	G.fasciularis	L		L		EGP0130	yes	6.18	4.09	2.11	7		mean site depth
PW486	HahaVillageOute	28.10.2016	P. Wepfer	G.fasciularis	L		L		EGP0130	na				7		mean site depth
PW487	HahaVillageOute	28.10.2016	P. Wepfer	G.fasciularis							5.55	3.34	2.02	7		mean site depth
PW488	HahaVillageOute	28.10.2016	P. Wepfer	G.fasciularis	L		L		EGP0130	yes	7.85	5.46	2.97	7		mean site depth
PW489	HahaVillageOute	28.10.2016	P. Wepfer	G.fasciularis	L		L		EGP0130	na	5.95	3.78	2.27	7		mean site depth
PW490	HahaVillageInne	28.10.2016	P. Wepfer	G.fasciularis										1.5		mean site depth
PW491	HahaVillageInne	28.10.2016	P. Wepfer	G.fasciularis										1.5		mean site depth
PW492	HahaVillageInne	28.10.2016	P. Wepfer	G.fasciularis										1.5		mean site depth
PW493	HahaVillageInne	28.10.2016	P. Wepfer	G.fasciularis	L									1.5		mean site depth
PW494	HahaVillageInne	28.10.2016	P. Wepfer	G.fasciularis			L		EGP0130	yes				1.5		mean site depth
PW495	HahaVillageInne	28.10.2016	P. Wepfer	G.fasciularis	L	LA	L		EGP0130	yes	15.9	9.67	4.28	1.5		mean site depth

specID	locality	Date	collector	taxon	mt type FA	mt type seq	RAD lineage	meta bar	RAD-plateNo	skeleton examined	polypDia Max [mm]	polypDia Min [mm]	polyp Dist	depth Situ	depth Tide Correct	notes
PW496	HahaVillageInne	28.10.2016	P. Wepfer	G.fascicularis	L						7.98	6.73	2.08	1.5		mean site depth
PW497	HahaVillageInne	28.10.2016	P. Wepfer	G.fascicularis										1.5		mean site depth
PW498	HahaVillageInne	28.10.2016	P. Wepfer	G.fascicularis										1.5		mean site depth
PW499	HahaVillageInne	28.10.2016	P. Wepfer	G.fascicularis	L						12.33	7.42	2.81	1.5		mean site depth
PW500	HahaVillageInne	28.10.2016	P. Wepfer	G.fascicularis										1.5		mean site depth
PW501	HahaVillageInne	28.10.2016	P. Wepfer	G.fascicularis	L		L		EGP0130	na	7.21	5.54	2.33	1.5		mean site depth
PW502	HahaVillageInne	28.10.2016	P. Wepfer	G.fascicularis	L						9.12	7.32	3.24	1.5		mean site depth
PW503	HahaVillageInne	28.10.2016	P. Wepfer	G.fascicularis	L		L		EGP0130	na	9.82	7.26	3.28	1.5		mean site depth
PW504	Chichi1	28.10.2016	P. Wepfer	G.fascicularis	L						6.02	4.47	2.4	9.5		
PW505	Chichi1	28.10.2016	P. Wepfer	G.fascicularis										9.2		
PW506	Chichi1	28.10.2016	P. Wepfer	G.fascicularis	L						8.5	6.26	2.89	8.7		
PW507	Chichi1	28.10.2016	P. Wepfer	?	L		L		EGP0130	na						
PW508	Chichi1	28.10.2016	P. Wepfer	G.fascicularis	L						5.48	4.36	1.97	9.7		
PW509	Chichi1	28.10.2016	P. Wepfer	G.fascicularis	L						10	6.75	3.51	10.5		
PW510	Chichi1	28.10.2016	P. Wepfer	G.fascicularis										9.8		
PW511	Chichi1	28.10.2016	P. Wepfer	G.fascicularis										10.7		
PW512	Chichi1	28.10.2016	P. Wepfer	G.fascicularis	L						5.24	4.36	2.09	8.5		
PW513	Chichi1	28.10.2016	P. Wepfer	G.fascicularis	L									9.2		
PW514	Chichi1	28.10.2016	P. Wepfer	G.fascicularis	L	LA	L		EGP0130	na				8.1		
PW515	Chichi1	28.10.2016	P. Wepfer	G.fascicularis	S		L		EGP0130	na	7.97	5.71	2.06	9		
PW516	Chichi1	28.10.2016	P. Wepfer	G.fascicularis	L									8.4		
PW517	Chichi1	28.10.2016	P. Wepfer	G.fascicularis	L									6.1		
PW518	Chichi1	28.10.2016	P. Wepfer	G.fascicularis	L		L		EGP0130	na	5.74	3.88	2.67	7.3		
PW519	Chichi1	28.10.2016	P. Wepfer	G.fascicularis	L									7.5		
PW520	Chichi1	28.10.2016	P. Wepfer	G.fascicularis	L						5.47	3.8	1.58	6.4		
PW521	Chichi1	28.10.2016	P. Wepfer	G.fascicularis	L		L		EGP0130	na				6.6		
PW522	Chichi1	28.10.2016	P. Wepfer	G.fascicularis										10.9		
PW523	Chichi1	28.10.2016	P. Wepfer	G.fascicularis	L									6		
PW524	Anijima	28.10.2016	P. Wepfer	G.fascicularis	L									6.3		mean site depth
PW525	Anijima	28.10.2016	P. Wepfer	G.fascicularis	L		L		EGP0130	na				6.3		mean site depth
PW526	Anijima	28.10.2016	P. Wepfer	G.fascicularis	L									6.3		mean site depth
PW527	Anijima	28.10.2016	P. Wepfer	G.fascicularis	L									6.3		mean site depth
PW528	Anijima	28.10.2016	P. Wepfer	G.fascicularis	L									6.3		mean site depth
PW529	Anijima	28.10.2016	P. Wepfer	G.fascicularis	L									6.3		mean site depth
PW530	Anijima	28.10.2016	P. Wepfer	G.fascicularis	L		L		EGP0130	na				6.3		mean site depth
PW531	Anijima	28.10.2016	P. Wepfer	G.fascicularis	L									6.3		mean site depth
PW532	Anijima	28.10.2016	P. Wepfer	G.fascicularis	L									6.3		mean site depth
PW533	Anijima	28.10.2016	P. Wepfer	G.fascicularis	L		L		EGP0130	yes				6.3		mean site depth
PW534	Anijima	28.10.2016	P. Wepfer	G.fascicularis	L									6.3		mean site depth
PW535	Anijima	28.10.2016	P. Wepfer	G.fascicularis	L									6.3		mean site depth
PW536	Anijima	28.10.2016	P. Wepfer	G.fascicularis	L		L		EGP0130	na				6.3		mean site depth
PW537	Anijima	28.10.2016	P. Wepfer	G.fascicularis	L									6.3		mean site depth
PW538	Anijima	28.10.2016	P. Wepfer	G.fascicularis	L									6.3		mean site depth
PW539	ChichiNihonIwa	29.10.2016	P. Wepfer	G.fascicularis	L		L		EGP0130	yes				6.4		
PW540	ChichiNihonIwa	29.10.2016	P. Wepfer	G.fascicularis										4.1		
PW541	ChichiSE	29.10.2016	P. Wepfer	G.fascicularis	L									9.3		
PW542	ChichiSE	29.10.2016	P. Wepfer	G.fascicularis	L									10.3		
PW543	ChichiSE	29.10.2016	P. Wepfer	G.fascicularis	L									9.2		
PW544	ChichiSE	29.10.2016	P. Wepfer	G.fascicularis	L		L		EGP0130	na				9.5		
PW545	ChichiSE	29.10.2016	P. Wepfer	G.fascicularis	L									8.1		
PW546	ChichiSE	29.10.2016	P. Wepfer	G.fascicularis	L									6.1		
PW547	ChichiSE	29.10.2016	P. Wepfer	G.fascicularis	L									5.8		
PW548	ChichiSE	29.10.2016	P. Wepfer	G.fascicularis	L									5.4		
PW549	ChichiSE	29.10.2016	P. Wepfer	G.fascicularis	L		L		EGP0130	yes				5		
PW550	ChichiSE	29.10.2016	P. Wepfer	G.fascicularis	L									3.9		
PW551	ChichiSE	29.10.2016	P. Wepfer	G.fascicularis	L		L		EGP0130	na				4.1		
PW552	ChichiSE	29.10.2016	P. Wepfer	G.fascicularis	L									4.9		
PW553	ChichiSE	29.10.2016	P. Wepfer	G.fascicularis	L									5		
PW554	ChichiSE	29.10.2016	P. Wepfer	G.fascicularis	L		L		EGP0130	na				4.3		
PW555	ChichiSE	29.10.2016	P. Wepfer	G.fascicularis										(4.6		
PW556	ChichiSE	29.10.2016	P. Wepfer	G.fascicularis										4.6)		
PW557	ChichiSE	29.10.2016	P. Wepfer	G.fascicularis	L									6.4		
PW558	ChichiSE	29.10.2016	P. Wepfer	G.fascicularis	L									5.4		
PW559	ChichiSE	29.10.2016	P. Wepfer	G.fascicularis	L									6		
PW560	ChichiSE	29.10.2016	P. Wepfer	G.fascicularis										8.9		
PW561	ChichiSE	29.10.2016	P. Wepfer	G.fascicularis	L									9.5		
PW562	ChichiSE	29.10.2016	P. Wepfer	G.fascicularis	L		L		EGP0130	na				10.9		
PW563	ChichiSE	29.10.2016	P. Wepfer	G.fascicularis	L									11.2		
PW564	ChichiSE	29.10.2016	P. Wepfer	G.fascicularis										10.7		
PW565	ChichiSE	29.10.2016	P. Wepfer	G.fascicularis	L									9.7		
PW566	ChichiSE	29.10.2016	P. Wepfer	G.fascicularis										8.8		
PW567	ChichiSE	29.10.2016	P. Wepfer	G.fascicularis	L									11.3		
PW568	ChichiSE	29.10.2016	P. Wepfer	G.fascicularis	L		L		EGP0130	na				12		
PW569	ChichiSE	29.10.2016	P. Wepfer	G.fascicularis										12.1		
PW570	ChichiSE	29.10.2016	P. Wepfer	G.fascicularis										12		
HK1	Hong Kong	Nov. 2016	Put Ang	G.fascicularis	S		S		EGP0130					1.2		
HK2	Hong Kong	Nov. 2016	Put Ang	G.fascicularis	S		S		EGP0130					1.2		
HK3	Hong Kong	Nov. 2016	Put Ang	G.fascicularis	S		S		EGP0130					1.2		
HK4	Hong Kong	Nov. 2016	Put Ang	G.fascicularis	S		S		EGP0130					2.9		
HK5	Hong Kong	Nov. 2016	Put Ang	G.fascicularis	S		S		EGP0130					2.2-3.1		
HK6	Hong Kong	Nov. 2016	Put Ang	G.fascicularis	S		S		EGP0130					2.2-3.1		
HK7	Hong Kong	Nov. 2016	Put Ang	G.fascicularis	S		S		EGP0130					2.2-3.1		
HK8	Hong Kong	Nov. 2016	Put Ang	G.fascicularis	S		S		EGP0130					2.6		
HK9	Hong Kong	Nov. 2016	Put Ang	G.fascicularis	S		S		EGP0130					2.8		
HK10	Hong Kong	Nov. 2016	Put Ang	G.fascicularis	S		S		EGP0130					2.7		
HK11	Hong Kong	Nov. 2016	Put Ang	G.fascicularis	S									3		
HK12	Hong Kong	Nov. 2016	Put Ang	G.fascicularis	S		S		EGP0130					2.4		
HK13	Hong Kong	Nov. 2016	Put Ang	G.fascicularis	S		S		EGP0130					2.4		
HK14	Hong Kong	Nov. 2016	Put Ang	G.fascicularis	S		S		EGP0130					2.4		
HK15	Hong Kong	Nov. 2016	Put Ang	G.fascicularis	S		S		EGP0130					6		
M013	Reethi Rah	30.03.2015	V. Radice	G.fascicularis		?			EGP0135					~30		mean site depth
M014	Reethi Rah	30.03.2015	V. Radice	G.fascicularis										~30		mean site depth
M015	Reethi Rah	30.03.2015	V. Radice	G.fascicularis					EGP0135					~30		mean site depth
M019	Reethi Rah	30.03.2015	V. Radice	G.fascicularis		LA			EGP0135					~10		mean site depth
M022	Reethi Rah	30.03.2015	V. Radice	G.fascicularis					EGP0135					~10		mean site depth
M032	Reethi Rah	30.03.2015	V. Radice	G.fascicularis					EGP0135					~10		mean site depth
M042	Mathiveri	1.04.2014	V. Radice	G.fascicularis		LA			EGP0135					~30		mean site depth
M044	Mathiveri	1.04.2014	V. Radice	G.fascicularis					EGP0135					~30		mean site depth

specID	locality	Date	collector	taxon	mt type FA	mt type seq	RAD lineage	meta bar	RAD-plateNo	skeleton examined	polypDia Max [mm]	polypDia Min [mm]	polyp Dist	depth Situ	depth Tide Correct	notes
M047	Mathiveri	1.04.2014	V. Radice	G.fascicularis					EGP0135					~30		mean site depth
M049	Mathiveri	1.04.2014	V. Radice	G.fascicularis		SA			EGP0135					~10		mean site depth
M051	Mathiveri	1.04.2014	V. Radice	G.fascicularis										~10		mean site depth
M052	Mathiveri	1.04.2014	V. Radice	G.fascicularis					EGP0135					~10		mean site depth
M221	Bodu huraa	8.04.2014	V. Radice	G.fascicularis					EGP0135					~30		mean site depth
M222	Bodu huraa	8.04.2014	V. Radice	G.fascicularis										~30		mean site depth
M226	Bodu huraa	8.04.2014	V. Radice	G.fascicularis		LA			EGP0135					~30		mean site depth
M242	Bodu huraa	8.04.2014	V. Radice	G.fascicularis										~10		mean site depth
M243	Bodu huraa	8.04.2014	V. Radice	G.fascicularis					EGP0135					~10		mean site depth
M244	Bodu huraa	8.04.2014	V. Radice	G.fascicularis					EGP0135					~10		mean site depth
CH033	Ile de la Passe	18.02.2015	V. Radice	G.fascicularis		LA			EGP0135					~30		mean site depth
CH037	Ile de la Passe	18.02.2015	V. Radice	G.fascicularis					EGP0135					~30		mean site depth
CH038	Ile de la Passe	18.02.2015	V. Radice	G.fascicularis					EGP0135					~30		mean site depth
CH048	Ile de la Passe	18.02.2015	V. Radice	G.fascicularis					EGP0135					~10		mean site depth
CH049	Ile de la Passe	18.02.2015	V. Radice	G.fascicularis					EGP0135					~10		mean site depth
CH054	Ile de la Passe	18.02.2015	V. Radice	G.fascicularis					EGP0135					~10		mean site depth
CH113	Nelson's Island	18.02.2015	V. Radice	G.fascicularis					EGP0135					~30		mean site depth
CH115	Nelson's Island	18.02.2015	V. Radice	G.fascicularis										~30		mean site depth
CH131	Nelson's Island	18.02.2015	V. Radice	G.fascicularis					EGP0135					~30		mean site depth
CH111	Nelson's Island	18.02.2015	V. Radice	G.fascicularis					EGP0135					~10		mean site depth
CH120	Nelson's Island	18.02.2015	V. Radice	G.fascicularis					EGP0135					~10		mean site depth
CH128	Nelson's Island	18.02.2015	V. Radice	G.fascicularis					EGP0135					~10		mean site depth
HGN07R	Harry's bommie	08.08.2016	V. Radice	G.fascicularis		SB			EGP0135					~8		mean site depth
HGN15R	Harry's bommie	08.08.2016	V. Radice	G.fascicularis		SB			EGP0135					~8		mean site depth
HGN24R	Harry's bommie	08.08.2016	V. Radice	G.fascicularis		SB			EGP0135					~8		mean site depth
HI1	Harry's bommie	08.08.2016	V. Radice	G.fascicularis		LA			EGP0135					~8		mean site depth
HI4	Harry's bommie	08.08.2016	V. Radice	G.fascicularis		LA			EGP0135					~8		mean site depth
HI5	Harry's bommie	08.08.2016	V. Radice	G.fascicularis		LA			EGP0135					~8		mean site depth
ZR#1	Rowley Shoals	unknown	Z. Richards	G. astreata		LA			EGP0135							K14 #227, Z89274
ZR#2	Rowley Shoals	unknown	Z. Richards	G. astreata		SA			EGP0135	yes						K14 #496, Z89272
ZR#3	Christmas Island	unknown	Z. Richards	G. astreata		LI			EGP0135							Xmas#42, Z65832
ZR#4	Ashmore Reef	unknown	Z. Richards	Galaxea horrescens					EGP0135	yes						K13#203, Z66352
ZR#5	Montebello Islan	unknown	Z. Richards	Galaxea fascicularis		LL			EGP0135	yes						MM#55, no rego yet
ZR#6	Rowley Shoals	unknown	Z. Richards	Galaxea fascicularis		LK			EGP0135							K14#321, Z89277
ZR#7	Rowley Shoals	unknown	Z. Richards	Galaxea fascicularis		LA			EGP0135	yes						K14#610, Z89279
ZR#8	Montebello Islan	unknown	Z. Richards	Galaxea fascicularis		LA			EGP0135	yes						MM#71, no rego yet
ZR#9	Montebello Islan	unknown	Z. Richards	Galaxea fascicularis		LA			EGP0135							MM#107, no rego yet
ZR#10	Rowley Shoals	unknown	Z. Richards	G. astreata		LA			EGP0135							K14#199, Z89273
ZR#11	Rowley Shoals	unknown	Z. Richards	Galaxea fascicularis		LA			EGP0135							K14#589, Z89278
ZR#12	Ashmore Reef	unknown	Z. Richards	Galaxea horrescens					EGP0135							K13site139, no rego yet
ZR#13	Cassini Island	unknown	Z. Richards	G. astreata												K10#51, Z66007
SC1	Sichang	Dec. 2016	Sitterporn	G. fascicularis	S											
SC2	Sichang	Dec. 2016	Sitterporn	G. fascicularis												
SC3	Sichang	Dec. 2016	Sitterporn	G. fascicularis	S		L		EGP0130							
SC4	Sichang	Dec. 2016	Sitterporn	G. fascicularis												
SC5	Sichang	Dec. 2016	Sitterporn	G. fascicularis	S											
SC6	Sichang	Dec. 2016	Sitterporn	G. fascicularis												
SC7	Sichang	Dec. 2016	Sitterporn	G. fascicularis	S											
SC8	Sichang	Dec. 2016	Sitterporn	G. fascicularis												
SC9	Sichang	Dec. 2016	Sitterporn	G. fascicularis	S											
SC10	Sichang	Dec. 2016	Sitterporn	G. fascicularis												
SC11	Sichang	Dec. 2016	Sitterporn	G. fascicularis	S											
SC12	Sichang	Dec. 2016	Sitterporn	G. fascicularis												
SC13	Sichang	Dec. 2016	Sitterporn	G. fascicularis	S											
SC14	Sichang	Dec. 2016	Sitterporn	G. fascicularis												
SC15	Sichang	Dec. 2016	Sitterporn	G. fascicularis	S											
SC16	Sichang	Dec. 2016	Sitterporn	G. fascicularis												
SC17	Sichang	Dec. 2016	Sitterporn	G. fascicularis	S											
SC18	Sichang	Dec. 2016	Sitterporn	G. fascicularis												
SC19	Sichang	Dec. 2016	Sitterporn	G. fascicularis	S											
SC20	Sichang	Dec. 2016	Sitterporn	G. fascicularis												
SC21	Sichang	Dec. 2016	Sitterporn	G. fascicularis	S											
SC22	Sichang	Dec. 2016	Sitterporn	G. fascicularis												
SC26	Sichang	Dec. 2016	Sitterporn	G. fascicularis	S											
SC27	Sichang	Dec. 2016	Sitterporn	G. fascicularis												
SC28	Sichang	Dec. 2016	Sitterporn	G. fascicularis	S											
SC29	Sichang	Dec. 2016	Sitterporn	G. fascicularis												
SC30	Sichang	Dec. 2016	Sitterporn	G. fascicularis	S											
SC31	Sichang	Dec. 2016	Sitterporn	G. fascicularis												
SC32	Sichang	Dec. 2016	Sitterporn	G. fascicularis	S											
SC33	Sichang	Dec. 2016	Sitterporn	G. fascicularis	S											
RMNH:10	Java-LeidenMuse	unknown	na	G. sp					EGP0135	yes						
RMNH:10	Java-LeidenMuse	unknown	na	G. sp.					EGP0135	yes						
89904	CookIslands	unknown	na	G. fascicularis						yes						
83301	Indonesia	unknown	na	G. fascicularis					EGP0135							
83316	Indonesia	unknown	na	G. fascicularis	L				EGP0135							
83317	Tanzania	unknown	na	G. clavus	S				EGP0135							
75180	Seychelles	unknown	na	G. sp.					EGP0135							
89396	Marshall_Islands	unknown	na	G. sp.												
93768	PapuaNewGuine	unknown	na	G. paucisepta						yes						
93769	PapuaNewGuine	unknown	na	G. paucisepta						yes						
93770	PapuaNewGuine	unknown	na	G. paucisepta					EGP0135	yes						
93774	PapuaNewGuine	unknown	na	G. paucisepta												
80004	Philippines	unknown	na	G. sp.					EGP0135							
95493	Philippines	unknown	na	G. astreata												
1154299	NewCaledonia	unknown	na	G. sp.					EGP0135							
1154300	Eritrea	unknown	na	G. sp					EGP0135							
1154337	Madagascar	unknown	na	G. sp												
1154345	Madagascar	unknown	na	G. sp					EGP0135							
1154454	Seychelles	unknown	na	G. sp.					EGP0135							
1154455	Seychelles	unknown	na	G. sp.												
MS01	Samoa_Aoa	14.07.2016	M. Sudek	G.fascicularis		LN			EGP0135		10.06	7.34	2.56	10.36		
MS02	Samoa_Fagaalu	26.06.2016	M. Sudek	G.fascicularis		LA			EGP0135		9.6	6.14	2.29	7.62		
MS03	Samoa_Fagamol	16.10.2016	M. Sudek	G.fascicularis		LA			EGP0135		9.41	7.27	2.55	8.84		
MS04	Samoa_Aasu	12.02.2016	M. Sudek	G.fascicularis		LM			EGP0135		6.02	3.98	1.78	9.14		
MS05	Samoa_Leone	26.10.2016	M. Sudek	G. astreata ?		LM			EGP0135		5.66	3.96	2.17	9.75		
AF-1	Agat_Cementary	Mar-2017	A. Fujimura	G. horrescens					EGP0130							

Appendix 3: Table S3.1 - List of specimens

specID	locality	Date	collector	taxon	mt type FA	mt type seq	RAD lineage	meta bar	RAD-plateNo	skeleton examined	polypDia Max [mm]	polypDia Min [mm]	polyp Dist	depth Situ	depth Tide Correct	notes
AF-2	Meriza_Pier	Mar-2017	A. Fujimura	G. horrescens					EGP0130							
AF-3	Meriza_Pier	Mar-2017	A. Fujimura	G. horrescens		LH			EGP0130							
AF-4	Meriza_Pier	Mar-2017	A. Fujimura	G. horrescens		LH			EGP0130							
AF-A	Agat_Cementary	Mar-2017	A. Fujimura	G. fascicularis		LA			EGP0130							
AF-B	Agat_Cementary	Mar-2017	A. Fujimura	G. fascicularis		SA			EGP0130							
AF-C	Agat_Cementary	Mar-2017	A. Fujimura	G. fascicularis		LA			EGP0130							
AF-D	Meriza_Pier	Mar-2017	A. Fujimura	G. fascicularis		LA			EGP0130							
AF-E	Meriza_Pier	Mar-2017	A. Fujimura	G. fascicularis		SA			EGP0130							
SA2718	Shark Reef	25/08/2016	T. Terraneo	G.fascicularis										21		
SA2719	Shark Reef	25/08/2016	T. Terraneo	G.fascicularis					EGP0135					23		
SA2720	Shark Reef	25/08/2016	T. Terraneo	G.fascicularis	L	LA			EGP0135					18		
SA2723	Shark Reef	25/08/2016	T. Terraneo	G.fascicularis										0.3		
SA2724	Shark Reef	25/08/2016	T. Terraneo	G.fascicularis										0.4		
SA2725	Shark Reef	25/08/2016	T. Terraneo	G.fascicularis										22		
SA2726	Shark Reef	25/08/2016	T. Terraneo	G.fascicularis	L	LA			EGP0135					23		
SA2727	Shark Reef	25/08/2016	T. Terraneo	G.fascicularis					EGP0135					23		
SA2728	Shark Reef	25/08/2016	T. Terraneo	G.fascicularis										24		
SA2729	Shark Reef	25/08/2016	T. Terraneo	G.fascicularis					EGP0135					24		
SA2730	Shark Reef	25/08/2016	T. Terraneo	G.fascicularis	L	LA								24		
SA2731	Shark Reef	25/08/2016	T. Terraneo	G.fascicularis					EGP0135					24		
SA2732	Shark Reef	25/08/2016	T. Terraneo	G.fascicularis										24		
SA2733	Shark Reef	25/08/2016	T. Terraneo	G.fascicularis	L	LA			EGP0135					24		
SA2734	Shark Reef	25/08/2016	T. Terraneo	G.fascicularis	L	LA			EGP0135					24		
SA3442	Yanbu 1	2017/07/15	T. Terraneo	G.fascicularis												
SA3443	Yanbu 1	2017/07/15	T. Terraneo	G.fascicularis	L	LA			EGP0135							
SA3469	Yanbu 2	2017/07/15	T. Terraneo	G.fascicularis												
SA3470	Yanbu 2	2017/07/15	T. Terraneo	G.fascicularis	L	LA			EGP0135							
SA3490	Yanbu 3	2017/07/15	T. Terraneo	G.fascicularis												
SA3491	Yanbu 3	2017/07/15	T. Terraneo	G.fascicularis												
SA3517	Farasan Banks 1	18.07.17	T. Terraneo	G.fascicularis	L	LJ			EGP0135					8		
SA3518	Farasan Banks 1	18.07.17	T. Terraneo	G.fascicularis	L	LA			EGP0135					18.4		
SA3529	Al Lith 1	20.07.17	T. Terraneo	G.fascicularis	L	LA			EGP0135					21		
SA3530	Al Lith 1	20.07.17	T. Terraneo	G.fascicularis	L	LA			EGP0135					2.8		
SA3566	Al Lith 2	20.07.17	T. Terraneo	G.fascicularis					EGP0135					3.8		
SA3567	Al Lith 2	20.07.17	T. Terraneo	G.fascicularis										4.2		
PW571	SeragakiRyugu	04.09.16	P. Wepfer	G. paucisepta		LA	L				3.31	3.06	2.72	23		
PW572	SeragakiRyugu	04.09.16	P. Wepfer	G. atreata / (crypto)		LA	L		EGP0135	yes	5.88	5.34	3.97	26		
PW573	SeragakiRyugu	04.09.16	P. Wepfer	G. astreata		LA	L		EGP0135	yes	4.2	3.51	2.7	26.6		
PW574	SeragakiRyugu	04.09.16	P. Wepfer	G. cryptoramosa			L		EGP0135	yes	5.52	5	2.07	23.2		
PW575	SeragakiRyugu	04.09.16	P. Wepfer	G. fascicularis			S		EGP0135	yes				23.7		
PW576	SeragakiRyugu	04.09.16	P. Wepfer	G. cryptoramosa		LA	L		EGP0135	yes	8.7	7.59	4.68	22.8		
PW577	Zanpa	Sept. 2016	P. Wepfer	Plerogyra sp.												
PW578	AnaHotelBeach	12.09.16	P. Wepfer	Pachyseris sp.										~10		
PW579	AnaHotelBeach	12.09.16	P. Wepfer	Plerogyra eurysepta										~20		
PW580	AnaHotelBeach	12.09.16	P. Wepfer	Euphyllia paraancoris										~20		
PW581	AnaHotelBeach	12.09.16	P. Wepfer	Pachyseris sp.										~15		
PW583PH	SeragakiRyugu	2016.6.11	P. Wepfer	G. astreata							4.83	4.07	3.49	29.9		
PW584PH	SeragakiRyugu	2016.6.11	P. Wepfer	G. paucisepta							2.79	2.58	1.74	29.9		
PW585PH	SeragakiRyugu	2016.6.11	P. Wepfer	G. astreata/paucisepta with long polyps							3.86	3.32	3.94	29.9		
Y331	Haemida	2014	Y. Nakajima	G.fascicularis	L		L	1	EGP0124							
Y332	Haemida	2014	Y. Nakajima	G.fascicularis	L			1	EGP0124							
Y333	Haemida	2014	Y. Nakajima	G.fascicularis	L		L	1	EGP0124							
Y334	Haemida	2014	Y. Nakajima	G.fascicularis	S		S	1	EGP0124							

Appendix 3: Table S3.1 - List of specimens

speID	locality	Date	collector	taxon	mt type FA	mt type seq	RAD lineage	meta bar	RAD-plateNo	skeleton examined	polypDia Max [mm]	polypDia Min [mm]	polyp Dist	depth Situ	depth Tide Correct	notes
Y335	Haemida	2014	Y. Nakajima	G.fascicularis	S		S	1	EGP0124							
Y336	Haemida	2014	Y. Nakajima	G.fascicularis	L		L	1	EGP0124							
Y341	Haemida	2014	Y. Nakajima	G.fascicularis	S			1	EGP0124							
Y343	Haemida	2014	Y. Nakajima	G.fascicularis	S		S	1	EGP0124							
Y344	Haemida	2014	Y. Nakajima	G.fascicularis	S		S	1	EGP0124							
Y349	Haemida	2014	Y. Nakajima	G.fascicularis	L		L	1	EGP0124							
Y435	Zampa	2014	Y. Nakajima	G.fascicularis	L		L	1	EGP0124							
Y436	Zampa	2014	Y. Nakajima	G.fascicularis	S		S	1	EGP0124							
Y437	Zampa	2014	Y. Nakajima	G.fascicularis	L		L	1	EGP0124							
Y439	Zampa	2014	Y. Nakajima	G.fascicularis	L		L	1	EGP0124							
Y440	Zampa	2014	Y. Nakajima	G.fascicularis	S		S	1	EGP0124							
Y441	Zampa	2014	Y. Nakajima	G.fascicularis	S		S	1	EGP0124							
Y442	Zampa	2014	Y. Nakajima	G.fascicularis	L		L	1	EGP0124							
Y443	Zampa	2014	Y. Nakajima	G.fascicularis	L		L	1	EGP0124							
Y447	Zampa	2014	Y. Nakajima	G.fascicularis	S		S	1	EGP0124							
Y452	Zampa	2014	Y. Nakajima	G.fascicularis	L		L	1	EGP0124							
Y1	Ayamaru	2014	Y. Nakajima	G.fascicularis	S				EGP0124							
Y2	Ayamaru	2014	Y. Nakajima	G.fascicularis	S				EGP0124							
Y3	Ayamaru	2014	Y. Nakajima	G.fascicularis	L				EGP0124							
Y4	Ayamaru	2014	Y. Nakajima	G.fascicularis	S				EGP0124							
Y5	Ayamaru	2014	Y. Nakajima	G.fascicularis	S				EGP0124							
Y7	Ayamaru	2014	Y. Nakajima	G.fascicularis	S				EGP0124							
Y8	Ayamaru	2014	Y. Nakajima	G.fascicularis	L				EGP0124							
Y9	Ayamaru	2014	Y. Nakajima	G.fascicularis	L				EGP0124							
Y10	Ayamaru	2014	Y. Nakajima	G.fascicularis	L				EGP0124							
Y11	Ayamaru	2014	Y. Nakajima	G.fascicularis	L				EGP0124							
Y141	Ikema	2014	Y. Nakajima	G.fascicularis	S				EGP0124							
Y142	Ikema	2014	Y. Nakajima	G.fascicularis	S				EGP0124							
Y143	Ikema	2014	Y. Nakajima	G.fascicularis	S				EGP0124							
Y144	Ikema	2014	Y. Nakajima	G.fascicularis	L				EGP0124							
Y145	Ikema	2014	Y. Nakajima	G.fascicularis	L				EGP0124							
Y146	Ikema	2014	Y. Nakajima	G.fascicularis	L				EGP0124							
Y147	Ikema	2014	Y. Nakajima	G.fascicularis	S				EGP0124							
Y148	Ikema	2014	Y. Nakajima	G.fascicularis	L				EGP0124							
Y149	Ikema	2014	Y. Nakajima	G.fascicularis	S				EGP0124							
Y150	Ikema	2014	Y. Nakajima	G.fascicularis	L				EGP0124							

Appendix 3: Table S3.2 - List of sampling sites

locality	country	island / province	LAT	LONG
Harry's bommie	Australia	Heron Island	-23.468	151.936
Ashmore Reef	Australia	WA	-12.2842	123.0287
Cassini Island	Australia	WA	-14.122	125.6069
Christmas Island	Australia	WA	-10.4913	105.6971
Montebello Islands	Australia	WA	-20.1106	115.8004
Rowley Shoals	Australia	WA	-17.4375	119.1919
Nelson's Island	Chagos	Great Chagos Bank	-5.685	72.317
Bodu huraa	Chagos	Meemu	2.811	73.366
Ile de la Passe	Chagos	Salomon	-5.286	72.250
HongKong_NE	China	HongKong	22.530158	114.366638
Agat Cementary	Guam	Guam	13.3900	144.6489
Merizo Pier	Guam	Guam	13.2682	144.6639
Guam	Guam	various	13.4	144.7
Ayamaru	Japan	Amami	28.4761111	129.7166667
Katetsu	Japan	Amami	28.1358333	129.3441667
Kuninao	Japan	Amami	28.3747222	129.4038889
Yadori Beach	Japan	Amami	28.1230556	129.3616667
Anijima	Japan	Anijima	27.111714	142.199749
Chichi-Nihoniwa	Japan	Chichi	27.052554	142.171022
Chichi1	Japan	Chichi	27.102365	142.21669
ChichiSE	Japan	Chichi	27.056147	142.228223
HahaEastPort	Japan	Haha	26.693478	142.151836
HahaNorthPort	Japan	Haha	26.701905	142.140603
HahaVillageBeach	Japan	Haha	26.636437	142.157501
HahaVillageOuter	Japan	Haha	26.635203	142.155223
North	Japan	Iheya	27.0927	128.01216
Amitori	Japan	Iriomote	24.3297222	123.6961111
Haemida	Japan	Iriomote	24.2683333	123.8297222
Nakano	Japan	Iriomote	24.4311111	123.7905556
Hirakubo	Japan	Ishigaki	24.6116667	124.3283333
Kannon	Japan	Ishigaki	24.3652778	124.1111111
North Shiraho	Japan	Ishigaki	24.4005556	124.2647222
Ohama	Japan	Ishigaki	24.34	124.1986111
KitaDaito	Japan	KitaDaito	25.95752	131.322
North Hateno-hama	Japan	Kume Island	26.3555556	126.8769444
Takenchi (South Hateno-	Japan	Kume Island	26.3208333	126.8566667
Kuroshima	Japan	Kuroshima	24.3013889	124.0155556
MinamiDaitoSouth	Japan	MinamiDaito	25.81694	131.22034
MinamiDaitoWest	Japan	MinamiDaito	25.87795	131.21427
Ikema	Japan	Miyako	24.93455	125.2297
Ikema	Japan	Miyako	24.9338889	125.2305556
Ueno	Japan	Miyako	24.7180556	125.3416667
Yoshino	Japan	Miykao	24.74841	125.44599
AnaHotelBeach	Japan	Okinawa	26.509882	127.853747
Maeda	Japan	Okinawa	26.443775	127.777357
Manza	Japan	Okinawa	26.51134	127.85831
Miyagi	Japan	Okinawa	26.36451	127.99891
Observatory1	Japan	Okinawa	26.713156	127.86884
Observatory2	Japan	Okinawa	127.87626	26.67884
Odo	Japan	Okinawa	26.0880556	127.7075
Oku	Japan	Okinawa	26.84922	128.28717
SeragakiRyugu	Japan	Okinawa	26.511133	127.880975
Sesoko	Japan	Okinawa	26.67894	127.87513
Zampa	Japan	Okinawa	26.4388889	127.7111111
Taketomi	Japan	Taketomi	24.3475	124.0775
Tanega	Japan	Tanega	30.827102	131.035352
Mathiveri	Maldives	North Ari	4.191	72.737
Reethi Rah	Maldives	North Male	4.521	73.362
Palau	Palau	various	7.5	134.5
Samoa_Aasu	Samoa	Tutuila	-14.291454	-170.758163
Samoa_Aoa	Samoa	Tutuila	-14.26153	-170.58679
Samoa_Fagaalu	Samoa	Tutuila	-14.293259	-170.677594
Samoa_Fagamale	Samoa	Tutuila	-13.439068	-172.348735
Samoa_Leone	Samoa	Tutuila	-14.339041	-170.787282
Al Lith 1	SaudiArabia		19.953871	40.261804
Al Lith 2	SaudiArabia		19.953871	40.261804
Farasan Banks 1	SaudiArabia		17.900723	40.997964
Shark Reef	SaudiArabia		22.465283	38.627835
Yanbu 1	SaudiArabia		23.945466	38.086245
Yanbu 2	SaudiArabia		23.945466	38.086245
Yanbu 3	SaudiArabia		23.945466	38.086245
Dongsha	Taiwan	Dongsha	20.710857	116.729739
Taiwan	Taiwan	Taiwan	21.941878	120.789388
Trat1	Thailand	KohBaiDang	11.901579	102.450841
Trat2	Thailand	KohKut-LaemAoSalat	11.704815	102.589848
KoPhangan1	Thailand	KoPhangan	9.75638	99.9587
KoPhangan2	Thailand	KoPhangan	9.79377	100.035
Sichang	Thailand	Sichang	13.1178667	100.807525
Chumphon1	Thailand		10.491507	99.417383
Chumphon2	Thailand		10.486858	99.417516
Chumphon3	Thailand		10.317731	99.298906
Chumphon4	Thailand		10.363112	99.308107
Trat3	Thailand		11.711015	102.578062
Trat4	Thailand		11.719483	102.570486
Trat5	Thailand		11.820244	102.445946

Appendix 3: Table S3.3 - Booster instability

Taxon	Instability	Taxon	Instability
Acropora_2	0.035401	Gcrypto_PW576	0.123231
Acropora_M	0.035401	GcryptoSer_PW249	0
Chagos_CH033	0.033986	GcryptoSer_PW572	0.283632
Chagos_CH037	0.017857	GcryptoSer_PW574	0
Chagos_CH038	0.018182	GpauciSer_PW571	0.296032
Chagos_CH048	0	GpauciSer_PW573	0.647465
Chagos_CH049	0.558459	Guam_AF-1	0
Chagos_CH054	0.911276	Guam_AF-2	0
Chagos_CH111	0	Guam_AF-3	0
Chagos_CH113	0	Guam_AF-4	0
Chagos_CH120	0.035401	Guam_AF-A	0.316951
Chagos_CH128	0	Guam_AF-B	0.141383
Chagos_CH131	0	Guam_AF-C	0.316951
Chichi_PW514	1.363954	Guam_AF-D	0.316951
Chichi_PW515	0	Guam_AF-E	0.141383
Chichi_PW518	1.294036	Haha_PW456	1.64313
Chichi_PW521	0	Haha_PW458	0
Chichi_PW525	0	Haha_PW468	0
Chichi_PW530	0	Haha_PW480	0.070532
Chichi_PW533	0	Haha_PW483	0.036062
Chichi_PW536	0.017544	Haha_PW485	0.018182
Chichi_PW539	0	Haha_PW486	0.016949
Chichi_PW544	0.052642	Haha_PW488	0.018519
Chichi_PW549	0.018182	Haha_PW489	0
Chichi_PW551	0	Haha_PW494	0
Chichi_PW554	0.016949	Haha_PW495	0
Chichi_PW562	0.016949	Haha_PW501	0.069409
Chichi_PW568	0.018519	Haha_PW503	0.052068
Daito_PW199	1.526056	Heron_HGN07R	0
Daito_PW200	1.278587	Heron_HGN15R	0
Daito_PW201	0.435799	Heron_HGN24R	0
Daito_PW202	0.035131	Heron_HI1	0
Daito_PW203	3.413489	Heron_HI4	0
Daito_PW204	0.016949	Heron_HI5	0
Daito_PW207	0	HK_HK1	0
Daito_PW208	5.847927	HK_HK10	0.087481
Daito_PW210	0	HK_HK12	0
Daito_PW211	0.120751	HK_HK13	1.252174
Daito_PW212	0.016949	HK_HK14	0
Daito_PW213	0.490971	HK_HK15	0
Daito_PW219	0.137609	HK_HK2	0
Daito_PW220	0	HK_HK3	0
Daito_PW221	1.368756	HK_HK4	0
Daito_PW222	0.705258	HK_HK5	0
Daito_PW223	3.074667	HK_HK6	0
Daito_PW224	0	HK_HK7	0
Daito_PW226	0.176273	HK_HK8	0.122924
Daito_PW229	0.068148	HK_HK9	0.016949
Daito_PW230	0.017241	Iheya_PW100	0.104377
Daito_PW232	0	Iheya_PW101	0.034493
Daito_PW233	0.051481	Iheya_PW102	0
Daito_PW235	0.206574	Iheya_PW103	0.034493
Daito_PW237	0.035468	Iheya_PW104	0
Daito_PW240	0.017544	Iheya_PW105	0.017241
Daito_PW242	0.103549	Iheya_PW106	0.017544
Daito_PW243	0	Iheya_PW107	0.035401
Daito_PW247	0.368757	Iheya_PW108	0.360771
Dongsha_D1	1.339026	Iheya_PW109	0
Dongsha_D2	0	Iheya_PW110	0.035131
Dongsha_D3	0.172455	Iheya_PW111	0.017241
Dongsha_D4	0	Iheya_PW112	0.034493
Dongsha_D5	2.911177	Iheya_PW113	1.440583
Dongsha_D6	2.911177	Iheya_PW114	0.051734
Euphyllia_PW453	0	Iheya_PW117	0.592018
Euphyllia_PW580	0	Iheya_PW119	0.034493
GastreOb2_PW448	0.087794	Iheya_PW123	0.034493
GastreOb2_PW449	0.034493	Iheya_PW126	0.18889

Appendix 3: Table S3.3 - Booster instability

Taxon	Instability	Taxon	Instability
Iheya_PW128	0.607071	RedSea_SA2733	0
Iheya_PW129	0	RedSea_SA2734	0.053571
Iheya_PW97	0	RedSea_SA3443	0
Iheya_PW98	0.03337	RedSea_SA3470	0
Iheya_PW99	0.034493	RedSea_SA3517	0.474682
Indonesia_83316	4.294028	RedSea_SA3518	0.403494
Maldives_M013	0.015625	RedSea_SA3529	0
Maldives_M015	0.159494	RedSea_SA3530	0
Maldives_M019	0.033898	RedSea_SA3566	0.033673
Maldives_M022	0.085985	Samoa_MS01	0
Maldives_M032	0.034493	Samoa_MS02	0
Maldives_M042	0.192569	Samoa_MS03	0
Maldives_M044	0.068684	Samoa_MS04	0
Maldives_M047	0.119506	Samoa_MS05	0
Maldives_M049	0.05392	Seragaki_PW575	1.483852
Maldives_M052	0	Taiwan_T1	0.788846
Maldives_M221	0.107816	Taiwan_T2	3.965684
Maldives_M226	0.086258	Taiwan_T3	0.788846
Maldives_M243	0.348709	Taiwan_T4	0.788846
Maldives_M244	0.067662	Tanega_PW158	0.155862
Miyako_PW37	0.174834	Tanega_PW159	0.017857
Miyako_PW39	0.034483	Tanega_PW160	0.174345
Miyako_PW40	1.980985	Tanega_PW161	0.034191
Miyako_PW41	0.016393	Tanega_PW162	0.035401
Miyako_PW42	0.138003	Tanega_PW163	0
Miyako_PW43	0.173479	Tanega_PW164	0.325775
Miyako_PW45	0.052663	Tanega_PW166	0.067581
Miyako_PW47	0.016667	Tanega_PW167	0.016393
Miyako_PW48	0.55415	Tanega_PW168	0
Miyako_PW49	0.053571	Tanega_PW170	0.03337
Miyako_PW50	0.035714	Tanega_PW171	0.034524
Miyako_PW51	0.089286	Tanega_PW173	0
Miyako_PW52	0.175828	Tanega_PW174	0.017857
Miyako_PW54	0.017857	Tanega_PW176	0.072727
Miyako_PW56	0	Tanega_PW177	0.083926
Miyako_PW58	0.017544	Tanega_PW178	0
Miyako_PW59	0.051149	Tanega_PW180	0
Miyako_PW60	0.472914	Tanega_PW181	0.103479
Miyako_PW61	0.279535	Tanega_PW182	0
Miyako_PW63	0.608033	Tanega_PW183	0.050847
Miyako_PW65	1.210974	Tanega_PW184	0
Miyako_PW66	0.293779	Tanega_PW185	0
Miyako_PW67	0.366917	Tanega_PW186	0.033898
Miyako_PW69	0	Tanega_PW187	0
Miyako_PW71	0.086882	Tanega_PW188	0
Miyako_PW73	0.086359	Tanega_PW190	0.169032
Miyako_PW75	0.051794	Tanega_PW194	0.050565
Oku_PW139	1.245706	Tanega_PW195	0.102642
Oku_PW141	0.156465	Tanzania_83317	0.260237
Oku_PW142	0.033482	Thai_PW287	0.244687
Oku_PW143	0	Thai_PW289	0
Oku_PW145	0.224471	Thai_PW337	0.036039
Oku_PW147	0.188871	Thai_PW348	0.036039
Oku_PW149	0.103782	Thai_SC3	0.036039
Oku_PW150	0.034493	Thai_STS27	0.261353
Oku_PW151	0	Thai_STS28	0.385436
Oku_PW152	0.595378	WA_ZR1	0.176843
Oku_PW153	0	WA_ZR10	0.036364
Oku_PW154	0.069624	WA_ZR11	0.05303
Oku_PW155	0.631048	WA_ZR12	0
Pachiseris_PW578	0	WA_ZR2	2.214481
Pachiseris_PW581	0	WA_ZR3	7.95424
RedSea_SA2719	0.051473	WA_ZR4	0
RedSea_SA2720	0.034524	WA_ZR5	0.315775
RedSea_SA2726	0.051228	WA_ZR6	0.036364
RedSea_SA2727	0.280009	WA_ZR7	0.335064
RedSea_SA2729	0	WA_ZR8	0.036364
RedSea_SA2731	2.444821	WA_ZR9	0.193739